THE DUAL ROLE OF LEF-2 IN DNA REPLICATION AND LATE GENE EXPRESSION DURING BACULOVIRUS-REPLICATION.

CLARE ALLEN

A thesis submitted in partial fulfilment of the requirements of Oxford Brookes University for the degree of Doctor of Philosophy.

This research programme was carried out in collaboration with the NERC Centre for Ecology & Hydrology, Oxford.

September 2006

Abstract

The dual role of *lef*-2 in DNA replication and late gene expression during baculovirus-replication.

Clare Allen.

Oxford Brookes University and the NERC Centre for Ecology & Hydrology.

Thesis for Doctor of Philosophy

September 2006

AcMNPV *lef*-2 is essential for DNA replication and is involved in expression of late and very late gene promoters. In earlier work, the isolation of a virus mutant (VLD1) deficient only in very late protein synthesis was attributed to a point mutation in *lef*-2. DNA replication and late protein production remained largely unchanged. In this study, real time or quantitative polymerase chain reaction (q-PCR) was used to re-examine virus DNA replication by VLD1 and AcORF6^{3260}-1, a virus containing the same mutation within *lef*-2 derived by directed methods. The results showed that AcORF6^{3260}-1 DNA replication was comparable to wild type AcMNPV, but that VLD1 exhibited slightly delayed DNA replication, suggesting that this virus might have other gene mutations. A second mutation was discovered within *lef*-2, but when this was introduced into AcMNPV it had no apparent effect on DNA replication. The q-PCR was also used to examine late and very late gene expression in virus-infected cells. The expression of late (*gp64* and *capsid*) genes was similar between AcORF6^{3260}-1 and AcMNPV whereas very late gene expression (*p10* and *polyhedrin)* was down regulated in the mutant. This evidence supports a dual role for *lef-2* in DNA replication and very late gene expression.

Further analysis of the region of *lef*-2 containing the mutation in VLD1 revealed 5 cysteine residues highly conserved between examples of the gene from 37 different baculoviruses. Mutation of four of these cysteines into serines and construction of recombinant viruses showed that budded virus production was reduced from 0 – 48% of that seen in AcMNPV controls. This suggests an important role for the cysteine rich region of LEF-2 in AcMNPV replication.

To facilitate the construction of a number of virus mutants in this study, a recombinant bacmid (AcΔ*lef-2*.neo) was used that lacked the *lef*-2 coding region. This virus should not have been replication-competent but insect cells transfected with AcΔ*lef-2*.neo DNA showed limited cytopathic effects. Subsequent titration of culture medium produced small, punctate plaques. The titres of these virus stocks were very low and made further characterisation difficult. Clearly, *lef*-2 is an important gene, but it can be deleted from the virus genome.

To assess the ability of other baculovirus *lef*-2s to complement AcΔ*lef-2*.neo, synthetic copies of genes with AcMNPV-specific flanking regions were constructed and used to rescue this virus. Only a *lef*-2 with at least 53% identity was able to produce a virus that replicated with 0.04% efficiency compared with wild type. *Lef*-2s with higher identity to that of AcMNPV are not yet available. This suggests that such examples of *lef*-2 may not be functional or more likely, that many other baculoviruses have yet to be identified.

List of Presentations.

Much of the information and results presented in this thesis have been presented in conferences and seminars. The following presentations are listed below:

Allen, C., King, L.A., and Possee, R. D. Mutational analysis of baculovirus late gene promoters. Oral Presentation at NERC Centre for Ecology & Hydrology First Postgraduate Seminar Day May 2003. I was awarded first prize for the best first year student oral presentation.

Allen, C., King, L.A., and Possee, R. D. Mutational analysis of baculovirus late gene promoters. Oral Presentation at Oxford Brookes University Postgraduate Research Student Symposium, December 2003.

Allen, C., King, L.A., and Possee, R. D. Mutational analysis of baculovirus late gene promoters. Oral Presentation at NERC Centre for Ecology & Hydrology Second Postgraduate Seminar Day May 2004.

Allen, C., King, L.A., and Possee, R. D. Examining the late-very late gene expression transition in baculovirus-infected cells. Poster Presentation at Oxford Brookes University Postgraduate Research Student Symposium, January 2005. I was awarded first prize for the best student poster presentation (Sponsored by Nature/ Nature jobs).

Allen, C., King, L.A., and Possee, R. D. Examining the late-very late gene expression transition in baculovirus-infected cells. Oral Presentation at NERC Centre for Ecology & Hydrology Third Postgraduate Seminar Day May 2005.

Allen, C., King, L.A., and Possee, R. D. Examining the late-very late gene expression transition in baculovirus-infected cells. Oral Presentation Oxford Brookes University School of Biological and Molecular Sciences Symposium, November 2005.

Allen, C., King, L.A., and Possee, R. D. *Lef*-2 dual role in DNA replication and late gene expression during baculovirus- infection. Oral Presentation at IX International Colloquium on Invertebrate Pathology and Microbial Control (ICIPMC), XXXIX Annual Meeting of the SIP And VIII International Conference on *Bacillus thuringiensis* (ICBt), Wuhan, Peoples Republic of China, 25th August- 1st September 2006. I was awarded third prize for the best overall student oral presentation and also a Society for Invertebrate Pathology Virology Division student travel award.

Acknowledgements.

My first and most humble thanks go most deservingly to my supervisor Prof Bob Possee who has been absolutely wonderful throughout my PhD. In the last four years, you have taught me what makes a good scientist and shown me what makes a great scientist, and that is something I will always take with me. I would also like to thank my other supervisor Prof Linda King for inspiring me to work with viruses through the virology module at Oxford Brookes University as an undergraduate student.

There are so many people I would like to thank but especially all those people both past and present that have worked in the baculovirus lab at NERC Centre for Ecology & Hydrology. My special appreciation goes to Dr John Burden for all his help and support with all the real-time PCR work plus being a good friend. To Miss (shortly to be Dr.) Carolyn Pritchard I have found someone to laugh with and to count on not only as a colleague but as a dear friend who has been there for me until the very end of this PhD. I would also like to thank Dr Sarah Lee Turner for her invaluable help on sequence alignments and phylogeny trees. Furthermore, Dr Rosie Hails for trying to explain everything statistical to me. To Mr Adam Chambers I wish to thank for the construction of the AcΔ*lef*-2.neo virus construct. To the rest of the lab, it has been great and thanks for the support and endless help.

I would also like to thank Oxford Brookes University and NERC Centre for Ecology and Hydrology for the financial support of a collaborative CASE- studentship throughout my PhD.

Finally, I would like to thank the most important people in my life- my parents and my fiancé Chris. To my parents, I am so blessed to have you in my life as you have constantly supported and had faith in me. Lastly, I thank my fiancé- Chris whose support and love have been boundless during my PhD. His humour and willingness to act as my personal taxis at some very unsociable hours in the pursuit of cells has been absolutely fantastic. Therefore, I dedicate my thesis to my parents and Chris.

The Road goes ever on and on
Out from the door when it began.
Now far ahead the Road has gone,
Let others follow it who can!
Let them a journey new begin,
But I at last with weary feet
Will turn towards the lighted inn,
My evening rest and sleep to meet.

(J.R.R. Tolkien, Lord of the Rings).

Contents

Table of Tables and Figures

Chapter Four:

Chapter Five:

Abbreviations

3 prime	3'
3-(N-Morpholino)propanesulfonic acid	MOPS
5 prime	5'
5-bromo-4-chloro-3-indolyl-beta-D-galactopyranoside	X-gal
5'- bromodeoxyuridine	BrdU
Adenosine Triphosphate	ATP
Base pairs	bp
Change in	Δ
Concentration	Conc. Or [ ]
Daltons	Da
Days post infection	dpi
Degree Celcius	°C
Deoxynucleotide Triphosphate	dNTP
Deoxyribonucleic acid	DNA
Dideoxyadenosine Triphosphate	ddATP
Dideoxycytidine Triphosphate	ddCTP
Dideoxyguanidine Triphosphate	ddGTP
Dideoxythymidine Triphosphate	ddTTP
Diethylpyrocarbonate	DEPC
Dithiothreitol	DTT
Double-stranded DNA	dsDNA
Ethylenediaminetetraacetic acid	EDTA
Foetal Calf Serum	FCS
Grammes	g
Hours post infection	hpi
isopropyl-beta-D-thiogalactopyranoside	IPTG
Kilo Base pairs	Kbp
Kilo Daltons	KDa
Less than	<

Luria broth	*Lb*
Magnesium Chloride	$MgCl_2$
Micro Farad (Capacitance)	µF
Microgrammes	µg
Microlitre	µl
Micromolar	µM
Millilitre	ml
Millimeters	mm
Millimolar	mM
Minutes post infection	mpi
Molar	M
Molecular Weight	M_W
Moles	mol
More than	>
Multiplicity of Infection	MOI
Nanogrammes	ng
Nanometers	nm
Ohm (Electrical Resistance)	Ω
Open Reading Frame	ORF
Percentage	%
Phosphate buffered saline	PBS
Picomoles	pmol
Plaque forming units	pfu
Polymerase Chain Reaction	PCR
Real time-PCR	q-PCR
Revolutions per minute	rpm
Ribonucleic acid	RNA
Single-stranded DNA	ssDNA
Sodium Carbonate	Na_2CO_3
Sodium Chloride	NaCl
Sodium Dodecyl Sulfate	SDS

Sodium Hydroxide	NaOH
T4 polynucleotide kinase	PNK
Thermus aquaticus	*Taq*
Tris (hydroxymethyl) aminomethane Hydrochloride	Tris-HCl
Tris-EDTA Buffer	TE
Ultra Violet	UV
United Kingdom	UK
Volts	V
Weight/ volume	w/v
Weight/ weight	w/w

Chapter One

Introduction

Chapter One

Introduction

1.1 General Introduction.

The *Baculoviridae* comprise a family of large double stranded DNA (dsDNA) viruses that have been described in the earliest written accounts of Chinese silkworms culture. Due to baculoviruses being host-specific, they have had an enormous attraction for use in microbial control against invertebrates such as forest, cotton and soybean pests. Unfortunately, a disadvantage is the length of time taken to kill the larval host. However, research has been undertaken to increase time to death by incorporating genes such as the scorpion toxin, or by combined application with other microbes (e.g. *Bacillus thuringiensis).* The other advantage of the baculoviruses is they can be used as an expression vector to produce large amounts of recombinant proteins. During very late gene expression, baculoviruses are able to hyper-express two genes - *polyhedrin* and *p10* that are involved in the formation and production of occlusion bodies. By inserting a foreign gene downstream of the very late promoters, recombinant proteins can be produced in large quantities from larvae or insect cells. These applications of baculovirus technology have out distanced our understanding of the molecular genetics of virus replication.

1.2 Baculovirus Genome Organisation.

The baculovirus genome is a large circular, covalently closed, dsDNA of calculated size between 90 – 160Kbp depending on the virus isolate (Figure 1.1). The prototype baculovirus genome and first to be sequenced was the *Autographa californica* nucleopolyhedrovirus (AcNPV) C6 isolate. This is 133,984bp and contains at least 154 open reading frames (ORF) 150 nucleotides or greater in length (Ayres *et al*, 1994; Possee and Rohrmann, 1997). Baculovirus genes are classified into distinct phases of immediate early, delayed early, late and very late transcription (Nissen and Friesen, 1989; Dickson and Friesen, 1991; Lu and Miller, 1995b; and Friesen, 1997). The locations of genes are dispersed throughout the baculovirus genome as illustrated in Figure 1.1. These genes are found on both strands of DNA and may overlap slightly.

The expression of the baculovirus genome follows a highly ordered temporally regulated cascade, with each successive phase dependent on gene expression within the previous phase. The early gene phase occurs before DNA replication and utilizes a host cell RNA polymerase II (Fuchs *et al*, 1983; Hoopes and Rohrmann, 1991; Kogan *et al*, 1995). However, the late phase succeeds viral replication and appears dependent on a α-amanitin resistant virus-specific RNA polymerase. The chemical α-amanitin is a powerful toxin from the toadstool *Amanita phalloides* (Stirpe and Fiume, 1967). Mice injected with this toxin died within 2-5 days and analysis of DNA, RNA and protein content of the liver nuclei revealed a decrease in RNA content (Stirpe and Fiume, 1967). Further analysis showed that α-amanitin caused impairment to RNA synthesis, and inhibited RNA polymerase, but did not affect the replication of RNA or DNA viruses (Stirpe and Fiume, 1967)

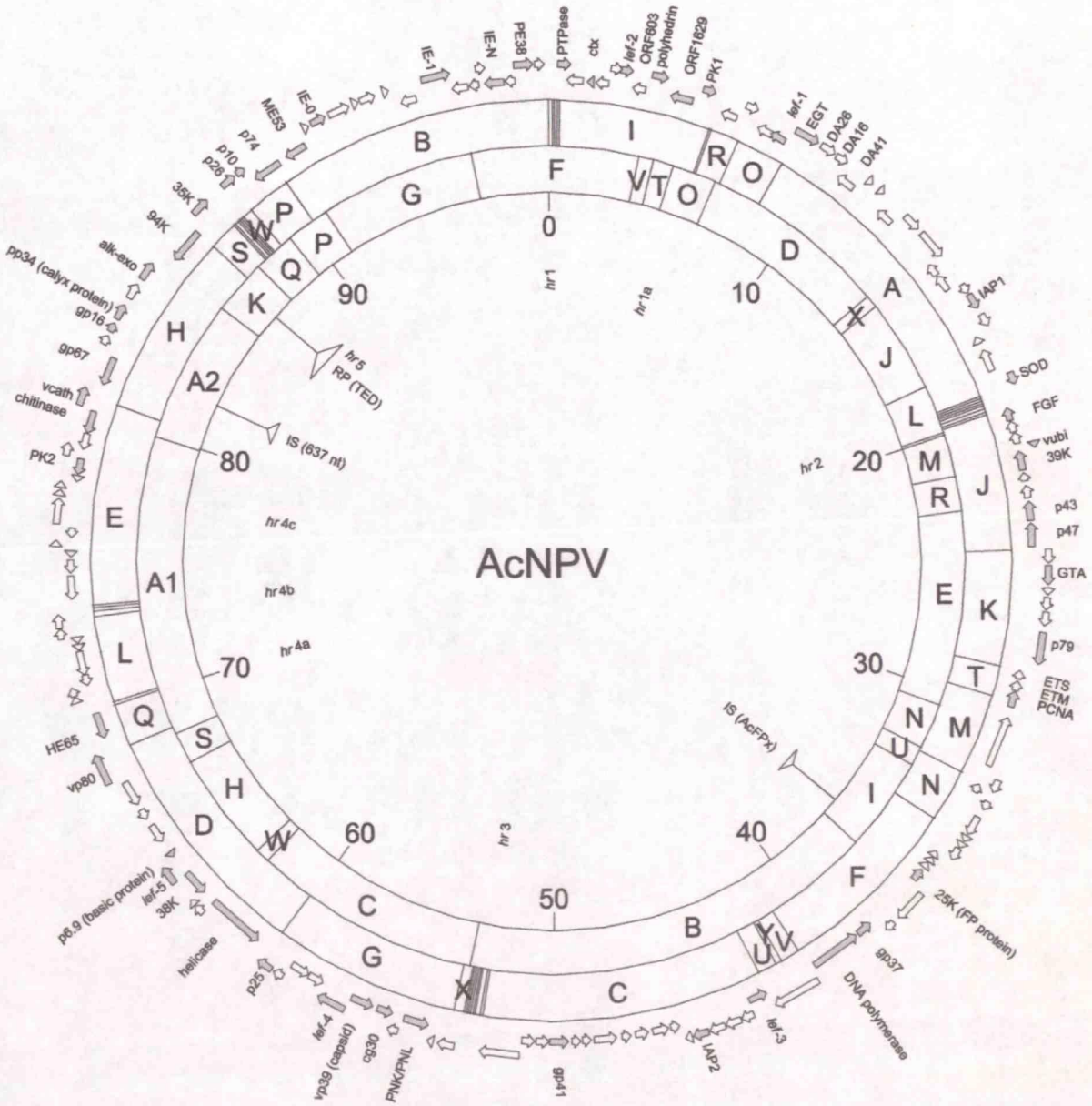

***Figure 1.1*- Circular map of AcMNPV** (Ayres *et al.*, 1994)**.** The outer ring represents *Eco*RI and the inner ring represents *Hind*III restriction enzymes. The positions of the 154 ORFs are indicated with arrows showing the direction of transcription. The scale of the inner circle is 100MU.

1.3 Baculovirus Classification.

Members of the invertebrate-specific *Baculoviridae* family are traditionally classified into two genera- Nucleopolyhedroviruses (NPV) or Granuloviruses (GV) based on the morphology of the occlusion bodies. The NPV form polyhedral occlusion bodies, with the major matrix protein consisting of polyhedrin (Herniou *et al.*, 2001). In addition, the NPV occlusion bodies characteristically contain one or many virions. In contrast, the GVs form ovoid based occlusion bodies with the protein granulin and only contain a single virion

(Herniou *et al*., 2001). The NPVs can be further sub-divided into two groups, denoted group I and II based on early phylogenetic analyses of the polyhedrin gene (Zanotto *et al*, 1993). In support for this division, is the identification of a F (fusion) protein only found in group II NPVs such as *Lymantria dispar* MNPV (LdMNPV) and *Spodoptera exigua* MNPV (SeMNPV) and GVs such as *Plutella xylostella* GV (PxGV) (Ijkel *et al*, 2000; Pearson *et al*, 2000). The F (fusion) protein is a functional alternative to the glycoprotein64 (GP64) that is found on BV of group I NPVs such as *Orgyia pseudotsugata* MNPV (OpMNPV). However, this classification is being challenged by the characterization of baculoviruses such as *Culex nigripalpus* (CuNPV), *Neodiprion lecontei* (NlNPV) and *Neodiprion sertifer* (NsNPV) that are both phylogenetically similar and distant to the current groupings (Jehle *et al*., 2006). Herniou *et al*. (2001) have attempted to reconstruct phylogenetic trees based on the use of the entire baculovirus genome. Single gene trees were used as well as sets of core genes, gene content and order (Herniou *et al*., 2001). However, a new classification has been recently proposed based on the alignment of 29 baculovirus core genes of 29 sequenced baculovirus genomes (Jehle *et al*., 2006). The newly proposed baculovirus phylogenetic tree consists of four groups- Alphabaculovirus, Betabaculovirus, Gammabaculovirus and Deltabaculovirus (Jehle *et al*., 2006). The alphabaculovirus genus includes all lepidopteran-specific NPVs, the betabaculovirus genus comprise of all lepidopteran-specific GVs; and the gammabaculovirus genus should include NlNPV, NsNPV and hymenopteran-specific NPV. Finally, the deltabaculovirus genus includes CnNPV and possibly other diptera-specific baculoviruses. The advantage of using this classification is that it is readily expanded to include additional groups.

1.4 Ultra Structure of Baculoviruses.

Baculoviruses have a unique bi-phasic lifecycle, which produces two structurally distinct viral phenotypes – Budded Virus (BV) and Occlusion Derived Virus (ODV) (Fig 1.2). During the late gene phase, the BV is formed by the migration of nucleocapsids from the nucleus, then budding through the heavily modified GP64 - rich plasma membrane. *Gp64* is regulated both by early and late promoters and plays an important role as a fusion protein for BV, spreading systemic infection *in vivo*. Electron microscope studies on BV structure appear to show a loosely associated lipid membrane surrounds this viral phenotype with

peplomers that are each composed of a single trimer of gp64 (Oomens *et al*, 1995). Initially, the *gp64* was identified and sequenced from group I NPVs- OpMNPV and AcMNPV (Blissard and Wenz, 1992). Analysis showed a high degree of conservation between the sequences especially with potential *N*-glycosylation, acylation sites and cysteine residues (Blissard and Wenz, 1992). In contrast, BV of group II NPVs and GV lack the *gp64* homolog (Westenberg *et al*., 2004). Instead, a *gp64* alternative was present and named the F protein (Westenberg *et al*., 2004). The F protein was identified in group II NPVs LdMNPV and SeMNPV and in GVs- PxGV (Ijkel *et al*, 2000; Pearson *et al*, 2000). Transfection of a *gp64*-null mutant in *Spodoptera frugiperda (*Sf-9) cells was unable to produce BV, but was rescued by introducing an F protein from either LdMNPV or SeMNPV (Lung *et al*., 2002). This highlighted that the F protein is functionally similar to GP64 (Lung *et al*., 2002).

As the levels of BV decrease, in favour of nucleocapsids destined to become ODV, a potential switch between the two viral phenotypes is formed. The viral ODV phenotype can be observed during both late phases, but is most dominant in the very late phase of infection. In contrast to BV, GP64 is not detected in the surrounding envelope of the ODV (Whitford *et al*., 1989). The source of the envelope remains unclear, but a *de novo* membrane synthesis process may be responsible. The production of occlusion bodies during replication is not only limited to the baculoviruses, but is a shared characteristic with other virus families such as insect reoviruses and poxviruses as reviewed by Cann, (1997). Whether the occlusion body is composed of polyhedrin (NPV) or granulin (GV), it offers a protective matrix around the virus particles and resists solublisation except under alkaline conditions found in the invertebrate host gut (Rohrmann, 1986).

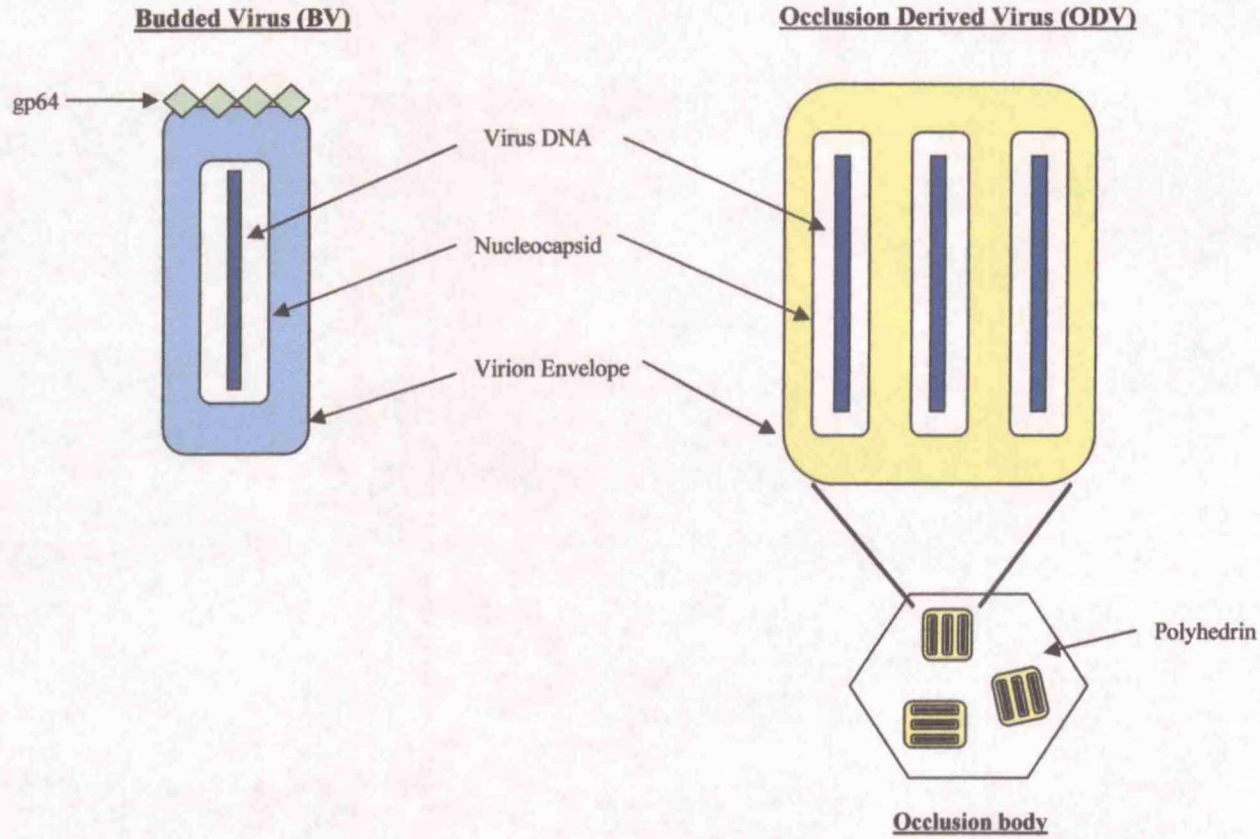

Figure 1.2 **Schematic of the two structurally distinct viral phenotypes of baculovirus (Funk *et al*, 1997).** Budded Virus (BV) and Occlusion Derived Virus (ODV).

1.5 Baculovirus Replication *in vivo*.

Baculoviruses are invertebrate-specific and their hosts have been described from insect orders such as Lepidopteran, Hymenoptera, Diptera, as well as the crustacean order Decapoda (Fauquet *et al.*, 2005). A common mode of infection for the baculovirus is through ingestion of the ODV by the invertebrate host (Granados and Williams, 1986) (Fig 1.3). Artificial modes of baculovirus infection that are feasible are injection of BV into the haemocoel and dispensing the virus onto medium using an atomizer (Biji *et al.*, 2006). The occlusion body matrix is dissolved by alkaline juices of the invertebrate midgut lumen, releasing nucleocapsids to bind to an unknown receptor on columnar epithelial cells.

Nucleocapsids of AcMNPV and *Heliothis zea* NPV (HzNPV) appear to migrate and uncoat within the nucleus, before releasing viral DNA (Granados and Lawler, 1981) Preceding DNA replication, the host nucleus swells, forming an electron-dense chromatin-like network or virogenic stroma (Granados and Lawler, 1981; and Volkman and Knudson, 1997). From 8hpi to 48hpi, the virogenic stroma is the predominant structure in the nucleus (Guarino *et al.*, 1992). Granados and Lawler (1981) observed the presence of nucleocapsids dispersed throughout the virogenic stroma. In addition, empty viral particles were shown to assemble in pockets between the chromatin filaments and then fill up with DNA from the stroma (Guarino *et al.*, 1992). The virogenic stroma is thought to be the site of DNA replication and late gene transcription.

Late in gene expression, progeny nucleocapsids migrate to the plasma membrane, acquiring a double envelope coat from budding though the inner and outer nuclear membranes (Granados and Lawler, 1981; Williams and Faulkner, 1997). By unknown processes, the double membranes of the nucleocapsids are lost in the cytoplasmic region of the cell. A new membrane is gained as the nucleocapsids bud through the plasma membrane, modified with gp64 (group I NPVs) or F-protein (group II NPVs and GV). Afterwards, the BVs systemically spread secondary infection to further tissues and are taken up by the cells via endocytosis. This is

mediated by the pH-dependent membrane fusion GP64 (in the case of group I NPVs) protein (Blissard and Wenz, 1992).

The very late phase is characterized by the hyper expression of late genes such as *polyhedrin* and *p10* that function in the formation and release of occlusion bodies. Polyhedrin is the major matrix protein of polyhedra in NPV (or granulin in GV), forming a structure that incorporates either singular or multiple numbers of nucleocapsids. Structural integrity of the developing occlusion bodies is enhanced by the acquisition of an additional envelope or calyx (Williams and Faulkner, 1997). From sequence and mutational analysis, the P10 has been implicated in the aggregation of self-molecules, liberation of the occlusion bodies and assembly of fibrillar structures in both the cytoplasm and nucleus of host cell (Williams and Faulkner, 1997).

The final stage of *in vivo* baculovirus infection is the liquefaction of the host invertebrate and release of occlusion bodies into the environment. Virus-encoded late genes *chitinase* and *cathepsin* are thought to be associated with this process, providing a stripping action of protein from the invertebrate cuticle, to allow extensive degradation of chitin (Hawtin *et al*, 1997)

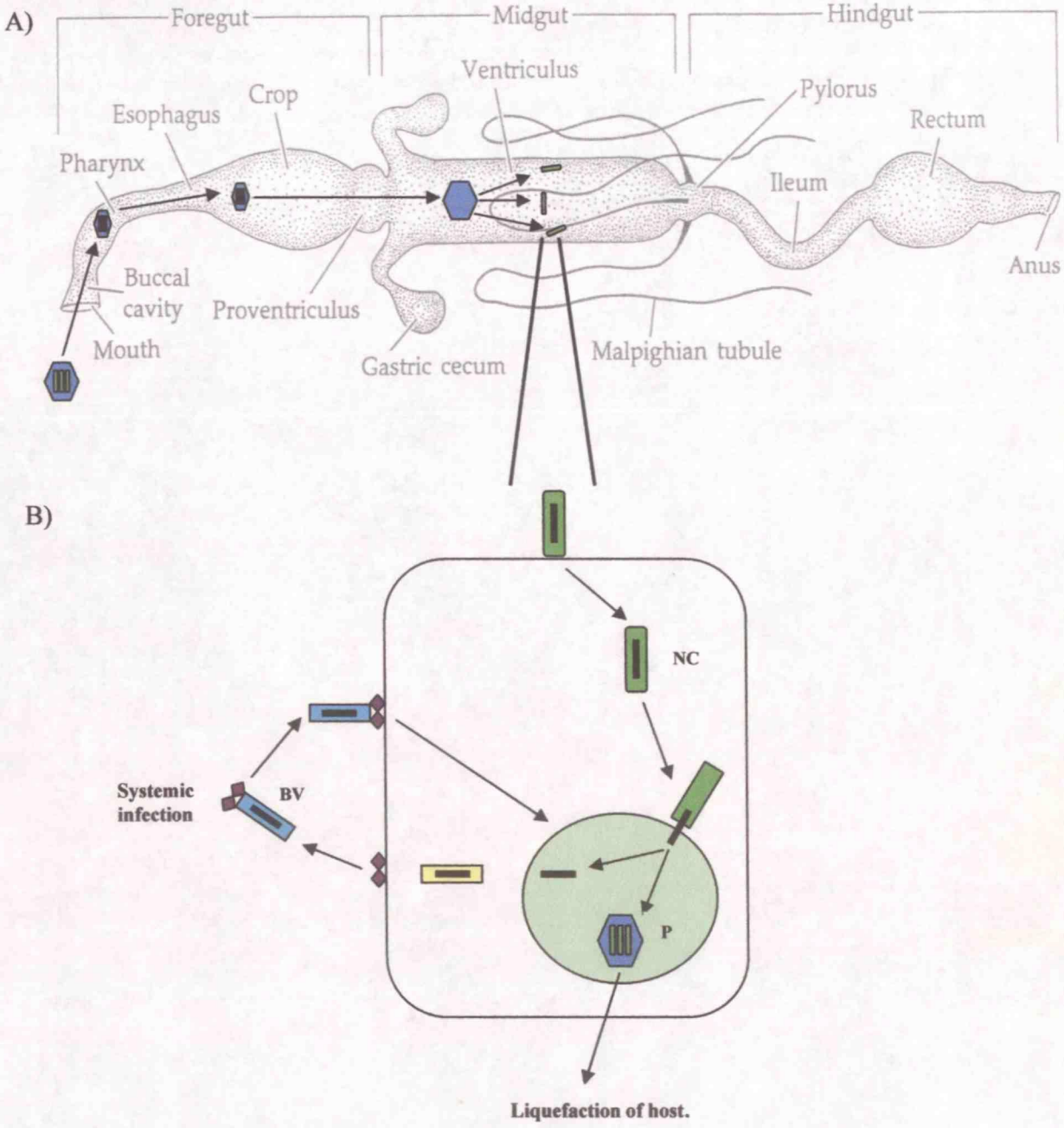

***Figure 1.3*- Baculovirus lifecycle.** Panel A illustrates the pathway of the polyhedra through the insect digestive system (Brusca and Brusca, 1990). Panel B represents the stage of the baculovirus lifecycle at the cellular level. P, Polyhedra, NC, Nucleocapsid, BV, Budded Virus.

1.6 Baculovirus Replication *in vitro*.

The replication and morphogenesis of the baculovirus family has been studied extensively throughout many cell culture-based systems (Williams and Faulkner, 1997). After initial exposure to the insect cells, viral particles can be observed to attach to the host membrane receptors at 5-10 minutes post infection (mpi). Following endocytosis, the viral nucleocapsids migrate into the cytoplasm. The nucleocapsids uncoat, penetrate the nucleopore and transcription of *ie*-1 reaches its maximal level at 1 hour post infection (hpi) (Guarino and Summers, 1987). After initiation of DNA replication (6-9hpi), a structure is observed to form inside the nucleus and is named the virogenic stroma (Granados and Lawler, 1981; Williams and Faulkner, 1997). This structure is present throughout baculovirus infection and is proposed to be the site of DNA replication and late gene transcription due to the high levels of progeny nucleocapsids (Granados and Lawler, 1981). During the late phase (12-15hpi), naked nucleocapsids migrate towards the GP64 modified plasma membrane. The commencement of BV release in an *in vitro* system is estimated to be around 17-20hpi (Rosinski *et al*, 2002). At approximately 14-16hpi, production of polyhedra can be observed inside the nucleus of the host cell, indicating the presence of occlusion bodies (Williams and Faulkner, 1997).

1.7 Baculovirus Gene Expression.

Baculovirus gene expression can be organized into four phases- immediate early, delayed early, late and very late genes. It is proposed that the timing of the gene levels is potentially regulated at the transcriptional level (Nissen and Friesen, 1989; Dickson and Friesen, 1991; Lu and Miller, 1995a; Friesen, 1997).

1.7.1 Early Gene Expression.

Baculovirus early genes are transcribed by a host RNA polymerase II and expression levels peak before the onset of DNA replication as late gene expression increases (Friesen, 1997). The products of early genes function to prepare the host for viral replication as well as regulation of the host against cellular mechanisms such as apoptosis (Friesen, 1997). Early transcription is often characterized by the synthesis

of overlapping RNA that form groups with a common 3' terminus but different 5' end (Lübbert and Doerfler, 1984). In addition, the synthesized RNA transcripts are capped and polyadenylated with only *ie*-1 known to be spliced to produce *ie*-0 (Chisholm and Henner, 1988). Early gene expression can be further differentiated into immediate early and delayed early genes. The classification of these two groups has caused some debate based on the methods used to evaluate either promoter activity or transcriptional levels during early viral infection (O'Reilly, 1992). In this study, immediate early and delayed early genes will be discussed. Immediate early genes such as *ie*-1, *ie*-2 and *ie*-0 function as a *trans*activation factor (Guarino and Summers, 1987; Ribeiro *et al.,* 1994; Slack and Blissard, 1997), a transcriptional factor plus cell cycle arrest gene (Prikhod'ko and Miller, 1998) and also a *trans*-activator factor (Huijskens *et al.*, 2004) respectively. Both *ie*-1 and *ie*-2 are described in further detail in section 1.8, due to their function as late gene expression factors (*lefs*). IE-0 is the alternative form of IE-1 with the addition of 54 amino acids at the N-terminus (Chisholm and Henner, 1988). It has been demonstrated that *ie*-0 is able to successfully replace *ie*-1 in transient late and very late assays with a plasmid containing a reporter gene under the control of a polyhedrin promoter (Huijskens *et al.*, 2004). This highlighted the importance of *ie*-0 in the *trans*-activating of early genes. Studies that used cyclohexamide (an inhibitor of protein synthesis) were able to identify immediate early genes such as *ie*-1, and aphidicolin, an inhibitor of DNA replication was used to distinguish between early and late genes (Rice and Miller, 1986; Friesen and Miller, 1987).

Delayed early genes are transcribed throughout baculovirus infection due to the presence of an early (CAGT) and late promoter (TAAG). The *39K* gene has provided a useful tool in the identification of potential *trans*-activating factors such as *ie*-1 in transient expression assays (Guarino and Summers, 1986; Carson *et al.*, 1988). Sequence analysis of *39K*, revealed the presence of both an early and late promoters (Nissen and Friesen, 1989; and Guarino and Smith, 1990; Dickson and Friesen, 1991). Another example of a delayed early gene is *gp*64, and identical to *39*K contains both an early and late promoter (Blissard and Rohrmann, 1989).

1.7.2 Late Gene Expression and Very Late Gene Expression.

Late and very late phases occur after the initiation of DNA replication, with genes being transcribed by a viral α-amantin resistant RNA polymerase (Huh and Weaver, 1990). Activation of late gene transcription seems to be dependent on DNA replication, as demonstrated by metabolic inhibitor studies using aphidicolin (inhibitor of DNA replication) (Rice and Miller, 1986; Friesen and Miller, 1987). This dependence was further supported by observations showing a delay or blockage of late gene expression when temperature sensitive (*ts*) mutants in genes such as *p143* (helicase) were generated (Gordon and Carstens, 1984; Erlandson *et al.*, 1984; Lu and Carstens, 1991; Laufs *et al.*, 1997; Liu and Carstens, 1999).

The late phase of infection actively transcribes structural genes such as *vp39* (major capsid protein) (Thiem and Miller, 1989) throughout this period (Lu and Miller, 1997). This phase is dominant between 6-18hpi in the cell and reaches optimum levels at approximately 12-18hpi (Wood, 1980).

Very late gene expression occurs approximately between 18-72hpi and is characterized by the production of occlusion bodies (Wood, 1980). Two genes characteristically hyper-expressed during this period are *polyhedrin* and *p10*.

1.8 Late Gene Expression factors (*lefs*).

Late gene expression factors or *lefs* are a library of early genes that are transcribed to function in the regulation of late gene expression and DNA replication. To date a total of nineteen *lefs* (*lefs* 1 to 12, *ie-1*, *ie-2*, *p35*, *p143*, *dnapol*, *p47*, and 39K) have been identified, although not all of their individual roles have been elucidated (Fig 1.4).

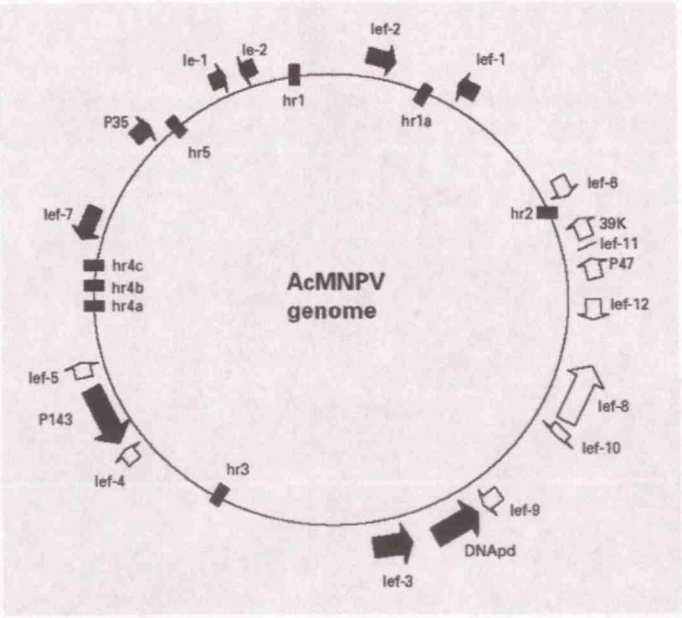

***Figure 1.4*- Orientation and location of AcMNPV nineteen *lefs* (Hefferon, 2004).** Each *lef* is represented through the corresponding ORFs with respect to orientation and location. Solid arrows indicate replication *lefs* and unfilled arrows represent transcription *lefs*. Homologus regions (hrs) are represented in location of the AcMNPV genome by bars.

1.8.1 Replication *lefs*.

Research by Kool *et al.* (1994), identified six essential genes (*ie-1*, *lef*-1, *lef*-2, *lef*-3, *dnapol*, and *p143*) and three stimulatory (*p35*, *ie-2* and *pe38*) for transient DNA replication. Assays of transient DNA replication in insect cells involved the use of minimal sub-clones expressing segments of the AcMNPV genome known to be involved in DNA replication. From these sub-clones, nine genes were identified, as noted previously. When plasmids expressing each of the essential genes were omitted from the transient assay, plasmid replication was not detected; and in the case of the stimulatory genes, replication levels were notably reduced (Kool *et al.*, 1994). In contrast to research conducted by Kool *et al.* (1994), further studies into replication *lefs* highlighted distinct differences between results, with particular reference to the involvement of *dnapol*, *p35*, *pe38* and *lef*-7 (Lu and Miller, 1995b). It was suggested by Lu and Miller (1995b) that *dnapol* was only stimulatory while *p35* was deemed essential to plasmid replication. Furthermore, the role of *pe38* was

found to moderate a stimulatory effect on plasmid replication according to Kool *et al* (1994), but was not included by Lu and Miller (1995b) based on only producing a 2 to 3-fold effect. The final difference was the inclusion of the *lef*-7 into the replication *lef* library (Lu and Miller, 1995b). It was observed that the *lef*-7 produced the largest stimulatory effect on plasmid replication (approximately 12-fold) compared to both *ie-2* and *dnapol* during the transient assay (Lu and Miller, 1995b). It is thought that *ie-1*, *lef*-1, *lef*-2, *lef*-3, *dnapol*, and *p143* are essential and *p35*, *ie-2* and *lef-7* are stimulatory factors for DNA replication (Hefferon, 2004).

1.8.1.1 Essential replication *lefs*.

Lef-1 was first identified by Passarelli and Miller (1993a), through the development of a transient expression assay. This gene encodes a protein of 266 amino acids and predicts a 31kDa polypeptide (Passarelli and Miller, 1993a). Evans *et al* (1997) identified a primase motif (WVVDAD) within the amino acid sequence of this protein that was essential for DNA replication. When the WVVDAD motif was changed to WVVQAD, the resulting mutant was unable to support transient-replication assays in place of the native *lef*-1 (Evans *et al.*, 1997). Additional evidence supporting the role of *lef*-1 as a primase has been provided by the direct comparison with the small subunit of eukaryotic-type DNA primases (EP) by multiple alignments (Koonin *et al*, 2000; Mikhailov and Rohrmann, 2002).

Studies involving yeast two hybrid analyses identified the interaction between LEF-1 and LEF-2 (Evans *et al*, 1997). *Lef*-2 was initially identified through DNA sequencing of a 633bp open reading frame (ORF) (Possee *et al*, 1991) but assigned a function later (Passarelli and Miller, 1993c). Similar to *lef*-1, *lef*-2 is an essential gene for DNA replication (Kool *et al*, 1994; Lu and Miller, 1995b) and is further involved in transient expression of late and very late promoters (Passarelli and Miller, 1993c; Lu and Miller, 1995b; Hefferon, 2004). The *lef*-2 gene encodes a 210aa protein of predicted 23.9kDa weight (Hefferon, 2004). Homologs of *lef*-2 have been found widely across the baculovirus family, including members of the GV genus (e.g. PxGV) and NPV genus, of both MNPV (e.g. *Choristoneura fumiferana*

MNPV) and SNPV (e.g. *Orgyia pseudotsugata* SNPV) (Zanotto *et al*, 1992; Federici and Hice, 1997; Jehle *et* al, 1997; Chen *et al*, 1999; Gomi *et* al, 1999; Kuzio *et* al, 1999; Afonso *et* al, 2001; Li *et al*, 2002; Garica-Maruniak *et al*, 2004). This gene is highly conserved throughout the baculovirus family with a distinct cysteine residue rich C-terminal (Chen *et al*., 1999). Sriram and Gopinathan (1998) showed that the removal of 96 amino acids within the C-terminus of the *Bombyx mori* NPV (BmNPV) LEF-2 resulted in the loss of the *trans*-activation of the minimal BmNPV polyhedrin promoter. Further to the involvement of *lef*-2 with late gene expression, Merrington *et al* (1996) observed a deficiency in very late gene expression when a point mutation was generated at position D178 within this gene. Marker rescue of wild type *lef*-2 sequence into the mutant restored the virus back to its original phenotype (Merrington *et al*, 1996). Due to the strong interactions with LEF-1, LEF-2 is suggested to function as a primase binding protein and this is further supported by the comparison with the eukaryotic–type DNA primase large subunit (Fig 1.5, Table 1.1 and Mikhailov and Rohrmann, 2002).

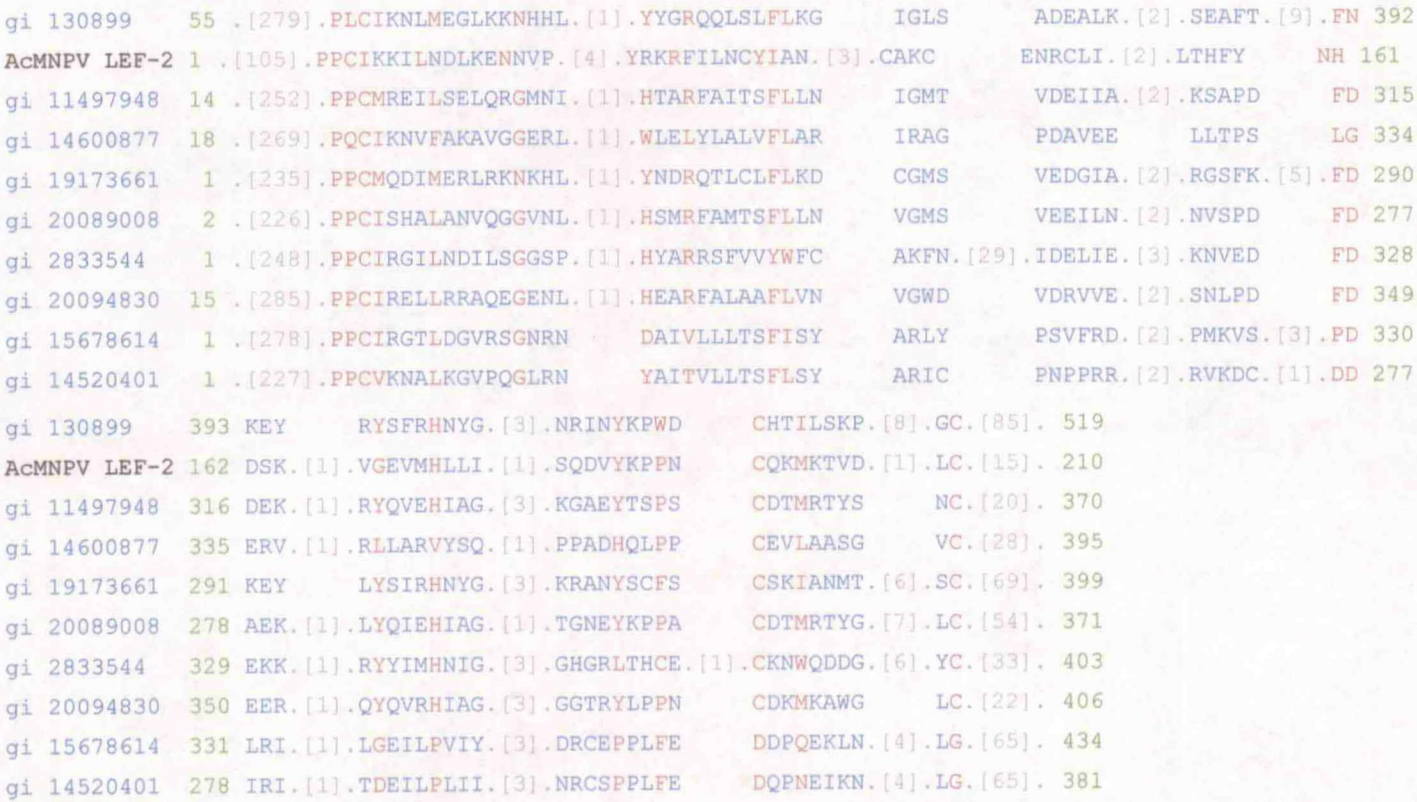

***Figure 1.5*- Conserved domain alignment of AcMNPV LEF-*2* with eukaryotic DNA primase large subunit (p58).** The AcMNPV *lef*-2 protein sequence was compared against the NCBI's Conserved Domain Database, to identify any potential conserved domains or modules. The top nine sequences are displayed by the NCBI GI identity number (further details are located in Table 1.1). The red font illustrates similar conserved amino acids between sequences. The numbers in brackets represent the amino acid gap in the sequence so that only the conserved domains are shown between all the sequences. The numbers in green those are located at the beginning and end of each sequence block represent the amino acid number in that particular protein sequence that is aligned with AcMNPV LEF-2.

***Table 1.1* - List of top nine protein sequences that display low homology with AcMNPV *lef*-2 (Fig 1.5) using NCBI conserved domains program.**

NCBI GI identity Number.	Accession Number.	Definition of protein sequence.	Organism
130899	P20457	DNA primase 58kDa subunit.	*Saccharomyces cerevisiae.*
9627748 **(AcMNPV *lef*-2)**	NP_054035	Eukaryotic-type DNA primase, large subunit	*Autographa californica* NPV.
11497948	NP_069172	DNA primase large subunit	*Archaeoglobus fulgidus* DSM4304.
14600877	NP_147402	Hypothetical protein including a eukaryotic-type DNA primase large subunit.	*Aeropyrum pernix* K1.
19173661	NP_597464	DNA polymerase α/primase large subunit.	*Encephalitozoon cuniculi* GB-M1.
20089008	NP_615083	DNA primase large subunit.	*Methanosarcina acetivorans* C2A.
2833544	Q58112	Hypothetical protein including a eukaryotic-type DNA primase large subunit.	*Methanocaldococcus jannaschii.*
20094830	NP_614677	DNA primase large subunit.	*Methanopyrus kandleri* AV19.
15678614	NP_275729	DNA primase large subunit.	*Methanothermobacter thermautotrophicus* Str.Delta H.
33356669	NP_125876	DNA primase large subunit.	*Pyrococcus abyssi* GE5.

A replication *lef* that was identified through the characterisation of a temperature sensitive mutant virus (ts8) was *p143* (Gordon and Carstens, 1984; Erlandson *et al.*, 1984; Lu and Carstens, 1991; Laufs *et al.*, 1997; and Liu and Carstens, 1999). The ts8 virus was shown to be defective for DNA replication at the non-permissive temperature of 33°C, but replicated normally at the permissive temperature of 25°C (Gordon and Carstens, 1984). A single point mutation was responsible for the ts phenotype. A guanine was changed to an adenine (Lu and Carstens, 1991). This alteration resulted in the substitution of a methionine residue for a valine residue. Lu and Carstens (1991) showed that this mutation was located seven amino acids downstream of the NTP-binding motif of the p143 gene. Furthermore, the predicted amino acid sequence of *p143*, highlighted seven motifs that were consistent with the super-family of viral, bacterial, and eukaryotic proteins involved in the functioning of duplex unwinding in DNA replication (Lu and Carstens, 1991). The seven motifs that were highlighted are two NTP-binding sequences, helix-turn-helix structure, leucine zipper, nuclear localisation signal (PKCKCYKKIK), DNA-binding and DNA unwinding (Lu and Carstens, 1991). Laufs *et al.* (1997) demonstrated that *p143* non-specifically binds to double-stranded DNA (dsDNA) to form a ladder of retarded protein-DNA complexes. Furthermore, elution profiles from cellulose chromatography of single stranded DNA (ssDNA) revealed a polypeptide of 46kDa in size, later identified to be *lef*-3 closely associated with *p143* (Laufs *et al.*, 1997)`.

Initially, *lef*-3 was identified and suggested to be required in transient assays for the expression from a reporter gene under the control of late and very late promoters (Li *et al.*, 1993). Omission of this *lef* from the library of sub-clones resulted in the dramatic reduction of expression levels (Li *et al.*, 1993). However, LEF-3 is suggested to function as a single stranded binding protein (SSBP) and is known to be essential for baculovirus DNA replication (Hang *et al*, 1995). The *lef-3* gene encodes for a polypeptide of a predicted molecular mass of 44.5kDa and has been shown to prefer binding to ssDNA over dsDNA during competition binding experiments (Hang *et al*, 1995). LEF-3 has been shown by immunofluoresence staining to be localised to the nucleus of infected cells, consistent with a gene that is essential to

baculovirus DNA replication (Wu and Carstens, 1998). As mentioned above, LEF-3 has been shown to be closely associated with P143. Wu and Carstens (1998) further demonstrated the close association of LEF-3 and P143 by showing that LEF-3 mediates the nuclear co-localisation of P143. Moreover, that LEF-3 may function to interact and transport P143 to the nucleus. Recent studies have shown that IE-1, P143 and LEF-3 are able to cluster together in the nucleus within regions of high IE-1 accumulation to form the fine basic structure of the virogenic stroma (Nagamine *et al.*, 2006). The IE-1/LEF-3/P143 complex is able to recruit other components such as a single stranded DNA binding protein (DBP) to localise to the structure (Nagamine *et al.*, 2006). It is further suggested that this model of IE-1/LEF-3/P143 structure expands and develops to form the virogenic stroma upon the initiation of DNA synthesis by the replication complex (Nagamine *et al.*, 2006)

The nucleotide sequence of the immediate early gene 1 (ie-1) was first determined by Guarino and Summers (1987). It was predicted to possess a molecular mass of 67kDa and encode a 582 amino acid IE-1 protein. Furthermore, the IE-1 was revealed to *trans*-activate the late *39K* and reached its maximal level at 1hpi (Guarino and Summers, 1987). IE-1 is essential for DNA replication and required for late gene expression (Passarelli and Miller, 1993c; and Rodems *et al.*, 1997). Rodems *et al.* (1997), concluded that residues required for *trans*-activation are confined to the N-terminus and subsequently multiple IE-1 domains involved in DNA binding are located in the C-terminus. The mutation responsible for the temperature sensitive phenotype *ts*B821 was mapped to a single nucleotide change in *ie-1*, which resulted in changing an alanine to a valine (Ribeiro *et al.*, 1994). Consequences of the *ts*B821 involved a delay in DNA replication and BV formation at 33°C by 12 hours (Ribeiro *et al.*, 1994). The *ts*B821 phenotype helped to determine the role of IE-1 in regulating gene expression of genes in AcMNPV infection (Ribeiro *et al.*, 1994; Slack and Blissard, 1997). Within AcMNPV infection, the only spliced gene is *ie*-0, which has two exons (Passarelli and Miller, 1993c). IE-0 is the alternative form of IE-1 with the addition of 54 amino acids at

the N-terminus (Passarelli and Miller, 1993c; Ribeiro *et al.*, 1994; and Huijskens *et al.*, 2004).

The final essential replication *lef* is the baculovirus DNA polymerase gene (*dnapol*). In contrast, it was suggested by Lu and Miller (1995b) that *dnapol* was only stimulatory, but it is reviewed as an essential *lef* by Hefferon (2004). Using an oligonucleotide probe corresponding to the predicted YGDTD sequence (conserved amongst viral polymerases), the AcMNPV *dnapol* was first identified by Tomalski *et al.* (1988). The observation of a new aphidicolin-sensitive DNA polymerase induced by baculovirus infection was recorded by Miller *et* al. (1981). The new virus-induced DNA polymerase could be separated from host cell DNA polymerase through sensitivity to heat inactivation and high salt concentrations (Miller *et al.*, 1981). According to Hang and Guarino (1999), following purification from virus-infected cells, the nuclear extract containing *dnapol* when electrophoresed on a SDS gel, showed a single polypeptide band with a predicted molecular mass of 110KDa, confirming previous results (Tomalski *et al.*, 1988). *Dnapol* expression increased to peak at 6hpi and declined by 12hpi (Tomalski *et al.*, 1988). It has been found to exhibit 3'- 5' exonuclease activity which is required by all viral DNA polymerases as a proofreading ability (Hang and Guarino, 1999). Further confirmation of *dnapol* requirement was obtained when a *dnapol* null bacmid transfected into *Sf*-9 cells was unable to replicate (Vanarsdall *et al.*, 2005).

Proteins that are classified as transcription factors such as the *lef*s can activate DNA replication in a number of different ways. Firstly, DNA replication may be activated by transcription factors being able to modulate chromatin structure. According to Bodmer-Glavas *et al* (2001) it was shown using *Saccharomyces cerevisiae* that the transcription factor- Abf1 is able to remodel chromatin by binding to the B3 element of *ARS*1 (origin of replication) in a manner very similar to other transcription factors that are capable of stimulating replication. A second method of activating DNA replication is the recruitment of replication proteins to form a replication complex. It has been shown that Epstein Barr Virus (EBV) cellular transcription factors Sp1 and

ZBP-89 are able to bind directly through activation domains to viral replication proteins BMRF1 (DNA polymerase accessory factor) and BALF-5 (DNA polymerase catalytic subunit) (Baumann *et al*, 1999). These findings led researchers to support the assumption that downstream components form a binding platform for EBV replication proteins, guided to the origin of replication site (*oriLyt*) by TD-binding transcription factors such as Sp1 and ZBP-89 (Baumann *et al*, 1999). Finally, DNA replication may be activated by the unwinding of the DNA duplex through the involvement of transcription factors. Transcription factors such as Jun and Fos have been found to interact with the polyomavirus large T antigen in the unwinding of the viral origin *in vivo* (Guo *et al*, 1996). It is though that this interaction provides the biochemical basis for the PEA1 site at the viral enhancer to activate DNA replication (Guo *et al*, 1996).

1.8.1.2 Stimulatory *lefs*.

Passarelli and Miller (1993c) found that IE-2 was involved in the transient expression of a reporter gene under the control of the late (*vp39*) or very late (*polyhedrin*) promoter. The *ie*-2 gene encodes for a 49kDa protein, IE-2 which *trans*-activates IE-1 (Prikhod'ko and Miller, 1998). While studying the effects of AcMNPV genes on apoptosis, transfection of plasmids expressing *ie*-2 showed enlarged cells through the blockage of the cell cycle in the S-phase (Prikhod'ko and Miller, 1998). Furthermore, there appeared to be no mitotic spindle formation present in the *ie*-2-transfected cells (Prikhod'ko and Miller, 1998). IE-2 contains a ring finger (or C_3HC_4 motif), which was determined by mutagenesis studies to be important for arresting the cell cycle, but does not appear to affect the *trans*-activating ability (Prikhod'ko and Miller, 1998). The function of IE-2 is known to be cell line specific and this is illustrated with isolated mutants of AcMNPV that were defective in *ie*-2 (Prikhod'ko *et al*., 1999). The *ie*-2 mutants exhibited a severe delay in viral replication, late gene expression, BV production and polyhedrin production in *Spodoptera frugiperda* (*Sf*-21) cells, but no delay in replication was observed in *Tn*-5B1-4d cells (Prikhod'ko *et al*., 1999). Furthermore, elevated levels of a 75kDa

protein were detected in Tn-5B1-4d cells, but no change was observed in *Sf*-21 cells (Prikhod'ko *et al.*, 1999).

Lef-7 was observed to produce the largest stimulatory effect on plasmid replication (approximately 12-fold) compared to both *ie-2* and *dnapol* during the transient assay (Lu and Miller, 1995b). It was found by Morris *et al.* (1994) that *lef*-7 is transcribed by both early and late promoters, and during transient assays acted as an early gene that was dependent on *ie*-1. It is thought that *lef*-7 may be host-specific. In two viral phenotypes expressing mutations within *lef*-7, DNA replication was delayed in *Trichoplusia ni* (*Tn*368) cells, but reached wild-type levels by 48hpi (Chen and Thiem, 1997). However, DNA replication in *Sf*-21 and *Spodoptera exigua* (*Se*-1) cells was reduced to less than 5% compared to AcMNPV (Chen and Thiem, 1997). Despite, this reduction in *Sf*-21 and *Se*-1 cells, DNA replication was still occurring in all cell lines. This reinforced the proposal of *lef*-7 being a stimulatory *lef*. LEF-7 sequence was compared to known databases, but showed no striking homology to other sequences (Morris *et al.*, 1994). Although analysis revealed that within the C-terminus, LEF-7 did contain a $CX_2CX_2CCX_8CCX_3CX_7C$ motif that is suggestive of a metal coordination site (Morris *et al.*, 1994). A region downstream of *lef*-7 within the AcMNPV genome was identified to exhibit a repressor activity of late gene expression (Hefferon, 2003a). To investigate which region was responsible for repressing late gene expression, four sub-clones that spanned the region were added singly or in combination to a *lef* library (Hefferon, 2003a). It was shown by Hefferon (2003a) that when none of the sub-clones were present that late gene expression was enhanced. In contrast, when all four sub-clones were simultaneously present, the greatest amount of repressor activity was observed (Hefferon, 2003a). Furthermore, it was suggested that the repressor activity of this sequence downstream of *lef*-7 was from a *cis*-acting element rather than ORF (Hefferon, 2003a).

P35 is an anti-apoptotic gene that is required to prevent the premature death of AMNPV-infected *Sf*-21 cells (Clem *et al.*, 1991; Hershberger *et al.*, 1994). This gene is detected early in the AcMNPV infection cycle, between 8hpi to 12hpi, and

was predominantly a soluble component of the cytosol (Hershberger *et al.*, 1994). In addition, *p35* is suggested to be cell line-specific, hence a host range determinant based on results that *Sf*-21 cells under went extensive cellular blebbing when infected with the *p35* mutant (vAcAnh) virus, but this was not observed in *Tn*368 cells (Clem *et al*, 1991; Hershberger *et al.*, 1992; Clem and Miller, 1993). Griffiths *et al.* (1999) extended the examination of *p35* observations in various cell lines to other cell types. It was found that a *p35*-deficient virus was able to replicate and produce both BV and ODV in both *Mamestra brassicae* and *Panolis flammea* cell lines (Griffiths *et al.*, 1999). However in *Spodoptera littoralis* cells infected with a *p35*-lacking virus, extensive blebbing was observed (Griffiths *et al.*, 1999).

1.8.2 Transcription *lefs*.

Transcription *lef*s were originally identified by transfection of an entire *lef* library into *Sf*-21 cells to support expression of a reporter gene under the control of a late promoter (Lu and Miller, 1995b). Omission of any *lef* plasmid from the library resulted in the significant decrease of the reporter gene. To determine which *lef* affected late gene transcription, an RNase protection assay was used to examine reporter gene levels (Lu and Miller, 1995b). From this study, it was suggested that *lef*-4, *lef*-5, *lef*-6, *lef*-8, *lef*-9, *lef*-10, *lef*-11, *39K,* and *p47* were likely to function in late gene expression (Lu and Miller, 1995b; Todd *et al.*, 1995). A further *lef* that was proposed to be involved in AcMNPV late and very late gene expression was *p35* (Todd *et al.*, 1995), which is probably just required to prevent apoptosis.

The viral-encoded RNA polymerase is responsible for the transcription of baculovirus late and very late genes during AcMNPV infection. Guarino *et al.* (1998b) purified the RNA polymerase and found it to be composed of equimolar proportions of four subunits LEF-8, LEF-9, LEF-4 and P47. When the baculovirus RNA polymerase was purified, Guarino *et al* (1998b) observed an altered transcription profile compared to infected cells. This altered profile involved late and very late gene promoters being transcribed with equal efficiencies with no "burst" being observed from late gene promoters (Guarino *et al.*, 1998b). This suggested

that the purification of RNA polymerase removed key transcription factors (perhaps *lef*-2) from this complex that were responsible for the transcription of very late genes and the repression of polyhedrin transcription during the late phase (Guarino *et al.*, 1998b). LEF-8 is proposed to be the largest subunit (Guarino *et al.*, 1998b) and was first described by Passarelli *et al.* (1994). LEF-8 is predicted to encode for a 101kDa polypeptide and revealed no significant homology to other sequences (Passarelli *et al.*, 1994). However, a conserved C-terminus motif of 13 amino acids $GXKX_4HG^{Q}/_{N}KG^{V}/_{I}$ was identified and listed amongst a number of eukaryotic and prokaryotic RNA polymerases (Passarelli *et al.*, 1994). These findings suggested that LEF-8 may be the catalytic site for the enzyme and this was further supported by Titterington *et al.* (2003) through the determination of the importance of the C-terminal motif by site-directed mutagenesis. The sequence of both *lef*-9 and *lef*-10 was originally determined by Lu and Miller (1994), and the amino acid sequence of LEF-9 was found to contain a motif (NTDCDGD) which was similar in five or seven positions to the DNA-directed RNA polymerases (Lu and Miller, 1994). In BmNPV- infected Bm cells, both *lef*-8 and *lef*-9 were transcribed from 12hpi, implying that they are early genes (Acharya and Gopinathan, 2002). The *lef*-4 is suggested to be localized to the nucleus, particularly the virogenic stroma in virus-infected cells (Durantel *et al.*, 1998). *Lef*-4 is an essential transcription *lef* in which late and very late genes depend upon as demonstrated in studies involving the silencing of LEF-4 by RNA interference and bacmid knockout technology (Knebel-Mörsdorf *et al*, 2004). The loss of LEF-4 was observed to have no effect on early gene expression, but severely reduced or abolished expression of late and very late genes (Knebel-Mörsdorf *et al*, 2004). According to Guarino *et al.* (1998a), over expression of LEF-4, confirmed that the single subunit of the baculovirus RNA polymerase possessed guanylyltransferase activity and this was also confirmed in other studies (Gross and Shuman 1998; Jin *et al*, 1998). Analysis of LEF-4 revealed the presence of a KXDG motif that was consistent with members of nucleotidyltransferases (Passarelli and Miller, 1993b; Gross and Shuman, 1998; Guarino *et al.*, 1998a; Jin *et al*, 1998). Guanylyltransferase is an enzymatic function that is involved in the formation of an m7G cap on the 5' end of mRNA (Jin *et al*,

1998). It has also been shown that *lef*-4 possesses RNA triphosphate activities suggesting that it act as a bi-functional enzyme (Gross and Shuman 1998; Jin *et al*, 1998). The final subunit of the baculovirus RNA polymerase is P47 and was first discovered by Carstens *et al.* (1993). The *p47* gene was identified through the discovery of a lesion within the temperature-sensitive mutant virus (*ts*317) (Carstens *et al.*, 1993). At the non-permissive temperature, it was observed that *ts*317-infected cells produced almost normal levels of viral structural proteins but the synthesis was restricted at a time before 20hpi (Carstens *et al.*, 1993). This led to the suggestion that *p47* was involved in the transcription of late and very late gene promoters.

Harwood *et al.* (1998) showed using a yeast two-hybrid system that LEF-5 is able to interact with itself. Amino acid sequence determination suggested the presence of a zinc ribbon-like domain with homology to RNAPII elongation factor TFIIS (Harwood *et al.*, 1998). LEF-5 was purified from over expression in a bacterial system and found that this protein strongly stimulated the transcription activity of the baculovirus RNA polymerase but did not increase the ability to synthesize long transcripts (Guarino *et al.*, 2002a). Furthermore, the authors suggested that LEF-5 functioned as initiation factor *in vitro* systems.

Lef-6 is predicted to encode for a 19kDa polypeptide with some limited sequence homology to the C-terminal of the DNA-dependent RNA polymerase subunit of the vaccinia virus (Passarelli and Miller, 1994). Lin and Blissard (2002a) observed by immunofluorescent microscopy that LEF-6 was localized to the nuclei of infected-cells and was consistent with classification of an early gene and role in regulating late transcription. *Lef*-6 null mutants in *Sf*-9 cells showed a reduction in BV and a subsequent delay in late transcription (Lin and Blissard, 2002a). This suggested that LEF-6 was not required for DNA replication, but accelerated late gene transcription (Lin and Blissard, 2002a).

The identification of transcription *lef*s was initially determined by transient origin-dependent DNA replication assays (Lu and Miller, 1995b; Todd *et al.*, 1995). *Lef*-11

was described in such a manner and it was estimated that LEF-11 contained a single zinc finger motif (C_2H_2) near the N-terminus and a basic charged region near the C-terminus (Lin *et al.*, 2001). Anti-LEF-11 antibodies were raised and used in immunofluoresence microscopy to show that LEF-11 was located within large and dense nuclear regions (Lin *et al.*, 2001). However, using a *lef*-11 knockout it was found that this virus was unable to grow in *Sf*-9 cells, and this was further supported by the reinsertion of *lef*-11 back into the BACmid to rescue the defect (Lin and Blissard, 2002b). This revealed that *lef*-11 is essential to DNA replication and should be reconsidered as a replication *lef*.

Lef-12 was discovered when a set of 18 plasmids expressing a single *lef* ORF with an eptiope-tagged fusion protein from the *Drosophila melanogaster* hsp70 promoter failed to support late gene expression in transient assays (Rapp *et al.*, 1998; Li *et al.*, 1999). *Lef*-12 is located next to *p47*, and potentially encodes a 181 amino acid polypeptide of molecular weight of 21kDa (Rapp *et al*, 1998). It is suggested that *lef*-12 has a role in late gene transcription and not DNA replication (Rapp *et al*, 1998), although Guarino *et al.* (2002b) concluded that *lef*-12 is not essential for late gene expression. Furthermore, Rapp *et al.* (1998) proposed that *lef*-12 was expressed as an early gene, which in contrast is suggested by Guarino *et al.* (2002b) to be expressed after DNA replication based on the treatment with aphidicolin.

1.8.3 Determination of Host Range.

As discussed throughout the section involving *lefs*, some genes are able to play a role in host determination. An example of this function is the antiapoptic gene *p35*. It was shown that *Sf*-21 cells under went extensive cellular blebbing when infected with the *p35* deficient mutant (vAcAnh) virus, but this was not observed in *Tn*368 cells (Clem *et al*, 1991; Hershberger *et al.*, 1992; Clem and Miller, 1993). The host range studies were extended by Griffiths *et al.* (1999) as it was found that the *p35*-deficient virus was able to replicate and produce BV and ODV in both *M. brassicae* and *P. flammea* cell lines. However in *S. littoralis* cells infected with a *p35*-lacking virus, extensive blebbing was observed (Griffiths *et al.*, 1999). Other genes that have

been implicated in determination of host range are IE-2, LEF-7. *P143* is another example of a cell specific *lef* that plays a role in host determination. Studies involving the substitution of AcMNPV *p143* with BmNPV *p143* in transient expression assays showed that this change was not able to support late gene expression or be imported into the nucleus of cells in the presence of AcMNPV or BmNPV LEF-3 (Berretta *et al*, 2006). Moreover, the same result was observed when SeNPV *p143* substituted for AcMNPV *p143* and was unable to support late gene expression in a transient expression assay (Berretta and Passarelli, 2006). A recombinant virus with null host cell-specific factor 1 gene (*hcf*-1) was able to replicate normally in *Sf*21 cells (Lu and Miller, 1996). In contrast, DNA replication plus late and very late gene expression was severely reduced in *Trichoplusia ni* (*Tn*368) cells (Lu and Miller, 1996). Furthermore, a complete shut off of host and viral protein synthesis at 18hpi was exhibited in *Tn*368 cells infected with AcMNPV *hcf*-1 null mutants (Lu and Miller, 1996). *Hcf*-1 was characterised to be an early gene that was localised to the nucleus and has the ability to only interact with itself and no other replication *lef*s (Hefferon, 2003b). According to Hefferon (2003b), using deletion analysis, it is suggested that HCF-1 functional activity is located at the N-terminus region of the protein. Further studies have identified a region within HCF-1 that is predicted to form a RING finger structure (Wilson *et al*, 2005). Mutagenesis studies of the cysteine residues within the RING finger structure showed that they are required for HCF-1 self-association and occlusion body production in *Tn*368 cells (Wilson *et al*, 2005). Further possible cell-specific *lef*s could be *lef*-2 or *lef*-12. Similar to *p143*, substituting AcMNPV *lef*-2 for SeNPV *lef*-2 showed that late gene expression is unable to be supported (Berretta and Passarelli, 2006). In contrast, late gene expression was supported when BmNPV *lef*-2 replaced AcMNPV *lef*-2 (Berretta *et al*, 2006). The cell-specific nature of *lef*-2 may be further illustrated by results in Chapter Five, which showed that CfMNPV *lef*-2 was only able to substitute AcMNPV *lef*-2 to a limited extent.

1.9 DNA Replication

1.9.1 Homologous Regions (*hrs*) and Non-*hrs* Origins of Replication.

Baculovirus DNA replication precedes the late and very late phase that results in the production of progeny virus either in the form of BV or in occlusion bodies by genes being transcribed by a viral α-amantin resistant RNA polymerase (Huh and Weaver, 1990). Two different classes of replication origins have been identified in the AcMNPV genome. The first class that is interspersed throughout the AcMNPV genome is known as homologous regions (*hrs*). Key features of *hrs* (in AcMNPV) are that they contain 2.8 imperfect palindromes of 28bp with an *Eco*RI restriction site at the in variant 10/12bp core (Cochran and Faulkner, 1983; and Guarino *et al.*, 1986). Furthermore, *hrs* are suggested to act as replication origins. This proposal was supported by evidence which showed that plasmids containing *hrs* 2, 3 and 5 were able to replicate when transfected into AcMNPV-infected *Sf*-9 cells (Kool *et al.*, 1993; and Pearson *et al.*, 1992). Furthermore, Kool *et al.* (1993) found that intracellular DNA from AcMNPV virus particles after 40 passages contained high levels of small *Eco*RI fragments that were derived from *hrs* 1, 3 and 5. Another key feature of *hrs* is to act as transcriptional enhancers of *cis*-linked viral promoters in plasmid transfection assays (Leisy and Rohrmann, 1993).

The second class of replication origins is non-*hrs*. Generation of AcMNPV defective genomes by serial, undiluted passages identified the *Hind*III-K region to carry a putative *ori* or non-*hr* (Lee and Krell, 1992; and Kool *et al.*, 1994). Sequence analysis by Kool *et al.* (1994) revealed the presence of palindromes and other motifs within the *Hind*III-K fragment. The essential part of the non-*hr* within the *Hind*III-K fragment was that it contained imperfect palindromes and an A/T rich flanking region (Kool *et al.*, 1994). Another potential non-*hr* origin is the promoter region of *ie*-1 and has been shown to be active in AcMNPV infection cycle (Wu and Carstens, 1996).

1.9.2 A Model for the Initiation of Baculovirus DNA Replication.

From the identification of nineteen *lef*s that have proposed roles in DNA replication and late gene expression, plus the comparison of AcMNPV replication with the Herpes Simplex virus type I (HSV-1), a model of the AcMNPV replication complex has been proposed (Fig 1.6).

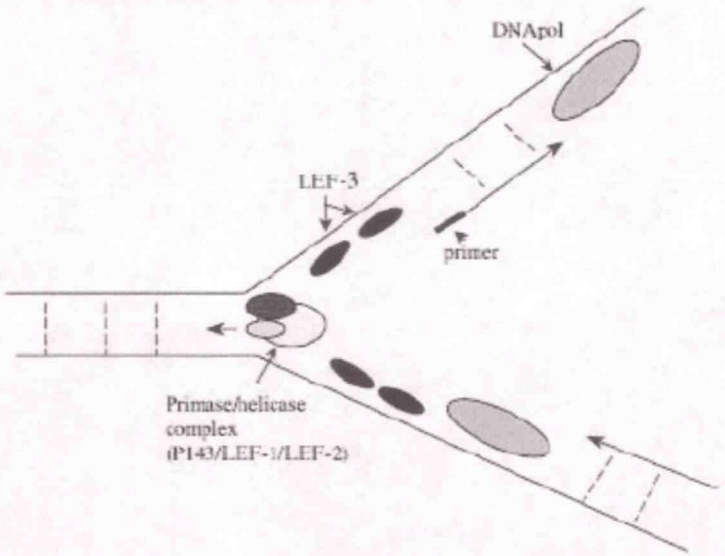

***Figure 1.6*- Model of the AcMNPV replication complex (Hefferon and Miller, 2002, pg 6239).** This model was constructed based on results in Hefferon and Miller. (2002) and on the proposed model of Herpes Simplex type I (HSV-1) replication from Knopfs (2000).

A possible scenario for the contribution of genes that are known to be involved in DNA replication was suggested by Lu *et al.* (1997). It was thought that initiation could be mediated by the binding of IE-1 to *hrs* to lead to the melting of duplex DNA to allow the assembly of the helicase-primase complex (P143, LEF-1 and LEF-2) at the replication fork (Lu *et al.*, 1997). Unwinding at the replication fork would be undertaken by the SSBP LEF-3 while the lagging strand was primed for DNA polymerase (Lu *et al.*, 1997). Other genes may be involved as an accessory factor (e.g. LEF-7, P35, IE-2, PE-38) to contribute towards maximal DNA replication, although the exact function of some proteins is not fully understood.

1.10 Very Late Deficient Phenotype (VLD).

A mutant virus displaying Very Late Deficient phenotype (VLD1) was isolated and identified to be deficient in late gene expression (Merrington *et al.*, 1996). Propagation of AcMNPV in the presence of 5'- bromodeoxyuridine (BrdU) induced a G:C – A:T mutation on the replication of the BrdU-containing template strand. Consequences of the VLD1 phenotype included reduced levels of viral titres plus delayed synthesis of virus-specific proteins such as chitinase and polyhedrin. To account for the deficiency in late gene expression, marker rescue studies mapped the putative mutation to the *Eco*RI-I region of the AcMNPV genome. Further digestion of the *Eco*RI-I fragment with *Eco*RV, deriving two smaller fragments and cotransfection into insect cells located the mutation to the 3.9Kbp *Eco*RI-*Eco*RV region of the *Eco*RI-I fragment. DNA sequencing identified two mutations within ORF-2 and *lef*-2, where a leucine residue replaced a phenylalanine and asparagine to an aspartic acid respectively. The mutation responsible for the VLD1 phenotype was located by marker rescue to be within the *lef*-2. To determine if the deficiency was a result of the *lef*-2 mutation, a recombinant virus (AcORF6^{3260}-1) was produced. Merrington *et al.* (1996) demonstrated using dot blot hybridisation that no difference in DNA replication levels occurred between AcMNPV, and AcORF6^{3260}-1. However, a temporal delay was observed in DNA replication of VLD1 compared to AcMNPV at 18hpi using dot blot hybridisation. Using a modified *Dpn* I protection assay to measure DNA synthesis, it was apparent that VLD1 exhibited lower levels compared to the other viruses (Merrington *et al.*, 1996).

Late gene expression is responsible for actively transcribing structural genes such as *vp39* (Thiem and Miller, 1989) throughout this period (Lu and Miller, 1997). This phase is dominant between 6-18hpi and reaches its optimal levels between 12-18hpi (Wood, 1980). However the timing of very late gene expression profile is different and occurs approximately between 18-72hpi (Wood, 1980). The promoters of late and very late genes share a common feature of possessing the late gene *TAAG (where * denotes either A, G or T not C) motif. This is the site at which late and very late genes are transcribed by the α-amantin RNA polymerase. A distinct feature

of very late gene promoters that contribute towards to the hyper expression *p10* and *polyhedrin* is the 5' untranslated leader region (5' UTR). This "burst" sequence is located between the transcription initiation codon (ATG) and the late *TAAG motif. It is an A-T rich region and data from mutational studies to investigate the *p10* and *polyhedrin* promoters showed that the burst sequence was required for optimal expression (Possee and Howard, 1987; Weyer and Possee, 1988; Qin *et al*, 1989; Weyer and Possee, 1989). Given that the VLD1 phenotype is deficient in very late gene expression, a key very late gene that should be considered is the Very Late Factor 1 (*vlf-1*). According to research that generated a *vlf-1* null bacmid mutant, VLF-1 was not essential for viral DNA synthesis and was a crucial capsid component, which may help to explain why it is important in the production of DNA containing virions (Vanarsdall *et al*., 2004; Vanarsdall *et al*., 2006). Interestingly, it was apparent that the absence of this gene only affected the transcription of very late genes; late genes were unaffected (Vanarsdall *et al*., 2004). These results supported data that proposed that VLF-1 transactivates the *polyhedrin* or *p10* promoters by interacting with the "burst" sequence, although the possibility of interaction with other factors cannot be dismissed (Yang and Miller, 1999). Other factors that may be considered in response to the VLD1 phenotype are perhaps involved in nuclear localization of replication proteins such as LEF-3 or factors responsible for nucleocapsids assembly.

Lef-2 is a well characterized gene that is highly conserved throughout the baculovirus family. Furthermore, it is proposed to be one of six genes essential for DNA replication. Studies have shown that *lef*-2 may function as a primase accessory factor. LEF-2 interacts with LEF-1, between 20-60 amino acids from the N-terminus. The C-terminus is cysteine-rich and previous results have highlighted the importance of this region in the successful functioning of *lef*-2.

The production of a recombinant virus (AcORF6^{3260}-1) that showed a deficiency in very late gene expression but exhibited normal levels of DNA replication compared to AcMNPV raised many interesting questions. Merrington *et al*. (1996) suggested a

dual function for *lef*-2 in DNA replication and late gene expression based on the results obtained. This was in contrast to research that had proposed that *lef*-2 was a replication *lef*. Could *lef*-2 really have a dual role in both of these processes? Is *lef*-2 really essential for DNA replication? Is the location of the mutation within LEF-2 important for either DNA replication or late gene expression? Could *lef*-2 be influencing other transcription factors such as *vlf*-1? Could the dual role of *lef*-2 be sequence or region-specific?

1.11 Aims of PhD Research.

Merrington *et al.* (1996) proposed a dual role for *lef*-2 in both DNA replication and late gene expression. Support for this proposal was obtained when analysis showed that AcORF6^{3260}-1 was deficient in very late gene expression but exhibited DNA replication levels comparable to AcMNPV (Merrington *et al.*, 1996). This was in contrast to previous research that suggested *lef*-2 was a replication *lef*.

The main objective of this PhD study was to investigate this dual role of *lef*-2 in DNA replication and late gene expression during baculovirus replication. The aim initially was to further characterise both VLD1 and AcORF6^{3260}-1 virus phenotypes. This involved the use of real time PCR (q-PCR) to examine both DNA replication and the expression of late (*gp64* and *capsid*) and very late (*polyhedrin* and *p10*) genes during a period of 48hpi.

To help answer questions relating to the importance of the location of the point mutation within LEF-2, other potentially critical residues within this sequence were identified for study. This was examined by multiple alignments of all sequenced LEF-2s across the baculovirus family including both the NPV and GV genera. Highly conserved residues were mutated by replacement with a similar residue through site-directed mutagenesis. This is aimed to expand our current knowledge of LEF-2 by identifying critical residues and constructing individual recombinant viruses to examine the consequences of such mutations on the functioning of the *lef*-2 gene. To produce these virus mutants, a parental virus lacking *lef*-2 was used for recombination. Although it was predicted that *lef*-2 was essential for virus replication, during the course of making the recombinant viruses, it became apparent that a *lef*-2 null virus was able to replicate in insect cells, albeit at a low level.

Expanding from the multiple alignments of all sequenced baculovirus genomes, a phylogenetic tree was produced to illustrate the grouping of viruses based on LEF-2 homology. Percentages of identical amino acid residues of individual baculoviruses compared to AcMNPV LEF-2 were determined. Based on this information, a

selection of NPV and GV *lef*-2s were used to replace the AcMNPV *lef*-2. This aimed to examine the relationship between gene homology and functioning in a heterologous background. Recombination between baculoviruses is possible in the insect host, but the production of a successful hybrid virus will depend on the ability of the exchanged genetic elements to function in a new background. This work was intended to address the question of how interchangeable are baculovirus *lef*-2s.

Chapter Two

Materials and Methods.

Chapter Two

2.1 Materials

2.1.1 Chemicals

General chemicals were obtained from BDH Laboratory supplies (UK) Sigma Chemical Company Limited (UK). SYBR green was purchased from Invitrogen (UK). All media preparations for the propagation and involvement of insect cell work were purchased from GIBCO of the Invitrogen Incorporation. Antibiotics were purchased from Sigma Alderich (UK) and X-gal from Nbl enzymes Limited. IPTG was purchased from Invitrogen. The chemicals required for primer extension work were purchased from National Diagnostics.

2.1.2 Radioactive isotopes

The [γ- ^{32}P] ATP isotope was purchased from Perkin Elmer Incorporation.

2.1.3 Enzymes

All restriction enzymes were purchased from New England Biolabs except for *Srf* I which was purchased from Stratagene. *Taq* DNA polymerase was purchased from Bioline and RNase A from Sigma (UK). DNase A was purchased from Promega. T4 DNA ligase was supplied as part of a kit for the pGem®T- Vector System I, purchased from Promega. T4 polynucleotide kinase (PNK) was purchased from New England Biolabs.

2.1.4 Nucleic Acids

The following nucleic acids were purchased from the corresponding sources;

2.1.5 Baculovirus DNA used in this study:

Autographa californica Multinucleopolyhedrovirus C6 Strain (AcMNPV)	R.D. Possee, R. I. Graham and J. Burden
Mamestra brassicae Nucleopolyhedrovirus (MbNPV)	J. Burden and C. Pritchard
Spodoptera exigua Nucleopolyhedrovirus (SeNPV)	A. Chambers

Plutella xylostella Granulovirus (PxGV)	R.D. Possee
Choristoneura fumfierana Multiple Nucleopolyhedrovirus (CfMNPV)	R.D. Possee

2.1.6 Plasmids and Vectors used in this study:

PGem®T- Vector System I	Promega

2.1.7 *Escherichia coli* strains used in this study

Library Efficiency® DH5α Chemically Competent Cells	Invitrogen
DH10B Electrocompetent Cells	Invitrogen

2.1.8 Viruses used in this study:

Autographa californica Multinucleopolyhedrovirus C6 strain	R.D.Possee.
Very Late Deficient Phenotype (VLD1)	C. Merrington.
AcORF6^{3620}-1	C. Merrington.
Ac*Δlef*-2^{100}.neo	R.D. Possee
Ac*Δlef*-2.neo	R.D Possee and A.Chambers
Temperature-sensitive 8b (Ts8b)	E.B Carstens

2.1.9 Insect cells used in this study:

Spodoptera frugiperda (*Sf*-21) cells	R. D. Possee.
Trichnoplusia ni (*Tn*368Ad) cells	R.D. Possee

2.2 Methods

2.2.1 Virus and Cell Work:

2.2.1.1 Cell lines and viruses.

The host cell lines of *Spodoptera frugiperda* (*Sf*-21) and *Trichoplusia ni* (*Tn*368Ad) were propagated at 28°C in TC100 medium supplemented with 10% foetal calf serum (FCS). The AcMNPV C6 isolate strain was propagated and titred according to standard procedures (King and Possee, 1992). VLD1 (Merrington *et al.*, 1996) possessed two mapped point mutations within in ORF2 and *Lef*-2 of the AcMNPV genome, at positions 1689 and 3620 respectively. AcORF6^{3620} -1 (Merrington *et al.*, 1996) possessed an induced point mutation at position 3620 within the AcMNPV genome. The virus stocks were maintained and titred according to standard procedures (King and Possee, 1992). A concentration of 10% FCS in TC100 medium was used for all cell-based procedures and maintenance.

2.2.1.2 Amplification of virus stocks.

Intermediate stock of virus:

This methods assumed that the virus starting material was from a seed stock or had been sent as a gift. A 75cm^2 T-flask was seeded at 5 x 10^5 *Sf*-21 cells and left at 28°C for 1-2 hours. The TC100/10% FCS medium was removed and the cells infected at <1PFU per cell. The virus inoculum was removed after adsorption for 1 hour and 10ml TC100/10% FCS was added. Incubated at 28°C for 4-6 days or until the cells became well infected. The medium was harvested and stored at 4°C.

***High titre stock of virus*:**

A cell culture flask was seeded at 1 x 10^5 *Sf*-21 cells/ml and left at 28°C for 2-3 days, stirring at >150rpm. The cells were infected at a multiplicity of infection (MOI) of 0.1-0.2PFU per cell when the culture had reached 5 x 10^5 *Sf*-21 cells/ml. The cell culture was then left at 28°C for 4-6 days. The medium was harvested and stored at 4°C.

2.2.1.3 Virus infection of cells.

Cell Monolayer:

Sf-21 sub-confluent monolayer seeded at 1 x 10^6 cells per 35mm dishes were left overnight at 28°C (or seeded at 1.5 x 10^6 *Sf*-21 cells per 35mm dishes and left at 28°C for 1-2 hours) and infected at 10 PFU per cell. The virus inoculum was removed after adsorption for 1 hour at room temperature and replaced with fresh medium. Zero hours post infection was defined as the time when the virus inoculum was added to the dishes.

Suspension Cultures:

Cell culture flasks were initially seeded at 1 x 10^5 *Sf*-21 cells/ml and left at 28°C for 2-3 days, stirring at >150rpm. After the *Sf*-21 cells had reached their exponential phase (~5 x 10^5 cells/ml), each flask was infected with virus at 0.1 or 0.2 PFU/cell and left to stir at 28°C for the specific time.

2.2.1.4 Titration of viruses by plaque assay.

Dishes of 35mm diameter were seeded at 1.5 x 10^6 (or 1.0 x 10^6 *Sf*-21 cells/ dish left overnight at 28°C) *Sf*-21 cells in 1.5ml of TC100 + 10% FCS. The dishes were incubated at 28°C for 1-2 hours. Serial log dilutions (1:10 dilutions) of the virus were prepared using TC100+ 10% FCS as a diluent. Medium was removed and the cells overlaid with 100µl of virus inoculum in a drop-wise manner into the centre of each dish. The dishes were left at room temperature for 1 hour to allow virus adsorption. Afterwards, virus inoculum was removed from the dishes and the cells overlaid with 2ml of agarose overlay (1ml 3% low melting temperature agarose and 1ml TC100+ 10% FCS pre-treated with 1.0% Streptomycin and Penicillin). After solidification of the agarose, the dishes were overlaid with 1ml TC100 +10% FCS and incubated at 28°C for 3-4 days. The plaques were visualised by staining the cells with 1ml liquid overlay of a 1:20 dilution of 0.5% w/v neutral red dye using PBS as a diluent. The dishes were incubated for 2-4hours at 28°C. The liquid overlay was discarded and the dishes inverted and stored in aluminium foil wrapped container for 2- 24 hours at room temperature to allow clearing of plaques.

2.2.1.5 Plaque Picking and Plaque-Purification of AcΔ*lef*-2^{100}.neo based rescued viruses.

After identifying well isolated plaques containing rescued viruses, they were picked using a sterile Pasteur pipette and washed into 0.5ml TC100/10% FCS. The agarose plug was then vortexed briefly to release the virus particles and stored at 4°C until further use. To ensure that a false-negative had not been picked it was essential to re-plaque the virus sample suspension using 10^{-1} to 10^{-3} dilutions (using TC100/10%FCS as a diluent) to infect duplicate 35mm dishes of *Sf*-21 cells. The purification of plaques was repeated at least twice to obtain pure stocks of rescued virus.

2.2.1.6 Co-transfection of PCR generated *lef*-2 mutant fragments with either AcΔ*lef*-2^{100}.neo or AcΔ*lef*-2.neo viral DNA:

Duplicate 35mm dishes were seeded at 3 x 10^5 *Sf*-21 cells and left overnight at 28°C. In a disposable bijou, 8.50µg of AcΔ*lef*-2^{100}.neo or AcΔ*lef*-2.neo viral DNA was mixed together with 500ng of the PCR generated *Lef*-2 mutant fragment. Afterwards, TC100 without FCS was added to the bijou to bring the total volume to 500µl. To the bijou, 500µl of TC100 plus 5µl of Lipofectin (Invitrogen) was added and pipetted thoroughly. The diluted lipid-reagent with the DNA solution was left at room temperature for 15 minutes. Meanwhile, the TC100/10%FCS medium was removed from each 35mm dish of *Sf*-21 cells and the cell monolayer washed twice with 1ml of TC100 without FCS. Afterwards, the 1ml of TC100 was removed and the DNA-lipid mixture was added to the dish. The dishes were incubated at 28°C for 5 hours (or overnight). At 5 hours (or overnight), an extra 1ml of TC100/10%FCS was added to each dish and the incubation at 28°C was continued until a total of 5 days post infection (dpi).

2.2.1.7 First Step Virus Growth Curves.

Cell culture flasks were seeded at 1 x 10^5 *Sf*-21 cells/ml and incubated at 28°C for 2-3 days, stirring at >150rpm. After 2-3 days when they had reached 5 x 10^5 *Sf*-21 cells/ml, each flask was infected at 0.1PFU per cell with either AcMNPV, VLD1, AcORF6^{3260}(1) or TC100/10% FCS. The flasks were left at 28°C, and three 0.5ml samples were collected at

24, 48, 72, 96, 120hpi. All samples were stored at 4°C. To determine each budded virus growth curves standard plaque assays were used.

2.3 Cloning Work:

2.3.1 Ligation of PCR generated fragments into pGem-T cloning vector.

To ligate the *Spodoptera frugiperda* actin gene into the pGem-T cloning vector (Promega), the following series of reactions were produced using the Promega System 1 cloning kit:

Table 2.1 **– Reaction components for the ligation of PCR fragments into pGem-T cloning vector.**

Reaction	Negative Control 1	Negative Control 2	Sample 1A (1:3 Volume Ratio)	Sample 1B (3:1 Volume Ratio)	Positive Control
2x Rapid ligation buffer	5.0µl	5.0µl	5.0µl	5.0µl	5.0µl
pGem-T Vector (50ng/µl)	0.5µl	0.5µl	0.5µl	1.5µl	0.5µl
PCR generated fragment insert	-	-	1.5µl	0.5µl	-
Positive DNA control insert (4ng/µl)	-	-	-	-	1.5µl
T_4 DNA ligase (3Units/µl)	-	1.0µl	1.0µl	1.0µl	1.0µl
Nuclease-free Water	4.5µl	3.5µl	2.0µl	2.0µl	2.0µl
Total Volume	10.0µl	10.0µl	10.0µl	10.0µl	10.0µl

With each sample to be ligated into the cloning vector, two reactions were set up. These two reactions represented either 1:3 or 3:1 vector to PCR insert volume ratios. Afterwards, all reactions were left at room temperature for 4 hours before being chilled prior to transformation.

2.3.2 Transformation into DH5α *Escherichia coli* chemically competent cells.

The appropriate volume of library efficient DH5α *Escherichia coli* chemically competent cells (Invitrogen) were thawed on ice for 40 minutes and mixed thoroughly by gently pipetting the mixture. To each of the 10µl ligation reactions, 25-100µl of DH5α *E.coli* competent cells was added. The samples were chilled on ice for 10 minutes and left at 42°C for exactly two minutes before placing immediately back on to ice. One ml of *Luria broth* medium (Lb) was added to each sample and left at 37°C for 1 hour, shaking at 150rpm. Afterwards, 100µl of the sample was spread out onto Lb agar plates containing IPTG (20µg/µl), X-gal (20µg/µl) and ampicillin (100µg/µl). The Lb agar plates were then inverted and left overnight at 37°C.

2.3.3 Propagation of DH5α *Escherichia coli* competent cells to amplify plasmid DNA stocks.

A single white colony was picked from Lb agar plates and placed into 2ml of Lb medium containing ampicillin (100µg/µl). The cultures were left overnight at 37°C, shaking at 150rpm. To amplify up a larger plasmid DNA stock, 0.5mls of the grown Lb culture was added to 100-200mls of Lb medium plus ampicillin (100µg/µl). The culture was left overnight at 37°C, shaking at 150rpm.

2.3.4 Qiagen Midi prep purification of plasmid DNA.

To purify plasmid DNA from a large grown culture of library efficient DH5α *E.coli* cells, a Qiagen midi prep kit using Qiagen-tip 100 was employed. The bacterial cells were harvested by centrifugation at 6000 x *g* for 15 minutes at 4°C. The pellet was resuspended in 4ml of Buffer P1 (50mM Tris-Cl pH 8.0, 10mM EDTA and 100µg/µl RNase A). Four ml of Buffer P2 (200mM NaOH and 1% SDS (w/v)) was added and the sample mixed thoroughly by inverting the tube 4-6 times. To each sample, 4ml of Buffer P3 (3.0mM

potassium acetate pH 5.0) was added and mixed immediately by inverting 4- 6 times. Each of the samples was chilled on ice for 15 minutes. Afterwards, the samples were centrifuged at ≥ 20, 000 x *g* for 30 minutes at 4°C and the supernatant containing the plasmid DNA was kept. A Qiagen-tip 100 for each sample was equilibrated by applying 4ml of Buffer QBT (750mM NaCl, 50mM MOPS pH 7.0, 15% isopropanol (v/v) and 0.15% Triton® X-100 (v/v)) to the column and allowing it to empty by gravity flow. The supernatant containing the plasmid DNA was applied to the column and allowed to empty by gravity flow. The column was washed twice with 10ml of Buffer QC (1.0mM NaCl, 50mM MOPS pH 7.0 and 15% isopropanol (v/v)). The plasmid DNA was eluted from the column by applying 5ml of Buffer QF (1.25M NaCl, 50mM Tris-Cl pH 8.5, and 15% isopropanol (v/v)). To the eluted plasmid DNA, 3.5ml (0.7 volumes) of room-temperature isopropanol was added and centrifuged at ≥15, 000 x *g* for 30 minutes at 4°C. The pellet was washed with 2ml of 70% ethanol and centrifuged at ≥15, 000 x *g* for 10 minutes. The pellet was allowed to air-dry before finally being redissolved in 50µl of 1 x TE. To determine the yield, the DNA concentration was analysed both by spectrophotometer readings at 260nm and agarose gel electrophoresis.

2.3.5 Restriction endonuclease digests to determine size of plasmid DNA and successful insertion of PCR product.

The following restriction endonuclease reaction was set up for every individual plasmid DNA sample purified from a Qiagen midi column:

Table 2.2 **– Reaction components for the restriction digestion of purified DNA.**

Reaction	Volume (µl)
10x NEB Buffer 2	2.0
RNase A (10mg/ml)	0.2
*Sac*I/ II (20Units)	1.0
Purified Plasmid DNA	2.0
Nuclease-free Water	14.8
Total Volume	20.0

Incubate for 2-3 hours (or overnight) at 37°C. Restriction digests of plasmids were examined on a 1.0% agarose gel.

2.4 DNA based Work:

2.4.1 Total DNA extraction from infected-insect cells.

Total DNA was purified from infected *Sf*-21 cells as described by King and Possee (1992). Infected *Sf*-21 cells were harvested from the surface of the 35mm diameter dishes with TC100+ 10%FCS. Cell pellets were formed by centrifugation at 7,000rpm for five minutes before being resuspended twice in 1ml Phosphate Buffered Saline (PBS); to remove any residual proteins or medium. The cell pellets were then stored at -80°C until ready to use. The cell pellets were resuspended in 250µl of 1x TBE and 250µl of Cell lysis buffer (10mM EDTA, 5% 2-Mercaptoethanol, 50mM Tris-HCl, pH8.0, 0.4% w/v SDS). The contents of the eppendorf were mixed gently and the cell lysate became clear and viscous as the *Sf*-21 cells released their DNA. Afterwards, 12.5µl proteinase K (10mg/ml in TE) and 2.5µl ribonuclease A (10mg/ml) were added and incubated at 37°C for 30 minutes. The lysate was then extracted with 515µl of 50% phenol: chloroform, mixed thoroughly and centrifuged at 13,000rpm for 2 minutes to separate the phases. The aqueous phase was removed and placed into a clean eppendorf. This process was repeated. Fifty µl of 3M sodium acetate and two volumes of 100% ethanol were added to the extracted aqueous layer to precipitate the DNA. The DNA was pelleted by centrifuging at 13,000rpm for 5 minutes and wash twice with 100µl of 75% ethanol. The last traces of ethanol were removed with a drawn-out Pasteur pipette and the DNA pellet was allowed to air dry. Afterwards, the cell pellet was soaked overnight at 4°C in 100µl 1x TE. The DNA was left at 37°C for 10 minutes before resuspending with a pipette. The total DNA was stored at 4°C until further use.

2.4.2 Purification of PxGV or CfMNPV occlusion bodies.

PxGV larvae were macerated in an equivalent volume of SDS using a Stomacher. To remove larger contaminants, the TE/ homogenised PxGV larvae mixture was filtered through a muslin filter and further centrifuged at 400 x g for 5 minutes. The pellet was resuspended in SDS and the process repeated, keeping both sets of supernatant fluids.

Afterwards, the supernatant fluids were combined and centrifuged at 10,000 x g for 30 minutes to remove lipid, soluble material and smaller contaminants. The pellet was resuspended in a small volume of SDS and further centrifuged on a rate zonal 30- 80% glycerol (in SDS) gradient at 12,000 x g for 40 minutes. The band containing the virus was harvested and placed into an eppendorf. The occlusion bodies were centrifuged at 7,000rpm for 3 minutes, and resuspend in 1ml 1 x TE. This step was repeated a further two times. Finally, the pellet was resuspended in 1ml 1 x TE, and stored at 4°C until needed.

2.4.3 DNA purification from PxGV or CfMNPV occlusion bodies.

Five hundred µl of PxGV occlusion body suspensions was added to 100µl of 0.5M EDTA and 15µl of proteinase K (20mg/ml). The mixture was incubated at 37°C for 90 minutes. Afterwards, 50µl of 1M Na_2CO_3 was added to the suspension and left at 37°C for 40 minutes. At this stage, the sample was not colourless, and an additional volume of 50µl of 1M Na_2CO_3 was added. The sample was left at 37°C for a further 40 minutes. Then 50µl of 10% SDS was added to the sample and further incubated at 37°C for 15 minutes to disrupt the virus particles and release the DNA. During this last incubation period, 25mm lengths of dialysis tubing were cut and moistened in 1 x TE buffer. Sides of the moistened dialysis tubing were slit using a sterile scalpel to produce two membranes of equal size (one per sample of DNA) that were boiled in TE buffer for 10-15 minutes. The virus/SDS mixture was centrifuged at 13,000 x g for 30 seconds. The supernatant was transferred to a clean eppendorf and an equal volume of 50% phenol: chloroform was added. The sample was mixed thoroughly by vigorous shaking and centrifuged at 13,000rpm for 3 minutes. The aqueous layer was extracted and placed into a clean eppendorf. The plasmid DNA was extracted again using 50% phenol: chloroform and the removed aqueous layer was placed into a 1.5ml eppendorf lid that formed part of the dialysis chamber. The dialysis chamber was constructed as illustrated by Hunter-Fujita *et al.* (1998). The sample was left in sterile 1x TE buffer, stirring for 48 hours at 4°C. During this time, the 1 x TE buffer was changed at least three times. The sample was then removed from the buffer and the purified PxGV DNA was transferred to a sterile eppendorf to be stored at 4°C.

2.4.4 Qiagen QIAquick® Purification of PCR Products.

A Qiagen QIAquick® purification kit was used to remove any excess primers, nucleotides, polymerases and salts from fragments generated by PCR that ranged in size from 0.1-1Kbp.

2.4.5 Qiagen QIAquick® Gel Extraction and Purification of DNA.

Qiagen QIAquick® Gel Extraction Kit was used to extract and purify DNA (ranging in size from 70bp-10Kbp) from low melting temperature agarose in 1 x TBE.

2.4.6 Amplification of AcΔ*lef*-2^{100}.neo or AcΔ*lef*-2.neo Bacmid DNA in DH10B *E.coli* Electrocompetent cells.

The appropriate volume of DH10B electrocompetent *E.coli* cells were thawed on ice for 40 minutes. One µg of AcΔ*lef*-2^{100}.neo Bac DNA was used to prepare 1:5 and 1:10 dilutions in a total volume of 10µl using water. To every sample of 40µl electrocompetent cells, 1µl of diluted DNA or 1µl of neat DNA was added and mixed gently by pipetting. The cuvette chambers and reactions were chilled on ice. One ml of SOC medium was placed into a tube per reaction. The transformation reaction was added to each cuvette chamber and electroporated using the following program:

Electroporation Program;

Voltage	2500V
Capacitance	25µF
Resistance	100Ω
Cuvette	1mm

Afterwards, the transformation reaction was added to the 1ml of SOC medium and incubated at 37°C, shaking at 150rpm for 70 minutes. One hundred µl of the transformation reaction was spread onto the Lb agar and Chloroamphenicol (15µg/µl) plates. The plates were inverted and left overnight at 37°C.

2.4.7 Purification of transformed of AcΔ*lef*-2^{100}.neo or AcΔ*lef*-2.neo Bacmid DNA in DH10B *E.coli* Electrocompetent cells

2.4.7.1 Small scale purification (< 5mls)

This method was designed and used to quickly examine colonies for potential sources of transformed DNA. A suitable colony was picked and used to inoculate 4mls of Lb medium with chloroamphenicol (15µg/µl). The culture was left overnight at 37°C, shaking at 150rpm. Two mls of DH10B electrocompetent *E.coli* cell culture was pelleted at 7,000rpm for 5 minutes. The supernatant was discarded and the pellet resuspended in 300µl of P1 buffer (without RNase A). Three hundred µl of buffer P2 was added to the sample and incubated at room temperature for 5 minutes. Afterwards, 300µl of P3 buffer was added and the sample chilled on ice for 10 minutes. The sample was centrifuged at 13,000rpm for 10 minutes, and the supernatant fraction was transferred to a clean eppendorf. 0.7 volumes of propanol was added to the supernatant fraction and mixed thoroughly before centrifuging at 13,000rpm for 10 minutes. The pellet was washed twice with 70% ethanol and allowed to air dry briefly to remove any last traces of ethanol. The pellet was soaked overnight in 30µl of 1x TE at 4°C. Then the pellet was gently resuspended. To confirm the presence of the bacmid DNA, restriction digests were performed and RNase A was added to each reaction.

2.4.7.2 Large scale purification (~400mls)

Once the small scale purification had established which cultures had successfully transformed the AcΔ*Lef*-2^{100}.neo or AcΔ*Lef*-2.neo Bac DNA, larger cultures were produced to further amplify DNA stocks. One ml of culture from 2.4.7.1 was used to inoculate 400mls of Lb medium plus chloroamphenicol (15µg/µl). The culture was left overnight at 37°C, shaking at 150rpm. Afterwards, the culture was centrifuged at 4,000rpm for 20 minutes at 4°C and the pellet resuspended in 30mls of P1 buffer with RNase A (100µg/ml). Thirty mls of P2 buffer was added and the sample incubated at room temperature for 5 minutes before adding 30mls of P3 buffer and mixing thoroughly. The sample was chilled on ice for 10 minutes and the precipitated material pelleted at 19,500rpm for 30 minutes at 4°C. The supernatant fraction was filtered through Whatman paper to remove any remaining large debris. The DNA was mixed The DNA pellet was resuspended in 1ml of

Ix TE. DNA was purified by applying it to a 5mls 50% w/w Caesium chloride gradient with 25µl of 10mg/ml Ethidium Bromide. The rest of the gradient was filled with paraffin oil to within 1cm of the top to prevent the centrifugation tube from collapsing. A swinging bucket rotor (SW41) was used to centrifuge for 18 hours at 35,000rpm. The two DNA bands were harvested and pooled together. For a cleaner DNA preparation, the 50% w/w Caesium Chloride gradient was repeated at 35,000rpm for 21 hours. The DNA was harvested and extracted against one volume of butanol. The sample was shaken and briefly centrifuged at 13,000rpm for 1-2 minutes. The aqueous layer was removed and extracted against one volume of butanol. The sample was subsequently shaken and centrifuged at 13,000rpm for 1-2 minutes. This step was repeated until both layers were the same colour. Then the butanol extraction was repeated a further two times. Suitable lengths of dialysis tubing were cut and boiled for 10-15 minutes in distilled water. Afterwards, the dialysis tubing was moistened by flooding them with 1 x TE. One end of the dialysis tubing was closed with a clip and the purified DNA pipetted into the chamber, finally sealing it with another clip. The dialysis tubing was placed in 1x TE stirring gently at 4°C for 48 hours, changing the TE buffer at least twice.

2.5. Sequencing Work:

2.5.1 Sequencing

To confirm or map any mutations within any of the NPVs or GVs *lef*-2 genes or for any other sequencing requirements, the following reaction components and volumes were set up;

Table 2.3 **– Reaction components for sequencing of purified DNA samples.**

Reaction	Sample 1A (Forward Primer)	Sample 1B (Reverse Primer)
Dye Terminator Mix	1.0µl	1.0µl
Primer (0.8pmol/µl)	1.0µl	1.0µl
DNA	1.0µl	1.0µl
Buffer	1.5µl	1.5µl
dH_20	4.5µl	4.5µl
Total Volume	10.0µl	10.0µl

The DNA was sequenced at least in quadruplicate reactions and with differentiating primers to ensure that the region of interest was determined on either strand and in both directions.

2.5.2 Purification of Extension Products from sequencing reactions.

A fresh spin column was prepared using washed Sephadex G-50 beads. The sephadex column was centrifuged at 3,000rpm for 2 minutes and any liquid waste discarded. The spin column was removed and placed into a labelled eppendorf. The sequencing reaction mix was carefully added to the top of the Sephadex column. The column was centrifuged at 3,000rpm for 2 minutes. Afterwards, the eppendorfs were placed into a speed vac concentrator until the samples had dried down and were stored at 4°C.

2.5.3 Analysis of sequenced data.

Sequenced data was assembled using Pregap (Bonfield., *et al*, 1996) and Gap4 (Bonfield., *et al*, 1995) in the Staden system. Raw ABI files were imported from a central filing system and the files assembled in pregap4 to form one file in gap4. A consensus sequence was

produced in gap4 and the fasta file saved. The sequence was then compared against known sequences using NCBI blast (Tatusova., *et al.*, 1999). Nucleotide sequences were translated using pDraw32 software (Anon, pDraw32, no date).

2.6 RNA based Work:

2.6.1 Qiagen RNeasy® Mini RNA extraction of virus-infected cells.

Viral RNA was prepared by infecting subconfluent monolayers of *Sf*-21 cells (1.0 x 10^6 cells per 35mm plate) at a multiplicity of 10 PFU per cell. The virus inoculum was removed after adsorption for 1 hour at room temperature and replaced with fresh medium. At a given time point, the cell monolayer was washed gently with TC100 + 10% FCS to detach cells from the surface. The cells were collected as a pellet by centrifugation at 7,000rpm for five minutes. Afterwards, the supernatant was discarded and the pellet resuspended in 1ml PBS, before being centrifuged at 7,000rpm for 5 minutes. This process was repeated twice to remove any excess protein or contamination. The cell pellet was stored at -80°C until required. Total RNA was extracted and purified using Qiagen RNeasy® Midi Kit, version 3.0.

2.6.2 Guanidinium/ Hot phenol method for total RNA extraction.

The infected cells were harvested and centrifuged at 300x *g* for 5 minutes so that a pellet formed. Any supernatant was discarded and 3mls of 4M guanidinum isothiocyanate (1ml of 4M guanidinum isothiocyanate for 10^7 *Sf*-21 cells or 5mls for every gram of tissue) was added to the pellet. The mixture was heated to 60°C and vortex thoroughly. An equal volume of phenol/water preheated to 60°C was added and the sample was continually vortexed. 0.5 volumes (1.5mls) of 0.1M Sodium acetate pH 5.2, 10mM Tris-HCl pH7.4 and 1mM EDTA was added and the sample was heated to 60°C in a water bath and left for 10 minutes. At regular intervals throughout the incubation period, the samples were vortexed thoroughly. Finally, 1 volume (3mls) of chloroform was added at the end. The samples were chilled immediately on ice and centrifuged at 2000x *g* for 10 minutes at 4°C. The aqueous phase was recovered and re-extracted with an equal volume of phenol/chloroform. Afterwards, the sample was centrifuged at 2000x *g* for 10 minutes and the aqueous phase was transferred to a fresh eppendorf. To each sample, $^1/_{20}$ volume of 3M sodium acetate pH

5.2 and then 2 volumes of 100% ethanol was added before mixing well. All samples were stored overnight at -20°C. Total RNA was recovered by centrifuging at 12,000x *g* for 20 minutes at 4°C. The total RNA pellet was washed twice with 1ml 75% ethanol, and during the second wash the sample was transferred to a fresh eppendorf. The sample was centrifuged at 13,000rpm for 5 minutes and any supernatant was discarded. The pellet was allowed to air dry. Afterwards, the pellet was allowed to soak in 100µl RNase-free water before storing at -70°C.

2.6.3 Formaldehyde agarose gel electrophoresis for RNA analysis.

All equipment was pre-washed with 20% SDS, rinsed with DEPC-treated distilled water and treated with 100% ethanol before use to minimise any RNase contamination. To prepare a formaldehyde agarose gel; 1.5gms of molecular grade agarose, 15mls 10x FA gel buffer (41.9gms MOPS, free acid, 6.8gms sodium acetate, 20mls 0.5M EDTA pH 8.0) and 135ml DEPC-treated distilled water were mixed and heated until molten. Cool the agarose to 65-70°C in a water bath and swirl occasionally. After cooling, 2.7mls of formaldehyde and 1.5µl ethidium bromide (10mg/ml) were added to the agarose before casting the gel. The agarose gel tank was filled with 1x FA gel running buffer (100mls 10x FA gel buffer, 20mls 37% (12.3M) formaldehyde and 880ml DEPC-treated distilled water). Two µl of 5x RNA loading buffer (2.5mgs bromophenol blue, 80µl 0.5M EDTA pH8.0, 750µl 37% (12.3M) formaldehyde, 2ml glycerol, 3.084ml formamide and 4ml 10x FA gel buffer) was added to 10µl of RNA sample and mixed thoroughly. The RNA was denatured by incubating the samples for 3-5 minutes at 65°C and then immediately placing on ice. The denatured samples were loaded onto the agarose gel and run at 50V for 2-3 hours or until the bromophenol blue dye had migrated approximately $^2/_3$ of the way down the gel. Afterwards the RNA samples on the agarose gel were visualised using a UV transluminator.

2.6.4 Primer Extension Work:

2.6.4.1 Preparation of 6% polyacrylamide gel:

To set up a 6% polyacrylamide gel to analyse the transcriptional site of the 5' end of the RNA transcripts the glass plates were washed in 2% liquid Nox (Sigma-Aldrich) solution and rinsed well. Afterwards the glass plates were sprayed with 70% ethanol and dimethychlorosiliane (BDH) applied before they were placed together. A 6% polyacrylamide gel required 80mls of Sequa Gel solution; 16mls of Sequa Gel complete buffer (National Diagnostics) and 64mls Sequa Gel Monomer solution (National Diagnostics) mixed together and degassed using a vacuum for 2 minutes. Six hundred and forty µl of freshly prepared 10% Ammonium persulphate was added to the degassed mixture and mixed immediately. Using a clean 50ml syringe, the prepared Sequa gel solution was administered between the glass plates to form a uniform layer. The shark comb was inserted into the gel with the teeth facing away. The gel was allowed to set for 1-2 hours at room temperature. The glass plates and polyacrylamide gel were placed into a vertical gel electrophoresis tank. The shark comb was removed and placed so that the teeth pierced the gel slightly. The wells were washed out with 1 x TBE to remove any air bubbles. The gel was pre-run for 15-20 minutes at 40 watts before loading the samples. Specific gene sequencing ladders (2µl) and primer extension products (2µl) were loaded and the gel was run at 40 watts until the front of the dye had migrated $^{2}/_{3}$ of the way down the glass plates. After the gel had been run, both glass plates were removed and the polyacrylamide gel was placed onto plastic film, backed with benchkote before being dried down by a vacuum. The gel was then exposed to a plastic screen and placed into a protective cassette and stored at -70°C. Moreover, the plastic screen was removed and the image of the gel on the plastic screen was exposed by using a phosphoimagine scanner (Biorad, Molecular imaginer FX).

2.6.4.2 Production of sequencing ladder with ^{32}P to size reaction products.

To radiolabel the respective primer, 100ng of oligonucleotide was mixed with 4µl [γ-^{32}P] ATP (2.5pmol ^{23}P), 2µl PNK buffer (50mM Tris pH 7.4, 10mM $MgCl_2$, and 5mM DTT), 1µl T_4 PNK plus water to make the reaction volume to 10µl. Afterwards, the reactions were incubated at 37°C for 30 minutes. The reaction was stopped by heating at 90°C for

3minutes. In one eppendorf, 1µg of plasmid or PCR DNA containing the specific gene sequence was mixed with 2µl of reaction buffer, 2µl of specific radiolabelled primer (0.5pmol ^{32}P), 2µl of Thermo Sequenase DNA polymerase and water to make up to the reaction volume of 17.5µl. For each gene sequencing ladder, four eppendorfs were needed and labelled T, C, A and G. Four µl of ddGTP termination mix was placed into the eppendorf labelled G. Similarly the A, T, and C eppendorfs were filled with 4µl of ddATP, ddTTP, ddCTP termination mix respectively and capped to prevent any evaporation. Four µl of the radiolabelled primer reaction was removed and transferred to an eppendorf labelled "G", before mixing gently. The same process was repeated for the "A, T, and C" eppendorfs, and 10µl of paraffin oil was added to each reaction. Afterwards, each reaction was placed into a robocycler (Stratagene, Robocycler Gradient 40) under the following cycling conditions;

Window 1:	95°C for 5 minutes
	55°C for 30 seconds
	72°C for 1 minute
Window 2 (34 cycles):	95°C for 30 seconds
	55°C for 30 seconds
	72°C for 1 minute
Window 3:	95°C for 30 seconds
	55°C for 30 seconds
	72°C for 5 minutes
	Store at 6°C.

Four µl of the stop solution was added to each of the termination reactions; mixed thoroughly and centrifuged briefly to separate the paraffin oil layer from the aqueous phase. Samples were stored frozen at -20°C in the correct protective housing and thawed out using the following PCR program in the robocycler (Stratagene, Robocycler Gradient 40) before being loaded on to the polyacrylamide gel:

Window 1 (1 cycle):	95°C for 3 minutes

2.6.4.3 Generation of primer extension products.

An appropriate primer sequence was designed that was anti-sense to the specific gene mRNA at the 5' end. The primer was located between 100-150 nucleotides from the predicted translation initiation codon and 18-25bp in length. To radiolabel the respective primer (100ng) 4µl of [γ-^{32}P] ATP (2.5pmol ^{23}P) was incubated at 37°C for 10 minutes with 2µl of 5x PNK labelling buffer (250mM Tris-HCl ph7.4, 50mM $MgCl_2$ and 25mM DTT), 1µl of T_4 PNK and water to bring the total reaction volume to 20µl. Afterwards the reaction was stopped by heating at 90°C for 5minutes. Five µg of extracted total RNA was mixed with 5ng of radiolabelled oligonucleotide in a 10µl annealing reaction (in water). The reaction was incubated at 80°C for 3 minutes and allowed to re-anneal for 45 minutes at room temperature. Ten µl of the annealing reaction was taken and placed and in one tube with the following; 4µl of 10 x primer extension buffer (120mM Tris-HCl, pH8.3, 80mM $MgCl_2$, and 40mM DTT), 0.1mM DTT, 10mM dNTPS, 0.5µl (5 units) Superscript Reverse Transcriptase and water to make the total reaction volume to 20µl. The reactions were incubated at 50°C for 45 minutes and terminated by adding 1µl of formamide to each tube. Before the primer extension products were loaded onto the polyacrylamide gel, 2µl formamide dye was added to each tube.

2.6.5 DNase A treatment of extracted RNA samples prior to RT-PCR.

To eliminate any carry over of contaminating DNA from the extracted RNA, each sample was treated with DNase A (Promega RQ1 RNase-free DNase). The following components for each sample were set up:

Table 2.4 – **Reaction components to DNase-treat purified RNA samples.**

Reaction Components	Volume (µl)
Extracted RNA (2µg)	X
RQ1 RNase-free DNase 10x Reaction Buffer	1.0
RQ1 RNase-free DNase A (1Unit/1µg RNA)	2.0
Nuclease-free Water	Y
Total Volume	10.0

Where X is the amount required for 2µg of extracted RNA based on calculated concentration readings from a spectrophotometer at 260nm. The Y value is the amount of nuclease-free water required to bring the total volume of the reaction to 10µl. Afterwards, each sample was incubated at 37°C for 30 minutes before adding 1µl of RQ1 DNase Stop solution to terminate the reaction. Incubate at 65°C for 10 minutes to inactivate the DNase. Store samples at -80°C until required.

2.6.6 RT-PCR of DNase –treated (2.6.5) RNA samples to produce cDNA.

To produce cDNA from DNase-treated RNA samples for the use in q-PCR, the Qiagen Omniscript® Reverse transcription kit was employed. DNase-treated RNA templates were thawed on ice. The OligodT $_{12\text{-}18}$ primer (Invitrogen), 10x buffer RT, and dNTP mix were further thawed on ice. All solutions were stored on ice immediately after thawing. Each solution was briefly vortexed and centrifuged to collect residual liquid. A fresh master mix was set up according to the following (per individual reaction):

Table 2.5 – **Reaction components for the RT-PCR of DNase-treated RNA samples.**

Reaction Components.	Volume (µl)
10x Buffer RT	2.0
dNTP Mix (5mM dNTP each)	2.0
OligodT $_{12\text{-}18}$ primer (0.5µg/µl)	1.0
Omniscript RT	1.0
RNase-free Water	4.0
DNase-treated RNA template (2µg)	10.0
Total Volume	20.0

The master mix was briefly vortexed for <5 seconds and centrifuged before storing on ice. To each individual eppendorf, 10µl of master mix was distributed. All eppendorfs were kept and left on ice for a period prior to addition of any solutions to keep them chilled. Afterwards, 10µl (2µg) of DNase-treated RNA template was added to each eppendorf, and mixed thoroughly by vortexing. The eppendorfs were centrifuged briefly to collect any residual liquid. The samples were incubated for 60 minutes at 37°C. Samples were stored at -20°C until required.

2.7 Real time-PCR (Q-PCR) Work:

2.7.1 DNA replication study:

2.7.1.1 Creating a *Spodoptera frugiperda* Actin construct or pSfActin standard curve:

To determine the number of pSfActin copies per microlitre (µl), the following calculations were made:

1) To calculate the molecular weight (M_w) of the pSfActin, the molecular weight calculator (Simakov, no date) was used. This program was used by inputting the nucleotide sequence for either the pGem-T vector or *Sf*-21 *Actin* fragment individually and the calculator determining the molecular weight in units of g/molecule respectively.

M_w of vector = M_w of pGem-T vector + M_w of *Sf*-21 *Actin* fragment

= 1820539g/molecule + 233662g/molecule

= 2054201 g/molecule,

2) Afterwards, the number of pSfActin copies per µl was determined:

M_w of pSfActin = 2054201 g/molecule

Avogadro's Constant = 6.023×10^{23} molecules/mol

Weight of pSfActin per molecule = M_w of pSfActin / Avogadro's Constant

= 2054201 [g/molecule]/ 6.023×10^{23} [molecules/mol]

= $3.4105943 \times 10^{-18}$g/molecule

If a stock of pSfActin DNA at concentration of 2.63µg/µl is used, this can be converted to the equivalent numeric value in g/ml to give 2.63×10^{-3}g/ml respectively.

Therefore, to calculate the number of DNA copies per µl, the following equation was used:

Number of DNA copies/µl = Conc. of DNA [g/ml] / Weight of DNA per molecule

By inserting the appropriate values calculated in this section (2.7.1.1), the following is achieved to give a final value of:

Number of pSfActin copies/µl = Conc. of pSfActin DNA / Weight of pSfActin per molecule

= 2.63×10^{-3} [g/ml]/ $3.4105943 \times 10^{-18}$ [g/molecule]

= $\underline{7.711 \times 10^{14} \text{copies of pSfActin/ml}}$

This means that for every ml of pSfActin DNA stock solution that there are 7.711×10^{14} copies of the pSfActin molecule.

2.7.1.2 Dilution Series of pSfActin for q-PCR standard curve

In this dilution series, the absolute stock of pSfActin DNA at concentration of 2.63µg/µl had been diluted down 1:1000 to a working stock of 2.63×10^{-3}µg/µl due to the increased sensitivity of the q-PCR.

***Table 2.6* – Dilution series of *Spodoptera frugiperda* Actin construct for q-PCR.**

[pSfActin] µg/µl	Copies of plasmid/µl	Copies of plasmid/ml
2.63×10^{-3} (Working Stock)	7.711×10^{8}	7.711×10^{11}
2.63×10^{-4}	7.711×10^{7}	7.711×10^{10}
2.63×10^{-5}	7.711×10^{6}	7.711×10^{9}
2.63×10^{-6}	7.711×10^{5}	7.711×10^{8}
2.63×10^{-7}	7.711×10^{4}	7.711×10^{7}

2.7.1.3 Creating a genomic DNA (AcMNPV) standard curve:

To determine the concentration of AcMNPV DNA required giving an identical dilution series as pSfActin, the following calculations were made:

1) The molecular weight of AcMNPV genomic DNA was calculated using the molecular weight calculator (Simakov, no date) to give a value of:

M_w AcMNPV genomic DNA= 81368426 g/molecule

2) Afterwards, the number of AcMNPV genomic copies per µl was determined as follows:

M_w of AcMNPV= 81368426 g/molecule

Avogadro's Constant = 6.023×10^{23} molecules/mol

Weight of AcMNPV per molecule = M_w of AcMNPV / Avogadro's Constant

= 81368426 [g/molecule]/ 6.023×10^{23} [molecules/mol]

= $1.3509616 \times 10^{-16}$ g/molecule

As we wanted the AcMNPV standard curve to have an identical dilution series as pSfActin (2.7.1.2), it was logical to calculate the starting concentration of AcMNPV DNA required producing a working stock of 7.711×10^{8} copies/µl. Therefore, to calculate the concentration of AcMNPV DNA required, the following equation was used from section 2.7.1.1:

Number of DNA copies/µl = Conc. of DNA [g/ml] / Weight of DNA per molecule

By inserting the appropriate values calculated within this section, the following was given:

7.711×10^{8} copies/µl = Conc. of AcMNPV DNA / $1.3509616 \times 10^{-16}$ [g/molecule]

The equation was rearranged accordingly to make the concentration of AcMNPV DNA required the value to be calculated:

Conc. of AcMNPV DNA = $1.3509616 \times 10^{-16}$ [g/molecule] * 7.711×10^{7} copies of DNA/µl

= 1.042×10^{-1} µg/µl of AcMNPV concentration required

This means that for every 1.042×10^{-1} µg/µl of AcMNPV DNA working solution that there is 7.711×10^{11} copies of the AcMNPV molecule.

2.7.1.4 Dilution Series of AcMNPV for q-PCR standard curve

The following concentrations highlight the dilution series used in q-PCR for the AcMNPV standard calibration curve:

Table 2.7 **– Dilution Series of AcMNPV DNA for q-PCR.**

[AcMNPV] µg/µl	Copies of plasmid/µl	Copies of plasmid/ml
1.042×10^{-1} (Working Stock)	7.711×10^{8}	7.711×10^{11}
1.042×10^{-2}	7.711×10^{7}	7.711×10^{10}
1.042×10^{-3}	7.711×10^{6}	7.711×10^{9}
1.042×10^{-4}	7.711×10^{5}	7.711×10^{8}
1.042×10^{-5}	7.711×10^{4}	7.711×10^{7}

2.7.1.5 Q-PCR Reaction components.

The following reaction components were added to all individual samples prior to q-PCR:

Table 2.8 **– Reaction components for q-PCR.**

Components	Sample DNA (2.63×10^{-4}µg/µl)	pSfActin/ AcMNPV Standard Curve	Negative Control
Platinum SYBR green (Invitrogen)	10.0	10.0	10.0
Primer 1 (10pmol/µl)	0.50	0.50	0.50
Primer 2 (10pmol/µl)	0.50	0.50	0.50
BSA (x100) (Invitrogen)	1.0	1.0	1.0
DNA	2.0	2.0	-
dH_2O	6.0	6.0	8.0
Total Volume (20µl)	20.0	20.0	20.0

Both Primer 1 and 2 relate to either primers designed for measuring host (SfrugiperdaActin-1 and SfrugiperdaActin-2) or viral (ACIE1-1 and ACIE1-2) copy number depending on the individual reaction.

2.7.1.6 Q-PCR program for determining DNA replication levels

The following cycling conditions were used in the measuring of DNA replication levels using the Corbett Research Rotor Gene 3000:

Hold 50°C for 2 minutes

Cycling 95°C for 15 seconds

57°C for 15 seconds

72°C for 15 seconds

Melt Ramp from 72°C to 99°C

Rising by 1°C each step

Wait 30 seconds on first step and then wait for 5 seconds for each step afterward.

2.7.2 Gene expression study:

2.7.2.1 Q-PCR Reaction components

Using the cDNA produced in section 2.6.6, the levels of late and very late gene expression were measured using q-PCR. The following reaction components were added to all individual samples prior to q-PCR:

Table 2.9 **– Reaction components for q-PCR.**

Components	Volume (µl)
Platinum SYBR Green	10.0
Primer 1 (10pmol/µl)	0.5
Primer 2 (10pmol/µl)	0.5
BSA (x20)	1.0
cDNA (100ng)	1.0
dH_20 (Total Volume is 20µl)	7.0

Primer 1 and 2 refer to the name of the late or very late gene that is being targeted by specific primers.

2.7.2.2. Q-PCR program for determining gene expression levels.

The following cycling conditions were used in the measuring of gene expression levels using the Corbett Research Rotor Gene 3000:

Hold 1	50°C for 2 minutes
Hold 2	95°C for 2 minutes
Cycling	95°C for 20 seconds
	57°C for 20 seconds
	72°C for 20 seconds
Melt	Ramp from 72°C to 99°C
	Rising by 1°C each step
	Wait 30 seconds on first step and then wait for 5 seconds for each step afterward.

2.8 Other PCR programs used.

2.8.1 PCR program for the generation of *lef*-2 and *lef*-2 mutant fragments.

Window 1:	95°C for 1 minute
	51°C for 1 minute
	72°C for 4 minutes
Window 2 (25 Cycles):	95°C for 1 minute
	51°C for 1 minute
	72°C for 4 minutes
Window 3:	95°C for 1 minute
	51°C for 1 minute
	72°C for 10 minutes
	Store at 6°C

2.8.2 PCR program for the sequencing of DNA (based on method from ABI Systems).

Window 1 (25 cycles):	96°C for 30 seconds
	50°C for 15 seconds
	60°C for 4 minutes
	Store at 6°C.

2.9 Primers:

2.9.1 Generalised *lef*-2 primers:

RDP558	CTCGCTTTTAATCATGCCGTC	21bp, 57.9°C
RDP561	CAACACACTCCGAAGAACTAC	21bp, 57.9°C

2.9.2 Primer Extension Primers

Polyhedrin:

RDP511	TTCGGCGAAGTGCTTCTTG	19bp, 56.7°C

Capsid:

RDP527	GATACTTGTTCGCCATCGTGG	22bp, 61.4°C
RDP513	GCAGCGATTAACTCTCATTTG	21bp, 55.9°C

39K:

RDP526	CAGCGTCAAGGCGCGTTTTG	20bp, 61.4°C
RDP514	AGATTGTTGCTCCGGCACG	19bp, 58.8°C

2.9.3 AcMNPV *lef*-2 Flanking Region Experiment primers:

Forward Primers:

AcMNPVLef250F	TCCAATCGACCGTTAGTCGA	20bp, 57.3°C
AcMNPVLef2100F	TTACCGAGTATGTCGGTGACGT	22bp, 60.3°C
AcMNPVLef2200F	CAACGTGCACGATCTGTGCA	20bp, 59.4°C
AcMNPVLef2300F	ATCGCACGTCAAGAATTAACAATG	24bp, 57.6°C
AcMNPVLef2400F	TATTCCCGAGTCAAGCGCAGCG	22bp, 64.0°C
AcMNPVLef2500F	ATC ATT GCG ATT AGT GCG ATT AA	23bp, 55.3°C

Reverse Primers:

AcMNPVLef250R	GTTGCGTTTGGTTTGTATCGTTAA	24bp, 55.3°C
AcMNPVLef2100R	ATTACCTCAGCGATTATAACTACG	24bp, 57.6°C
AcMNPVLef2200R	AGAGAAGGAATACGAAGAAGAAGA	24bp, 57.6°C
AcMNPVLef2300R	AAGACATATATATTTATGACAACAA	25bp, 51.5°C
AcMNPVLef2400R	TAATTAAGCAACACACTCCGAAG	24bp, 57.6°C
AcMNPVLef2500R	AATGGTGTAATTGAACTAGAAGA	23bp, 53.5°C

2.9.4 DNA Replication Study Primers:

SfrugiperdaActin-1	CGAGGCCCAGAGCAAGAGAG	20bp, 63.5°C
SfrugiperdaActin-2	CGCACTGGACGAGAGACACC	20bp, 63.5°C
ACIE1-1	AAGGTGTGGTGGGCCAGTTT	20bp, 64.0°C
ACIE1-2	TGGTCGGAGAACCTGTTGGA	20bp, 64.0°C

2.9.5 *Lef*-2 cysteine-serine Mutants viruses

Forward Primers:

AcMNPVLef2C1F	ACGCAGCAAGAGAAACATTTCTATGAAA GAAT	32bp, 63.1°C
AcMNPVLef2C2F	TGGTTTCGTCTGCCAAGTGTGA	22bp, 60.3°C
AcMNPVLef2C3F	TGTGCCAAGTCTGAAAACCGATGT	24bp, 61.0°C
AcMNPVLef2C4F	TGTGAAAACCGATCTTTAATCAAGGCT	27bp, 60.4°C
AcMNPVLef2C5F	ACTCCAAGTCTGTGGGTGAAGT	22bp, 60.3°C

Reverse Primers:

AcMNPVLef2C1R	ATTCTTTCATAGAAATGTTTCTCTTGCTGC GT	32bp, 63.2°C
AcMNPVLef2C2R	TCACACTTGGCAGACGAAACCA	22bp, 60.3°C
AcMNPVLef2C3R	ACATCGGTTTTCAGACTTGGCACA	24bp, 61.0°C
AcMNPVLef2C4R	AGCCTTGATTAAAGATCGGTTTTCACA	27bp, 60.4°C
AcMNPVLef2C5R	ACTTCACCCACAGACTTGGAGT	22bp, 60.3°C

2.9.6 NPVs and GVs *lef*-2 Mutant viruses:

***Mamestra brassicae* NPV (MbNPV):**

MbNPVLef2ftF	TCGAATCAGGACCGCTGGTGCGAGAAGCCG CGAAGTATGACGTCGGTACCGCGGTT	56bp, >75°C
MbNPVLef2ftR	AAAACAAATTTAGCATTTATAATTGTTTTA TTATCTAAAAGTTACAAACTGGGTT	55bp, 65.7°C
MbNPVLef2AcftF	CAATCGACCGTTAGTCGAATCAGGACCGC TGGTGCGA	37bp, >75°C
MbNPVLef2AcftR	TTTGTATCGTTAATAAAAAACAAATTTAGC	

	ATTTATAAT	39bp, 58.9°C

***Autographa californica* MNPV (AcMNPV):**

AcMNPVLef2PosF	CAATCGACCGTTAGTCGAATCAGGA	22bp, 58.4°C
AcMNPVLef2PosR	TTTGTATCGTTAATAAAAAACA	26bp, 50.6°C

***Plutella xylostella* GV (PxGV):**

PxGVLef2ftF	TCAGGACCGCTGGTGCGAGAAGCCGCGAAG	
	TATGGAAAAGGCGGTGCCCTACA	53bp, >75°C
PxGVLef2ftR	AAAACAAATTTAGCATTTATAATTGTTTTATT	
	ATTTAAAATGGTTTTAGCAGGT	54bp, 64.9°C
PxGVLef2AcftF	CAATCGACCGTTAGTCGAATCAGGACCGCTG	
	GTGCG	37bp, >75°C
PxGVLef2AcftR	TTTGTATCGTTAATAAAAAACAAATTTAGCA	
	TTTATAAT	39bp, 58.9°C

***Choristoneura fumiferana* MNPV (CfMNPV):**

CfMNPVLef2ftF	TCGAATCAGGACCGCTGGTGCGAGAAGC	
	CGGCAAGTATGGACCAGGTGTGGAACC	55bp, >75°C
CfMNPVLef2ftR	AAAACAAATTTACGATTTATAATTGTTTT	
	ATTATCTAATAGTTGCAAATTGGATTCA	57bp, 65.8°C
CfMNPVLef2AcftF	CAATCGACCGTTAGTCGAATCAGGACCG	
	CT	37bp, >75°C
CfMNPVLef2AcftR	TTTGTATCGTTAATAAAAAACAAATTTAGCA	
	TTTATAAT	39bp, 58.9°C

***Spodoptera exigua* NPV (SeNPV):**

SeNPVLef2ftF	TCAGGACCGCTGGTGCGAGAAGCCGCGA	
	AGTATGCCACCGTTGCTGTCGTGGACA	55bp, >75°C
SeNPVLef2ftR	AAAACAAATTTAGCATTTATAATTGTTTT	
	ATTAAAAAGTTACAAATTGGATT	55bp, 63.4°C

SeNPVLef2AcftF	CAATCGACCGTTAGTCGAATCAGGACCG CT	37bp, >75°C
SeNPVLef2AcftR	TTTGTATCGTTAATAAAAAACAAATTTAGCA TTTATAAT	39bp, 58.9°C

2.9.7 VLD1 New mutant primers:

VLD1Lef2NewMutF	TGTTTAATCAAGACTCTGACGCATT	25bp, 58.1°C
VLD1Lef2NewMutR	AATGCGTCAGAGTCTTGATTAAACA	25bp, 58.1°C

2.9.8 Sequencing:

RDP558	CTCGCTTTTAATCATGCCGTC	21bp, 57.9°C
RDP561	CAACACACTCCGAAGAACTAC	21bp, 57.9°C
AcMNPVLef2PosF	CAATCGACCGTTAGTCGAAT AGGA	22bp, 58.4°C
AcMNPVLef2PosR	TTTGTATCGTTAATAAAAAACA	26bp, 50.6°C
AcMNPVLef2400F	TATTCCCGAGTCAAGCGCAGCG	22bp, 64.0°C
AcMNPVLef2400R	TAATTAAAGCAACACACTCCGAAG	24bp, 57.6°C
AcMNPVLef2SeqF	AATTGACCCTAACTCCATACA	21bp, 54.0°C
AcMNPVLef2SeqR	TGCGTCAGAGCCTTGATTA	19bp, 54.5°C
MbNPVLef2SeqF	TGTGTCGCTAGCCGACAT	18bp, 56.0°C
MbNPVLef2SeqR	AATTCGGCGGTAGATAGAC	19bp, 54.5°C
PxGVLef2SeqF	ATTTGAAACTGGCGGACTG	19bp, 54.5°C
PxGVLef2SeqR	AGCAGTGTCTGTTGATGGT	19bp, 54.4°C
CfMNPVLef2SeqF	TACACCGTGTTTGAGCGCGGA	21bp, 61.8°C
CfMNPVLef2SeqR	TCAAACACGCCGCCTTGCA	20bp, 59.4°C

2.9.9 Gene expression q-PCR study primers:

Polfin-1	CCGTTATCAAGAACGCTAAGCGCAAG	26bp, 64.8°C
Polfin-2	TCCATCCAACGACAAGCTTCATCGTG	26bp, 64.8°C
GP64fin-1	AATGTACAGCAGGCTCGAGTGCCA	24bp, 64.4°C
GP64fin-2	GTCACCGACTCGGGGTTATTTTTGTC	26bp, 64.8°C
P10fin-1	GACGCAAATTTTAGACGCCGTTACGGA	27bp, 65.0°C

P10fin-2	AACTGCGTTTACCACGACGAGCGT	24bp, 64.4°C
Capfin-1	GCGAGACGAATTGCGTTTCTTTGACG	26bp, 64.8°C
Capfin-2	CTGCTTCTTATCGGGTTGTACAACTCG	27bp, 65.0°C
Actin-1	GGACAGAAGGACTCGTACGTAGG	23bp, 64.2°C
Actin-2	ACAGCCTGGATGGCGACGTAC	21bp, 63.7°C

2.10 Computer analysis of thirty-seven baculovirus *lef*-2 genes:

2.10.1 Multiple alignment and phylogenetic analysis of *lef*-2 amino acid sequences:

Thirty-seven baculovirus *lef*-2 amino acid sequences were taken from the Pubmed database and aligned using Clustal X version 1.83 (Thompson *et al.*, 1997). From this multiple alignment, a phylogenetic tree was generated using bootstrap analysis (1000 replicates) and options were chosen to exclude positions with gaps and to present labels on the tree nodes. The phylogenetic tree was visualised using Treeview (Page, 1996).

Table 2.10 **– Protein and nucleotide sequences of thirty-seven baculoviruses *lef*-2 taken from Pubmed database.**

Virus Name	NPV/GV	Abbreviation	Nucleotide Accession Number.	Protein Accession Number.
Adoxophyes honmai	NPV	AhNPV	NC_004690	NP_818747
Adoxophyes orana	GV	AoGV	NC_005038	NP_872486
Amsacta albistriga	NPV	AaNPV	AF118112	AAD26699
Anagrapha falcifera	NPV	AfNPV	U64896	AAB53355
Antheraea pernyi	NPV	ApNPV	AY685706	AAU89800
Anticarsia gemmatalis	NPV	AgNPV	Y17753	CAC03566
Autographa californica	NPV	AcNPV	NC_001623	NP_054035
Bombyx mori	NPV	BmNPV	NC_001962	NP_047556
Buzura suppressaria	NPV	BsNPV	AF060564	AAC77814
Choristoneura fumiferana defective	NPV	CfdefNPV	NC_005137	NP_932612
Choristoneura fumiferana	MNPV	CfMNPV	NC_004778	NP_848315
Chrysodixis chalcites	NPV	CcNPV	NC_007151	YP_249740
Cryptophlebia leucotreta	GV	ClGV	NC_005068	NP_891885
Culex nigripalpus	NPV	CnNPV	NC_003084	NP_203329
Cydia pomonella	GV	CpGV	NC_002816	NP_148825
Epiphyas postvittana	NPV	EpNPV	NC_003083	NP_203173
Helicoverpa armigera G4 strain	NPV	HaG4NPV	NC_002654	NP_075186
Helicoverpa armigera	NPV	HaNPV	NC_003094	NP_203673
Helicoverpa zea	SNPV	HzSNPV	NC_003349	NP_542744
Lymantria dispar	NPV	LdNPV	NC_001973	NP_047774
Mamestra brassicae	NPV	MbNPV	*	*
Mamestra configurata 90. 2 strain	NPV	Mc90/2NPV	U59461	AAM09122
Mamestra configurata A isolate	NPV	McANPV	NC_003529	NP_613097

Mamestra configurata B isolate	NPV	McBNPV	NC_004117	NP_689188
Neodiprion lecontei	NPV	NlNPV	NC_005906	YP_025254
Neodiprion sertifer	NPV	NsNPV	NC_005905	YP_025164
Orgyia ericae	NPV	OeNPV	AJ629189	CAF32809
Orgyia pseudotsugata	MNPV	OpMNPV	NC_001875	NP_046162
Orgyia pseudotsugata	SNPV	OpSNPV	D50053	BAA08770
Perina nuda	NPV	PnNPV	AF162787	AAD48439
Phthorimaea operculella	GV	PoGV	NC_004062	NP_663202
Plutella xylostella	GV	PxGV	NC_002593	NP_068251
Rashiplusia ou	NPV	RoNPV	NC_004323	NP_702996
Spodoptera exigua	NPV	SeNPV	NC_002169	NP_037772
Spodoptera litura	NPV	SlNPV	NC_003102	NP_258382
Trichoplusia ni	SNPV	TnSNPV	DQ017380	AAZ67498
Xestia c-nigrum	GV	XcGV	NC_002331	NP_059183

The * denotes that the nucleotide and protein sequence of MbNPV *lef*-2 was given by Dr S. L .Turner, NERC Centre for Ecology & Hydrology, Oxford.

Chapter Three

Characterisation of genotypic and phenotypic differences between AcMNPV, VLD1 and AcORF6^{3260}-1

Chapter Three

3.1 Introduction.

The *lefs* comprise a group of genes transcribed early in baculovirus infection that function to regulate late gene expression and DNA replication. The *lefs* group can be further differentiated into sub-groups that are classified according to individual roles such as DNA replication, late gene regulation or host range. Through previous research employing the use of temperature-sensitive mutants and assays of transient DNA synthesis or late gene expression, a total of nineteen *lefs* have been identified, although not all of their roles have been fully characterised (Hefferon, 2004). The involvement of the *lef* group in late gene expression is very significant, with some of the genes taking on vital roles such as in the formation of the viral RNA polymerase complex (Hefferon, 2004).

Past research isolated and identified a viral phenotype that was deficient in very late gene expression through the mutagenesis of an AcMNPV recombinant genome containing a beta-galactosidase gene (AcUW1.lacZ) with 5'-bromodeoxyuridine (BrdU) treatment (Merrington *et al.*, 1996). The viral phenotype was designated VLD in recognition of its Very Late Deficiency with respect to the reduction in polyhedrin and β-galactosidase production. Marker rescue studies and sequence analysis revealed the presence of a single point mutation within *lef*-2 at position 3260, where a guanine nucleotide had been substituted by an adenine. This substitution thus altered the primary amino acid sequence of LEF-2 from an asparagine to an aspartic acid at position 154. Consequences of this mapped mutation ranged from lower viral titres, temporal delay in DNA replication, and a delay in virus-specific proteins such as chitinase. The VLD1 genotype was recreated by using site-directed mutagenesis to modify the *lef*-2 coding region in a plasmid vector and then *in vitro* recombination to insert the modified *lef*-2 back into the AcMNPV genome. This produced AcORF6^{3260}-1, which appeared to be phenotypically identical to VLD1 (Merrington *et al.*, 1996).

The initial objective of this chapter was to compare gene expression in cells infected with AcMNPV, VLD1 and AcORF6^{3260}-1. The scope of the work, however, was broadened

when it was discovered that there were obvious differences in cell morphology in cultures infected with VLD1 and AcORF6^{3260}-1. These results led me to examine the sequence of *lef*-2 in AcMNPV, VLD1 and AcORF6^{3260}-1 and discover an additional mutation in the VLD1 *lef*-2. This finding had consequences for the later strategy pursued in my work. To assess if the mutation within AcORF6^{3260}-1 was the result of a temperature sensitive mutant and to further determine if previous published results by Merrington *et al.* (1996) could be validated using PCR, DNA replication was investigated.

Merrington *et al.* (1996) demonstrated using dot blot hybridisation that no difference in DNA replication levels occurred between AcMNPV, and AcORF6^{3260}-1. However, a temporal delay was observed in DNA replication of VLD1 compared to AcMNPV at 18hpi using dot blot hybridisation. Using a modified *Dpn* I protection assay to measure DNA synthesis, it was apparent that VLD1 exhibited lower levels compared to the other viruses (Merrington *et al.*, 1996) Following on from research conducted by Merrington *et al.* (1996), it was possible using technology such as real time PCR (q-PCR) to measure more sensitively both RNA and DNA levels throughout infection. The use of q-PCR permitted the examination of viral DNA replication by focusing on the number of viral copies per cell present at specific time-points during infection. To account for the numeric differences in host and viral DNA levels during infection, individual standard calibration curves were established. Host DNA was differentiated in this system using a calibration curve targeting the *Spodoptera frugiperda* actin gene. In contrast, viral DNA levels were calculated based upon a standard curve aimed at the AcMNPV Immediate Early-1 (ie-1) gene. The DNA from virus-infected *Sf*-21 cells was used and the DNA replication levels calculated based on the viral copy number per cell.

To assess if the mutation within AcORF6^{3260}-1 was the result of a temperature sensitive virus, an additional control was employed. A temperature-sensitive mutant virus (Ts8b), that was defective in DNA replication at the non-permissive temperature of 33°C but replicated normally at the permissive temperature of 25°C (Gordon and Carstens, 1984; Erlandson *et al.*, 1984) was used. Using the q-PCR technology adopted in this chapter, the

viral replication levels of AcMNPV and AcORF6^{3260}-1 were measured over 24hpi, with Ts8b providing both a positive and negative control for DNA replication.

3.2 Results

3.2.1 Morphology of AcMNPV, VLD1 or AcORF6^{3260}-1-infected insect cells.

Polyhedrin synthesis is reduced in VLD1-infected cells (Merrington *et al.*, 1996). Virus-infected cell morphology was examined in *Spodoptera frugiperda* (*Sf*-21) and *Trichoplusia ni* (*Tn*-368Ad) cells infected with AcMNPV, VLD1 or AcORF6^{3260}-1, since this was never analysed in detail by Merrington *et al.* (1996).

_Sf_-21 cell morphology:

Sf-21 cells were set up and left overnight at 28°C until a cell monolayer had been established. The cells were infected in duplicate with the respective virus at a multiplicity of infection (MOI) of 10 and left to incubate at 28°C for the rest of the time course. The *Sf*-21 cells (virus-infected and controls) were photographed at 24, 48 and 72hpi at a magnification of x320 (Fig 3.1 to 3.3, respectively). The uninfected *Sf*-21 cells (Fig 3.1 to 3.3, panel A) exhibited normal division and morphology, with increasing cell numbers present in the dish as the time course progressed. In contrast, AcMNPV-infected *Sf*-21 cells exhibited typical signs of infection, indicated by the increasing accumulation of polyhedra between 24-72hpi onwards and the characteristic rounding of cells (Fig 3.1 to 3.3, panel B). Furthermore, the AcMNPV-infected cells appeared larger and more granular in appearance compared to uninfected cells. As an indication of infection, the *Sf*-21 cell density during AcMNPV-infection appeared lower compared to uninfected cells. Towards the end of the time course, AcMNPV-infected cells became detached from the monolayer and floated in the surrounding medium.

The VLD1 nor AcORF6^{3260}-1-infected *Sf*21 cells neither produced polyhedra in the form of occlusion bodies through out the time course (Fig 3.1 to 3.3, panels C and D). Similar to AcMNPV, both VLD1 and AcORF6^{3260}-1-infected cells exhibited a lower cell density compared to uninfected cells as the virus infection progressed. The only visible sign of any alteration in cell morphology was the irregular elongation of *Sf*-21 cells (indicated by triangles in panels C and D in Fig 3.1 to 3.3), which was not detected in AcMNPV-infected cells. This sign of altered *Sf*-21 cell morphology was detected in all virus infections throughout this PhD research study involving either the VLD1 or AcORF6^{3260}-1 virus. An

apparent difference between the two mutant viruses became evident when observing the *Sf*-21 cells from 24hpi. The AcORF6^{3260}-1-infected *Sf*-21 cells were observed to show viral infection (Fig 3.1, panel D) at an earlier time point of 24hpi compared to VLD1, which reached a comparable state at 48hpi (Figure 3.2, panel C).

A: Mock-infected *Sf*-21 cells.

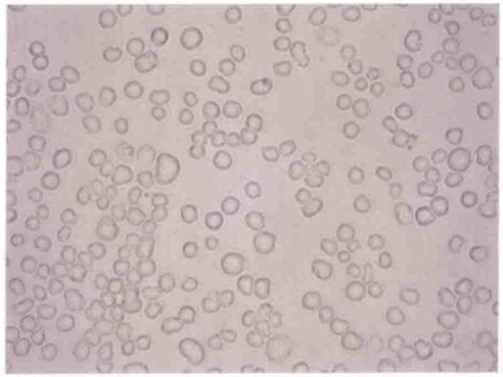

B: AcMNPV-infected *Sf*-21 cells.

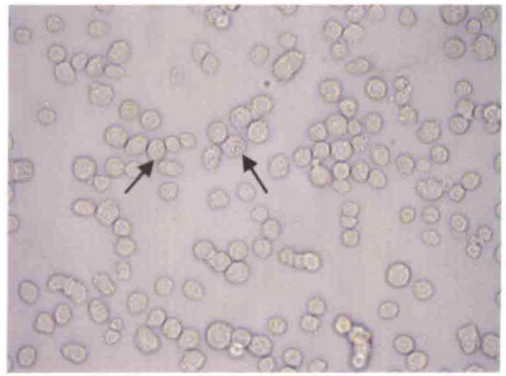

C: VLD1-infected *Sf*-21 cells.

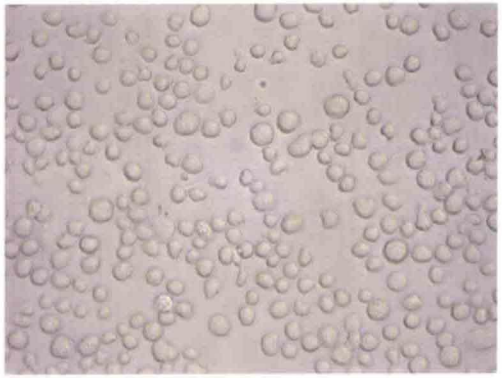

D: AcORF6^{3260}-1- infected *Sf*-21 cells.

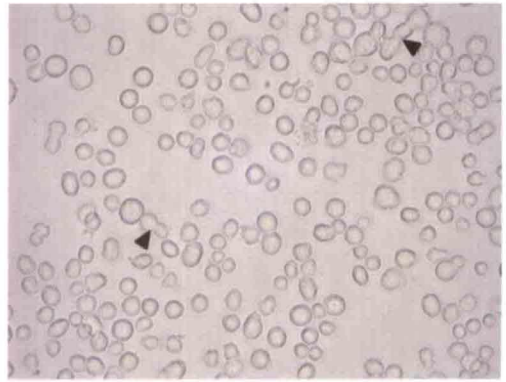

***Figure 3.1* – *Sf*-21 Cell Morphology at 24hpi.** 35mm dishes were seeded with 1x 10^6 *Sf*-21 cells and left at 28°C overnight. Afterwards the dishes were infected at MOI of 10 PFU with either AcMNPV, VLD1, AcORF6^{3260}-1 or TC100/10% FCS (mock) and left at room temperature for 1 hour (T_0 = Time the virus was added to individual dishes). The virus inoculum was removed and replaced with 2ml TC100/10% FCS and incubated at 28°C until 24hpi. Panel A represents mock-infected *Sf*-21 cells. Panel B represents AcMNPV-infected *Sf*-21 cells. Finally, panels C and D represent VLD1 and AcORF6^{3260}-1-infected *Sf*-21 cells respectively. Arrows indicate the presence of cells positive for polyhedrin, and triangles represent cells negative for polyhedrin in the form of occlusion bodies. Magnification at x320.

A: Mock-infected *Sf*-21 cells.

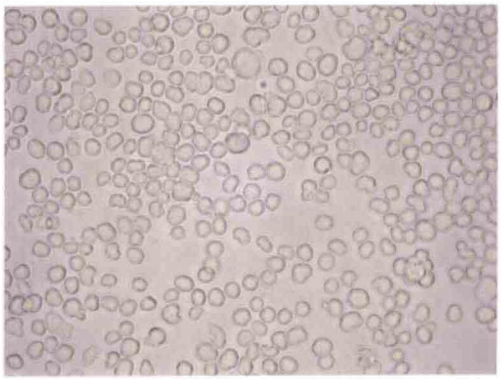

B: AcMNPV-infected *Sf*-21 cells.

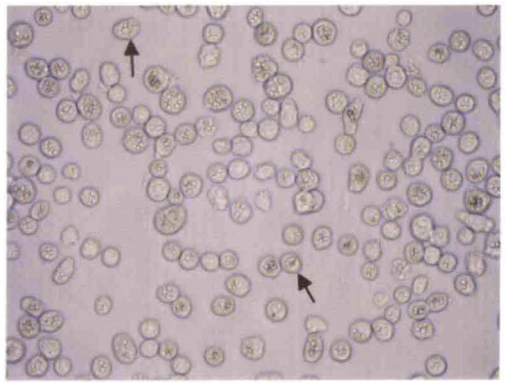

C: VLD1-infected *Sf*-21 cells.

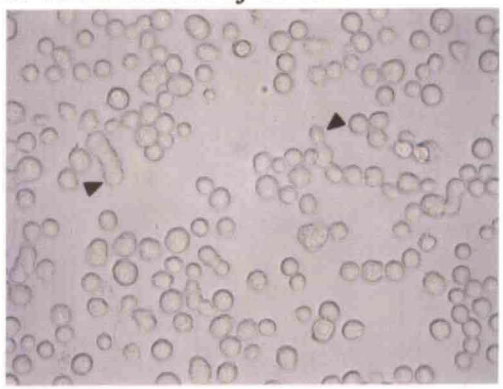

D: AcORF6^{3260}-1- infected *Sf*-21 cells

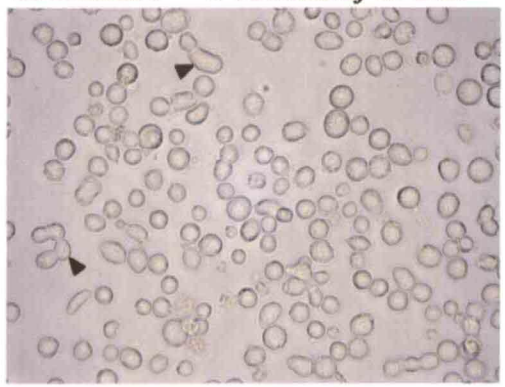

***Figure 3.2* – *Sf*-21 Cell Morphology at 48hpi.** *Sf*-21 cells were infected with AcMNPV, VLD1 or AcORF6^{3260}-1 in the same manner as Figure 3.1. Panel A represents mock-infected *Sf*-21 cells. Panel B represents AcMNPV-infected *Sf*-21 cells. Finally, panels C and D represent VLD1 and AcORF6^{3260}-1-infected *Sf*-21 cells respectively. Arrows indicate the presence of cells positive for polyhedrin, and triangles represent cells negative for polyhedrin in the form of occlusion bodies. Magnification at x320.

A: Mock-infected *Sf*21 cells

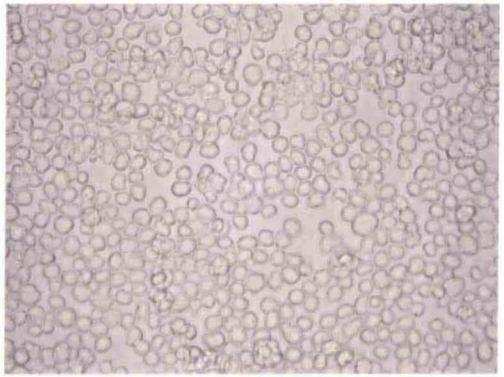

B: AcMNPV-infected *Sf*-21 cells

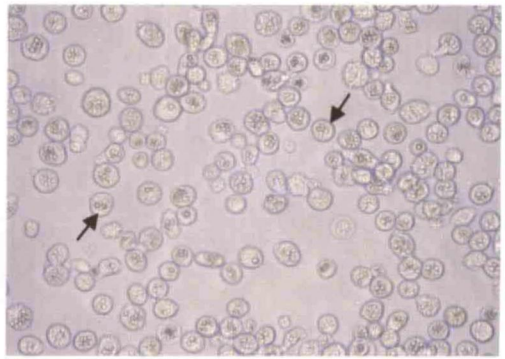

C: VLD1-infected *Sf*-21 cells

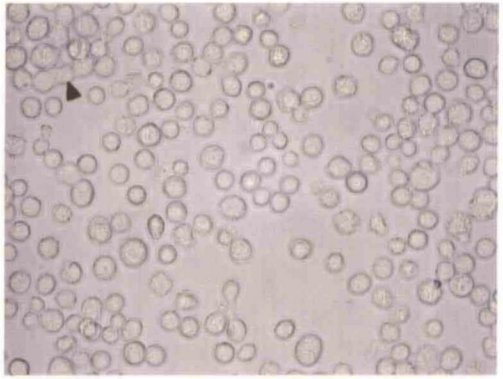

D: AcORF6^{3260}-1- infected *Sf*-21 cells

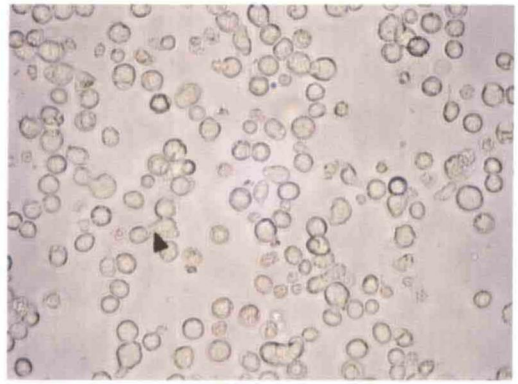

***Figure 3.3* – *Sf*-21 Cell Morphology at 72hpi.** *Sf*-21 cells were infected with AcMNPV, VLD1 or AcORF6^{3260}-1 in the same manner as Figure 3.1. Panel A represents mock-infected *Sf*-21 cells. Panel B represents AcMNPV-infected *Sf*-21 cells. Finally, panels C and D represent VLD1 and AcORF6^{3260}-1-infected *Sf*-21 cells respectively. Arrows indicate the presence of cells positive for polyhedrin, and triangles represent cells negative for polyhedrin in the form of occlusion bodies. Magnification at x320.

***Tn*-368Ad cell morphology:**

The *Tn*-368Ad cells were infected with AcMNPV, VLD1 or AcORF6^{3260}-1 at 10MOI and incubated at 28°C for the remainder of the time course. Identical to the examination of the *Sf*-21 cell morphology, the cells were photographed at a magnification of x320. The only difference between the two studies was the first time point of 25.5hpi instead of 24hpi as specified for *Sf*-21 cells. Similar to uninfected Sf-21 cells, the *Tn*-368Ad cells exhibited signs of normal morphology and growth, with increasing numbers of cells contributing to the monolayer (Fig 3.4 to 3.6, panel A). The process of cell growth was well illustrated within uninfected *Tn*-368Ad cells as they were observed as newly elongated spherical cells or fibroblasts. The wild-type AcMNPV infection rapidly spread between cells throughout the time course with increasing accumulation of polyhedra within the cells (Fig 3.4 to 3.6, panel B). At 72hpi, the AcMNPV-infected Tn-368Ad cells lysed under the pressure of increasing levels of occlusion bodies releasing the progeny virus (Fig 3.6, panel B). Additionally, the AcMNPV appeared to be more progressive within *Tn*-368Ad cells compared to *Sf*-21 cells at 24hpi (panel B, figures 3.1 and 3.4). Both the VLD1 and AcORF6^{3260}-1-infected *Tn*-368 cells did not exhibit any signs of polyhedra in the form of occlusion bodies through out the time course (Fig 3.4 to 3.6, panels C and D); identical to the morphology observed in *Sf*-21 cells. Signs of viral infection were observed by the cellular morphology altering to involve cells taking on a more spherical form and increasing in size (indicated by triangles in the appropriate panels). Between 48-72hpi, no obvious differences in morphology were observed between VLD1 and AcORF6^{3260}-1-infected cells.

A: Mock-infected *Tn*368Ad cells

B: AcMNPV-infected *Tn*368Ad cells.

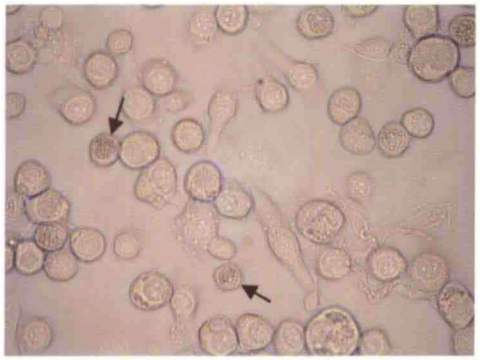

C: VLD1-infected *Tn*368Ad cells

D: AcORF6^{3260}-1-infected *Tn*368Ad cells.

***Figure 3.4* – *Tn*368Ad Cell Morphology at 25.5hpi.** 35mm dishes were seeded at 5x10^5 *Tn*368Ad cells and left at 28°C for overnight. Afterwards the dishes were infected at MOI of 10 PFU with AcMNPV, VLD1, AcORF6^{3260}-1 or TC100/10% FCS (Mock) and left at room temperature for 1 hour (T_0 = Time the virus was added to individual dishes). The virus inoculum was removed and replaced with 2ml TC100/10% FCS and incubated at 28°until 25.5hpi. Panel A represents mock-infected *Tn*368Ad cells. Panel B represents AcMNPV-infected *Tn*368Ad cells. Finally, panels C and D represent VLD1 and AcORF6^{3260}-1-infected *Tn*368Ad cells respectively. Arrows indicate the presence of cells positive for polyhedrin, and triangles represent cells negative for polyhedrin in the form of occlusion bodies. Magnification at x320.

A: Mock-infected *Tn*368Ad cells

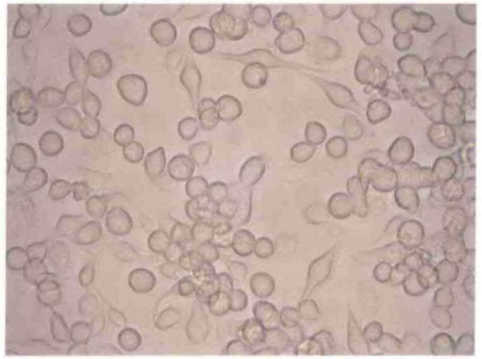

B: AcMNPV-infected *Tn*368Ad cells

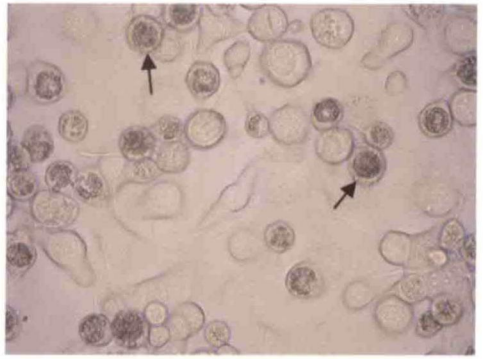

C: VLD1-infected *Tn*368Ad cells

D: AcORF6^{3260}-1-infected *Tn*368Ad cells

***Figure 3.5* – *Tni*368Ad Cell Morphology at 48hpi.** *Tn*368Ad cells were infected with AcMNPV, VLD1 or AcORF6^{3260}-1 in the same manner as Figure 3.4. Panel A represents TC100/10% FCS-infected *Tni*368Ad cells. Panel B represents AcMNPV-infected *Tni*368Ad cells. Finally, panels C and D represent VLD1 and AcORF6^{3260}-1-infected *Tn*368Ad cells respectively. Arrows indicate the presence of cells positive for polyhedrin, and triangles represent cells negative for polyhedrin in the form of occlusion bodies. Magnification at x320.

A: Mock-infected *Tn*368Ad cells

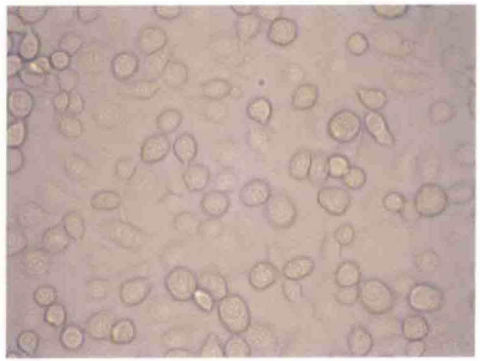

B: AcMNPV-infected *Tn*368Ad cells

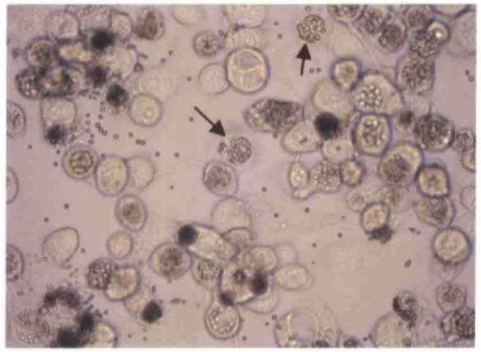

C: VLD1-infected *Tn*368Ad cells

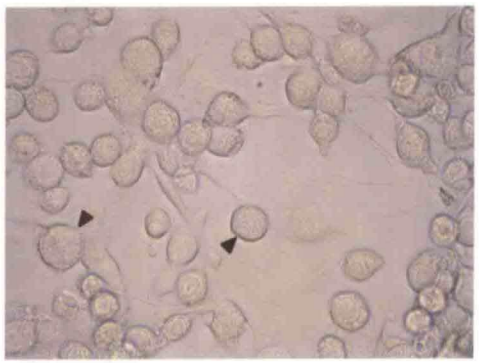

D: AcORF6^{3260}-1-infected *Tn*368Ad cells

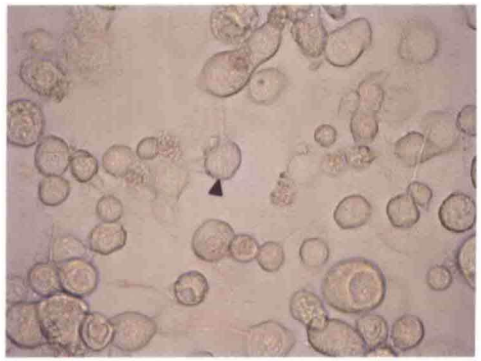

***Figure 3.6* – *Tni*368Ad Cell Morphology at 72hpi.** *Tn*368Ad cells were infected with AcMNPV, VLD1 or AcORF6^{3260}-1 in the same manner as Figure 3.4. Panel A represents TC100/10% FCS-infected *Tni*368Ad cells. Panel B represents AcMNPV-infected *Tni*368Ad cells. Finally, panels C and D represent VLD1 and AcORF6^{3260}-1-infected *Tn*368Ad cells respectively. Arrows indicate the presence of cells positive for polyhedrin, and triangles represent cells negative for polyhedrin in the form of occlusion bodies. Magnification at x320.

3.2.2 Multi-step viral growth curve analysis of AcMNPV, VLD1 and AcORF6^{3260}-1 viruses at 0.1PFU/cell over 96hpi.

Merrington *et al.* (1996) showed that during a one step growth curve initiated with 5 PFU/cell, no significant difference in budded virus titre was observed between VLD1, AcORF6^{3260}-1 viruses compared to the original parental virus (AcUW1.*lacZ*) that was used in BrdU treatment to give rise to the isolation of the very late deficient phenotype (VLD). Utilising the same technology and protocols, but using AcMNPV instead of AcUW1.*lac*Z, cell culture flasks were seeded at 1 x 10^5 *Sf*-21 cells/ml stirring for 2-3 days, until the cells had reached the exponential phase (~5 x 10^5 *Sf*-21 cells/ml). Each flask was infected with VLD1, AcORF6^{3260}-1 or AcMNPV virus at 0.1PFU/cell and incubated at 28°C. Using such a low virus infection rate of 0.1PFU allowed the *Sf*-21 cells to undergo several rounds of baculovirus replication in contrast to the high multiplicity of infection used for protein production. Three samples of medium (1ml) were extracted at 24, 48, 72 and 96hpi. A plaque assay was used to determine the budded virus titre over the time-course with an average being taken for each point (Fig 3.7). It was decided to only use AcMNPV and not AcUW1.*lac*Z in the multi-step viral growth curve because this virus was to be used continually through out this PhD study as a control measure and therefore act as a comparison to analyse the other mutant viruses against.

At time point 0hpi, the budded virus titre value is representative of the predicted input titre to each dish. Both AcMNPV and AcORF6^{3260}-1 exhibited a steady increase in budded virus titre over 48hpi before reaching a plateau that lasted for 24 hours. VLD1 virus replicated more slowly compared to the other two viruses. Budded virus titre in the VLD1 phenotype appeared to reach its potential peak at 48hpi, but at approximately 1.5 log values below that of the other viruses. The negative control of TC100/10% FCS showed no visible plaques during any point throughout this time-course.

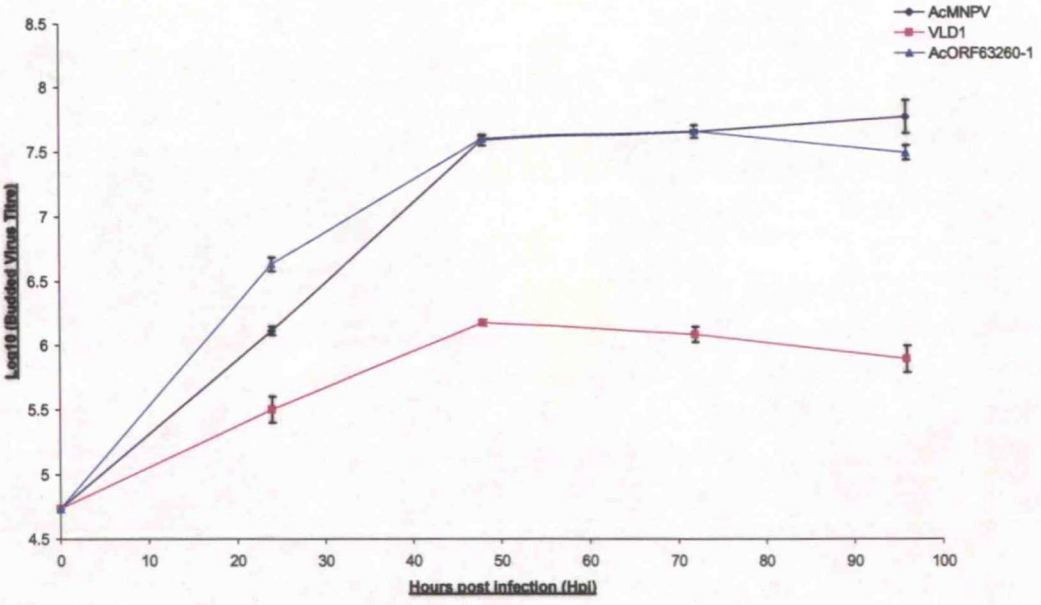

***Figure 3.7* - Viral growth curve analysis.** *Sf*-21 cells were infected at MOI of 0.1PFU with AcMNPV, VLD1, AcORF6^{3260}-1 and Uninfected (data not shown). At the indicated time-points, triplicate samples of the supernatants were collected and the budded virus titre determined by standard plaque assay. Each point indicates the average of triplicate samples taken and the y-axis error bars represents the standard error.

3.2.3 Sequencing of AcMNPV, VLD1 and AcORF6^{3260}-1 *lef*-2 coding region to ensure the presence of the original identified point mutations.

The apparent differences in VLD1 and AcORF6^{3260}-1 suggested genotypic differences between the two viruses. Hence, the *lef*-2 nucleotide sequence in each virus was determined. Dishes of 35mm diameter seeded with *Sf*-21 cells were infected with AcMNPV, VLD1 or AcORF6^{3260}-1 at a MOI of 10 and left at 28°C until the cells had become well-infected (4-6 days). Afterwards, the total DNA was extracted from virus-infected cell pellets and stored at 4°C. The DNA concentration of each sample was determined and the integrity of the nucleic acid examined by agarose gel electrophoresis. Using primers RDP558 (5'- CTC GCT TTT AAT CAT GCC GTC -3') and RDP561 (5'- CAA CAC ACT CCG AAG AAC TAC – 3'), the *lef*-2 coding region was amplified using PCR. The size (1500bp) of the PCR products was determined using agarose gels. The purified PCR products were then sequenced and software programs pregap4 and gap4 used to produce a consensus nucleotide sequence. The PCR and sequencing of different virus *lef*-2s was not done directly from virus stocks because it was by force of habit that the total DNA was extracted

from virus-infected cells. It would be possible in theory to extract DNA from BV particles and after a minimal purification step to amplify the product by PCR. However, how many BV particles are required to ensure a sufficient concentration of DNA is unknown and with VLD1 and AcORF6^{3260}-1 virus stocks that are 10-fold lower than AcMNPV it might be a costly method. Furthermore, using DNA extracted from virus-infected cells yields the advantage of providing enough material to run an agarose gel and analysing the DNA by restriction digest profiling. Whatever method is used, both give the same end result of extracted DNA to be further used as dictated by the researcher.

The nucleotide mutation that was originally located in VLD1 was a guanine that had been substituted by an adenine. A further point mutation was discovered in VLD1 *lef-2*. In this instance, a cytosine had been replaced by a thymidine. Individual nucleotide sequences were translated into their respective protein identities using pDraw software. Using the program Clustal X (version 1.83), the AcMNPV, VLD1 and AcORF6^{3260}-1 LEF-2 protein sequences were aligned and visualised using Gene Doc. This allowed the identification of conserved regions and shading according to percentage identity (Fig 3.8). The LEF-2 protein alignment was shaded for 100% (purple) between all three viruses. At position 178 in the alignment, the native amino acid of asparagine is present in AcMNPV, while the original mutation in both VLD1 and AcORF6^{3260}-1 correctly shows an aspartic acid residue instead. A new amino acid mutation was found in the VLD1 LEF-2 protein at position 154. This single point mutation resulted from an alanine amino acid residue being changed for a threonine residue. This alteration had not been documented before and was not reported by Merrington *et al* (1996).

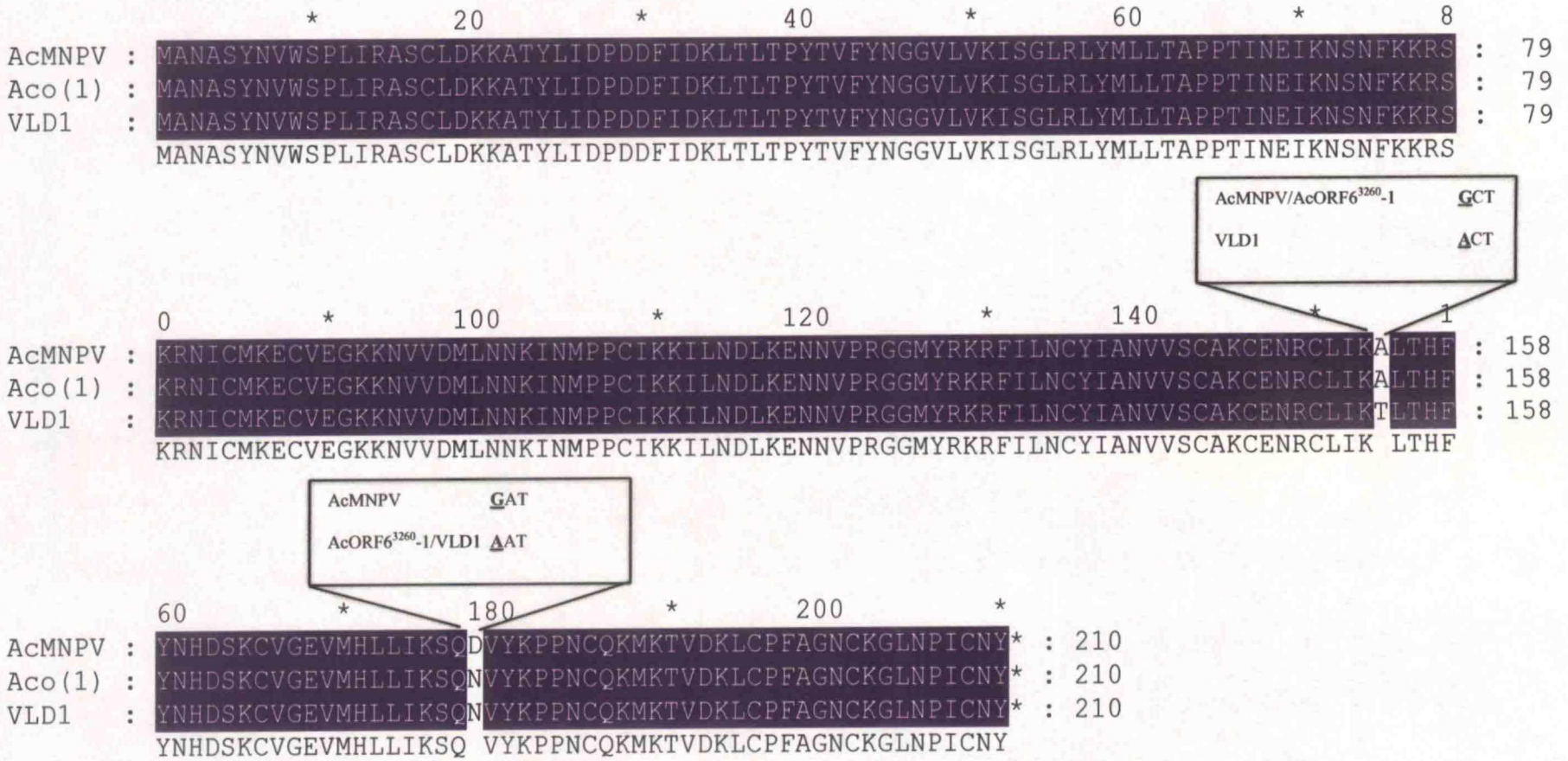

***Figure 3.8*- Complete LEF-2 protein alignments of AcMNPV, VLD1 and AcORF6^{3260}-1 viruses.** Total DNA was extracted from virus-infected *Sf*-21 cells after 6dpi. *Lef-2* fragment from each virus was generated by PCR using primers RDP558 and RDP561. Afterwards the entire coding region of the *lef*-2 gene was sequenced consecutively and translated using pDraw. The sequences were aligned using Clustal X (Version 1.83). GeneDoc software was subsequently used for homology shading. Two shading levels were set: Purple for 100% identity. Each of the two black lined boxes represents the nucleotide mutation responsible for the change in amino acid residue.

3.2.4 DNA replication study examining the consequences of the VLD1 mutation.

Total DNA was extracted from duplicate samples of *Sf*-21 cells infected with AcMNPV or AcORF6^{3260}-1 from specific time points encompassing early, late and very late phases of the baculovirus life cycle. More time points were taken when DNA replication was expected to be maximal. To differentiate between host and viral DNA, standard calibration curves were established targeting specific genes unique to each. Using both the viral and host standard curves as a baseline for measurement, DNA replication levels for each virus was calculated as a number of viral *ie-1* copies per *Sf*-21 cell.

3.2.4.1 Establishing host and viral calibration curves.

The host DNA calibration curve was calculated using the *S. frugiperda* actin coding sequence inserted into pGem®-T cloning vector. Total DNA was extracted from uninfected *Sf*-21 cells at 5dpi at 28°C. Using primers (denoted Act-1, Act-2) designed to amplify the *actin*A3a region of the *Helicoverpa armigera* genome (Genbank: X97614), a 386bp product was generated by PCR using the *Sf*-21 total DNA as a template. The purified PCR fragment was ligated into pGem®-T cloning vector at position 52 (Fig 3.9, panel A). The insertion of the DNA fragment at position 52 (*lac*Z region) of the pGem-T vector allowed the benefit of blue/white screening, which helped to differentiate between parental and recombinant plasmids. White colonies were amplified in Luria broth to produce recombinant plasmid for purification. Successful insertion of the *S. frugiperda* actin coding region into the pGem®-T cloning vector was determined by restriction digest with *Sac*I, which linearised the DNA for analysis by agarose gel electrophoresis. Final confirmation was obtained by sequencing analysis. The sequencing data was compared with the *S. frugiperda* actin mRNA partial sequence (Genbank AF548015) using NCBI blast, which yielded a 100% alignment between the two sequences. Using the available actin DNA sequence from *H. armigera*, plasmid construct and the partial cDNA sequence from *S. frugiperda*, a nucleotide alignment was performed using Clustal X (version 1.83) (Fig 3.10).

A)

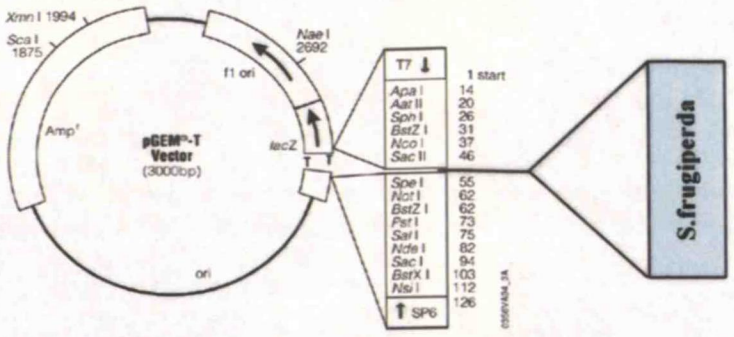

B)

Act-1 **S. frugiperda Actin-1**

```
  1 GGACAGAAGG ACTCGTACGT AGGTGACGAG GCCCAGAGCA AGAGAGGTAT

    CCTGTCTTCC TGAGCATGCA TCCACTGCTC CGGGTCTCGT TCTCTCCATA

 51 CCTCACCCTC AAGTACCCCA TCGAGCACGG CATCGTCACC AACTGGGACG
    GGAGTGGGAG TTCATGGGGT AGCTCGTGCC GTAGCAGTGG TTGACCCTGC

101 ATATGGAGAA GATCTGGCAC CACACCTTCT ACAACGAGCT GCGTGTGGCG
    TATACCTCTT CTAGACCGTG GTGTGGAAGA TGTTGCTCGA CGCACACCGC

151 CCCGAGGAAC ACCCCGTGCT GCTCACGGAG GCTCCCCTCA ACCCCAAGGC
    GGGCTCCTTG TGGGGCACGA CGAGTGCCTC CGAGGGGAGT TGGGGTTCCG

201 CAACAGGTAG GTGTCTCTCG TCCAGTGCGT CCGCACTTGT ATACATCTTG
    GTTGTCCATC CACAGAGAGC AGGTCACGCA GGCGTGAACA TATGTAGAAC
```

S. frugiperda Actin-2

```
251 ATTGTACTTG ATACATGCCG TCCCAGTTTG TATAGAGCGC CAGCTGACCG
    TAACATGAAC TATGTACGGC AGGGTCAAAC ATATCTCGCG GTCGACTGGC

301 TGCCGTTTGT TTCGCAGAGA GAAGATGACA CAGATCATGT TCGAGACCTT
    ACGGCAAACA AAGCGTCTCT CTTCTACTGT GTCTAGTACA AGCTCTGGAA

351 CAACACGCCC GCCATGTACG TCGCCATCCA GGCTGT

    GTTGTGCGGG CGGTACATGC AGCGGTAGGT CCGACA
```

Act-2

***Figure 3.9*- Sequence of *S. frugiperda Actin* plasmid.** Panel A shows the ligation of the *S. frugiperda* actin sequence into position 52 of the Promega pGem-T Vector. Panel B shows the complete sequence of *S. frugiperda* actin plasmid sequence. Using purified *S. frugiperda* total DNA as a template, the actin sequence was amplified by PCR using primers Act-1 (5'–GGACAGAAGGACTCGTACGTAGG-3') and Act-2 (5'–CAGCCTGGATGGCGACGTACAT-3') that are illustrated in red to produce a 386bp product. The purified DNA fragment was ligated into pGem-T vector at position 52 (panel A). Afterwards, the completed *S. frugiperda* actin plasmid was sequenced (panel B). The sequence highlighted in blue indicates an intron. The sequence underlined in black indicates the position of the q-PCR primers *Sfrugiperda*Actin-1 (5'-CGAGGCCCAGAGCAAGAGAG-3') and *Sfrugiperda*Actin-2 (5'-CGCACTGGACGAGAGACACC-3') to give a 203bp product.

To visualise the homology between the three sequences, the program Gene Doc was used. Predominantly, the 100% identity (green) between sequences was observed at the exon sequences that are located either side of the intron. The intron of the *S. frugiperda* actin DNA sequence spanned positions 207 to 317 in contrast to *H. armigera* actin sequence, which was 24bp shorter in length.

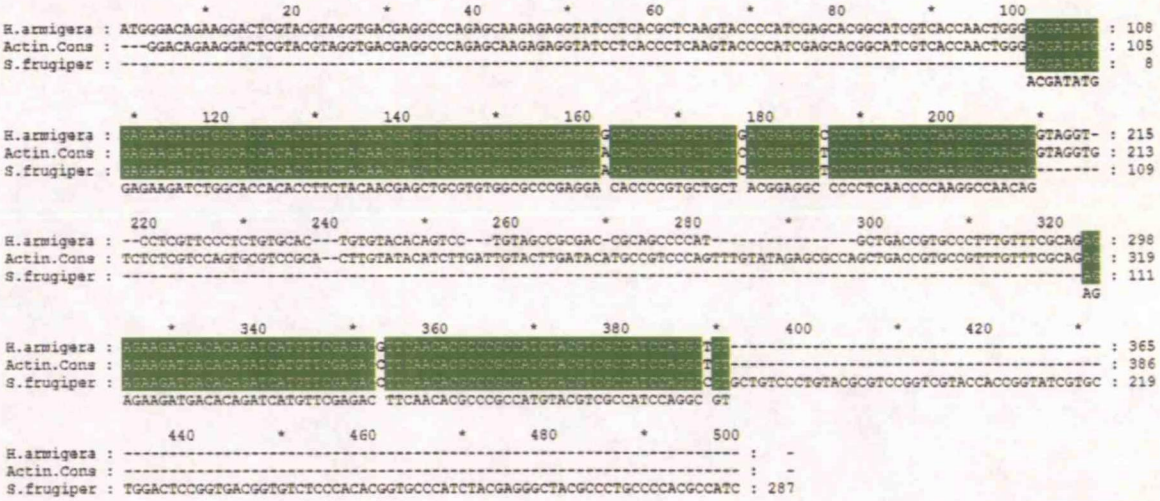

***Figure 3.10* – Complete alignment of actin nucleotide sequences.** Nucleotide sequences from *H. armigera* actA3a gene (Genbank: X97614), *S. frugiperda* partial actin cDNA (Genbank: AF548015) and *S. frugiperda* actin construct (Figure 3.9) were aligned using Clustal X (version 1.83).Using Gene Doc software one shading level was set: Green for 100% identity.

Finally, using the confirmed sequence as a template, two primers (S.frugiperda-1 and S.frugiperda-2) were designed to amplify a 203bp product of the *S. frugiperda* actin coding region during the q-PCR cycling process (Fig 3.9, panel B). The viral DNA calibration curve was established using *ie1*-specific primers (denoted ACIE1-1 and ACIE1-2) that are located at genomic coordinates of 127629 and 127858 respectively. The resulting product amplified from the use of these primers was a 229bp product of the AcMNPV genome (data not shown).

Prior to the commencement of the study, each standard was serially diluted a total of five to six times to check the correlation of the curve with respect to the concentration of DNA and the cycle threshold (Ct). The Ct corresponds to the value where the amplification curve crosses the threshold line (Anon, Rotorgene 6000 Online help, no

date). The threshold was calculated automatically by the Rotorgene 6000 program by scanning a graph like Figure 3.11, to find a setting that gave optimal estimates of the standard concentrations (Anon, 2006). In Figure 3.11, the threshold line was automatically calculated at 0.018 normal fluorescence units. According to Anon (2006), the Rotorgene 6000 program then scanned the threshold levels of the listed standards to obtain the best fit of a standard curve by maximising the R^2 value (Correlation coefficient) to approach 1.0 as closely as possible. This step was essential in determining the concentration of total sample DNA required that would be detectable within the limits of the standard curves. Using the actin construct, it was determined that the optimum concentration of extracted total sample DNA per sample was 2.63 x 10^{-4}µg/µl (Fig 3.11). However, within the water control (Fig 3.11, sample 6), one of the replicates showed the presence of a product with a high Ct value. This may be due to the presence of a primer dimer reaction product, which is a more probable explanation as the Ct value is so high compared to the samples.

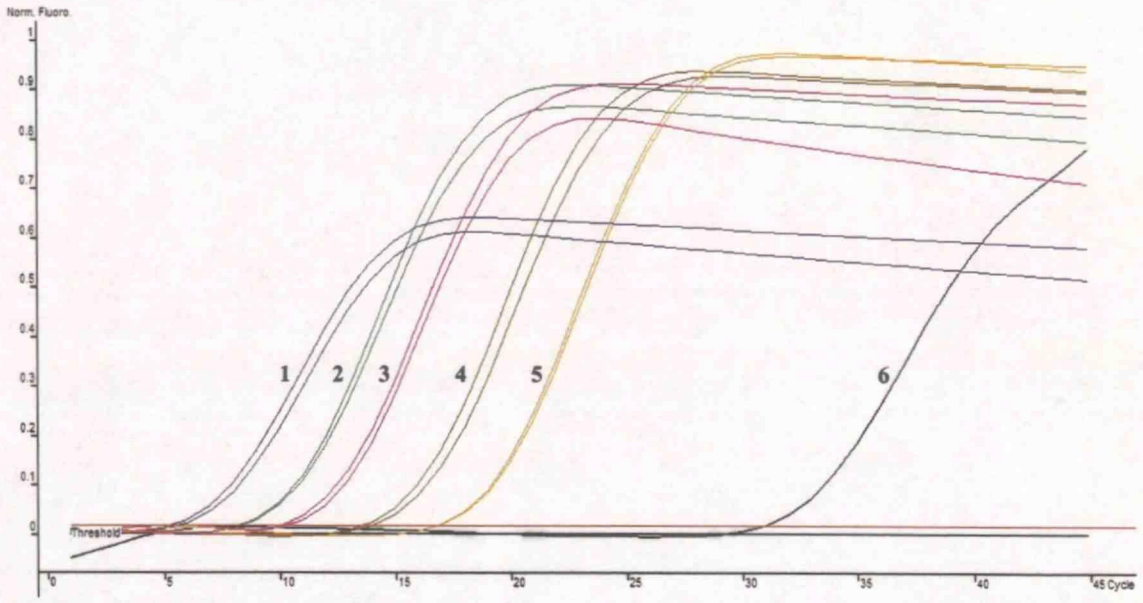

***Figure 3.11* - Cycling profile of serial dilutions of *S. frugiperda* actin standards using q-PCR.** *S. frugiperda* actin construct was serially diluted from 2.63 x 10^{-3} µg/µl to 2.63 x 10^{-7} µg/µl. Lines 1 to 5 represent *S. frugiperda* actin construct concentration from 2.63 x 10^{-3}µg/µl to 2.63 x 10^{-7}µg/µl in serial dilutions. Line 7 represents water as a negative control. Each pair of lines on the graph represents the fluorescence value of the two replicates. The threshold line is represented by a pink horizontal line set at 0.018 normal fluorescence values, which was calculated automatically by the Rotorgene 6000 program.

3.2.4.2 Analysis of DNA replication in AcMNPV, VLD1 and AcORF6^{3260}-1-infected cells.

To measure DNA replication by each virus, the number of *ie-1* copies per host cell was calculated. For each virus experiment, total DNA was analysed at 260nm to calculate DNA concentration and by agarose gel electrophoresis to check the integrity of the DNA sample. The samples were diluted to 2.63 x 10^{-4}µg/µl and mixed with SYBR green fluorescent dye and either *Sf*-21 actin or AcMNPV *ie-1*-specific gene primers before commencement of q-PCR. Each virus sample was set up in duplicate and q-PCR repeated three times before an average copy number value determined. Using Rotor-gene, version 6.0 software the fluorescent levels received from the q-PCR were interpreted graphically and numerically. Only *actin* or *ie-1* calibration curves (Fig 3.12, panels A or B) with a R^2 value of >0.99 were accepted and used as a means to calculate individual copy numbers of host *actin* or viral *ie-1* products. The R^2 value or correlation coefficient is defined by Anon (2006) as the percentage of data which matches the hypothesis that the given standards for the actin construct or AcMNPV DNA forms a standard curve. After each cycling run, a melt step was used and the sample or standard temperature increased at a linear rate and the fluorescent recorded (Anon, 2006). The recorded data is represented on a graph (data not shown) to help visualise the dissociation kinetics of the amplified products (Anon, 2006). The melt curve analysis examined the derivative of raw data from each experiment and calculated the melting temperature for each sample and standard; grouping them together according (Anon, 2006). This analysis was essential and helped to detect any significant levels of unspecific binding of the negative control (Water).

A)

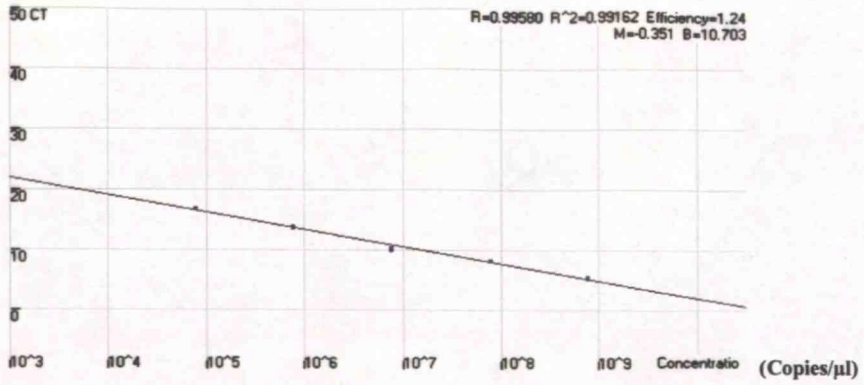

B)

***Figure 3.12* – Examples of standard calibration curves used for real-time PCR analysis of viral DNA replication.** Panel A represents the *S. frugiperda* actin plasmid construct calibration curve generated from duplicate samples of purified plasmid DNA serially diluted from 2.63 x 10^{-3}µg/µl to 2.63 x 10^{-7}µg/µl. Panel B represents AcMNPV IE-1 calibration curved generated from duplicate samples of AcMNPV DNA purified from a caesium chloride gradient serially diluted from 1.042 x 10^{-2}µg/µl to 1.042 x 10^{-6}µg/µl. The cycle threshold (Ct) corresponds to the value where the amplification curve crosses the threshold line (Corbett Research, Rotor-gene 6000 Program, and Online help). Correlation value (R^2) for panel A = 0.99162, panel B = 0.99599). The correlation value of all the standard curves was >0.99.

After each *ie-1* copy number value was calculated for each virus, the number of viral copies per cell was determined by simple division of the corresponding actin and *ie-1* values at the same time-point (Table 3.1). These final values are represented on the graph in Figure 3.13, which displays each virus DNA replication level as a measurement of log virus copy number per host cell number over 24hpi.

Typically, the wild-type virus showed a steady increase in DNA replication between 3 and 16hpi, peaking at the latter time before increasing only slightly up to 24hpi.

The AcORF6^{3260}-1 viral phenotype exhibited DNA replication levels very similar to the wild-type. The only exception to this observation was the apparent increase in viral copy number per cell from 9hpi, peaking at 3.7 log values at 12hpi compared to the wild type virus of 3.25 log values. Meanwhile, the VLD1 phenotype had a more delayed response with lower levels of DNA replication compared to wild-type AcMNPV at a time up to 16hpi. Progression into the late phase of infection yielded higher values of replication for the VLD1 virus, with similar results observed at 24hpi with AcMNPV. Uninfected total DNA was used as a negative control and unsurprisingly yielded negligible results of very low log values.

3.2.4.3 Comparison of DNA replication levels between VLD1 and AcORF6^{3260} -1 viral phenotypes.

By extrapolating data from the graph in Figure 3.13, the differences in DNA replication between the two viral *lef*-2 phenotypes were readily apparent (Fig 3.14). Up to 16hpi, higher levels of DNA replication were observed with the AcORF6^{3260}-1 virus. The initial delay in DNA replication that characterised the VLD1 phenotype in *Sf*-21 cells and resulted in less newly synthesized DNA in these cells was largely overcome by 24hpi. At 48hpi, the VLD1 copy number had surpassed that of AcORF6^{3260}-1.

Table 3.1- **Viral and host copy number calculations for AcMNPV, VLD1 and AcORF6^{3260}-1 viruses over 48hpi.**

AcMNPV	**3hpi**	**6hpi**	**9hpi**	**12hpi**	**16hpi**	**24hpi**	**48hpi**
Viral (*ie1*)	2636.45	16369.51	81529.17	104666.83	2404678.59	935066.35	632301.63
Host (*Actin*)	437.04	505.33	164.25	110.14	1818.17	497.90	145.78
Viral copy number/cell	**6.03**	**32.39**	**496.36**	**950.30**	**1322.58**	**1878.01**	**4337.47**
VLD1							
Viral (*ie-1*)	31.44	50.48	988.59	3326.44	15059.25	409378.98	168934.85
Host (*Actin*)	14.28	18.43	61.10	25.66	14.63	120.10	9.44
Viral copy number/cell	**2.20**	**2.74**	**16.18**	**129.61**	**1029.27**	**3408.62**	**17895.16**
AcORF6^{3260}-1							
Viral (*ie-1*)	122.63	6530.45	64566.91	122.63	96118.56	187873.31	79200.80
Host (*Actin*)	19.32	144.01	189.24	99.22	20.26	24.59	8.61
Viral copy number/cell	**6.35**	**45.35**	**341.19**	**2694.99**	**4744.87**	**7641.66**	**9195.04**
Uninfected							
Viral (*ie-1*)	12.21	7.13	6.95	7.28	8.60	3.50	1.56
Host (*Actin*)	9.62	6.45	6.08	11.39	10.87	10.56	4.52
Viral copy number/cell	**1.27**	**1.11**	**1.14**	**0.64**	**0.79**	**0.33**	**0.35**

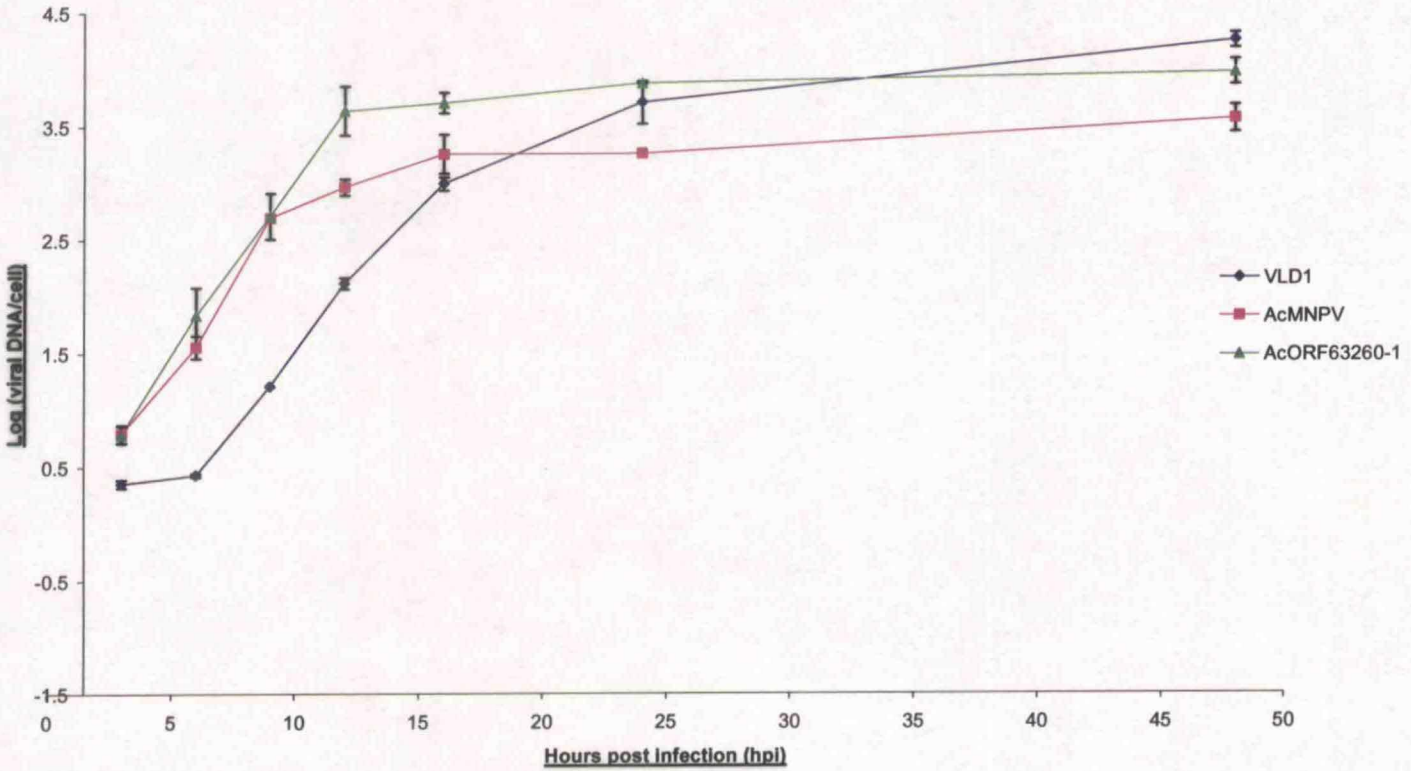

Figure 3.13 - **Quantitative analysis of replicated viral DNA in infected-*Sf*21 cells (MOI 10) over 48hpi.** Total intracellular DNA was isolated from duplicate samples from each time-point per virus. Each point indicates the average over three runs of q-PCR and the y-axis error bars represents the standard error.

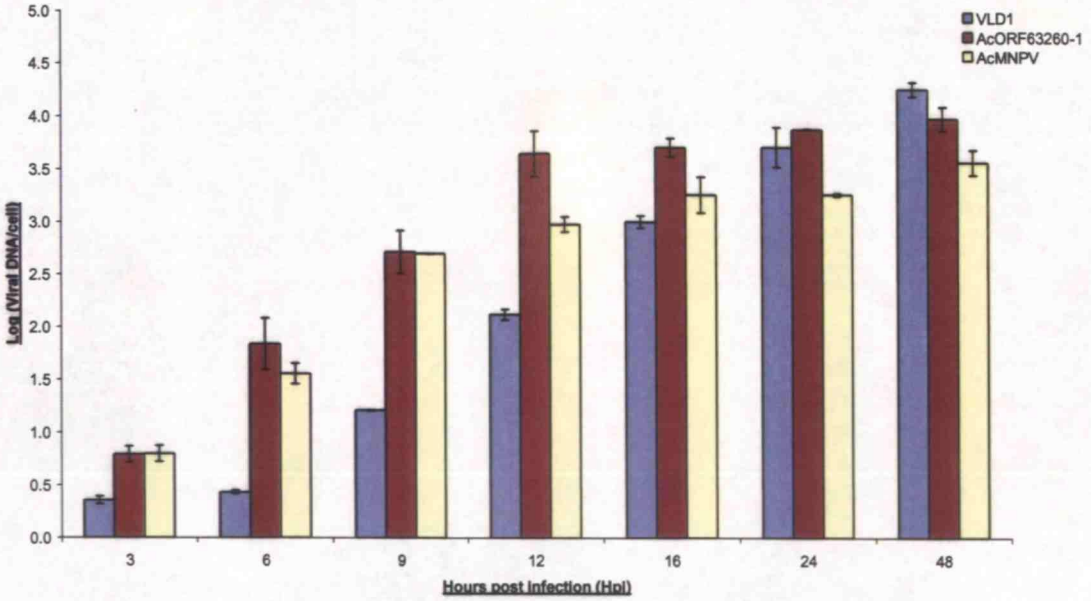

***Figure 3.14* – Comparison of DNA replication levels between AcMNPV and two *lef*-2 mutants by q-PCR analysis.** Results have been extrapolated from Figure 3.13 to highlight the apparent differences in DNA replication between viruses.

3.2.5 Analysis of DNA replication levels of AcMNPV and AcORF6^{3260}-1, over 48hpi.

The examination of DNA replication levels in AcMNPV, VLD1 and AcoRF6^{3260}-1 viruses over 24hpi were in approximate agreement with past research (Merrington *et al.*, 1996). Moreover, the discovery of an additional mutation within the VLD1 *lef*-2 at position 154 (Fig 3.8), led to the elimination of this virus from future work investigating the consequences to DNA replication. To further validate the apparent similarities between AcMNPV and AcORF6^{3260}-1 DNA replication levels an additional control was employed.

The temperature-sensitive mutant (Ts8b) is deficient in DNA replication at the non-permissive temperature 33°C and does not form plaques (Fig 3.15). In contrast, the Ts8b virus does replicate normally and produce plaques at the permissive temperature of 25°C (Fig 3.16). By using the Ts8b virus, I wanted to check that an expected difference in DNA replication was actually recorded in the q-PCR. The Ts8b virus

further provided a positive and negative control for virus replication in *Sf*-21 cells. The same method of measuring DNA replication by q-PCR was employed throughout this study as used in 3.2.4. Total DNA was extracted from AcMNPV, AcORF6^{3260}-1 and mock infected-cells incubated at 28°C, plus Ts8b-infected cells at either 25°C or 33°C. The replication profile for each virus was obtained by measuring the viral copy number (*ie-1*) per cell copy number (*actin*) (Fig 3.17).

In agreement with the results shown in Figure 3.8, the AcORF6^{3260}-1 virus DNA replication levels were slightly higher than AcMNPV (Fig 3.17). Furthermore, DNA replication of Ts8b incubated at 25°C was also similar to the wild-type AcMNPV. The same Ts8b mutant virus incubated at the non-permissive temperature of 33°C yielded significantly lower DNA replication levels than at the permissive temperature of 25°C. The levels of Ts8b DNA replication was higher than expected at the non-permissive temperature. According to Gordon and Carstens (1984); Erlandson *et al*, (1984), DNA replication by Ts8b should have been negligible. This led to the question of how accurate the incubator temperatures were during the study. As with all of the work concerning the Ts8b virus, a tiny tag extra monitor TGX-3580 (Serial Number 255506) was placed inside the incubator 1-1½ hours prior to record the temperature at five minute intervals before and during the experiment. To account for the apparent observation of DNA replication with the Ts8b virus at 33°C, the temperature inside the incubator was analysed. To confirm that the incubator responsible for the non-permissive temperature was inaccurate, it was monitored on a further two occasions. This involved monitoring the incubator over 3 days at different temperatures to determine the correct setting for 33°C.

To determine if Ts8b DNA replication was prevented at 33°C, the above experiment was repeated with the incubator set to the apparent temperature of 34.5°C, which empirical testing had shown to produce an actual temperature of 33.8°C. Therefore, a second experiment was repeated with AcMNPV, AcORF6^{3260}-1, Ts8b and uninfected- *Sf*-21 cells at permissive and non-permissive temperatures. The *Sf*-21 cell pellets were harvested at 9.6hpi and 24.0hpi from both incubator temperatures. Afterwards, the total DNA was extracted from each sample and stored at 4°C. The

replication of viral DNA was determined by q-PCR and calculated based on the number of *ie-1* copies per cell. According to Figure 3.18, both the AcMNPV and AcORF6^{3260}-1 exhibited DNA replication at the permissive temperature of 25°C at 9.6hpi. In contrast, both AcMNPV and AcORF6^{3260}-1 DNA replication levels were higher at the non-permissive temperature, extracted at 9.6hpi. The Ts8b virus exhibited DNA replication at 25°C but was defective at 33°C.

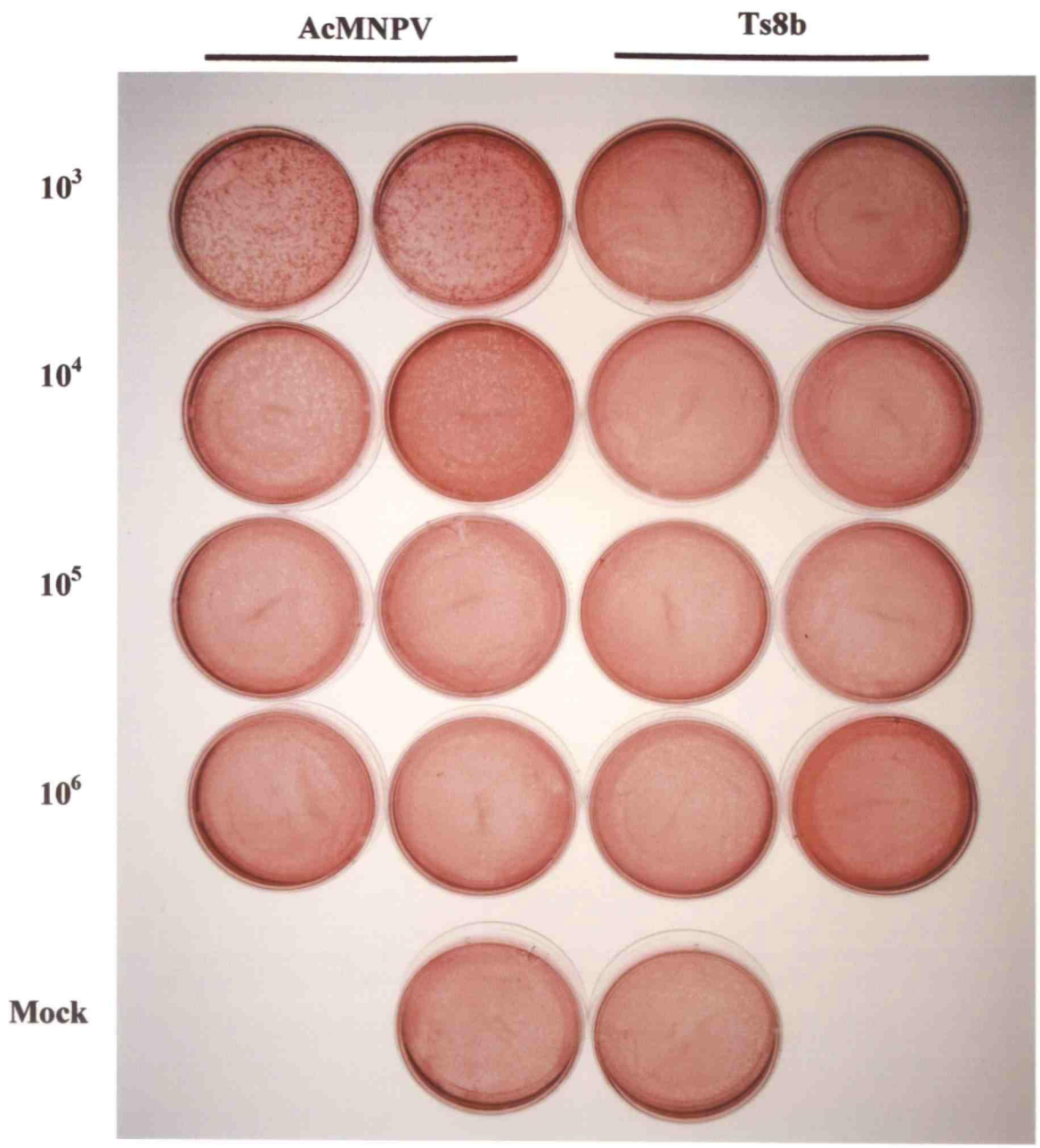

Figure 3.15 **–Standard Plaque Assay of AcMNPV and Ts8b virus at 33°C after 4 days post infection.** Dishes of 35mm diameter seeded at 1.5 x 10^6 *Sf*-21 cells infected with serial dilutions of AcMNPV or Ts8b and left at 33°C for 6 days until plaques were clearly visualised with neutral red stain.

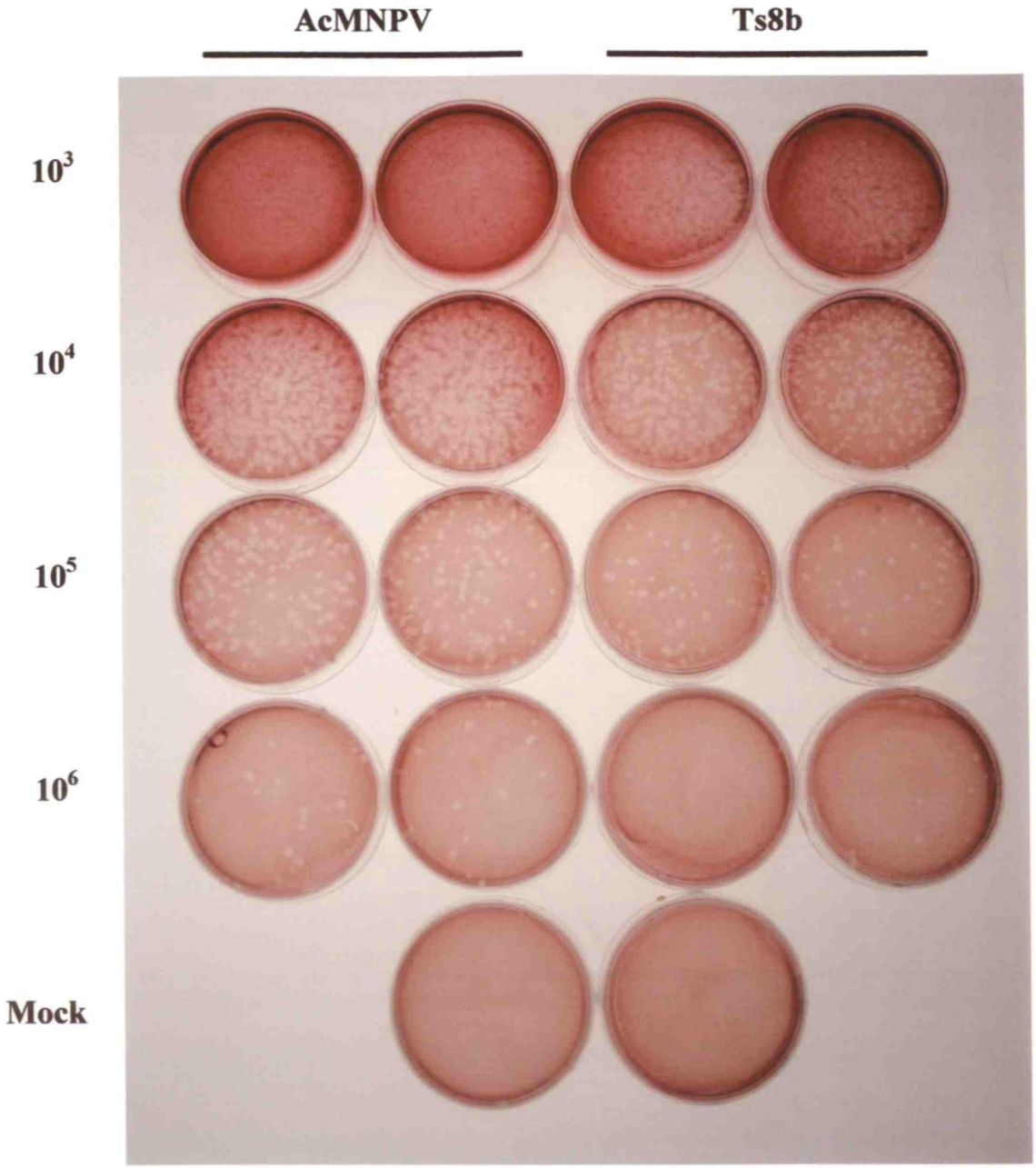

Figure 3.16 **–Standard Plaque Assay of AcMNPV and Ts8b virus at 25°C after 6 days post infection.** Dishes of 35mm diameter seeded at 1.5 x 10^6 *Sf*-21 cells infected with serial dilutions of AcMNPV or Ts8b virus and left at 25°C for 4 days until plaques were clearly visualised with neutral red stain.

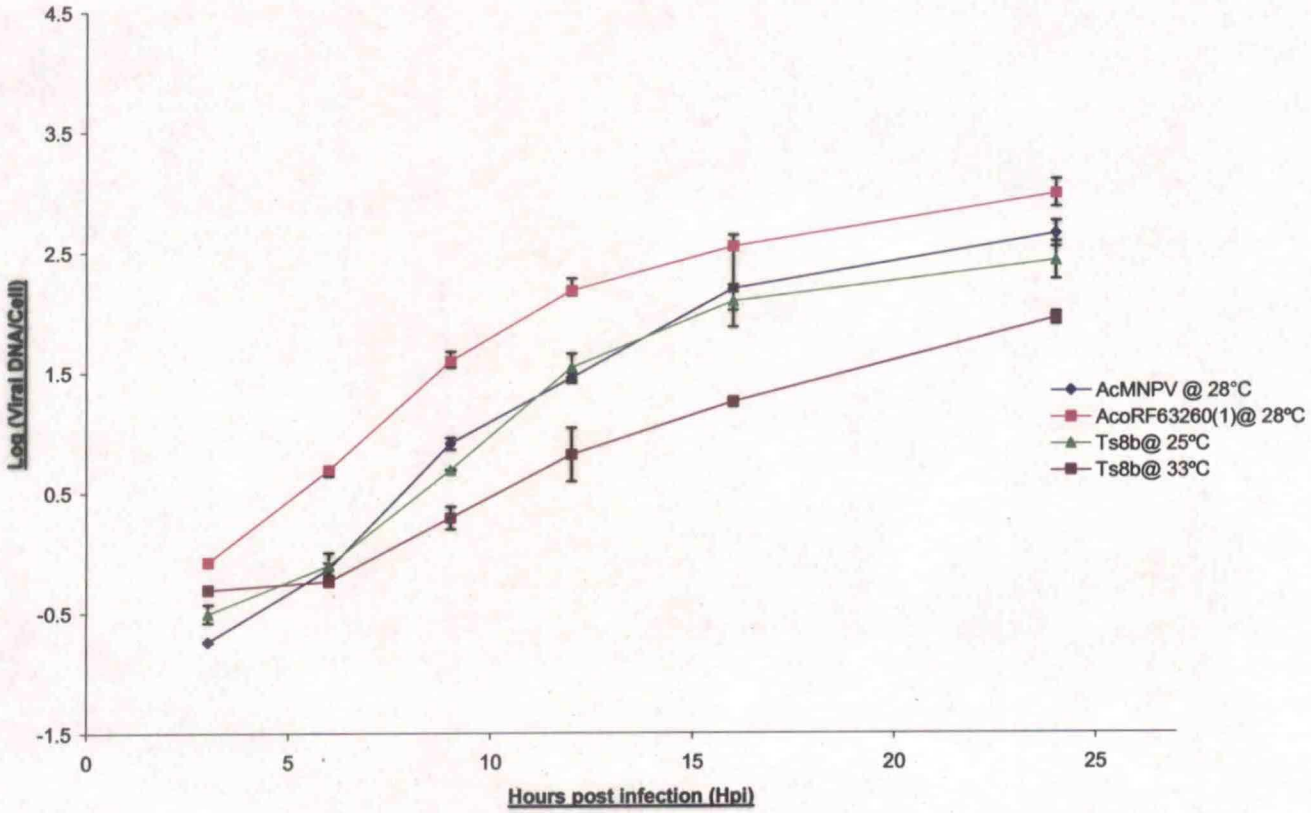

***Figure 3.17* - Quantitative analysis of replicated viral DNA detected in infected-*Sf*21 cells (MOI 10) over 24hpi.** Total intracellular DNA was isolated from duplicate samples from each time-point per virus. Each point indicates the average over three runs of q-PCR and the y-axis error bars represents the standard error.

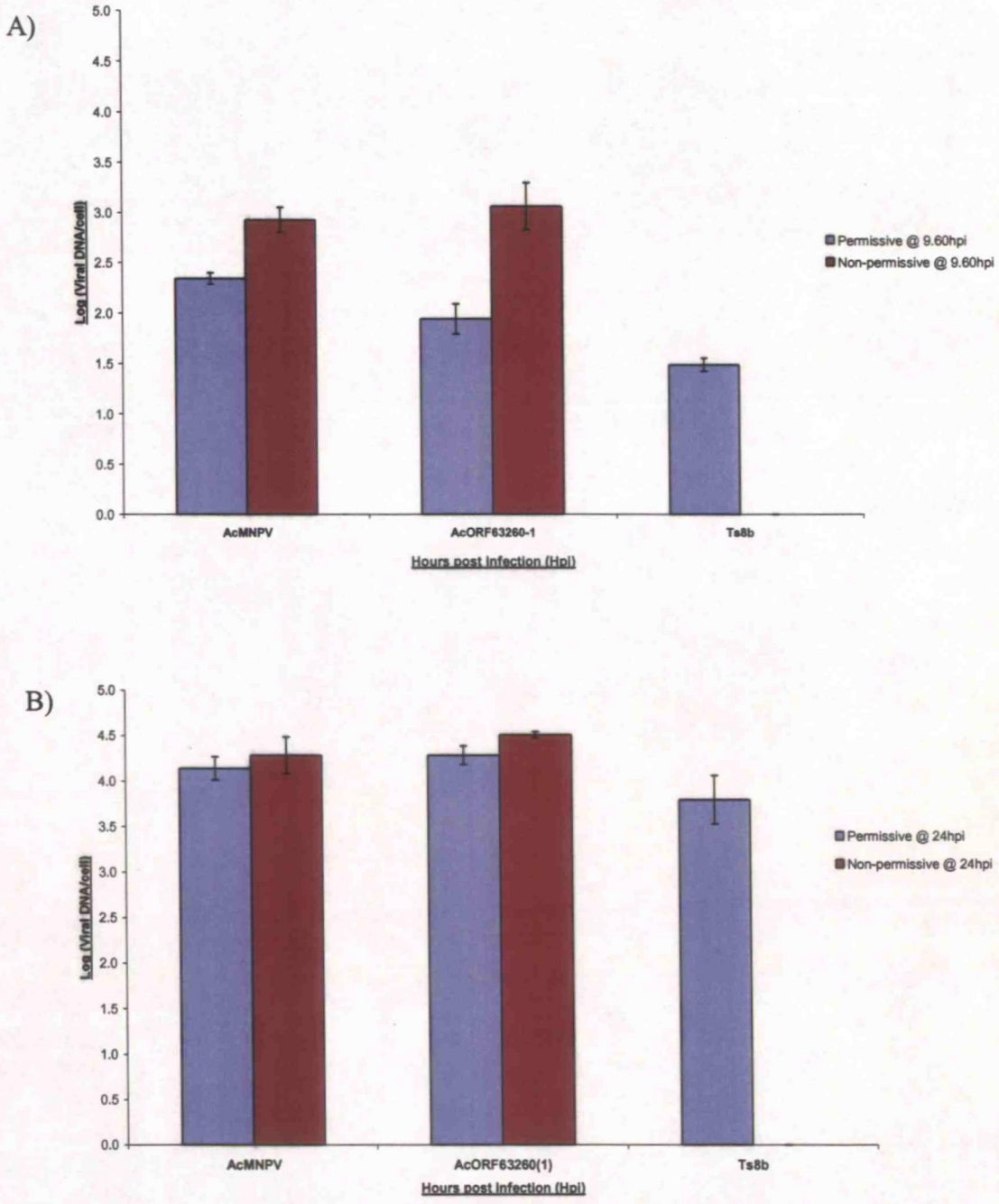

***Figure 3.18*- Quantitative analysis of viral DNA replication detected in infected-*Sf*21 cells (MOI 10) at permissive or non-permissive temperatures at 9.60 and 24hpi respectively.** Total intracellular DNA was extracted from virus infected cells at 9.60hpi (panel A) or 24hpi (panel B) (Permissive temperature of 25°C, non-permissive temperature of 33°C) from duplicate samples from each time-point per virus. Each point indicates the average over three runs of q-PCR and the y-axis error bars represents the standard error.

3.2.6 Primer extension analysis of late and very late genes transcribed by either AcMNPV or AcORF6^{3260}-1 virus.

The extra mutation within *lef*-2 of VLD1 rendered it unsound to analyse any gene expression by this virus, as any differences with AcMNPV could not be attributed to a point mutation. Therefore, AcORF6^{3260}-1 was used in further analysis. To determine the transcription site and level of specific late and very late RNA transcripts expressed by AcMNPV and AcORF6^{3260}-1 at 24hpi, primer extension analysis was used. Dishes of 2.5 x 10^7 *Sf*-21 cells were left overnight at 28°C and infected at a MOI of 6 with either AcMNPV or AcORF6^{3260}-1. Afterwards total RNA was extracted from each cell pellet harvested at 24hpi using the guanidinum/hot phenol method. The extracted RNA concentration was determined and the integrity of the nucleic acid analysed by agarose gel electrophoresis. The total RNA was then mixed with [γ-^{32}P] ATP-labelled primer either designed for *polyhedrin* (RDP511), *capsid* (SIDEX), or *39K* (RDP514). After the primer had annealed, cDNA was produced using the total RNA as a template. The samples were then loaded onto a 6% polyacrylamide gel and run alongside the respective sequencing ladder depending on the gene to be examined. The *polyhedrin* sequencing ladder was generated from a plasmid and both the *capsid* and *39K* ladders were generated by PCR with primers RDP527/ SIDEX and RDP514/RDP526 respectively using AcMNPV DNA as a template. Then, 1µg of each plasmid or PCR DNA template was mixed with individual [γ-^{32}P] ATP-labelled primers (*polyhedrin* – RDP511, *capsid* – SIDEX, and *39K* – RDP514) and Thermo Sequenase DNA polymerase to produce four separate lanes on the polyacrylamide gel through PCR that correspond to the four letters adenine, thymine, cytosine, and guanine of the DNA sequence.

The AcORF6^{3260}-1 virus was clearly deficient in very late gene expression, which was evident from analyses from virus-infected cells (Fig 3.19). Figure 3.19, panel A indicated a difference in *polyhedrin* transcription between AcMNPV and AcORF6^{3260}-1. AcMNPV-infected *Sf*-21 cells exhibited high levels of *polyhedrin* transcription at 24hpi (Fig 3.19, panel A, lane 1). In comparison, transcription levels produced by AcORF6^{3260}-1-infected cells were much reduced. Both sets of

polyhedrin transcripts were initiated at the T base pair of the late TAAG promoter motif. The AcORF6 ^{3260}-1 virus was derived from a cotransfection into insect cells with linearised pBacPAK6 and a *lef*-2 modified baculovirus transfer vector pAcCL29 (Merrington *et al.*, 1996). This produced small and colourless virus plaques. According to Merrington *et al* (1996), the *LacZ* coding region of the parental virus was replaced by a polyhedrin gene retaining only the sequence for the polyhedrin promoter and 3' untranslated region. However the polyhedrin coding region was replaced back into the recombinant viruses by cotransfection with a plasmid containing the polyhedrin gene and the viruses selected as polyhedrin positive plaques. Table 3.2 summarises the generation of viruses such as AcORF6^{3260}-1 that were used or referenced to in this chapter.

From previous work by Thiem and Miller (1989), it was suggested that at least three initiation sites for *capsid* transcription are present as described by nuclease protection and primer extension studies. This was further confirmed by primer extension experiments (Fig 3.19, panel B) comparing both viruses at 24hpi. Both viruses showed three sets of transcripts being expressed at 24hpi, with the two major *capsid* transcripts being initiated at the first A of the TAAG sequence. A third *capsid* transcript was identified as the least abundant of the three and was located much further away from the primer site. Interestingly, both viruses exhibited *capsid* transcripts levels that were visibly very similar to each other. The apparent difference that was observed with primer extension of *polyhedrin* transcription between AcMNPV and AcORF6^{3260}-1 viruses was not present with the *capsid* late gene. The same pattern of similarity examined during *capsid* primer extension analyses between both viruses was moreover observed with *39K* transcripts (Fig 3.19, panel C). Only one late transcript was evident per virus and was initiated at the T base pair of the TAAG promoter sequence.

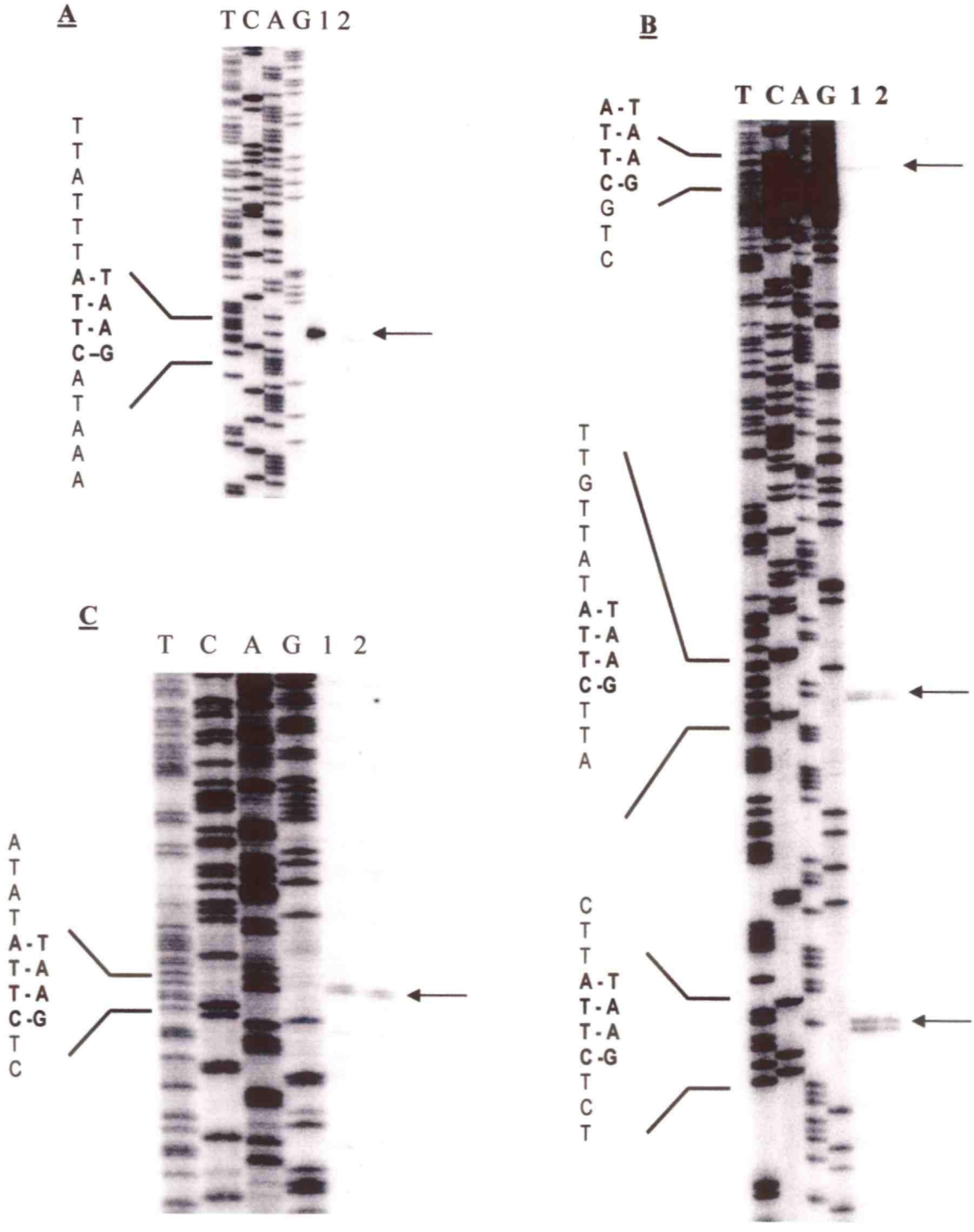

***Figure 3.19* - Primer extension analysis from late and very late promoters.** All primer extension product RNA transcripts were isolated and extracted from either AcMNPV (Lane 1) or AcORF6^{3260}-1 (Lane 2) infected *Sf*-21 cells at 24hpi. All of the primer extension products were run on a polyacrylamide sequencing gel alongside a DNA sequencing ladder generated from the same primers used in each sample. Panel A is the primer extension analysis of the *in vitro* transcribed polyhedrin, panel B, capsid and panel C, 39K. Arrows indicate the presence of primer extension RNA transcripts.

***Table 3.2*- A description of AcUW1.*lacZ*, AcMNPV, VLD1, BacPAK6 and AcORF6^{3260}-1 viruses used or referenced to in Chapter Three.**

Virus	Reference	Description of Virus
VLD1	Merrington *et al* (1996).	This virus was generated through the use of *Sf*-21 cells to propagate the AcUW1.*lacZ* recombinant virus in the presence of BrdU. The progeny viruses produced from theses cells were re-titred using a plaque assay to provide 1 to 20 plaques per dish. The dishes were screened for the presence of colourless, polyhedrin-negative plaques by staining with X-gal and neutral red. From a total of 160 plaques, 64 plaques exhibited the correct phenotype. Subsequent titrations were carried out and only 5 of the viruses produced colourless, polyhedrin-negative plaques. These viruses were denoted Very Late Deficient (VLD) 1-5.
AcORF6^{3260}-1	Merrington *et al* (1996).	This virus was generated by the cotransfection into insect cells of linearised BacPAK6 and a modified baculovirus transfer vector pAcCL29 (that possessed the single point mutation identified within *lef*-2 in VLD1). This produced small colourless virus plaques. The *LacZ* coding region of the parental virus was replaced by a polyhedrin gene retaining only the sequence for the polyhedrin promoter and 3' untranslated region. However the polyhedrin coding region was replaced back into the recombinant viruses by cotransfection with a plasmid containing the polyhedrin gene and the viruses selected as polyhedrin positive plaques.
AcMNPV		*Autographa californica* multinucleopolyhedrovirus C6 Strain
AcUW1.*lacZ*	Merrington *et al* (1996).	A recombinant virus with a normal polyhedrin gene and the *lacZ* coding region under the control of the *p10* promoter replacing the native *p10* coding sequence. *Polyhedrin* is retained at its native locus.
BacPAK6	Kitts and Possee (1993).	BacPAK6 contains an *E. coli lacZ* insert at the polyhedrin locus and Bsu36I restriction enzyme sites in the two flanking genes on either side of *lacZ*. Digestion with Bsu36I removes the *lacZ* insert and a fragment of an essential gene (ORF 1629) producing linear virus DNA that is unable to replicate within insect cells.

3.2.7 Analysis of late and very late gene expression profiles of AcMNPV and AcORF6^{3260}-1 viruses using q-PCR.

The use of primer extension for quantitative work was time consuming and difficult due to the need for extensive use of polyacrylamide gel analysis. Therefore, primer extension was superseded by real time-PCR (q-PCR) technology that offered a better way of looking at expression and provided statistical analysis. Dishes of *Sf*-21 cells (in duplicate) were infected with AcMNPV or AcORF6^{3260}-1 at MOI of 10 and incubated at 28°C. Total RNA was extracted from each sample using RNeasy Mini extraction kit. Afterwards, 2µg of total RNA was treated with DNase A to eliminate any carry over of contaminating DNA from the purification columns.

As an additional measure in the experiment, a negative control (RNase-free water) was employed to undergo the same treatment as the RNA samples. This control was important in determining any background contamination that may be present in cDNA samples as a result of the methods used. Using first strand synthesis, cDNA was produced from the 2µg RNA sample using the Oligo dT Omniscript kit. One µl of each cDNA sample was mixed with SYBR green fluorescent dye and gene-specific primers before commencement of the q-PCR. Five pairs of gene-specific primers were designed to amplify a ~200bp PCR product. The gene-specific primers were representative of both late and very late baculovirus phases.

The late primers were designed to target *gp64* (GP64fin-1 and GP64fin-2) and *capsid* (Capfin-1 and Capfin-2) genes. The very late gene primers were for the *polyhedrin* (Polfin-1 and Polfin-2) and *p10* (P10fin-1 and P10fin-2) genes. Primers targeting the housekeeping *S. frugiperda* actin gene (Actin-1 and Actin-2) were designed to function as an internal control. Each set of virus samples were initially set up in duplicate and the extracted total RNA samples pooled together to increase volume levels. Afterwards, the cDNA samples produced from the total RNA were set in replicates of two and run twice with q-PCR before an average comparative concentration was calculated.

The comparative concentration for each sample was determined by calculating the relative concentration compared to the *S. frugiperda actin* internal control at the set time point. For results that yielded large y-axis error bars, the number of replicates was increased to three or five in a further different experiment. Using this range it was possible to observe any trends in values and eliminate any potential outliers that did not fit into the overall consensus.

Using the gene-specific primers denoted previously, expression profiles were generated for each of the viruses over 48hpi. The *gp64* profile of AcMNPV and AcORF6^{3260}-1 (Fig 3.20) were very similar and showed no difference in expression during 24hpi and 36hpi. As the infection progressed into the very late phase (48hpi), AcMNPV *gp64* expression increased 1.7-fold compared to a 1.1-fold increase by AcORF6^{3260}-1. The level of *capsid* expression (Fig 3.21) was greatly higher (peaking at 589.50) compared to the *gp64* expression profile which peaked at 89.44 in the instance of AcMNPV respectively. Initially, both viruses exhibited similar *capsid* expression profiles up to 36hpi. At this time point, AcORF6^{3260}-1 *capsid* expression increased and became significantly different from the wild type. Similar to the *gp64* profile (Fig 3.20) at 48hpi, the AcMNPV *capsid* expression levels dramatically increased and peaked at 559.50 compared to a value of 252.60 for the AcORF6^{3260}-1 virus.

The *p10* expression profile (Fig 3.22) showed a strong increase in expression levels between 36 and 48hpi. During the late phase (24hpi and 36hpi), both virus *p10* profiles exhibited a similar pattern to *capsid* analysis. At the peak of expression, both *p10* and *polyhedrin* expression profiles of AcMNPV yielded similar values of approximately 1600-1800. Throughout the *polyhedrin* expression analysis (Fig 3.23), it was very clear that there was a difference between both viruses. AcMNPV *polyhedrin* expression increased gradually up to 36hpi, and then in a dramatic burst it peaked at a concentration of 1804.4. In contrast, the AcORF6^{3260}-1 virus showed a much reduced level of *polyhedrin* expression.

Using a 2-sample t-test, the differences between the AcMNPV and AcORF6^{3260}-1 means per time point of a specific gene based on q-PCR data was inferred. The p-value was calculated for each time point per gene at a 95% confidence interval, assuming equal variances (Fig 3.20 to 3.23). The null hypothesis assumed that the means of the two viruses were equal and therefore no significant difference was observed. The alternative hypothesis assumed that the two virus means were not equal and therefore a significant difference was observed. If a p-value of <0.05 was calculated, then the null hypothesis was rejected and it was proposed at a 95% confidence interval that the two virus means were significantly different. However, if a p-value of >0.05 was calculated, then the null hypothesis was accepted and it was proposed that at a 95% confidence interval that there was no significant difference between the two virus means at a specific time point of that gene.

The 2-sample t-test only measured the significant difference statistically between AcMNPV and AcORF6^{3260}-1 means at a given time point for a specific gene. To try and examine the statistical differences between the two viruses as a series rather than single time points, the general linear model (GLM) was used. According to (Anon, Minitab Help, no date), the GLM is able to use analysis of variance (ANOVA) with the ability to perform multiple comparisons and fit unbalanced data. Using GLM to examine both the AcMNPV and AcORF6^{3260}-1 expression profiles over 48hpi, the only model that was determined statistically different (p-value of <0.05) between the two viruses was the factor of time (hpi). Other statistical significant differences between the two viruses were not evident despite using other models in GLM. This may have been contributed to by the number of replicates used or that the duplicates of RNA samples were pooled together to increase the small volume for q-PCR analysis.

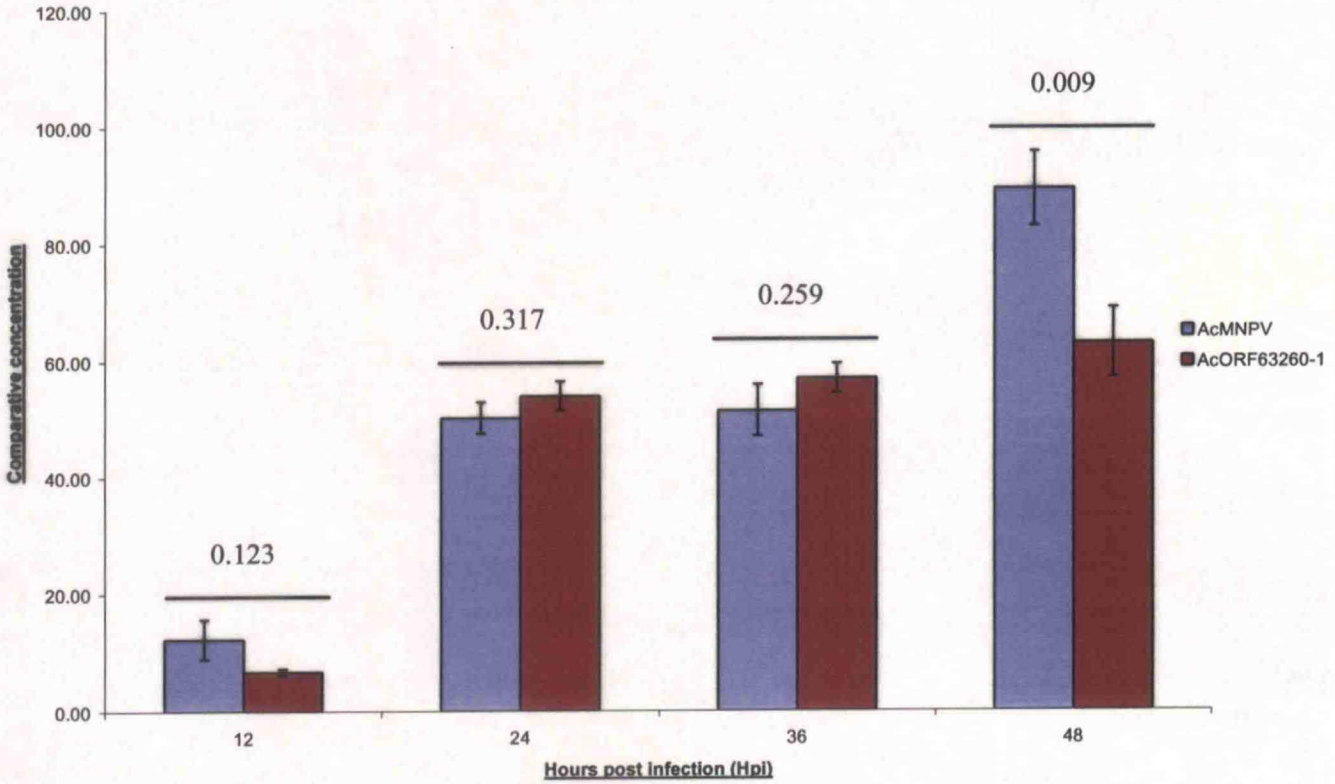

***Figure 3.20* – Q-PCR analysis of *gp64* expression over 48hpi in virus-infected cells (MOI 10).** Total intracellular RNA was isolated from each time point per virus. Each point indicates the average over two runs of q-PCR and the y-axis error bars represents the standard error. The value above the horizontal line for each time point corresponds to the p-value calculated at 95% confidence interval using a 2-sample t-test.

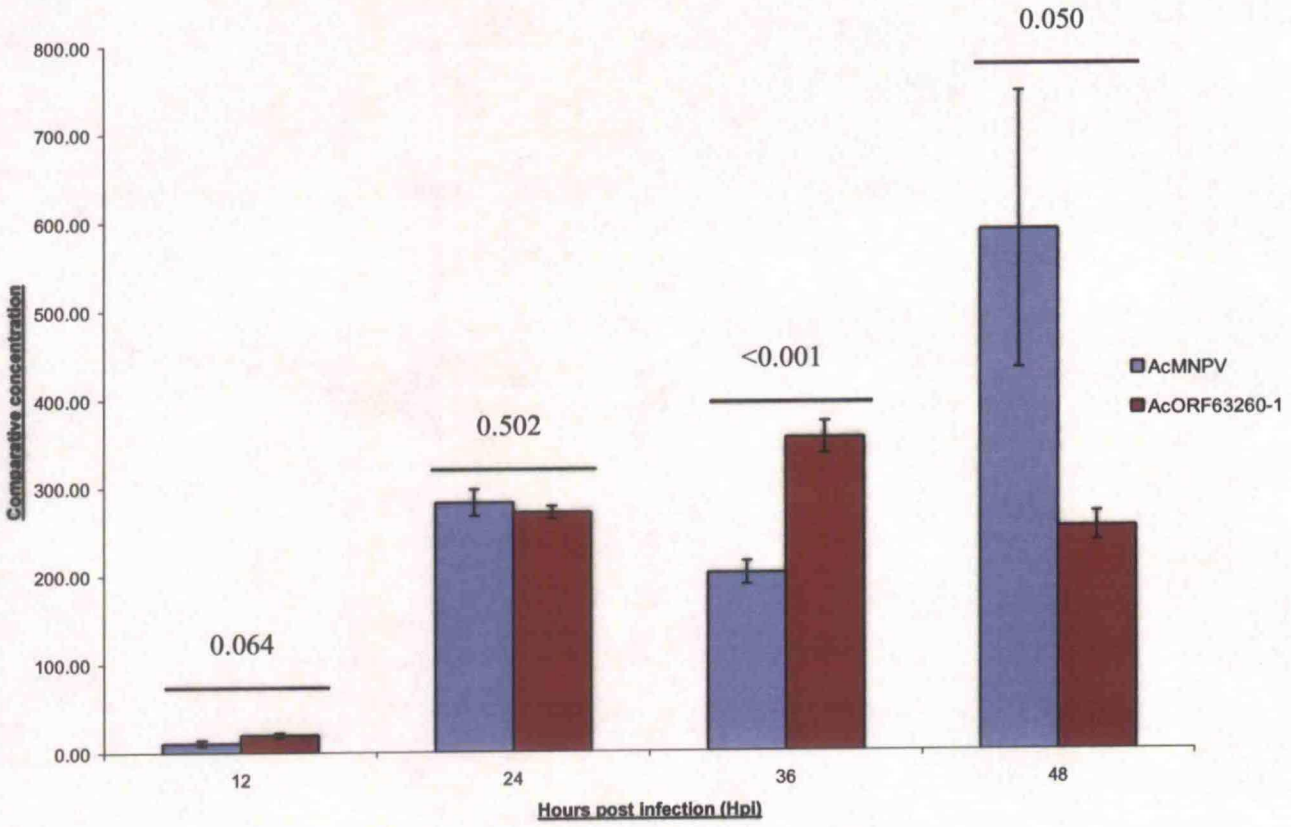

***Figure 3.21* – Q-PCR analysis of *capsid* expression over 48hpi in virus-infected cells (MOI 10).** Total intracellular RNA was isolated from each time point per virus. Each point indicates the average over two runs of q-PCR and the y-axis error bars represents the standard error. The value above the horizontal line for each time point corresponds to the p-value calculated at 95% confidence interval using a 2-sample t-test.

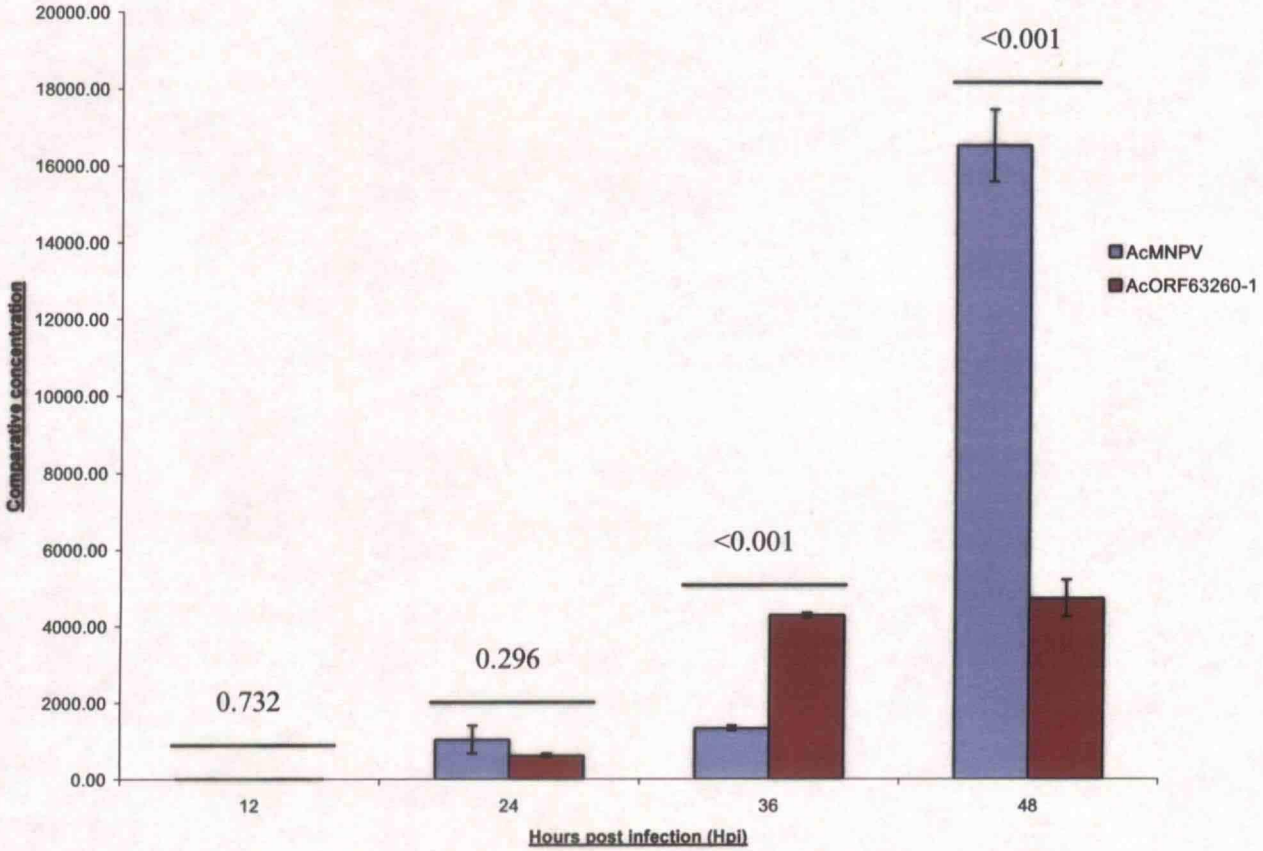

***Figure 3.22* – Q-PCR analysis of *p10* expression over 48hpi in virus-infected cells (MOI 10).** Total intracellular RNA was isolated from each time point per virus. Each point indicates the average over two runs of q-PCR and the y-axis error bars represents the standard error. The value above the horizontal line for each time point corresponds to the p-value calculated at 95% confidence interval using a 2-sample t-test.

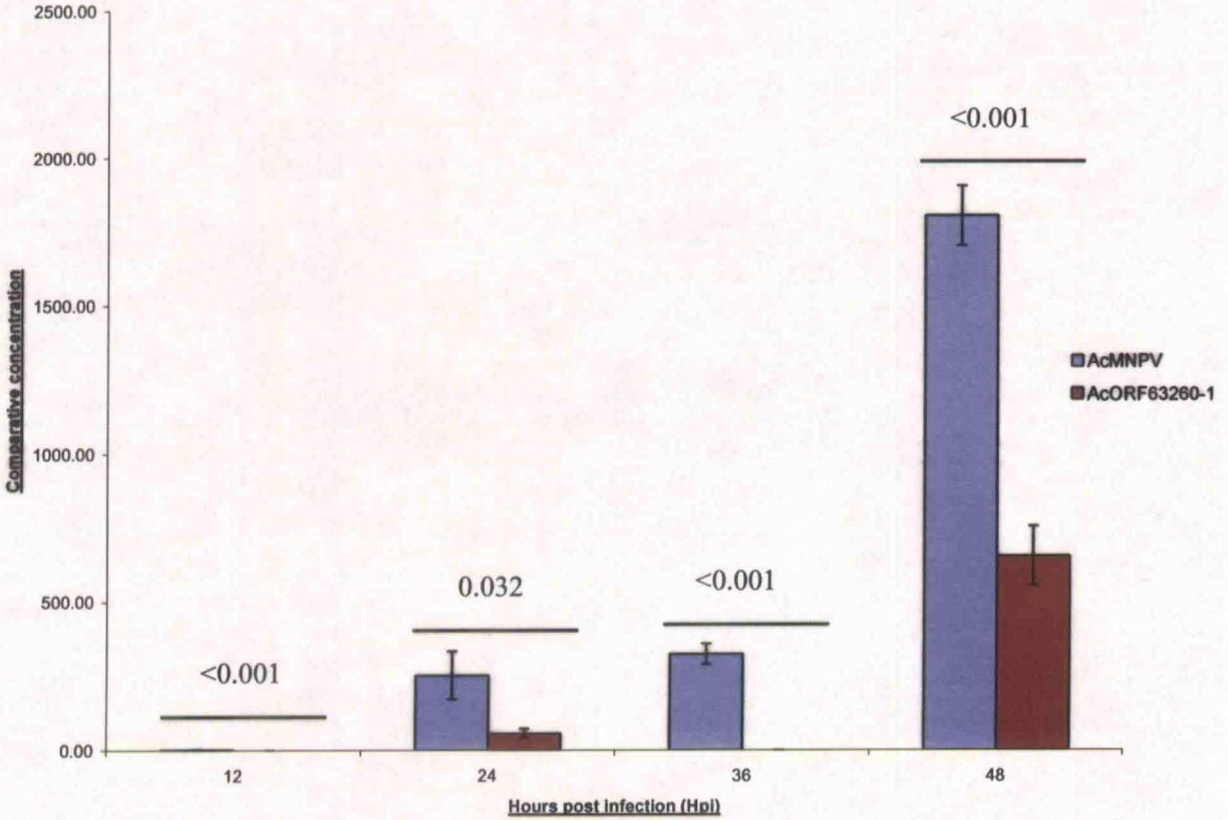

***Figure 3.23* – Q-PCR analysis of *polyhedrin* expression over 48hpi in virus-infected cells (MOI 10).** Total intracellular RNA was isolated from each time point per virus. Each point indicates the average over two runs of q-PCR and the y-axis error bars represents the standard error. The value above the horizontal line for each time point corresponds to the p-value calculated at 95% confidence interval using a 2-sample t-test.

3.3 Discussion

The aim of this chapter was to examine and identify differences between AcMNPV, VLD1 and AcORF6^{3260}-1 during gene expression and DNA replication. *Lef*-2 is well characterised for being one of six genes identified as essential for baculovirus DNA replication. The omission of this gene from a library of sub-clones during transient assays resulted in no detectable levels of plasmid replication being observed (Lu and Miller, 1995b). Further transient assays investigating late and very late gene expression suggested the involvement of *lef*-2 (Passarelli and Miller, 1993b; Lu and Miller, 1995b; Hefferon, 2004).

To identify any phenotypic differences between AcMNPV, AcORF6^{3260}-1, and VLD1 each virus was examined in either *Sf*-21 or *Tn*368Ad cell culture over 72hpi. Research examining *p35* deletion mutants found that the differential growth of these viruses in *Tn*368Ad cells was comparable to wild type AcMNPV (Kelly *et al.*, 2006). Therefore, a similar strategy was employed to observe AcMNPV, VLD1 and AcORF6^{3260}-1 in both *Sf*-21 and *Tn*368Ad cell lines. No obvious differences in cell morphology were observed between VLD1 and AcORF6^{3260}-1 in either *Sf*-21 or *Tn*368Ad cell lines between 48-72hpi. Therefore, it was decided that *Sf*-21 cells were to be used for further work. However, unlike *p35*, *p143*, *ie-2* and *lef-7*, it is apparent that in the two cell lines tested that *lef*-2 does not have cell-specific activities. To further examine the ability of all the viruses to replicate in cell culture, individual multi-step viral growth curves were established at 0.1MOI. Budded virus titres were determined by plaque assay for AcMNPV, VLD1 and AcORF6^{3260}-1. Each of the viruses initially infected at a MOI of 0.1 (Fig 3.7) to allow the cells to undergo several rounds of replication. This decision was in contrast to past research (Merrington *et al.*, 1996) that produced different VLD1 and AcORF6^{3260}-1 virus growth curves by infecting cells at a much higher MOI of 5. In Figure 3.13 the cells were infected at a MOI of 10 to study virus DNA replication. It was decided to use a higher MOI in Figure 3.13 so that every cell would be synchronously infected at once and produce abundant copies of total DNA to investigate viral replication profiles. It would be interesting to repeat the one-step viral growth curves at a MOI of 10 so that

a direct comparison could be made between viral titres and DNA replication levels. Results from Merrington *et al* (1996) showed that during the one step growth curves, no difference in budded virus titre was observed between VLD1, AcORF6^{3260}-1 viruses compared to the parental virus (AcUW1.*lacZ*). During my study, VLD1 showed a delayed and reduced virus growth curve that helped to confirm previous research (Merrington *et al.*, 1996). However, AcORF6^{3260}-1 was clearly different from VLD1 and displayed budded virus levels more similar to AcMNPV up to 72hpi. The end titre of AcMNPV was always found to be approximately 10-fold higher than the other mutant virus phenotypes in both suspension and monolayer cultures.

Due to apparent phenotypic differences between VLD1 and AcORF6^{3260}-1, it was decided to fully sequence both *lef*-2 coding regions. Analysis revealed the presence of a second mutation within the VLD1 *lef*-2 coding region that had not been documented before. The point mutation was located at position 3188 within ORF6; as a result of a guanine being substituted for a thymidine. Translation of VLD1 LEF-2 protein further revealed that the point mutation had altered the amino acid sequence by converting an alanine to a threonine residue. Sequencing analysis by Merrington *et al* (1996), did reveal two mapped point mutations within *lef*-2 and ORF2 respectively, but did not rule out further unmapped mutations within the AcMNPV genome as a consequence of the BrdU treatment.

To determine DNA replication levels of AcMNPV, VLD1 and AcORF6^{3260}-1 throughout baculovirus infection, a more sensitive and accurate method was employed in favour of other established techniques. The q-PCR technique allowed the sensitivity of measuring very low amounts of total DNA from virus-infected cells and had the option of automation by a robot to prepare samples and standards. To differentiate between viral and host DNA within a mixture of total DNA extracted from virus-infected cells, two calibration standard curves were established. To measure host DNA levels, *S. frugiperda actin* was chosen to amplify a ~200bp product. The gene chosen to measure viral DNA replication levels was *ie-1*. With both standard curves, two values for each sample were obtained and the number of

viral copies per cell was determined by simple division of one value against the other. Using q-PCR it was clear that the DNA replication levels of AcORF6^{3260}-1 virus were similar if not higher than AcMNPV during baculovirus infection from 12hpi.

In contrast, VLD1 replication was slightly delayed and lower than both AcMNPV and AcORF6^{3260}-1. This result was further evident when both mutant virus phenotypes were directly compared for DNA replication levels. Predominantly the AcORF6^{3260}-1-infected cells showed significantly higher levels of DNA replication up to 24hpi compared to VLD1. Both viruses exhibited the same cytopathic effects (CPE) in *Sf*-21 cells over 72hpi which resulted in an irregular and elongated cellular morphology. The only distinct difference between the CPE induced by both viruses was the timing and this was observed by light microscopy. AcORF6^{3260}-1-infected *Sf*-21 cells exhibited visible CPE at 24hpi compared to VLD1-infected *Sf*-21 cells that possessed the same CPE 24 hours later at 48hpi. The delayed timing and decrease in VLD1 DNA replication levels may be contributable for the apparent absence of CPE not being observed until 48hpi. Further reasons for the apparent absence of CPE in VLD1 infection could be the lack of cytotoxicity of the virus to function in inhibiting or preventing the functioning of the host cell. Even though VLD1 is replicating DNA it could be suggested that the virus is not budding correctly, hence the spread of systemic infection could be compromised and that CPE timing is altered. The DNA replication level at 48hpi for VLD1 was higher than AcMNPV. By 48hpi, the AcMNPV virus infection had progressed towards the very late gene phase and subsequently DNA replication levels started to plateau. In contrast, VLD1 DNA replication levels still increased, which could be the result of unmapped mutations present within the viral genome that further affected the transcription of very late genes by delaying the process of DNA replication.

Previously Merrington *et* al. (1996) had demonstrated using a modified *Dpn* I assay that no significant difference in plasmid DNA replication occurred between AcMNPV and AcORF6^{3260}-1 viruses. However, a temporal delay was observed in plasmid DNA replication of VLD1 confirmed to the wild-type AcMNPV. Despite

both the VLD1 and AcORF6^{3260}-1 phenotypes possessing mutation(s) within the *lef*-2 gene, DNA replication still occurred. These observations were confirmed by q-PCR results that not only demonstrated the point mutation within AcORF6^{3260}-1 did not alter DNA replication levels compared to the wild type AcMNPV, but that VLD1 virus did exhibit delayed and lower replication levels.

As the VLD1 was different from AcORF6^{3260}-1 at both the genotypic and phenotypic level; it was decided to reject this virus from future work because any results could not be attributed to one point mutation.

To further validate results obtained by q-PCR and to be confident that AcMNPV and AcORF6^{3260}-1 exhibited similar DNA replication levels, an additional control was employed. The temperature sensitive mutant (ts8b) has the dual ability of replicating at the permissive temperature of 25°C, but is defective for DNA replication at the non-permissive temperature of 33°C (Gordon and Carstens, 1984; Erlandson *et al.*, 1984). Characterisation of the ts8b virus identified a mutation with a single amino acid change in the *p143* (Gordon and Carstens, 1984; Lu and Carstens, 1991). The *p143* is suggested to be a helicase based on the existence of seven motifs that were observed in a super family of bacterial, viral and eukaryotic proteins involved in the unwinding of DNA duplexes (Lu and Carstens, 1991). Q-PCR results showed that AcORF6^{3260}-1 DNA replication levels were similar if not higher compared to AcMNPV. Ts8b exhibited DNA replication at 25°C, which was measured by q-PCR and standard plaque assay. Despite the absence of budded virus, Ts8b did exhibit a reduced level of DNA replication during q-PCR. Therefore, the incubator set at 33°C was measured and shown to be 1.5°C below the required temperature. To determine the set temperature required to achieve the correct non-permissive temperature, two studies were conducted. During these studies, the incubator was set at 35°C and 34.2°C respectively on two consecutive occasions and monitored for 2-3 days. Afterwards, the experiment to measure AcMNPV, AcORF6^{3260}-1 and ts8B DNA replication levels was repeated at the correct non-permissive temperature of 33°C.

As DNA replication was similar between AcMNPV and AcORF6^{3260}1, the apparent decrease in virus titre could be attributed to transcription of genes or synthesis of mRNA that are involved in the formation of BV and the spread of systematic infection.

A gene that is expressed both early and late that is essential in the spread of systemic infection throughout the cellular host is *gp64*. During the early and late phase of baculovirus infection, gp64 accumulates at the plasma membrane. Nucleocapsids become enveloped in the gp64 modified plasma membrane as they bud from the cell during the late phase and intitate systematic infection throughout the host. Analysis of *gp64* profile during the late phase of infection showed no difference in expression levels between AcMNPV and AcORF6^{3260} -1. Although in the very late phase (36hpi onwards) there was a difference between the viruses. Therefore, the apparent reduction in AcORF6^{3260}-1 virus titre was suggested not to be the consequence of DNA replication or *gp64* transcription.

A further gene that was involved as a structural component of the BV had been examined for any differences in expression levels using q-PCR. The *capsid* profile of both AcMNPV and AcORF6^{3260}-1 up to 24hpi exhibited no difference in viral gene expression levels. The very late phase is often associated with the hyper-expression of structural genes *polyhedrin* and *p10*. A clear difference between AcMNPV and AcORF6^{3260}-1 very late gene expression profiles was observed. At 48hpi, AcMNPV very late gene expression levels were significantly higher compared to AcORF6^{3260}-1. Although very low expression levels of *polyhedrin* are present within the q-PCR study, no visible evidence is available of the presence of occlusion bodies within cell culture. It is suggested that the point mutation within *lef*-2 does exert a negative effect on very late gene expression, but whether this extends to translation of the mRNA into proteins of other genes remains to be investigated. Possible hypotheses for the reduction in very late gene expression as displayed in AcORF6^{3260}-1-infection, could take on the form of either direct or indirect affects as a consequence of the *lef*-2 point mutation. It could be surmised that LEF-2 is unable to directly bind to the "burst"

sequences that are located between the late gene promoter TAAG motif and the translational start site of *polyhedrin* or *p10*. It is proposed that this region is responsible for the characteristic hyper expression of these very late genes. An indirect affect of the *lef*-2 point mutation could mean the loss of another gene product such as the subunits (*lef-4*, *lef-8*, *lef*-9 and *p47*) of the viral encoded RNA polymerase II. Furthermore, an indirect affect of the *lef-2* mutation could be more specifically targeted to the loss of the Very Late Factor 1 (*vlf-1*). According to research that generated a *vlf-1* null bacmid mutant, VLF-1 was not essential for viral DNA synthesis and was a crucial capsid component, which may help to explain why it is important in the production of DNA containing virions (Vanarsdall *et al.*, 2004; Vanarsdall *et al.*, 2006). Interestingly, it was apparent that the absence of this gene only affected the transcription of very late genes; late genes were unaffected (Vanarsdall *et al.*, 2004). These results supported data that proposed that VLF-1 transactivates the *polyhedrin* or *p10* promoters by interacting with the "burst" sequence, although the possibility of interaction with other factors cannot be dismissed (Yang and Miller, 1999). Other indirect affects as a consequence of the *lef*-2 mutation may potentially contribute towards a loss in host protein effects or in the ability of *lef*-2 to self-regulate.

Many previous research studies have shown that *lef*-2 is a highly important gene for baculovirus replication. However, the role of *lef*-2 during late and very late gene expression is less well understood. The production of AcORF6^{3260}-1 has challenged the view that *lef*-2 is only regarded as a replication *lef*. The distinct characteristics that belong to the AcORF6^{3260}-1 phenotype, which have been further demonstrated in this chapter and work by Merrington *et al.* (1996) show a deficiency in very late gene expression, despite possessing normal DNA replication levels. This evidence further indicates a possible dual role of *lef*-2 in both DNA replication and very late gene expression. Sriram and Gopinathan (1998) showed that the removal of 96 amino acids within the LEF-2 C-terminal of *Bombyx mori* NPV (BmNPV) virus resulted in the loss of the *trans*-activation of the minimal BmNPV polyhedrin promoter. Moreover, Evans *et al.* (1997) showed using a two yeast hybrid assay involving

various deletion clones that the interaction site of *lef*-2 with *lef*-1 appears to be located between 20-60amino acids of the N-terminus. Based on the evidence, it could be suggested that *lef*-2 contains sites or sequences that are specific to either DNA replication or late gene expression.

Chapter Four

Characterisation of an additional mutation within VLD1 *lef*-2 and a *lef*-2 deletion mutant.

Chapter Four

4.1 Introduction

In chapter three, a new mutation was discovered within VLD1 *lef*-2 that had not been documented by Merrington *et al*. (1996). The point mutation was located at position 460 nucleotides within *lef*-2, and was the result of a guanine being replaced by an adenine. When *lef*-2 was translated by pDraw, the amino acid sequence showed an alteration from an alanine to a threonine residue. In order to study the effects of the newly discovered mutation it was necessary to recreate a recombinant virus with only this mutation.

To recreate the point mutation, a two-stage PCR strategy was employed. Before the PCR fragment possessing the point mutation could be generated, the optimum length of AcMNPV *lef*-2 flanking regions was determined for homologous recombination. PCR fragments with AcMNPV *lef*-2 flanking regions of 50, 100, 200, 300, 400, and 500bp were generated and cotransfected into insect cells with AcΔ*lef*-2^{100}.neo. The AcΔ*lef*-2^{100}.neo virus construct was created by Professor R. D. Possee to replace the entire *lef*-2 coding region with a neomycin phosphotransferase fragment by ET recombination. According to Angrand *et al* (1999) "ET recombination is a way to engineer DNA in *E.coli* cells using homologous recombination" to introduce site-directed mutagenesis or knockout specific genes using a selectable marker. However, this virus DNA did not successfully remove the entire *lef*-2 coding region but still retained approximately 100bp of the 5' end. Using PCR technology similar to that described in this chapter, the entire *lef*-2 coding region was removed by Mr. A. Chambers and the virus was denoted as AcΔ*lef*-2.neo. To generate the new point mutation, two DNA fragments were generated. These primers created two DNA fragments that shared a region of 20-25bp, which were complementary to each other. During the second round of PCR, the two templates were able to anneal together to produce a completed fragment possessing the induced mutation. To establish the mutation into a viable genome, homologous recombination was used by cotransfection of the *lef*-2 mutant fragment with AcΔ*lef*-2^{100}.neo DNA into insect cells.

It became apparent during this study that the AcΔ*lef*-2^{100}.neo virus was able to persist in cell culture by a proposed helper mechanism provided by the recombinant virus. This made the separation of parental and recombinant virus very difficult even by serial plaque picking. Furthermore, when the AcΔ*lef*-2^{100}.neo DNA was transfected into insect cells as a negative control, small punctate plaques were observed during plaque assay analysis after 5dpi. The same observations were made also for the AcΔ*lef*-2.neo virus.

These observations were made in contrast to previous research that proposed *lef*-2 was essential for DNA replication (Kool *et al.*, 1994; and Lu and Miller., 1995). The overall objective of my PhD study was the investigation of the dual role of *lef*-2 in DNA replication and late gene expression during baculovirus replication. The discovery that *lef*-2 may not be essential for baculovirus replication broadened the scope of this chapter because the consequences of the results could be vital for future work. Therefore, it was decided to change direction and further characterise both the AcΔ*lef*-2.neo viruses. The DNA replication profile was obtained by q-PCR and virus growth curve by measuring BV through plaque assay analysis.

4.2 Results

4.2.1 Construction and production of VLD1 *lef*-2 virus containing the newly mapped mutation.

To investigate if the newly mapped mutation within the VLD1 *lef*-2 gene was responsible for delayed DNA replication respectively, a recombinant virus (AcORF6^{3188}-1) was constructed containing just the mutation.

4.2.1.1 Determination of the optimum length of flanking region required for successful insertion into AcΔ*lef*-2^{100}.neo virus construct by homologous recombination.

Before the new mutant PCR fragment could be generated, it was necessary to determine the optimum length of AcMNPV flanking regions outside *lef*-2 for successful insertion into the AcΔ*lef*-2^{100}.neo construct by homologous recombination. It was decided to investigate AcMNPV flanking regions of 50, 100, 200, 300, 400 and 500bp (Fig 4.1). Pairs of primers were designed to amplify as close to the chosen size of flanking region as possible to produce optimum sequences that shared a similar annealing temperature and avoided areas of highly repetitive nucleotides. Using AcMNPV DNA as a template, DNA fragments were generated and checked for correct size by agarose electrophoresis (Fig 4.2). The purified PCR products (500ng) were cotransfected with AcΔ*lef*-2^{100}.neo viral DNA into *Sf*-21 cells and left to incubate at 28°C.

At 48hpi and 168hpi, one ml of medium was removed from each cotransfection plate and the BV titred by plaque assay. The average value of BV titre (based on duplicate samples) calculated from the plaque assay was represented in Figure 4.3. From this analysis it was apparent that the average BV titre extracted at either 48hpi or 168hpi was similar across all recombinant viruses with 50, 100, 200, 300, 400 or 500bp flanking regions. Therefore, it was proposed that any of the flanking regions would provide sufficient length either side of *lef*-2 for its insertion into the AcΔ*lef*-2^{100}.neo virus DNA.

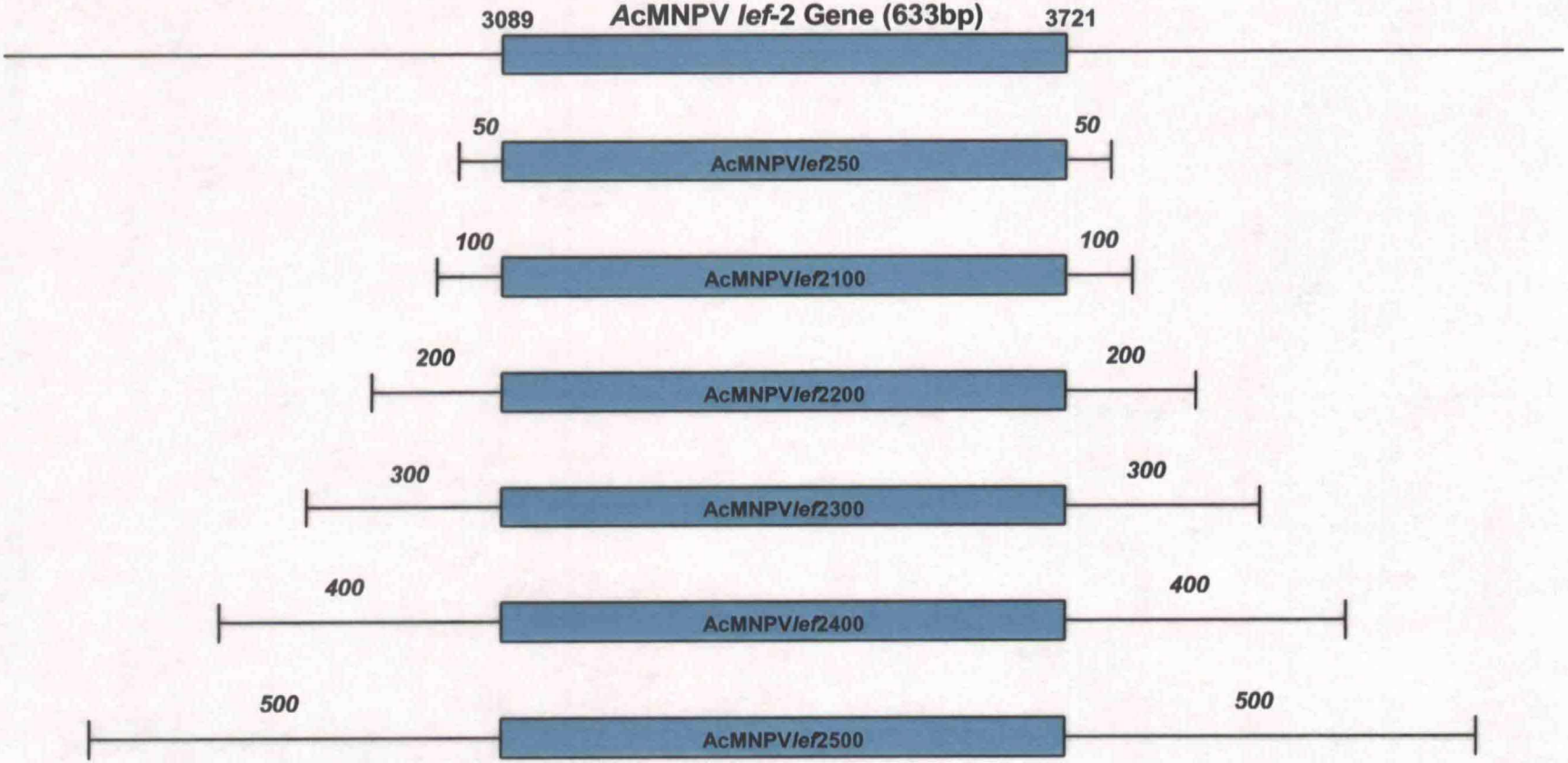

***Figure 4.1* - Generation of flanking regions surrounding the AcMNPV *lef-2* gene.** To determine the optimum length of insertion into the AcΔlef2.neo virus construct, PCR products were generated by primers designed to give (Numbers in brackets indicate AcMNPV genomic positions relative to 5' end of primer): 50bp AcMNPVLef250F (3039) / AcMNPVLef250R (3782), 100bp AcMNPVLef2100F (2999) / AcMNPVLef2100R (3841), 200bp AcMNPVLef2200F (2891) AcMNPVLef2200R (3945), 300bp AcMNPVLef2300F (2783)/ AcMNPVLef2300R (4048), 400bp AcMNPVLef2400F (2687) / AcMNPVLef2400R (4144) and 500bp AcMNPVLef2500F (2578) / AcMNPVLef2500R (4238) flanking regions. *Numbers in bold italic indicate the length in base pairs of the lef-2 flanking regions.*

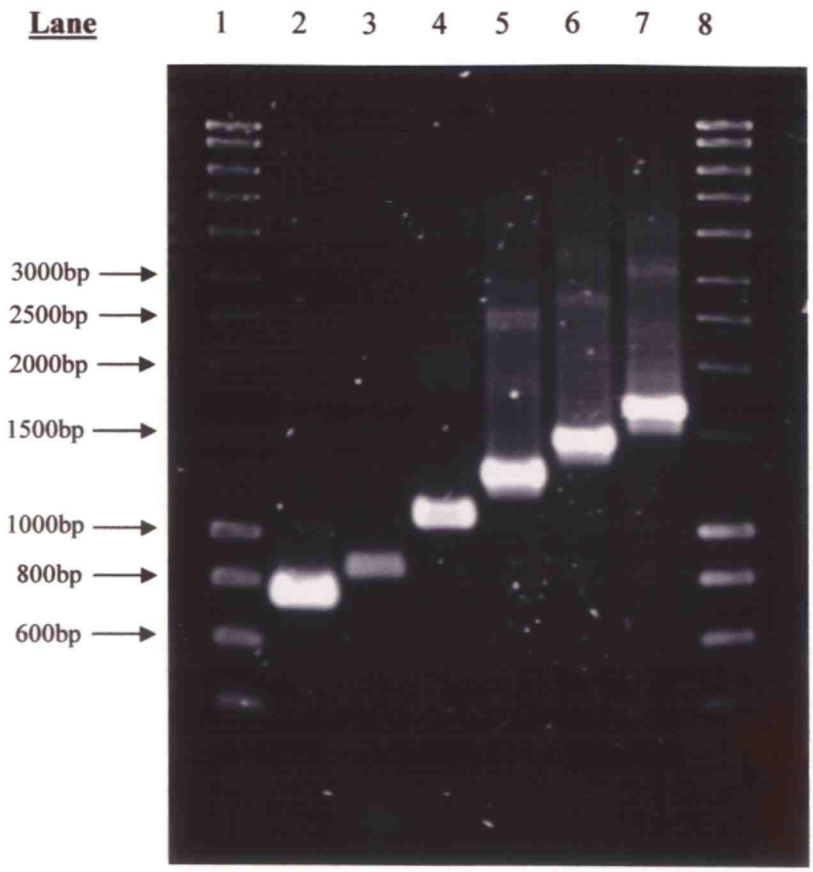

***Figure 4.2* - 1.0% agarose gel electrophoresis of the generation of flanking regions surrounding the *lef*-2 gene by PCR.** Lanes 1 and 8 are Bioline Hyperladder Number 1. Lanes 2 to 7 are completed 50, 100, 200, 300, 400 and 500bp flanking regions PCR fragments respectively.

4.2.1.2 Constructing the new VLD1 mutant virus

Total DNA extracted from AcMNPV or VLD1-infected *Sf*-21 cells was used as a template for the first round of PCR (Fig 4.4). A forward PCR product was produced from VLD1 total DNA using primers VLD1Lef2NewMutR and RDP558 (Fig 4.5, lane 2). In contrast, a reverse PCR product was produced using primers VLD1Lef2NewMutF and RDP561 from AcMNPV (Fig 4.5, lane 3). The reason why two sources of DNA were used as templates is that the VLD1 *lef*-2 possesses both the newly mapped and the original mutation and the AcMNPV DNA is the native sequence.

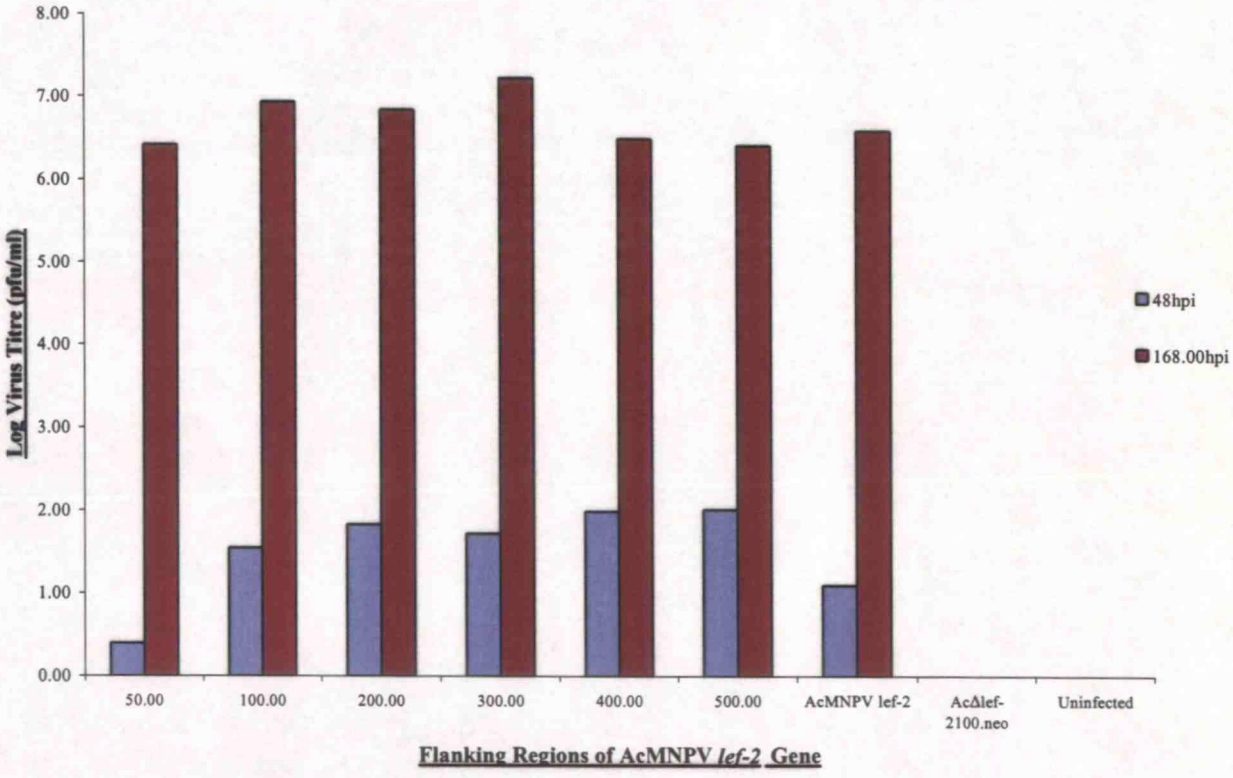

Figure 4.3* – Standard plaque assay analysis of rescued *lef*-2 viruses with different lengths of flanking regions.** 35mm dishes seeded at 1 x 10^6 *Sf*-21 cells (left overnight at 28°C) co-transfected with Ac**Δlef*-2.neo^{100} virus and respective *lef*-2 flanking region PCR fragment. The budded virus titres were extracted from *Sf*-21 cell culture at 48hpi and 168hpi. To determine the optimum length of the flanking regions, plaque assays were used to examine the budded virus titres. (Standard errors are not present on this graph to enhance the clarity of the data).

Therefore, by producing PCR products that contained the forward region of the VLD1 *lef*-2 region and the reverse region of the AcMNPV *lef*-2 region, the end product solely possessed the newer mutation. Both the VLD1Lef2NewMut F and R primers contained the mutation to be induced into the PCR product. Each of the PCR products was purified by agarose gel extraction to ensure no carry over of original template.

During the second round of PCR, the region of complementation created by the primers annealed together both the forward and reverse fragments to produce one template. Using the primers RDP558 and RDP561, a PCR product expressing the specific mutation was generated. The mutant PCR product was checked by agarose gel electrophoresis for size (approximately 1500bp) and purity (Fig 4.5, lane 4). The mutant PCR product was ligated into the pGem-T vector at position 52 (Fig 4.5, lane 5) and transformed into DH5**α** *E.coli*

chemically competent cells. Viable white (recombinant) colonies were picked and amplified further into larger *Lb* stocks before being purified and screened for the correct insert by restriction digestion with *Sac* I and II (Fig 4.5, lane 6).

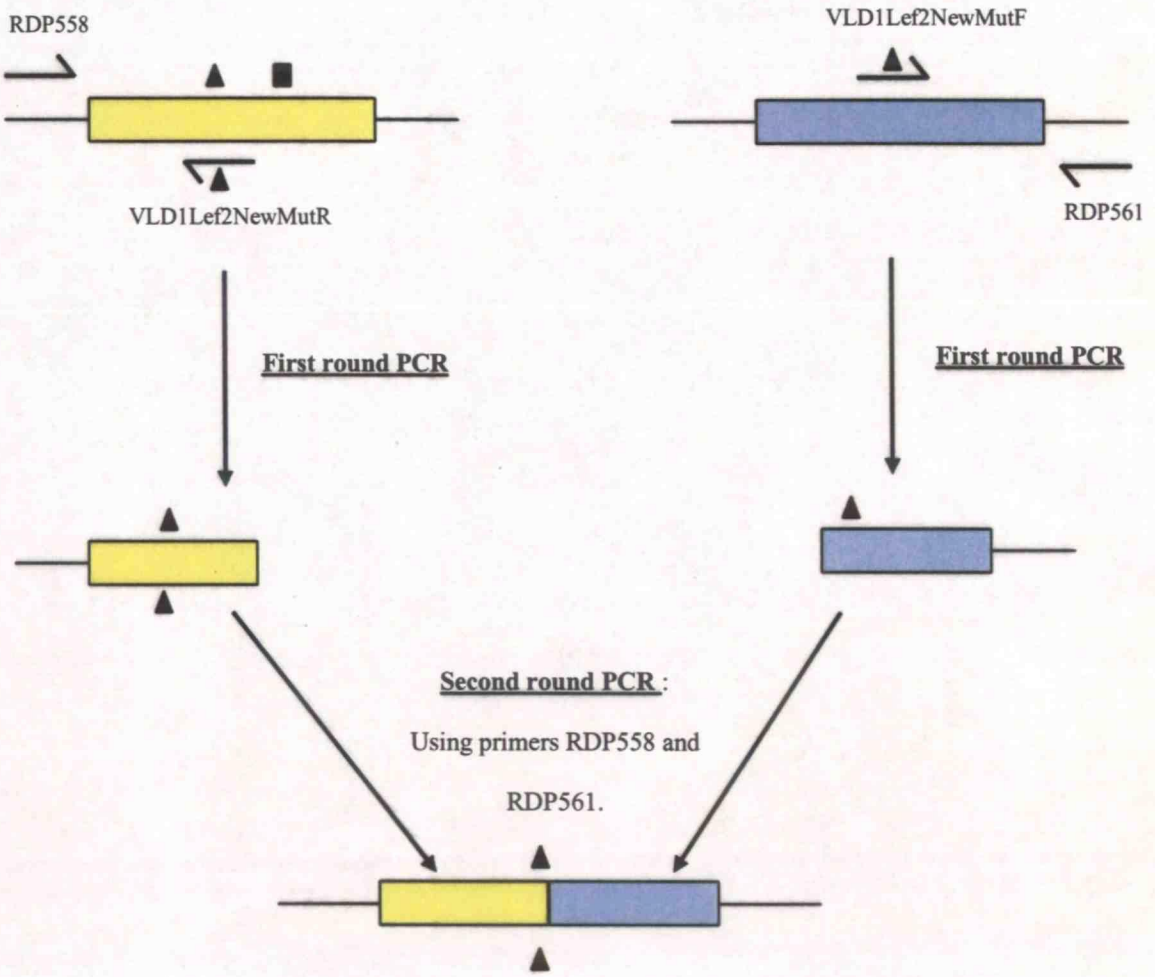

***Figure 4.4* – Construction of the second mapped mutation sequenced from the VLD1 *lef*-2 gene into a pGem-T vector.** The VLD1 *lef*-2 gene is indicated by the yellow box. The AcMNPV *lef*-2 gene is indicated by the blue box. The original mutation discovered in the VLD1 *lef*-2 gene is indicated by a solid black square. The newer second mapped mutation within the VLD1 *lef*-2 is indicated by a solid black triangle. To construct a PCR fragment that possessed only the newer point mutation, both AcMNPV and VLD1 total DNA was used as templates. The construction involved a two step PCR approach. Firstly, forward and reverse PCR fragments were generated by RDP558/VLD1Lef2NewMutR and VLD1Lef2NewMutF/RDP561 primers respectively. Afterwards the purified mutant fragments were annealed together in second round PCR using primers RDP558 and RDP561 to generate a 1500bp fragment represented by only the newer mutation indicated by a black triangle. The mutant AcMNPV *lef*-2 fragment was cloned into Promega pGem-T vector. Numbers in brackets indicate AcMNPV genomic positions relative to 5' end of primer for RDP558 (2612) and RDP561 (4137).

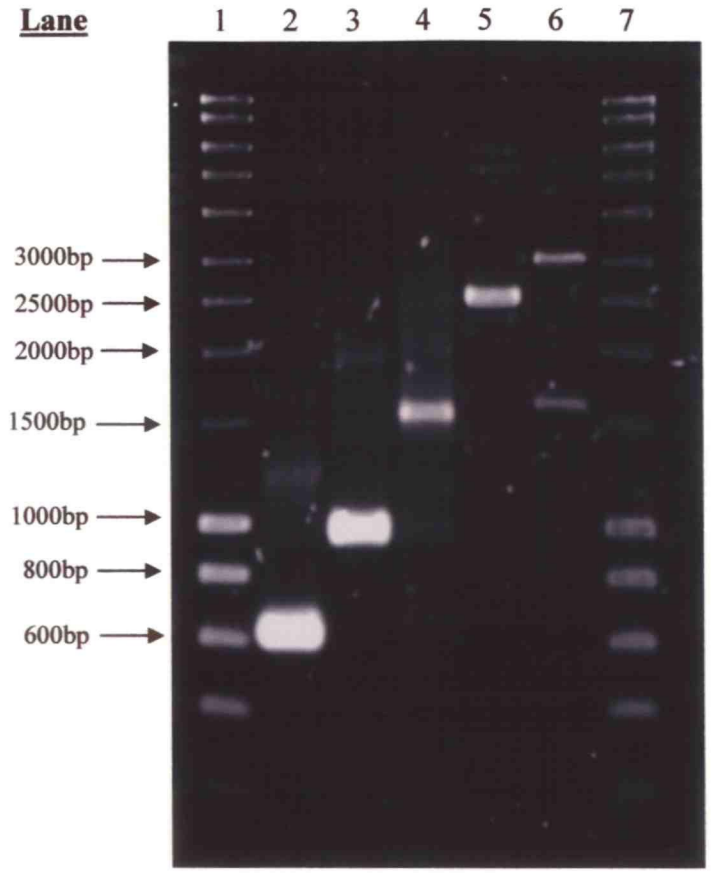

***Figure 4.5* - 1.0% agarose gel electrophoresis of the construction of the newly mapped point mutant within the VLD1 *lef*-2 gene.** Lanes 1 and 7 are Bioline Hyperladder Number 1; lanes 2 and 3 are first round PCR forward and reverse fragments respectively. Lane 4 is the completed product from second round PCR as a result of the annealing of the forward and reverse PCR fragments (lanes 2 and 3) together and using primers RDP558 plus RDP561. Lane 5 is the uncut pGem-T vector ligated with the completed new mutant PCR fragment (lane 4). Lane 6 is the plasmid (lane 5) digested with *Sac*I and *Sac* II.

Final confirmation of the correct PCR fragment insert into the pGem-T vector was obtained by sequencing analysis (Fig 4.6). The *lef*-2 mutant plasmid (500ng) was originally cotransfected into *Sf*-21 cells with 5.2µg of circular AcΔ*lef*-2^{100}.neo viral DNA, and left to incubate at 28°C for 4dpi prior to titration of the recombinant virus in a plaque assay conducted over 3 days. Plaque picks were taken and P_1 stocks of the recombinant viruses were established by infecting 25cm^3 T-flasks seeded with *Sf*-21 cells. Titres were obtained by plaque assay and the presence of recombinant viruses verified by PCR of total intracellular DNA with *lef*-2-specific primers and sequencing analysis. However, agarose

gel analysis showed the presence of *lef*-2 (1500bp) and the neomycin fragment (2000bp), indicating that a mixed virus population was present (data not shown). Each of the virus recombinant virus stocks obtained were denoted AcORF6^{3188} -1, -3, -4, -5 and -6 respectively. Each name depicted that the recombinant viruses were modified from an AcMNPV genome, and that the point mutation was located at genomic position 3188 within ORF6

To separate the new recombinant virus (denoted AcORF6^{3188}) from the parental AcΔ*lef*-2^{100}.neo virus, further plaque picks were isolated from subsequent titrations. From these plaques picks, plaque assays were set up and left for 5dpi to allow the plaques to develop. Plaque assay analysis (5dpi) revealed the presence of both large and small plaques on dishes that represented AcMNPV and mutant *lef*-2 PCR products cotransfected with viral DNA respectively (Fig 4.7). Furthermore, control dishes with only circular AcΔ*lef*-2^{100}.neo that had been previously transfected into insects expressed very small, punctuate plaques during plaque assay analysis at 5dpi (data not shown). The plaques were picked from the dishes and used to further infect *Sf*-21 cells. To characterise the recombinant virus, total DNA was extracted and used in a PCR reaction with *lef*-2-specific primers. Agarose gel electrophoresis showed that the parental (AcΔ*lef*-2^{100}.neo) virus still persisted (data not shown).

To confirm that the small, punctuate plaques on control dishes from the transfection medium of AcΔ*lef*-2^{100}.neo were really plaques and not a disruption to the cell monolayer, light microscopy photographs were taken at different magnifications (Fig 4.8). Uninfected cells (Fig 4.8, panel A) exhibited a healthy monolayer with live cells readily taking up the neutral red stain. In contrast, AcMNPV-infected cells showed large plaques that were surrounded by live red stained insect cells (Fig 4.8, panel B). Both the dishes for AcMNPV and mutant *lef*-2 fragments cotransfected into AcΔ*lef*-2^{100}.neo showed a mixture of both large well-defined plaques and small, punctuate plaques (Fig 4.8, panels C and D respectively). However, AcΔ*lef*-2^{100}.neo-infected cell monolayer showed small areas of clearing or plaques with transparent (dead) cells that had not taken up the neutral red stain.

Higher magnification of these plaques showed very small areas of dead cells as a result of virus infection (Fig 4.8, panel E).

At this point in the investigation, it was proving impossible to completely isolate the AcORF6^{3188} virus from the small plaques (AcΔ*lef*-2^{100}.neo) despite several rounds of plaque picking. Even after further infecting *Sf*-21 cells with the plaque picks, agarose gel electrophoresis of PCR samples using *lef*-2 primers showed the presence of two distinct bands at 1500bp and 2000bp (data not shown). The DNA band of 2000bp represented the neomycin fragment in the parental virus, and the 1500bp DNA band indicated *lef*-2 and the presence of the recombinant virus. Furthermore, the AcΔ*lef*-2^{100}.neo virus had shown it had the ability to replicate from the presence of small plaques despite only possessing 100bp of the *lef*-2 N-terminus. This observation was made in contrast to previous research that proposed that *lef*-2 is essential for DNA replication (Kool *et al.*, 1994; and Lu and Miller., 1995). Therefore, I decided to characterise in more detail both AcΔ*lef*-2.neo viruses.

RDP558

```
  1 CTCGCTTTTA ATCATGCCGT CGATTAAATC GCGCAATCGA GTCAAGTGAT
    GAGCGAAAAT TAGTACGGCA GCTAATTTAG CGCGTTAGCT CAGTTCACTA

 51 CAAAGTGTGG AATAATGTTT TCTTTGTATT CCCGAGTCAA GCGCAGCGCG
    GTTTCACACC TTATTACAAA AGAAACATAA GGGCTCAGTT CGCGTCGCGC

101 TATTTTAACA AACTAGCCAT CTTGTAAGTT AGTTTCATTT AATGCAACTT
    ATAAAATTGT TTGATCGGTA GAACATTCAA TCAAAGTAAA TTACGTTGAA

151 TATCCAATAA TATATTATGT ATCGCACGTC AAGAATTAAC AATGCGCCCG
    ATAGGTTATT ATATAATACA TAGCGTGCAG TTCTTAATTG TTACGCGGGC

201 TTGTCGCATC TCAACACGAC TATGATAGAG ATCAAATAAA GCGCGAATTA
    AACAGCGTAG AGTTGTGCTG ATACTATCTC TAGTTTATTT CGCGCTTAAT

251 AATAGCTTGC GACGCAACGT GCACGATCTG TGCACGCGTT CCGGCACGAG
    TTATCGAACG CTGCGTTGCA CGTGCTAGAC ACGTGCGCAA GGCCGTGCTC

301 CTTTGATTGT AATAAGTTTT TACGAAGCGA TGACATGACC CCCGTAGTGA
    GAAACTAACA TTATTCAAAA ATGCTTCGCT ACTGTACTGG GGGCATCACT

351 CAACGATCAC GCCCAAAAGA ACTGCCGACT ACAAAATTAC CGAGTATGTC
    GTTGCTAGTG CGGGTTTTCT TGACGGCTGA TGTTTTAATG GCTCATACAG

401 GGTGACGTTA AAACTATTAA GCCATCCAAT CGACCGTTAG TCGAATCAGG
    CCACTGCAAT TTTGATAATT CGGTAGGTTA GCTGGCAATC AGCTTAGTCC

451 ACCGCTGGTG CGAGAAGCCG CGAAGTATGG CGAATGCATC GTATAACGTG
    TGGCGACCAC GCTCTTCGGC GCTTCATACC GCTTACGTAG CATATTGCAC
                                  M   A   N   A   S   Y   N   V

501 TGGAGTCCGC TCATTAGAGC GTCATGTTTA GACAAGAAAG CTACATATTT
    ACCTCAGGCG AGTAATCTCG CAGTACAAAT CTGTTCTTTC GATGTATAAA
    W   S   P   L   I   R   A   S   C   L   D   K   K   A   T   Y   L

551 AATTGATCCC GATGATTTTA TTGATAAATT GACCCTAACT CCATACACGG
    TTAACTAGGG CTACTAAAAT AACTATTTAA CTGGGATTGA GGTATGTGCC
      I   D   P   D   D   F   I   D   K   L   T   L   T   P   Y   T   V

601 TATTCTACAA TGGCGGGGTT TTGGTCAAAA TTTCCGGACT GCGATTGTAC
    ATAAGATGTT ACCGCCCCAA AACCAGTTTT AAAGGCCTGA CGCTAACATG
      F   Y   N   G   G   V   L   V   K   I   S   G   L   R   L   Y

651 ATGCTGTTAA CGGCTCCGCC CACTATTAAT GAAATTAAAA ATTCCAATTT
    TACGACAATT GCCGAGGCGG GTGATAATTA CTTTAATTTT TAAGGTTAAA
    M   L   L   T   A   P   P   T   I   N   E   I   K   N   S   N   F

701 TAAAAAACGC AGCAAGAGAA ACATTTGTAT GAAAGAATGC GTAGAAGGAA
    ATTTTTTGCG TCGTTCTCTT TGTAAACATA CTTTCTTACG CATCTTCCTT
      K   K   R   S   K   R   N   I   C   M   K   E   C   V   E   G   K

751 AGAAAAATGT CGTCGACATG CTGAACAACA AGATTAATAT GCCTCCGTGT
    TCTTTTTACA GCAGCTGTAC GACTTGTTGT TCTAATTATA CGGAGGCACA
      K   N   V   V   D   M   L   N   N   K   I   N   M   P   P   C

801 ATAAAAAAAA TATTGAACGA TTTGAAAGAA AACAATGTAC CGCGCGGCGG
    TATTTTTTTT ATAACTTGCT AAACTTTCTT TTGTTACATG GCGCGCCGCC
    I   K   K   I   L   N   D   L   K   E   N   N   V   P   R   G   G

851 TATGTACAGG AAGAGGTTTA TACTAAACTG TTACATTGCA AACGTGGTTT
    ATACATGTCC TTCTCCAAAT ATGATTTGAC AATGTAACGT TTGCACCAAA
      M   Y   R   K   R   F   I   L   N   C   Y   I   A   N   V   V   S

901 CGTGTGCCAA GTGTGAAAAC CGATGTTTAA TCAAGACTCT GACGCATTTC   VLD1Lef2NewMutF
    GCACACGGTT CACACTTTTG GCTACAAATT AGTTCTGAGA CTGCGTAAAG   VLD1Lef2NewMutR
      C   A   K   C   E   N   R   C   L   I   K   T   L   T   H   F
```

```
 951 TACAACCACG ACTCCAAGTG TGTGGGTGAA GTCATGCATC TTTTAATCAA
     ATGTTGGTGC TGAGGTTCAC ACACCCACTT CAGTACGTAG AAAATTAGTT
     Y  N  H  D   S  K  C   V  G  E   V  M  H  L   L  I  K

1001 ATCCCAAGAT GTGTATAAAC CACCAAACTG CCAAAAAATG AAAACTGTCG
     TAGGGTTCTA CACATATTTG GTGGTTTGAC GGTTTTTTAC TTTTGACAGC
      S  Q  D   V  Y  K  P   P  N  C   Q  K  M   K  T  V  D

1051 ACAAGCTCTG TCCGTTTGCT GGCAACTGCA AGGGTCTCAA TCCTATTTGT
     TGTTCGAGAC AGGCAAACGA CCGTTGACGT TCCCAGAGTT AGGATAAACA
       K  L  C   P  F  A   G  N  C  K   G  L  N   P  I  C

1101 AATTATTGAA TAATAAAACA ATTATAAATG CTAAATTTGT TTTTTATTAA
     TTAATAACTT ATTATTTTGT TAATATTTAC GATTTAAACA AAAAATAATT
     N  Y  *

1151 CGATACAAAC CAAACGCAAC AAGAACATTT GTAGTATTAT CTATAATTGA
     GCTATGTTTG GTTTGCGTTG TTCTTGTAAA CATCATAATA GATATTAACT

1201 AAACGCGTAG TTATAATCGC TGAGGTAATA TTTAAAATCA TTTTCAAATG
     TTTGCGCATC AATATTAGCG ACTCCATTAT AAATTTTAGT AAAAGTTTAC

1251 ATTCACAGTT AATTTGCGAC AATATAATTT TATTTTCACA TAAACTAGAC
     TAAGTGTCAA TTAAACGCTG TTATATTAAA ATAAAAGTGT ATTTGATCTG

1301 GCCTTGTCGT CTTCTTCTTC GTATTCCTTC TCTTTTTCAT TTTTCTCCTC
     CGGAACAGCA GAAGAAGAAG CATAAGGAAG AGAAAAAGTA AAAAGAGGAG

1351 ATAAAAATTA ACATAGTTAT TATCGTATCC ATATATGTAT CTATCGTATA
     TATTTTTAAT TGTATCAATA ATAGCATAGG TATATACATA GATAGCATAT

1401 GAGTAAATTT TTTGTTGTCA TAAATATATA TGTCTTTTTT AATGGGGTGT
     CTCATTTAAA AAACAACAGT ATTTATATAT ACAGAAAAAA TTACCCCACA

1451 ATAGTACCGC TGCGCATAGT TTTTCTGTAA TTTACAACAG TGCTATTTTC
     TATCATGGCG ACGCGTATCA AAAAGACATT AAATGTTGTC ACGATAAAAG

1501 TGGTAGTTCT TCGGAGTGTG TTG
     ACCATCAAGA AGCCTCACAC AAC
```

RDP561

***Figure 4.6* - Completed sequence of the newly mapped point mutant *lef*-2 PCR fragment ligated into the pGem-T vector.** Sequencing analysis was carried out using purified preparations of the plasmid as a template. A detailed outline of the construction of this plasmid is located in figure 3.8. The blue lines and font indicate the universally used *lef*-2 primers RDP558 (5' – CTC GCT TTT AAT CAT GCC GT – 3') and RDP561 (5' –CAA CAC ACT CCG AAA ACT AC – 3'). The purple lines and font represent the primers VLD1Lef2NewMutF (5' – TGT TTA ATC AAG ACT CTG ACG CAT T – 3') and VLD1Lef2NewMutR (5'- AAT GCG TCA GAG TCT TGA TTA AAC A – 3'). The point mutation responsible for the change in amino acid sequence from the native AcMNPV Alanine (A) to a Threonine (T) residue is highlighted in red font. The amino acid sequence for the *lef*-2 gene was generated by using the program pDraw32.

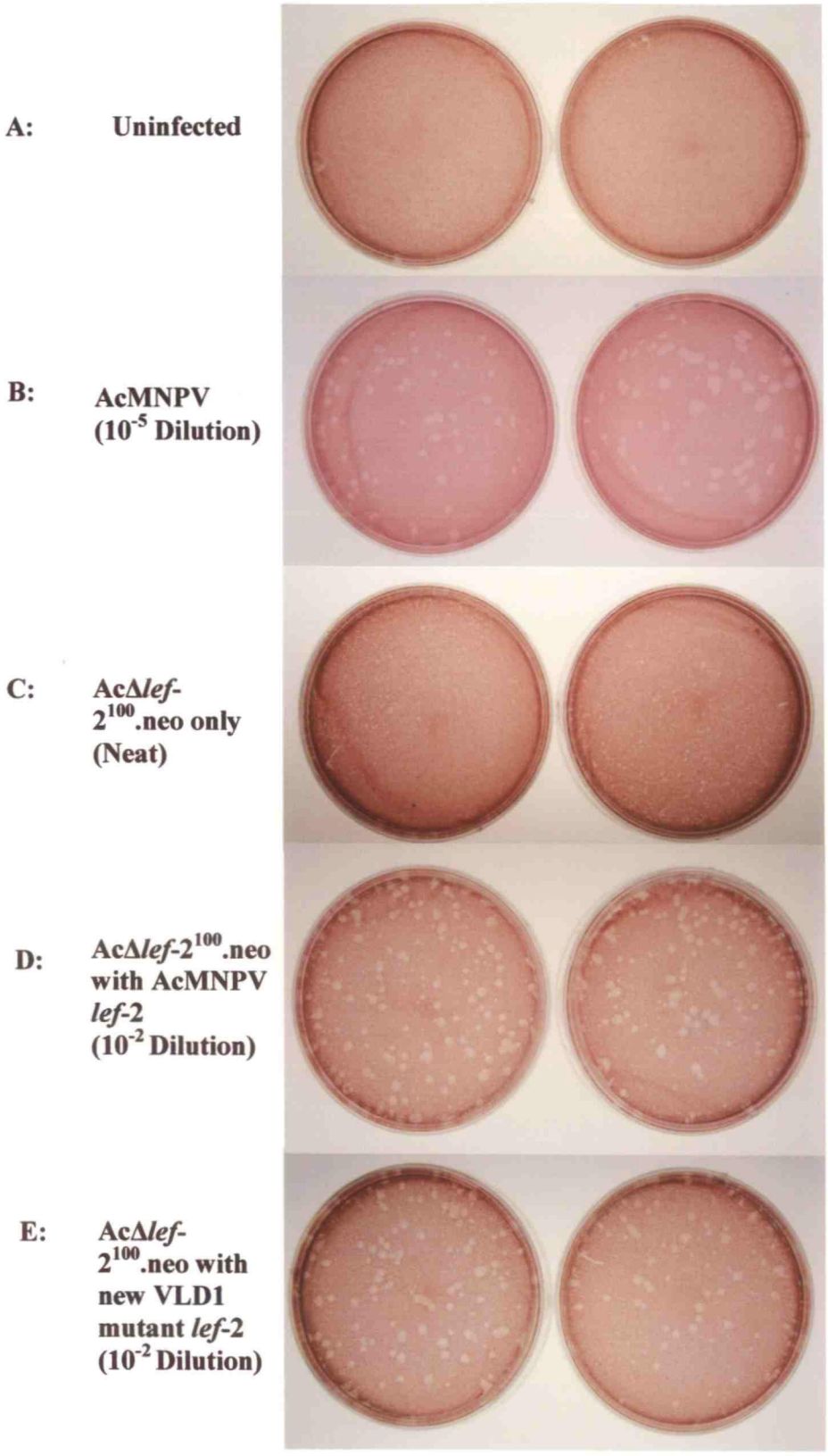

***Figure 4.7* - Plaque assay analysis of cotransfections with *lef*-2 based plasmids and AcΔ*lef*-2^{100}.neo virus DNA.** Serial dilutions from Neat to 10^{-2} were made from samples of cotransfection mixtures from circular AcΔ*lef*-2^{100}.neo DNA with AcMNPV *lef*-2 plasmid or VLD1 new mutant plasmid and left for 5dpi. Plaques were visualised by staining with neutral red.

A) Uninfected-*Sf*-21 cells (x200)

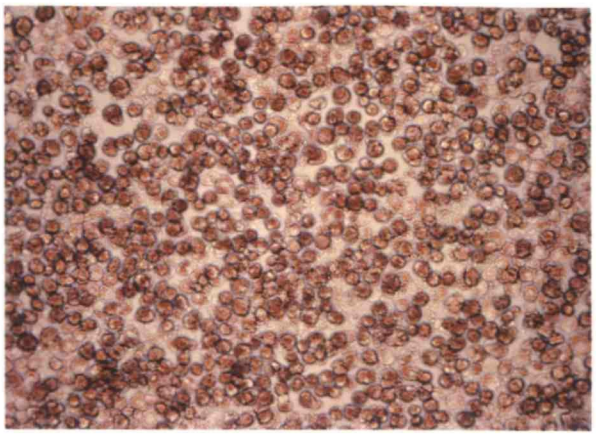

B) AcMNPV-infected *Sf*-21 cells (x40)

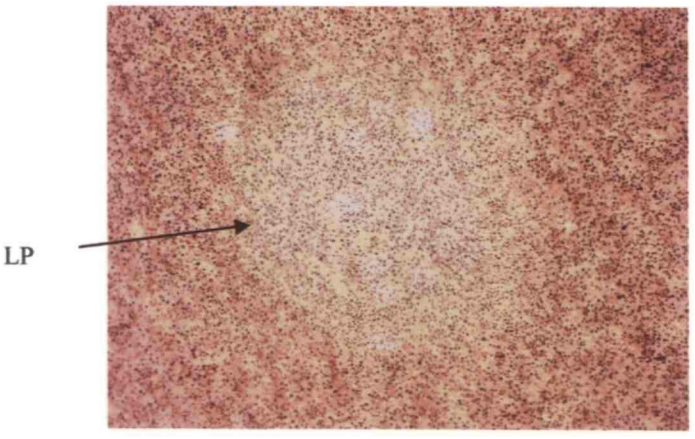

C) AcΔ*lef*-2^{100}.neo with AcMNPV *lef*-2 -infected *Sf*-21 cells (x40)

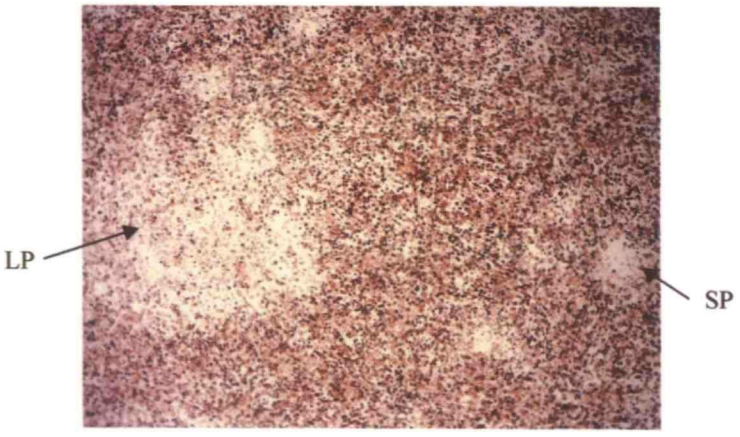

D) AcΔ*lef*-2^{100}.neo with new VLD1 mutant-infected *Sf*-21 cells (x40)

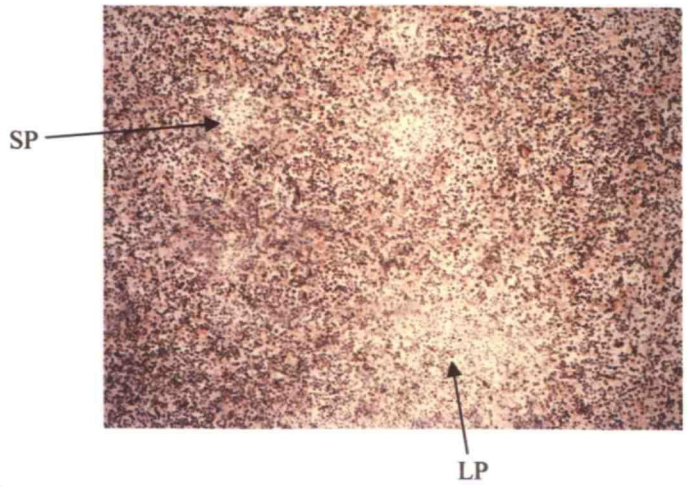

E) (i): AcΔ*lef*-2^{100}.neo (x40)

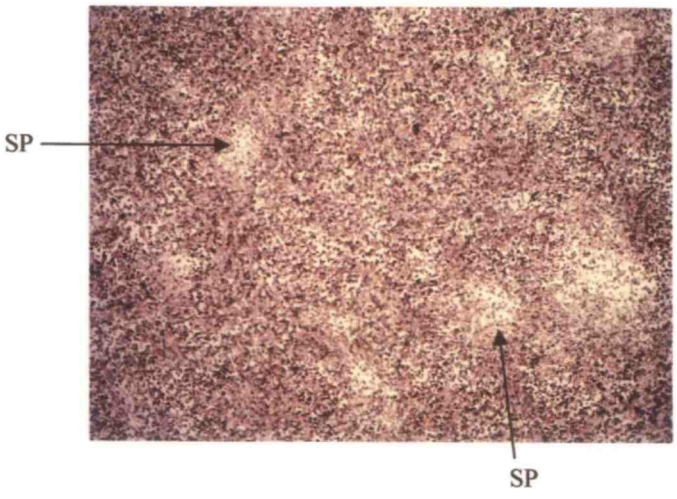

E (ii): AcΔ*lef*-2^{100}.neo (x200)

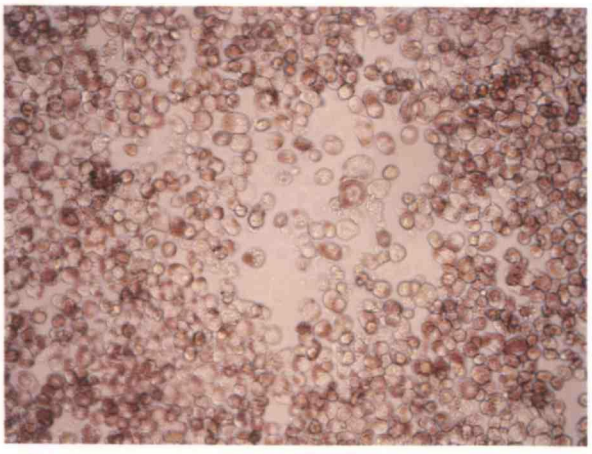

***Figure 4.8*- Light microscopy photographs of plaque assay analysis of results from Figure 4.7.** Photographs of virus-infected *Sf*-21 cells from plaque assays left at 28°C for five days see Figure 4.7. Magnification of each photograph is indicated in the brackets of each individual heading. LP, Large plaques, SP, Small plaques.

4.2.2 Characterisation of AcΔ*lef*-2.neo virus DNA replication.

The AcΔ*lef*-2.neo virus stock was amplified by transfecting the viral DNA into *Sf*-21 cells and incubating for 5-6dpi. The reason why the virus-infected *Sf*-21 cells were incubated for so long is because the AcΔ*lef*-2.neo virus is very slow growing. Afterwards, the AcΔ*lef*-2.neo BV stock was collected by harvesting the 2ml medium from infected dishes. The BV was titred by plaque assay at 5dpi in *Sf*-21 cells. As the AcΔ*lef*-2.neo virus appeared to have the ability to replicate, as was evident by the presence of small, punctate plaques, DNA replication was examined. Total DNA was extracted from AcMNPV, AcΔ*lef*-2.neo and mock-infected *Sf*-21 cells at 24, 48 and 72hpi at a MOI of 0.02. It was determined by plaque assay that the AcΔ*lef*-2.neo BV stock titres were very low, hence the use of a low MOI. The extracted total DNA concentration was determined by spectrophotometer and the integrity examined using agarose gel electrophoresis. Using the same technique employed in Chapter Three for the calculation of viral copy number per cell, the DNA replication profile for each virus was obtained (Fig 4.9). AcMNPV-infected *Sf*-21 cells exhibited a DNA replication profile that was similar to results observed in chapter three. In contrast, the AcΔ*lef*-2.neo virus DNA replication levels remained constant throughout the time course, except for a minor increase between 48hpi and 72hpi. The uninfected cells showed no evidence of viral DNA replication as expected.

4.2.3 Viral Growth curve of AcΔ*lef*-2.neo virus over 72hpi.

To investigate the viral growth curve dynamics of the AcΔ*lef*-2.neo virus, dishes of *Sf*-21 cells were infected at MOI of 0.02 with the respective virus and incubated at 28°C. Medium was harvested from the corresponding dishes at 1, 24, 48 and 72hpi respectively. The BV titre was determined by plaque assay (in duplicate) and a multi-step virus growth curve obtained for each virus (Fig 4.10). AcMNPV exhibited a steady increase in BV titre from 1hpi to 72hpi to reach a peak of approximately 6.30 log values. In contrast, AcΔ*lef*-2.neo multi-step BV growth did not exhibit a typical curve pattern similar to AcMNPV, rather a constant line. The line of AcΔ*lef*-2.neo did gradually increase to 2.03 log values at 72hpi; approximately a 2.9 fold reduction compared to AcMNPV at the same time-point. Uninfected *Sf*-21 cells did not exhibit any plaques and hence no BV titre.

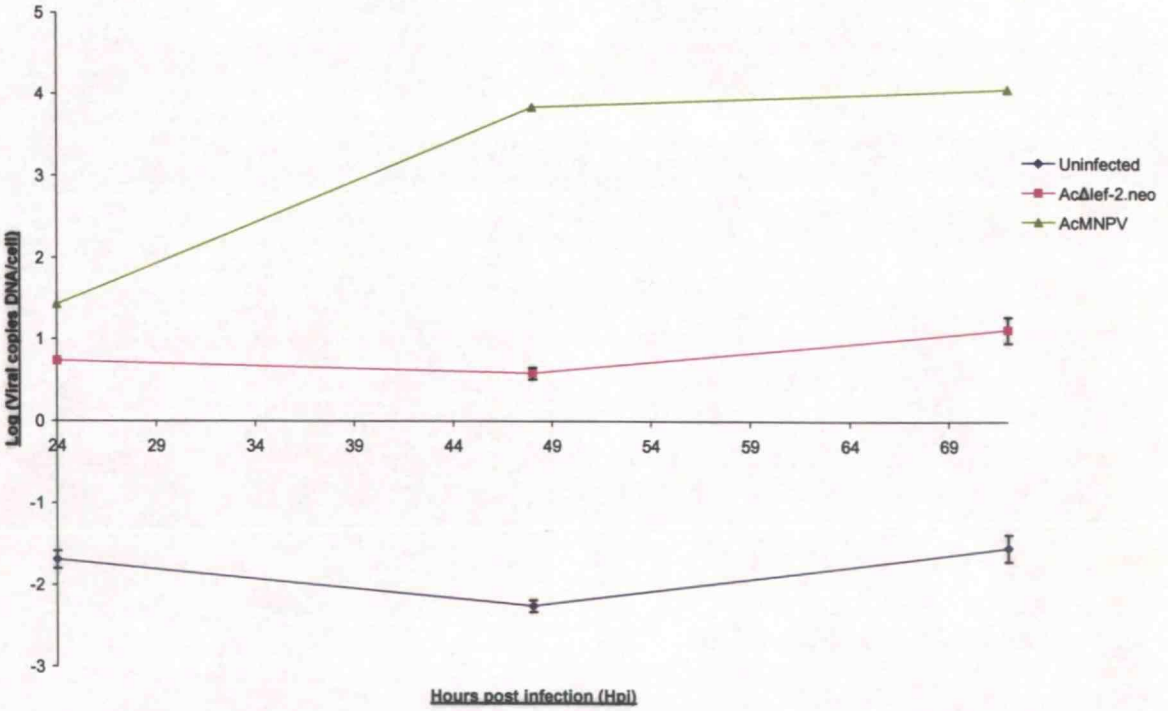

***Figure 4.9* - Quantitative analysis of replicated viral DNA in infected-*Sf*21 cells (MOI 0.02) over 72hpi.** Total intracellular DNA was isolated from duplicate samples from each time-point per virus. Each point indicates the average over three runs of q-PCR and the y-axis error bars represents the standard error.

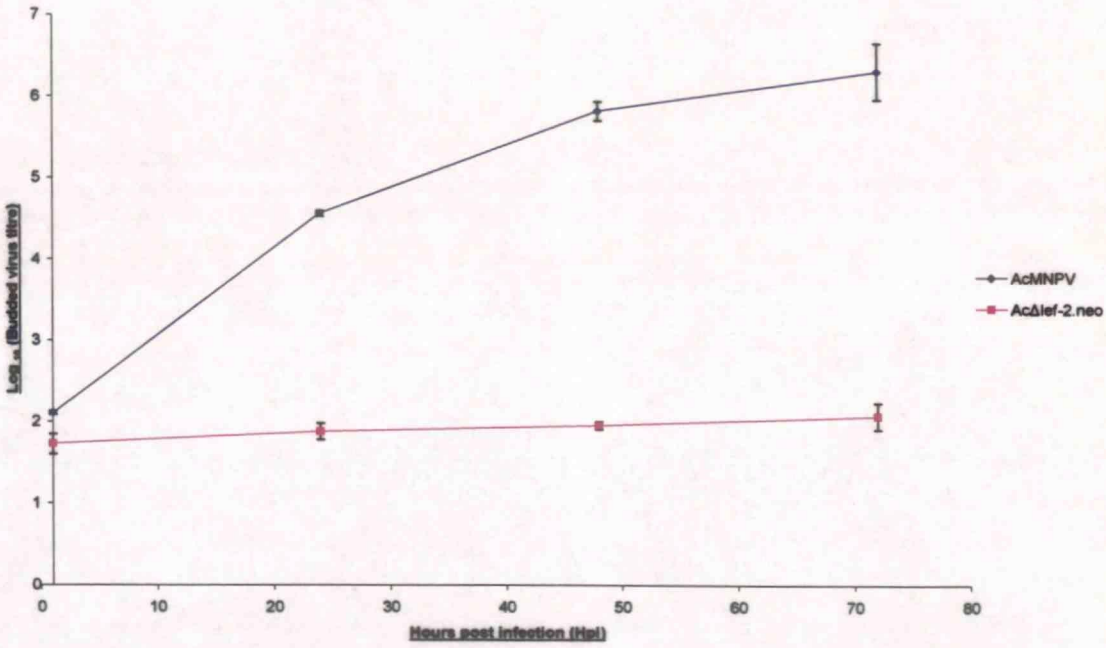

***Figure 4.10*- Viral growth curve analysis.** *Sf*-21 cells were infected at MOI of 0.02 with AcMNPV, Ac*Δlef*-2.neo and uninfected. At the indicated time-points, triplicate samples of the supernatants were collected and BV titre determined by standard plaque assay. Each point indicates the average of triplicate samples taken and the y-axis error bars represent the standard error.

4.2.4 DNA replication study examining the consequences of the second mapped mutation within the VLD1 *lef*-2.

As the separation of the parental (AcΔ*lef*-2^{100}.neo) and recombinant (AcORF6^{3188}-3) viruses was impossible despite serial plaque picking, it was decided to investigate the overall DNA replication from this sample. The DNA replication profile of AcΔ*lef*-2.neo had already been obtained (Fig 4.9). Results suggested a linear relationship of AcΔ*lef*-2.neo DNA replication, with a slight increase from 48hpi to 72hpi. The DNA replication results for AcΔ*lef*-2.neo was distinct from AcMNPV. Therefore, if any alteration in DNA replication levels were present within the mixture of AcΔ*lef*-2.neo and AcORF6^{3188}-3, then the difference could be suggested to be attributed by the recombinant virus. *Sf*-21 cells were infected with AcMNPV or a mixture of AcΔ*lef*-2.neo and AcORF6^{3188}-3 at MOI of 5 and incubated at 28°C. Total DNA was extracted from harvested virus-infected *Sf*-21 cells at 8, 16, and 24hpi. The DNA concentration was determined by spectrophotometer. Using q-PCR as outlined in chapter three, the DNA replication profile for each virus was obtained (Fig 4.11).

Typically the AcMNPV showed a steady increase in DNA replication up to 24hpi, peaking at 4.1 log values. However, the AcORF6^{3188}-3 and AcΔ*lef*-2^{100}.neo mixture showed DNA replication levels similar to AcMNPV. At 8hpi, the DNA replication levels of AcORF6^{3188}-3 and AcΔ*lef*-2^{100}.neo were slightly higher than AcMNPV, but continued to rise slowly to peak at 3.7 log values. The pattern of AcMNPV DNA replication is represented by a curve, but this was not observed in AcORF6^{3188}-3 and AcΔ*lef*-2^{100}.neo, which showed a consistent line. The uninfected cells showed no evidence of viral DNA replication as expected.

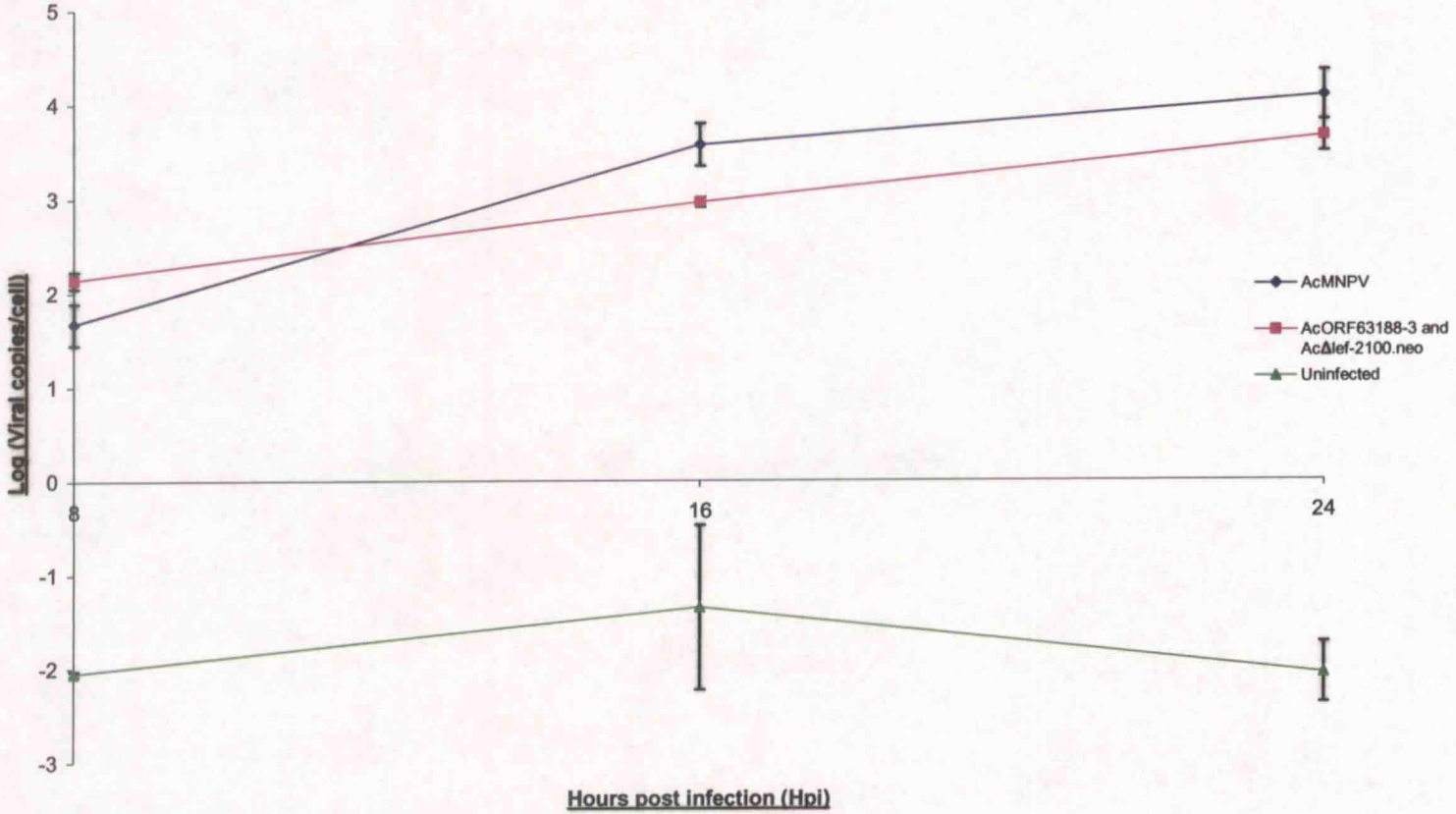

***Figure 4.11* - Quantitative analysis of replicated viral DNA in infected-*Sf*21 cells (MOI 5) over 24hpi.** Total intracellular DNA was isolated from duplicate samples from each time-point per virus. Each point indicates the average over two runs of q-PCR and the y-axis error bars represents the standard error.

4.3 Discussion.

Sequencing analysis in chapter three revealed an additional point mutation at a position of 460 nucleotides within VLD1 *lef*-2. The mutation was the result of a guanine being replaced by an adenine, hence altering the amino acid code from an alanine residue to a threonine residue. It was decided to construct and produce a recombinant virus (AcORF6^{3188}) that solely possessed the point mutation within *lef*-2 and so to be able to investigate its effect on virus replication.

Before the construction of the recombinant virus could commence, the optimum length of AcMNPV *lef*-2 flanking regions for insertion into an AcMNPV genome by homologous recombination was determined. This involved the generation of PCR fragments with AcMNPV *lef*-2 flanking regions ranging in length of 50, 100, 200, 300, 400 and 500bp. Afterwards, the PCR fragments were cotransfected with AcΔ*lef*-2^{100}.neo into insect cells and the BV calculated by plaque assay analysis at 4dpi. Results suggested that any length of AcMNPV *lef*-2 flanking regions would provide successful insertion into AcΔ*lef*-2^{100}.neo. At this stage of the investigation, no plaques were observed on dishes with only AcΔ*lef*-2^{100}.neo transfected into insect cells.

To recreate the new point mutation within *lef*-2, a two-stage PCR approach was taken. This involved the use of AcMNPV and VLD1-extracted DNA with specifically-designed primers to produce a 1500bp *lef*-2 PCR mutant fragment. The PCR fragment was ligated into pGem-T and cotransfected into insect cells with AcΔ*lef*-2^{100}.neo. The plaques were picked and used to further infect *Sf*-21 cells. Total DNA was extracted and used as a template in PCR to determine the presence of the *lef*-2 fragment, to indicate the presence of the AcORF6^{3188} virus. Agarose gel electrophoresis clearly showed the presence of two DNA fragments of approximately 1500bp and 2000bp in size. The 1500bp DNA band was consistent with the presence of *lef*-2, hence the AcORF6^{3188} virus. The 2000bp DNA band was likely to be the result of the neomycin fragment from the parental AcΔ*lef*-2^{100}.neo virus. The next step taken was to try and separate the parental and recombinant viruses by serial plaque picking. Despite this effort, PCR and agarose gel electrophoresis still confirmed the persistence of the Ac*lef*-2^{100}.neo virus. It is thought that the AcΔ*lef*-

2^{100}.neo persistence in cell culture may have been possible due to a proposed helper mechanism initiated by the AcORF6^{3188} virus. An alternative explanation for the presence of a mixed population is that a single crossover recombination event could have taken place between the parental virus and the *lef*-2 mutant plasmid so that they were both incorporated together. This could have transpired from the recombination of only one of the two flanking regions of the *lef*-2 mutant plasmid with the flanking region of neomycin phosphotransferase fragment of the parental virus. Ideally, a double recombination crossover event would take place between the flanking regions of the *lef*-2 mutant plasmid and the *lef*-2 regions that flanked the neomycin phosphotransferase fragment. Then the *lef*-2 mutant coding region would have replaced the neomycin phosphotransferase fragment, to produce a recombinant virus possessing the specific mutation.

It was at this point that the aim of this chapter changed direction to investigate the AcΔ*lef*-2^{100}.neo virus and to characterise this phenomenon further. The small, punctate plaques that had been characteristic of the AcΔ*lef*-2^{100}.neo were observed by light microscopy. Photographs revealed small areas of clearing in the monolayer, which upon higher magnification showed dead (infected) cells surrounded by red (live) stained *Sf*-21 cells. Potentially, this indicated that the AcΔ*lef*-2^{100}.neo virus was able to replicate, hence producing BV. This observation was made in contrast to previous research that proposed *lef*-2 to be essential for DNA replication (Kool *et al.*, 1994; and Lu and Miller., 1995). Before any conclusions could be made, further characterisations of AcΔ*lef*-2.neo including a multi step virus growth curve and DNA replication profiling was determined. As the AcΔ*lef*-2^{100}.neo was thought to possess approximately 100bp of the *lef*-2 N-terminus, the AcΔ*lef*-2 virus was chosen because the entire *lef*-2 coding region had been replaced by neomycin. Furthermore, the AcΔ*lef*-2.neo virus had shown the same results as AcΔ*lef*-2.neo of small, punctate plaques on plaque assay dishes.

Using q-PCR technology established in chapter three, the DNA profile of AcΔ*lef*-2.neo over 72hpi at a MOI of 0.02 was obtained. The AcΔ*lef*-2.neo virus was very slow growing, as indicated by the presence of plaques at 5dpi. Often the virus titre was very

low despite scaling up the virus stocks in comparison to AcMNPV, which explained why the low infection MOI of 0.02 was used compared to Figure 3.13 that used a MOI of 10. Throughout the time-course, AcΔ*lef*-2.neo showed a very linear DNA replication profile, with a slight rise between 24hpi to 72hpi. In contrast, the wild-type AcMNPV virus exhibited a typical DNA replication curve. These results are only limited at 24 hour intervals up to a total time of 72hpi. To gain a fuller understanding of the profile of AcΔ*lef*-2.neo, more time points are required to focus around DNA replication (6-12hpi) and later. The same AcΔ*lef*-2.neo pattern was observed when the multi-step virus growth curve was investigated. AcΔ*lef*-2.neo consistently exhibited a linear relationship that expressed a minor rise in BV titre throughout the 72 hour period. These results were very different to AcMNPV that showed a steady increase in BV titre up to 72hpi. Due to the slow growing nature of AcΔ*lef*-2.neo, a wider virus growth curve is needed by expanding the time-course to 168hpi.

The AcΔ*lef*-2.neo DNA replication profile obtained was very distinct and clearly different from the wild type AcMNPV virus. With the impossible separation of AcORF6^{3188} and AcΔ*lef*-2.neo, it was decided to investigate DNA replication over 24hpi by q-PCR of both these viruses as a mixture. Results showed that despite the presence of the AcΔ*lef*-2.neo virus that DNA replication levels were similar to AcMNPV over 24hpi. The DNA replication profile did not echo results as observed in VLD1-infected cells that were infected a higher MOI of 10 (chapter three). This may suggest based on this early study that the point mutation within the AcORF6^{3188}-3 virus is not responsible for the delay in DNA replication, which is characteristic of VLD1. Although further work is needed to try and separate the recombinant and parental virus before any conclusions can be made. The separation of recombinant and parental virus can be extremely difficult especially if using a virus knockout, which has been evident in this chapter. *Lac*Z has been used to knock out genes such as *p10* or *cathepsin* in order to make the separation easier through the production of blue and white plaques to highlight parental and recombinant viruses respectively. However, even this system is not perfect and picking of white plaques can sometimes result in a mixed virus population being present. It can take up to 10 rounds of plaque picking before obtaining a clean recombinant virus stock. It is

thought that the defective parental virus may persist by a helper mechanism from the recombinant virus and by using low dilutions it might be possible to separate the two viruses.

Reviewed by Hefferon (2002), baculovirus replication has often been compared to Herpes simplex type-1 virus (HSV-1), which requires the coordination of early, late and very late gene expression. Although similar to each other, both types of viruses do have differences between them. A heterotrimeric complex of UL5/ UL52 and UL8 can be isolated from triple-infected *Sf*-9 cells with recombinant viruses (Dodson *et al.*, 1989). The isolated heterotrimeric complex consisted of helicase, NTPase and primase activities (Tenney *et al.*, 1994). Although the exact function of each component is not known, it is suggested that UL52 functions as a primase, UL5 a helicase in the helicase-primase complex (Biswas and Weller, 1999) and UL8 stimulates primer primase activity of the UL52/ UL5 complex (Tenney *et al.*, 1994). Furthermore, UL8 is required for efficient primer utilisation on natural DNA templates as proposed by Sherman *et al.* (1992). If the same roles are transferred to an AcMNPV-based DNA replication process, then *p143* is suggested to function as a helicase, *lef*-1 a primase and *lef*-2 a primase accessory protein. Could the role of UL8 have parallel functions to *lef*-2 in function? The presence of *lef*-2 in AcMNPV contributes to the full functioning of the viral DNA replication process. However, the production of a virus without *lef*-2, but still being able to replicate and produce BV to a limited level as indicated by early studies suggests that the role of *lef*-2 may need to be re-thought. In contrast to UL8 which is essential to HSV-1 DNA replication, results in this chapter provide potential evidence that *lef*-2 could be suggested to actually be a stimulatory replication *lef* instead of a essential *lef*. Although more detailed studies are required to investigate the AcΔ*lef*-2.neo virus before any decision can be made.

Chapter Five

Examination of critical residues located within AcMNPV LEF-2 by multiple alignment and the conservation of baculovirus LEF-2 by phylogenetic analysis.

Chapter Five

5.1 Introduction.

Lef-2 is a highly conserved gene throughout the baculovirus family and is vital for DNA replication and late gene expression. The aim of this chapter was to examine LEF-2 for critical residues within the C-terminus as the VLD1 mutation documented by Merrington *et al.* (1996) was located within this region. Studies characterising the closely related BmNPV LEF-2 observed that the removal of 96 amino acids within the C-terminus resulted in the abolition of transcriptional activation (Sriram and Gopinathan, 1998). This study was based on the deletion of 96 amino acids from BmNPV LEF-2 by *Sal* I digestion; still retaining the last 19 amino acids of the C-terminus. Expressed under the *lef*-2 promoter, the plasmid was constructed and co-transfected into insect cells along with a plasmid possessing a minimal BmNPV polyhedrin promoter, harbouring a luciferase gene. Analysis showed that the deletion of the cysteine-rich domain within *lef*-2 resulted in the loss of the *trans*-activation of the minimal BmNPV polyhedrin promoter.

To examine the range and conservation of the cysteine-rich domain, a complete LEF-2 multiple alignment of thirty-seven baculoviruses spanning both NPV and GVs was produced. Subsequent analysis of the alignment revealed the presence of five highly conserved cysteine residues with 95% identity across all known baculovirus LEF-2 sequences. The importance of these cysteine residues together with previous evidence that the VLD1 phenotype original mutation was sub-mapped to position 154 to produce a virus deficient in late gene expression indicated that this region potentially was essential to the successful functioning of *lef*-2. Therefore, it was decided to produce recombinant viruses carrying single point mutations at the locations of the five cysteines to convert these to serine residues. Serine is a polar, hydrophilic amino acid and cysteine is a non-polar, hydrophilic amino acid. Both serine and cysteine amino acids possess very similar molecular weights of 105.09 and 121.15 respectively. In contrast, the cysteine R group contains a single sulphur atom that is essential in di-sulphide bonds and the forming of tertiary structures of some proteins. The only other known amino acid with a sulphur atom in the R side group is methonine, which was not appropriate for this study. Methonine is

encoded by the triple codon ATG and forms the sequence for the start site that is recognised by the ribosome for translation into a protein. Furthermore, methonine possessed a larger molecular weight of 149.21 compared to the other amino acids. Methonine was not used in this study because it would require a change from TGT for cysteine to ATG for methonine. It was more logical to introduce a single base pair change from TCT for cysteine to TGT for serine in *lef*-2 plus both amino acids shared a similar molecular weight.

The use of PCR technology and specifically-designed primers that possessed a single nucleotide change allowed the production of five cysteine-serine *lef*-2 PCR fragments that were ligated into pGem-T vector. Each individual cysteine-serine mutant plasmid was cotransfected with AcΔ*lef*-2.neo DNA into *Sf*-21 cells.

A phylogenetic tree was produced incorporating the results from the multiple alignments of the thirty-seven LEF-2 sequences. From the phylogenetic tree, the percentage of identical residues between all baculovirus LEF-2s compared to AcMNPV LEF-2 was calculated. To extend the investigation into the conservation of *lef*-2, it was decided to examine the percentage identity calculated for different viral *lef*-2s. From these results a selection of different viral *lef*-2s were chosen to see if AcMNPV *lef*-2 could be successfully replaced. Five baculovirus *lef*-2 sequences were selected to give an overall reflection of group I (AcMNPV, CfMNPV) and II (MbNPV, SeNPV) NPVs and GV (PxGV). Utilising PCR technology described in chapter four, baculovirus *lef*-2 PCR fragments with AcMNPV 50bp flanking regions were generated. As before, each of the baculovirus *lef*-2 PCR products was ligated into pGem-T and cotransfected into insect cells with AcΔ*lef*-2.neo.

5.2 Results

5.2.1 Multiple alignment of thirty-seven baculovirus LEF-2 protein sequences.

To construct a comprehensive analysis of *lef*-2 conservation within the baculovirus family, a multiple alignment of all known sequences was performed. Using the Genbank database, a total of thirty-seven nucleotide and corresponding protein sequences were collected from listed baculoviruses, including both GV and NPVs (For accession numbers, see chapter two). Using Clustal X, a multiple alignment of all thirty-seven baculovirus LEF-2 sequences was produced (figure 5.1). To visualize the degree of conservation within the baculovirus LEF-2 proteins, the program GeneDoc was used. This program not only allowed the percentage of identity similarity across the sequences, but the manual rearrangement of sequences for the purpose of producing a phylogenetic tree (See section 5.2.3.1).

Analysis of the completed multiple alignment of all the sequences highlighted 10 positions with 95% identity and a further 21 positions with 80% identity across the baculovirus LEF-2 family. However, five highly conserved (95%) cysteine residues were identified close to the original VLD1 mutation at D154. These five cysteines were located within the C-terminal of LEF-2 (with respect to AcMNPV sequence) at positions: 84 (cysteine 1), 143 (cysteine 2), 146 (cysteine 3), 150 (cysteine 4) and 165 (cysteine 5). In contrast, the NPV genera of the baculovirus family exhibited a further three highly conserved cysteine residues across the multiple alignment with an 80% identity at positions (with respect to AcMNPV): C185, C195, and C201. When examined in greater detail using only the NPV LEF-2 sequences, the three conserved cysteines showed a 100% identity.

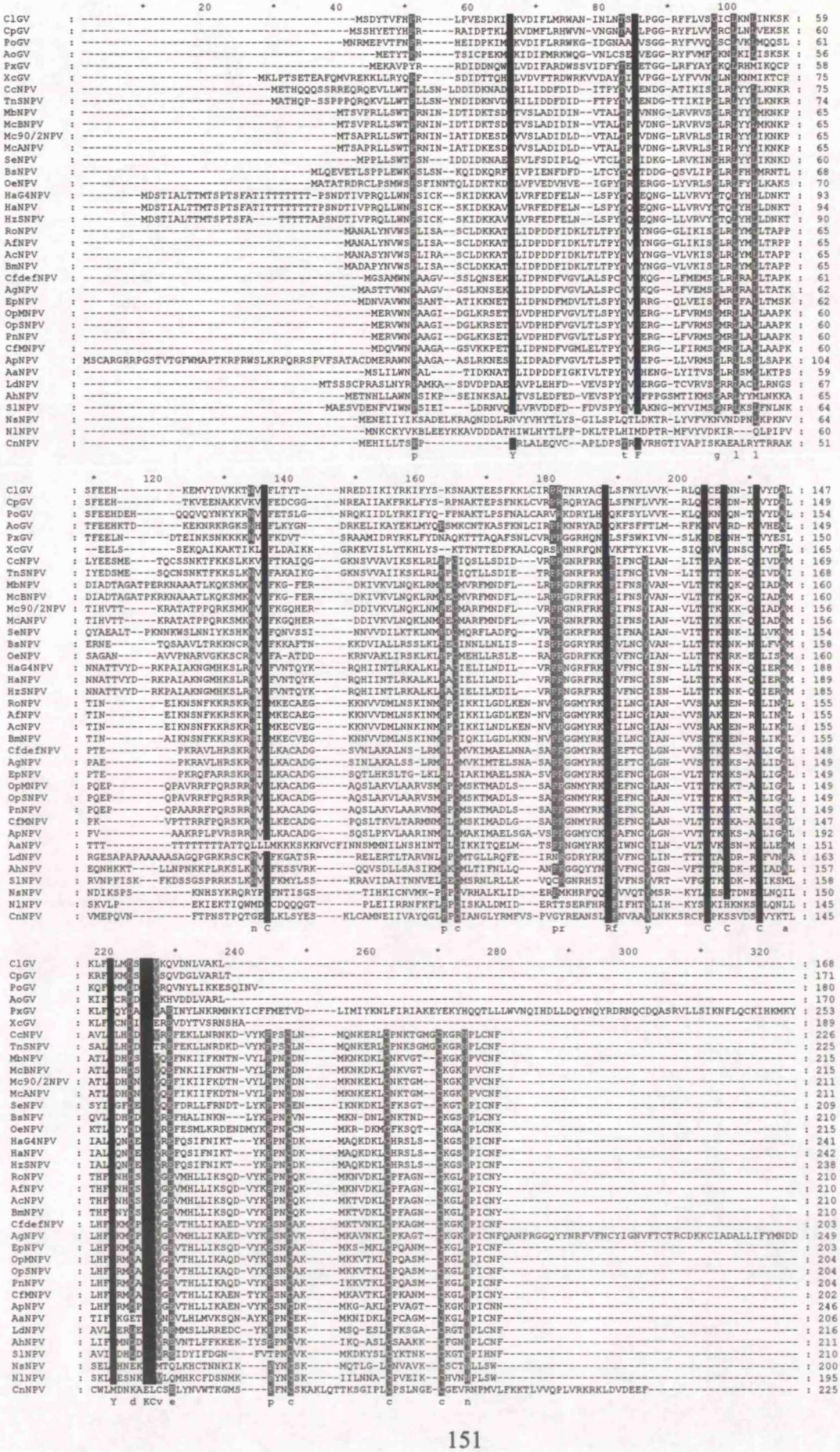

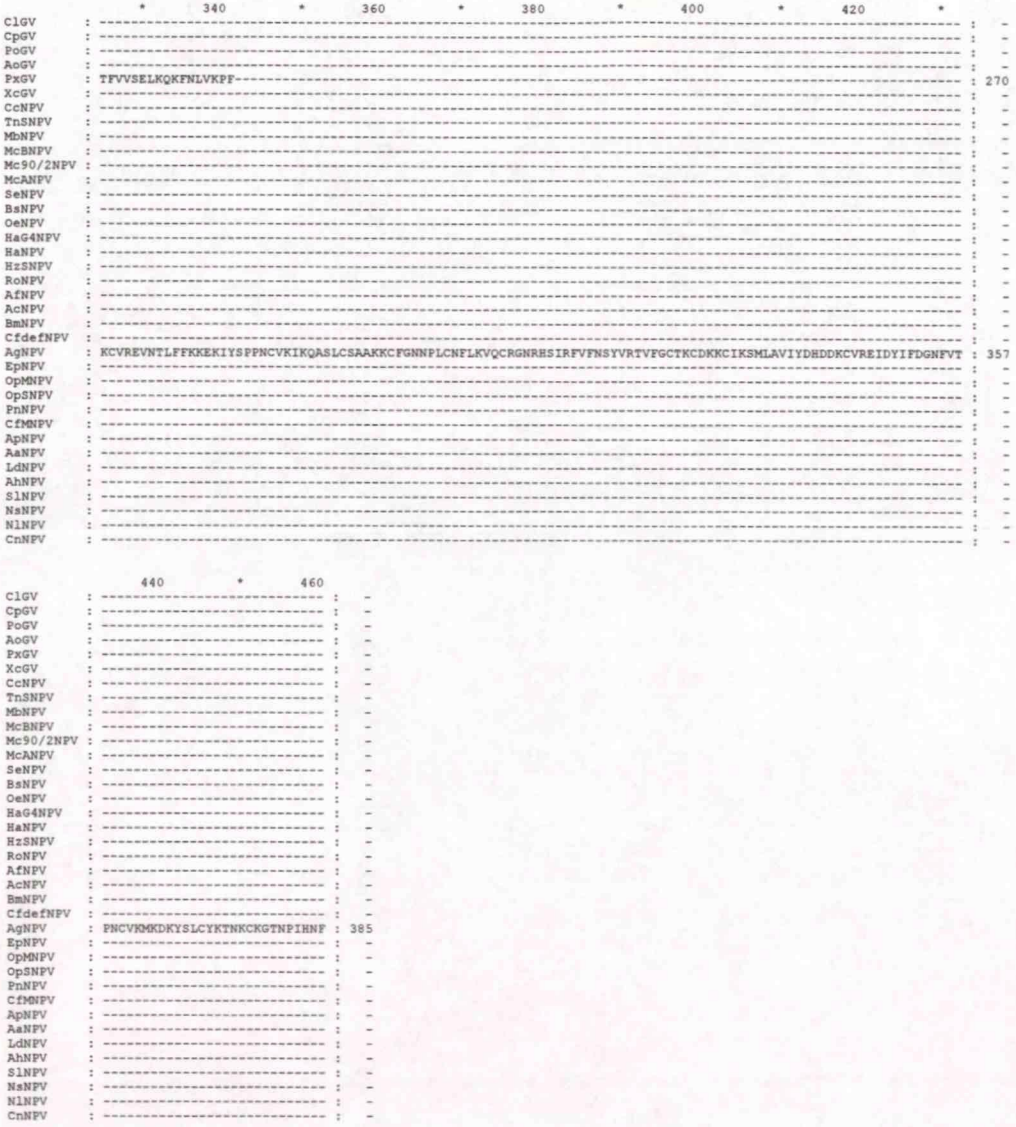

***Figure 5.1* – Multiple alignments of thirty-seven baculovirus LEF-2 proteins.** Thirty-seven amino acid baculovirus LEF-2 sequences (Chapter two for accession numbers) were taken from Genbank and aligned using Clustal X, version 1.83. Using Gene Doc software two shading levels were set: Black for 95% identity and Grey for 80% identity.

5.2.2 Construction and production of five highly conserved cysteine-serine mutant plasmids.

To examine the importance of the cysteine residues in the successful functioning of *lef*-2, five cysteine mutant plasmids were constructed. The five most highly conserved cysteine residues across the baculovirus family were chosen at positions (with respect to AcMNPV) at 84 (cysteine 1), 143 (cysteine 2), 146 (cysteine 3), 150 (cysteine 4) and 165 (cysteine 5). To knock out the cysteine residue, but to retain an amino acid replacement similar to the original as possible, the serine residue was chosen. The code for a cysteine residue is TGT, and with a single nucleotide change to TCT, the codon is translated into a serine instead.

With the ease of using only a single mutation change to convert the cysteine to a serine residue, specific primers possessing the point mutation were designed. The forward and reverse primers were designed to be overlapping so that a region of complementation was produced, which was essential to the second round of PCR (Fig 5.2, where in AcMNPVLef2CxF and AcMNPVLef2CxR primers the x denotes the cysteine number). The cysteine-serine mutant fragment was produced in two consecutive stages by PCR. Using AcMNPV DNA as a template, forward and reverse fragments were generated using primers AcMNPVLef2CxF/ RDP561 and AcMNPVLef2CxR/ RDP558 respectively (Fig 5.3). The second round of PCR involved the mixing of the corresponding purified forward and reverse fragments with RDP558 and RDP561 primers to produce a 1500bp product (Fig 5.4). However, as agarose gel electrophoresis (Fig 5.4) shows, a range of sizes was produced along with the desired 1500bp fragment size. These fragment sizes were screened out during the cloning stage. The purified PCR fragment was ligated into pGem-T cloning vector at position 52 and transformed into DH5α *E.coli* chemically competent cells. Viable white colonies were selected and grown into 2ml cultures of *Lb* to amplify stocks before purification. Successful insertion of the 1500bp PCR fragment was initially determined by restriction digestion with *Sac* I and II and agarose gel electrophoresis. To confirm the presence of the mutation within the 1500bp PCR fragments chosen from the restriction digest work, sequencing analysis was performed. Figure 5.5 illustrates the completed alignments of cysteine-serine mutant number 1 to 4 LEF-2s. Unfortunately, the cysteine-serine number 5 despite several attempts at sequencing yielded very obscure results that

suggested the annealing of PCR fragments at different locations. Therefore, this cysteine-serine mutant was discarded from further study.

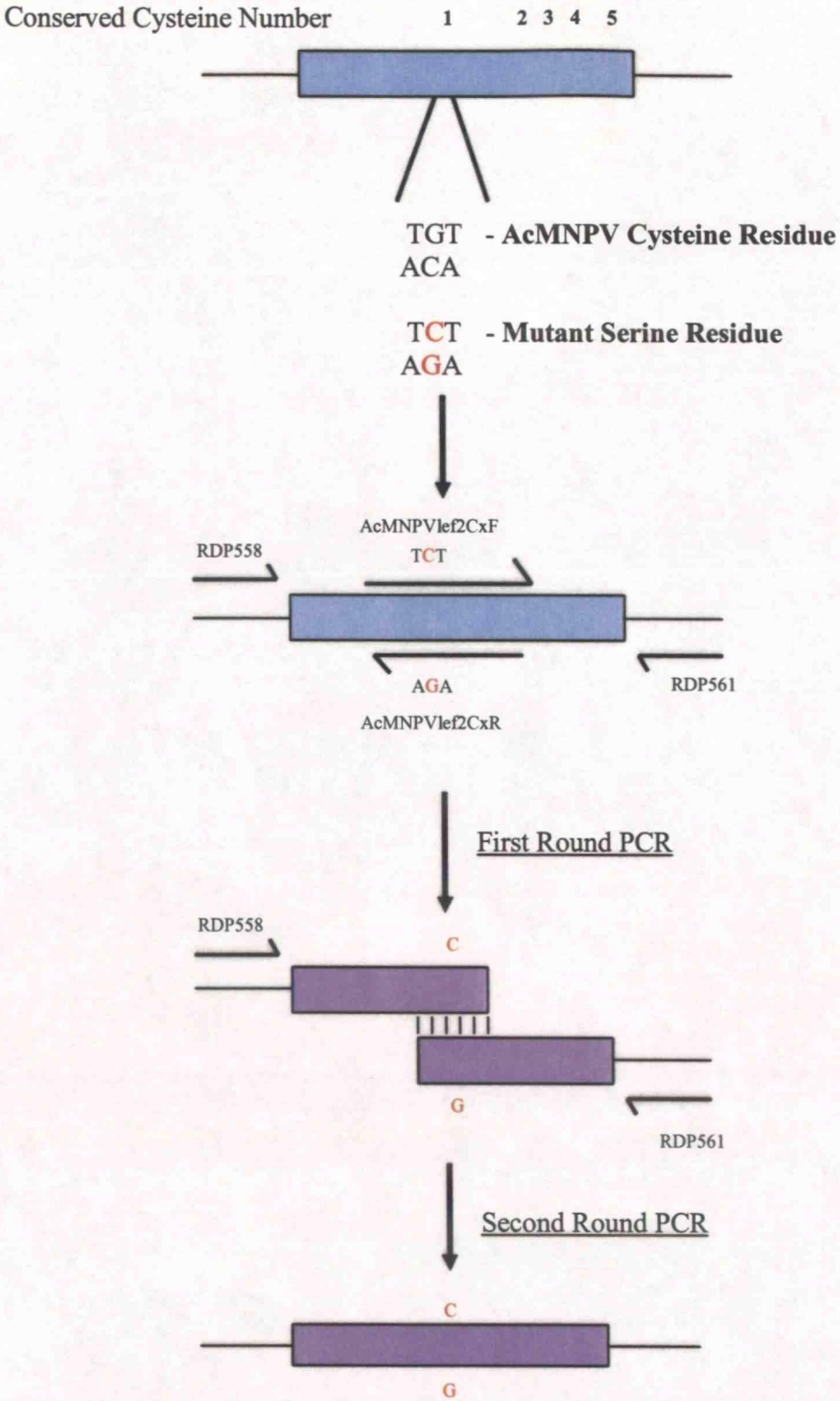

***Figure 5.2*- The production of five highly conserved cysteine-serine mutant fragments by PCR.** The blue box represents the AcMNPV *lef*-2 coding region with the schematic locations of the five highly conserved cysteine residues that are located in the C-terminal of the gene. These cysteines residues are translated by the presence of a TCT codon. To change the cysteine residue individually, the codon was changed by a single point mutation to TGT. Using the AcMNPV *lef*-2 DNA as a template, forward (AcMNPVlef2CxF and RDP561) and reverse (AcMNPVlef2CxR and RDP558) fragments expressing the corresponding mutation are produced by first round PCR (represented by the purple boxes). The purified PCR products were then annealed together in a single reaction, which was possible due to the AcMNPVlefCxF and AcMNPVlef2CxR primers producing a short region of nucleotides that are complementary to each other. The final 1500bp cysteine-serine mutant fragment is generated by second round PCR with RDP558 and RDP561 primers.

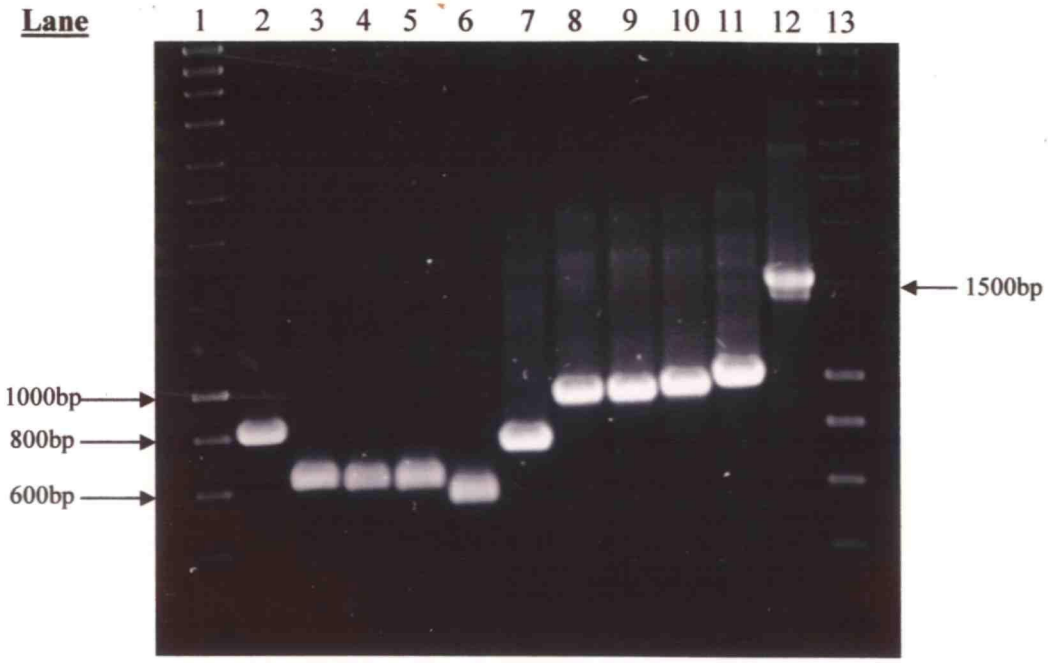

***Figure 5.3* - 1.2% agarose gel electrophoresis analysis of cysteine-serine mutants C1 to C5 forward and reverse fragments generated by first round PCR.** Lane 1 and 13- Bioline Hyperladder Number 1, lanes 2 to 6 are C1, C2, C3, C4, and C5 forward fragments, lanes 7 to 11 are C1, C2, C3, C4, and C5 reverse fragments. Lane 12- AcMNPV 1500bp fragment generated by first round PCR using primers RDP558 and RDP561.

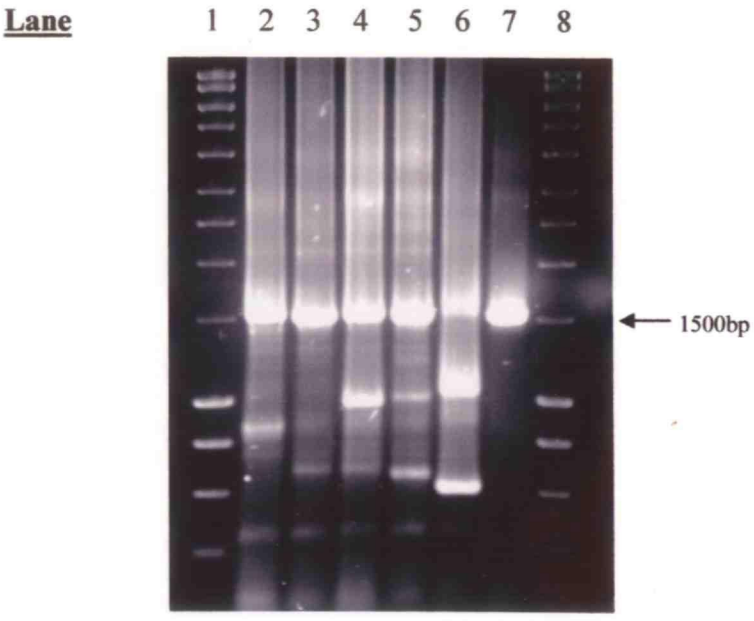

***Figure 5.4* - 1.2% agarose gel electrophoresis of completed cysteine-serine mutants C1 to C5 generated by second round PCR combining respective forward and reverse fragments.** Lanes 1 and 8 are Bioline Hyperladder 1; lanes 2 to 6 are completed C1, C2, C3, C4 and C5 mutant 1500bp fragments respectively. Lane 7- AcMNPV 1500bp fragment generated by first second PCR using primers RDP558 and RDP561

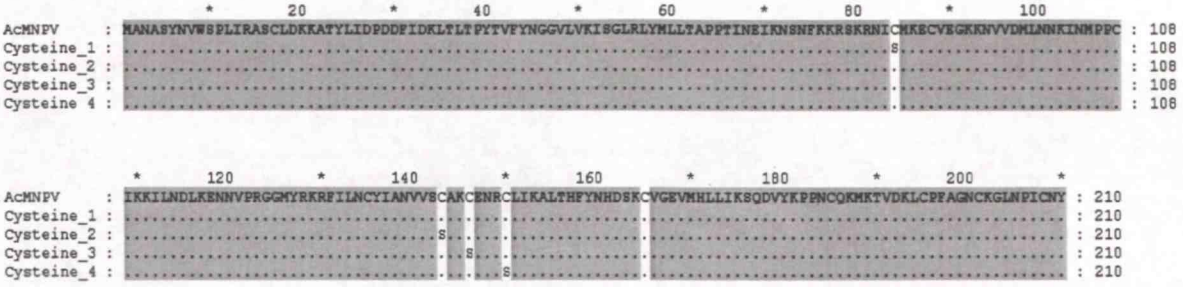

***Figure 5.5*- Confirmation of completed protein alignments of cysteine-serine *lef*-2 mutants viruses.** The entire amino acid coding region of the cysteine-serine *lef*-2 mutant genes were translated using pDraw. The sequences were aligned using Clustal X (Version 1.83). GeneDoc software was subsequently used for homology shading. Two shading levels were set: Grey for 100% identity and white for 60% identity. A dot represents the sequence that is identical to the AcMNPV LEF-2 sequence. The induced serine mutations are indicated by the presence of the letter "S" interrupting the amino acid sequence. The final highlighted cysteine shows the position of where the fifth cysteine-serine mutation was meant to be located upon successful sequencing analysis.

In chapter four, it was found that the AcΔ*lef*-2.neo DNA was infectious, evident by the production of BV. Therefore, to eliminate any possibility of background noise caused by the AcΔ*lef*-2.neo, this viral DNA was digested with *Srf* I. The AcΔ*lef*-2.neo DNA was constructed so that either side of the neomycin fragment was flanked by a *Srf* I restriction site, which was unique to this construct. By digesting with this enzyme the AcΔ*lef*-2.neo DNA was linearised, so that any parental virus was rendered non-infectious unless a suitable *lef*-2 fragment could be inserted to produce a viable virus.

Therefore, each cysteine-serine plasmid was co-transfected into insect cells with the digested AcΔ*lef*-2.neo DNA and left for 6dpi at 28°C. BV titres were determined by plaque assay. Figure 5.6 shows the results of the plaque assay at neat, 10^{-1} and 10^{-2} dilutions of the cotransfection mixture. It was clear from the linearised AcΔ*lef*-2.neo plaque assay dishes that the linearised virus DNA was unable to initiate replication, as shown by the absence of plaques. The recombinant viruses were not further plaque picked because it would be evident if *Srf* I had not successfully digested the AcΔ*lef*-2.neo DNA by the presence small punctate plaques on the plaque assay dishes. Furthermore, prior to cotransfection, the *Srf* I digested DNA was run on an agarose gel alongside uncut AcΔ*lef*-2.neo DNA for comparison (data not shown). Although it can never be assured that *Srf* I has cut every DNA molecule, the steps

taken at this stage before establishing a larger stock of the recombinant virus gave an initial idea of the potential consequences of these mutations. AcMNPV *lef*-2 rescued very successfully and higher serial dilutions were required to further titre the BV levels to give a final titre of 3.05 x 10^6 pfu/ml (Table 5.1). However, cysteine-serines numbers 1 to 3 also produced plaques but at a much lower level compared to AcMNPV *lef*-2. Further plaque assay serial dilutions were required for both cysteine-serine mutants 1 and 2 to give final calculated titres of 1.45 x 10^5pfu/ml and 1.45 x 10^6 pfu/ml respectively. According to Table 5.1, cysteine-serine number 3 produced a lower final titre of 2.73 x 10^3 pfu/ml; just 0.08% of the AcMNPV titre. In contrast, cysteine-serine number four did not produce any plaques.

To further characterize cysteine-serine mutants 1 to 3, plaque picks were taken and used to further infect *Sf*-21 cells. The total DNA was extracted and used as a template in a PCR with *lef*-2-specific primers- RDP558 and RDP561. The DNA fragments of approximate size of 1500bp were analysed using agarose gel electrophoresis (Fig 5.7). Cysteine-serine mutants number 1 to 3 (in duplicate) showed the presence of the 1500bp *lef*-2 fragment (Fig 5.7, lanes 2- 7), which was confirmed by AcMNPV (Fig 5.7, lane 8).

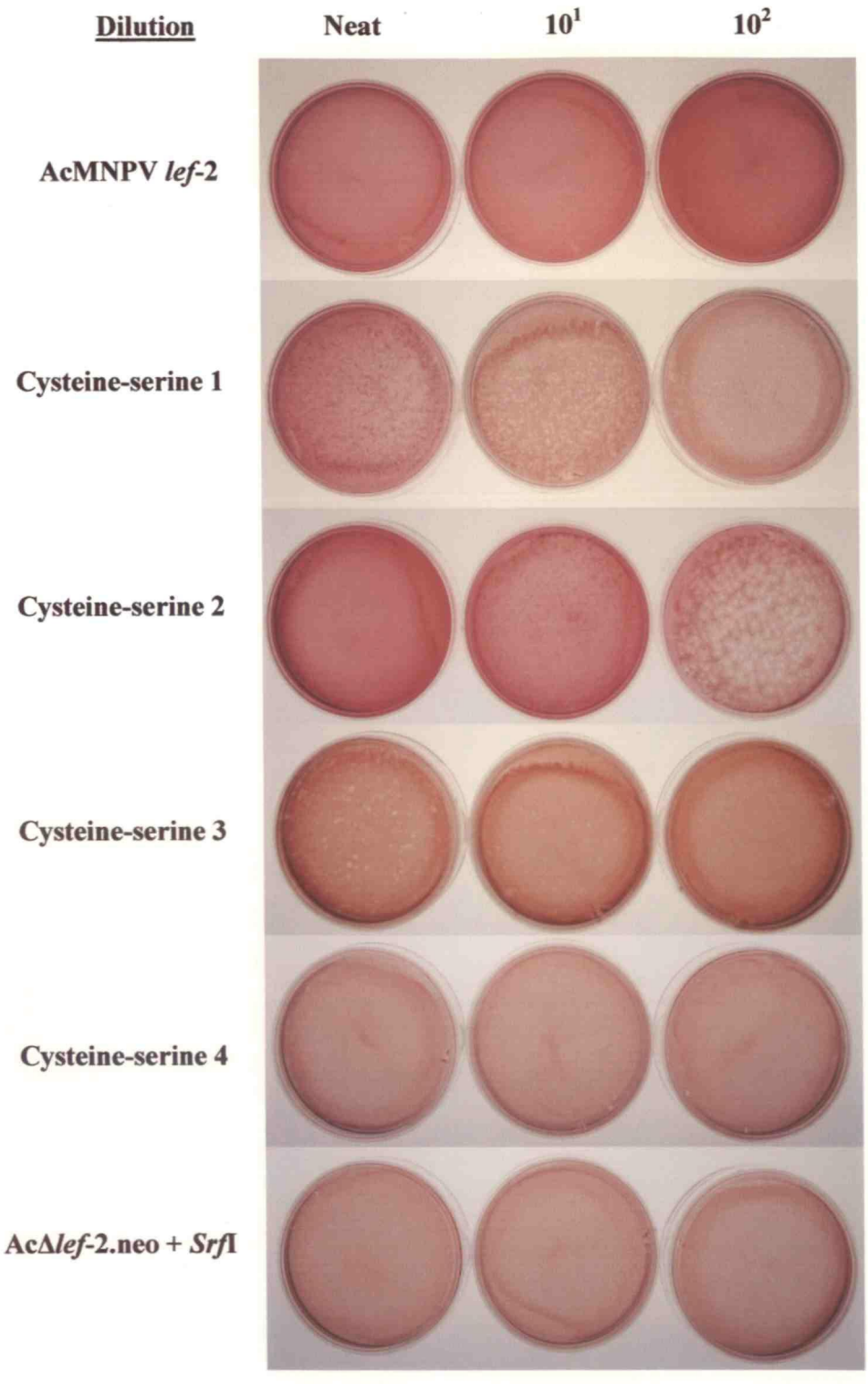

***Figure 5.6* - Plaque assay analysis of Cysteine-serine mutants 1 to 4 cotransfected into linear AcΔ*lef*-2.neo.** Cysteine-serine mutant plasmids with linear AcΔ*lef*-2.neo DNA (digested with *Srf* I) were cotransfected into *Sf*-21 cells and left for 5dpi at 28°C. Afterwards, the medium was removed and titred by plaque assay. Plaques were visualized using neutral red at 5dpi.

***Table 5.1*- BV titre of Cysteine-Serine Mutants 1 to 4 produced by rescuing linear AcΔ*lef*-2.neo DNA.**

Sample	Titre (pfu/ml)	Relative titre to AcMNPV *lef*-2 BV titre (%).
AcMNPV *lef*-2	3.05×10^6	100.00
Cysteine-Serine 1	1.45×10^5	4.75
Cysteine-Serine 2	1.45×10^6	47.50
Cysteine-Serine 3	2.73×10^3	0.08
Cysteine-Serine 4	0.00	0.00
AcΔ*lef*-2.neo + *Srf* I	0.00	0.00

***Figure 5.7* – 1.0% agarose gel electrophoresis of cysteine-serine recombinant viruses' *lef*-2 fragment generated by PCR.** Total DNA was used as a template to generate a PCR fragment of approximate 1500bp using RDP558 and RDP561 primers. Lanes 1 and 10 Bioline Hyperladder. Lanes 2 and 3 are cysteine-serine mutant number 1; lanes 4 and 5 are cysteine-serine mutant number 2 and lanes 6 and 7 are cysteine-serine mutant number 3. Lane 8 is AcMNPV DNA; Lane 9 is water (Negative Control).

5.2.3.1 Construction of a phylogenetic tree to display the multiple alignments of thirty-seven baculovirus LEF-2.

Lef-2 homologs are present in all baculovirus genomes sequenced to date. A phylogenetic tree was produced to examine the relationship between individual LEF-2s across the baculovirus family. At described in 5.2.1, a multiple alignment was produced for thirty-seven baculovirus LEF-2 sequences. From this analysis, a phylogenetic tree was generated using bootstrap analysis (1000 replicates) and options were chosen to exclude positions with gaps and to present labels on the tree nodes. As any gap in the sequence would be excluded from the final phylogenetic analysis, the alignment was manually rearranged to allow the minimization of sequence that would be removed and to align certain amino acids, which shared a common biochemistry.

According to Figure 5.8, it is clear that the baculovirus LEF-2 are clearly divided into their respective genera, either GV or NPVs. In agreement with Chen *et al.*, (1999), AcMNPV, BmNPV, RoNPV, AfNPV plus AaNPV clustered together as did ApNPV, CfdefNPV and AgNPV, with CfMNPV, PnNPV, OpMNPV, OpSNPV with EpNPV to form group I NPV. The GV group, including PxGV, XcGV, AoGV, PoGV, ClGV and CpGV formed a distinct cluster that was separated from group I NPVs but closer to group II NPVs. The cluster supporting CcNPV, TnSNPV, SeNPV, MbNPV, McBNPV, Mc90/2NPV, and McANPV formed group II NPVs. In contrast NsNPV and NlNPV formed a distinct cluster that was completely separated from any of the other groupings.

From the phylogenetic tree, a table was generated that illustrated the percentage of identical residues of every baculovirus LEF-2 compared to AcMNPV LEF-2 (Table 5.2). These ranged from 94-95% for BmNPV, AfNPV and RoNPV, via 28-54% amongst the rest of the NPVs in comparison to AcMNPV LEF-2. The overall amino acid with the GV LEF-2s was very low (13-18%). In contrast, NlNPV exhibited an amino acid identity of 19%, comparable to the GV group identity value.

Therefore, it was decided to investigate if any *lef*-2 from a different baculovirus species could effectively substitute AcMNPV *lef*-2 using the AcΔ*lef*-2.neo construct. Virus *lef*-2 from both group I and II NPVs and GV were examined. Due to availability of different baculovirus samples, the following were chosen to represent group I NPVs- AcMNPV and CfMNPV, group II NPVs– SeNPV and MbNPV and GV- PxGV. All AcMNPV, CfMNPV, SeNPV, MbNPV and PxGV had a percentage of identical amino acid residues to AcMNPV LEF-2 of 100, 53, 36, 37 and 13% respectively.

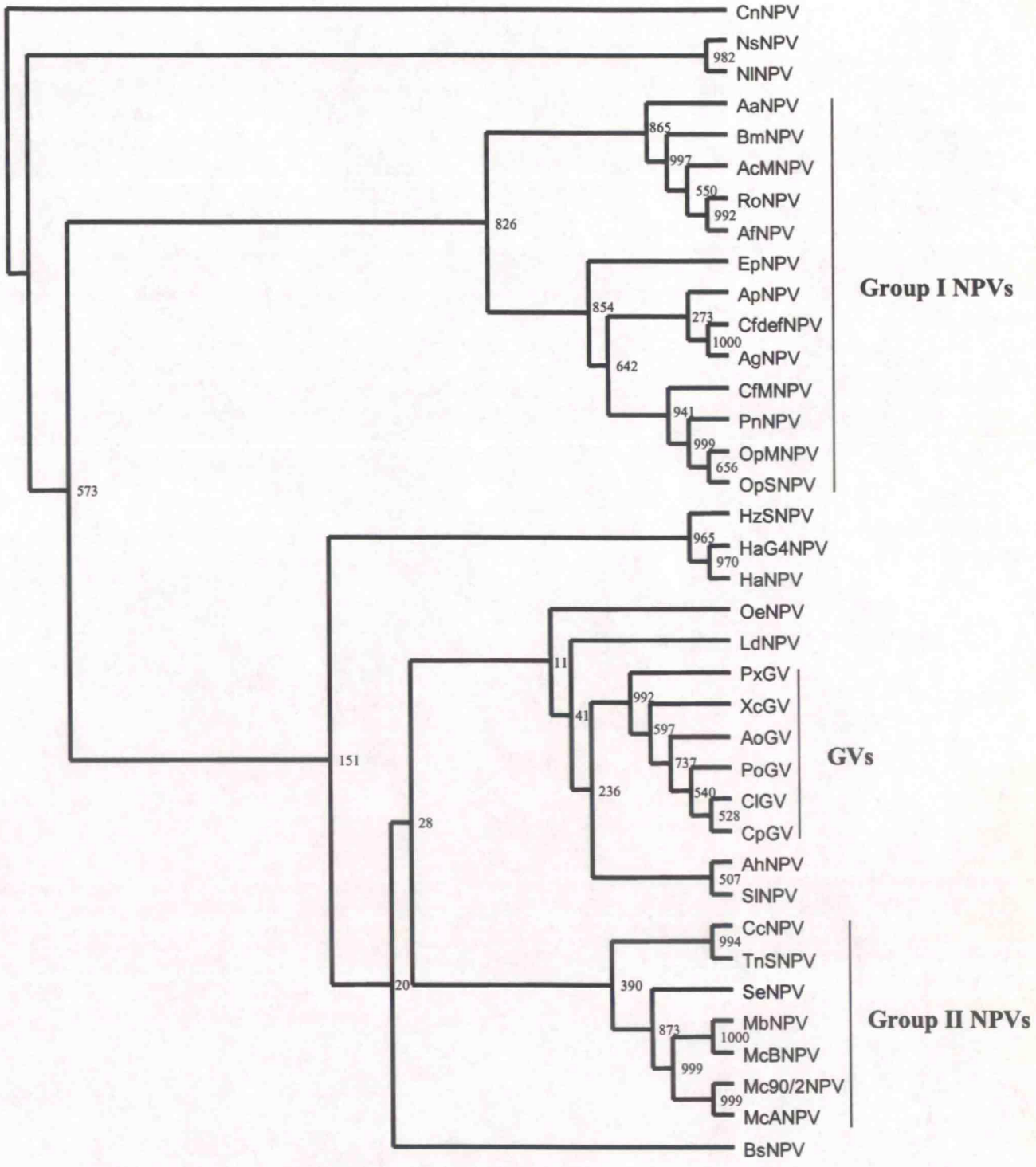

***Figure 5.8*- A phylogenetic tree of baculovirus LEF-2 sequences.** The amino acids of thirty-seven baculovirus LEF-2 were used based on the alignment in Figure 5.1 and rooted to CnNPV. Internal node labels indicate the frequency of a given cluster after bootstrap analysis (1000 replicates). The phylogenetic tree was constructed using Clustal X, version 1.83, and visualized by Treeview.

***Table 5.2* – Pairwise amino acid identity between different baculovirus LEF-2 used in the alignment (Fig 5.1) and phylogeny (Fig 5.8).**

Virus	Number of identical residues between AcMNPV and baculovirus LEF-2 amino acids used in the alignment (Fig 5.1) or phylogeny (Fig 5.8), expressed as percentage (%)
AcMNPV	100
AfNPV	95
RoNPV	95
BmNPV	94
CfdefNPV	54
EpNPV	54
CfMNPV	53
OpMNPV	52
OpSNPV	52
PnNPV	52
AaNPV	50
ApNPV	44
AhNPV	39
BsNPV	38
CcNPV	38
SeNPV	38
MbNPV	37
Mc90/2NPV	37
McANPV	37
McBNPV	37
OeNPV	37
TnSNPV	37
LdNPV	33
HaG4NPV	32
HaNPV	32
HzSNPV	32
SlNPV	31
AgNPV	28
NlNPV	19
ClGV	18
PoGV	17
NsNPV	16
AoGV	16
CpGV	16
XcGV	16
CnNPV	15
PxGV	13

5.2.3.2 Construction and production of AcMNPV, CfMNPV, SeNPV, MbNPV and PxGV *lef*-2 AcΔ*lef*-2.neo based constructs.

Results from chapter four which examined the optimum length of AcMNPV *lef*-2 flanking regions for insertion into AcΔ*lef*-2.neo identified that any length down to 50bp would be successful. The flanking region of 50bp was chosen as it provided enough length for insertion and reduced the overall number of nucleotides to be sequenced. To introduce AcMNPV flanking regions into a foreign baculovirus *lef*-2 sequence, specially designed primers and a two round PCR approach was taken (Fig 5.9). A two round PCR approach was taken to minimise errors in oligonucleotide construction that may have occurred from using larger primers such as 70-mers. However, I have since found that 70-mers work successfully and produce results from other work conducted in the laboratory. The foreign baculovirus DNA was obtained either as a gift or through Proteinase K extraction (see chapter two) from virus-infected larvae. Figure 5.10 represents the alignment of different viral *lef*-2 to be generated with 50bp AcMNPV flanking regions. Initially, virus-specific primers were designed to encode for 32bp of AcMNPV *lef*-2 flanking regions at the end of each sequence. During first round PCR, a product was generated of 705bp (AcMNPV), 681bp (CfMNPV), 702bp (SeNPV), 720bp (MbNPV) and 885bp (PxGV) respectively. The approximate sizes were analysed by agarose gel electrophoresis. After PCR purification each of the first round PCR products were used as a template in the second round stage of PCR. The primers used in the second round of PCR recognised and encoded only for the AcMNPV flanking region to complete the 50bp required for insertion.

Afterwards each of the PCR products was ligated into pGem-T and grown up in *Lb* from recombinant white colonies before extraction and purification of plasmid DNA. The correct insert was initially determined by digestion with *Sac* I and II, and final confirmation obtained by sequencing analysis (Table 5.3). As illustrated by Table 5.3, not all of the flanking regions possessed the total 50bp in length. Furthermore, both SeNPV and CfMNPV contained mutations that altered the amino acid sequence in comparison to the original sequence obtained from Genbank.

However, from the sequencing of other clones obtained, the same amino acid alterations appeared to be present in the immediate virus population.

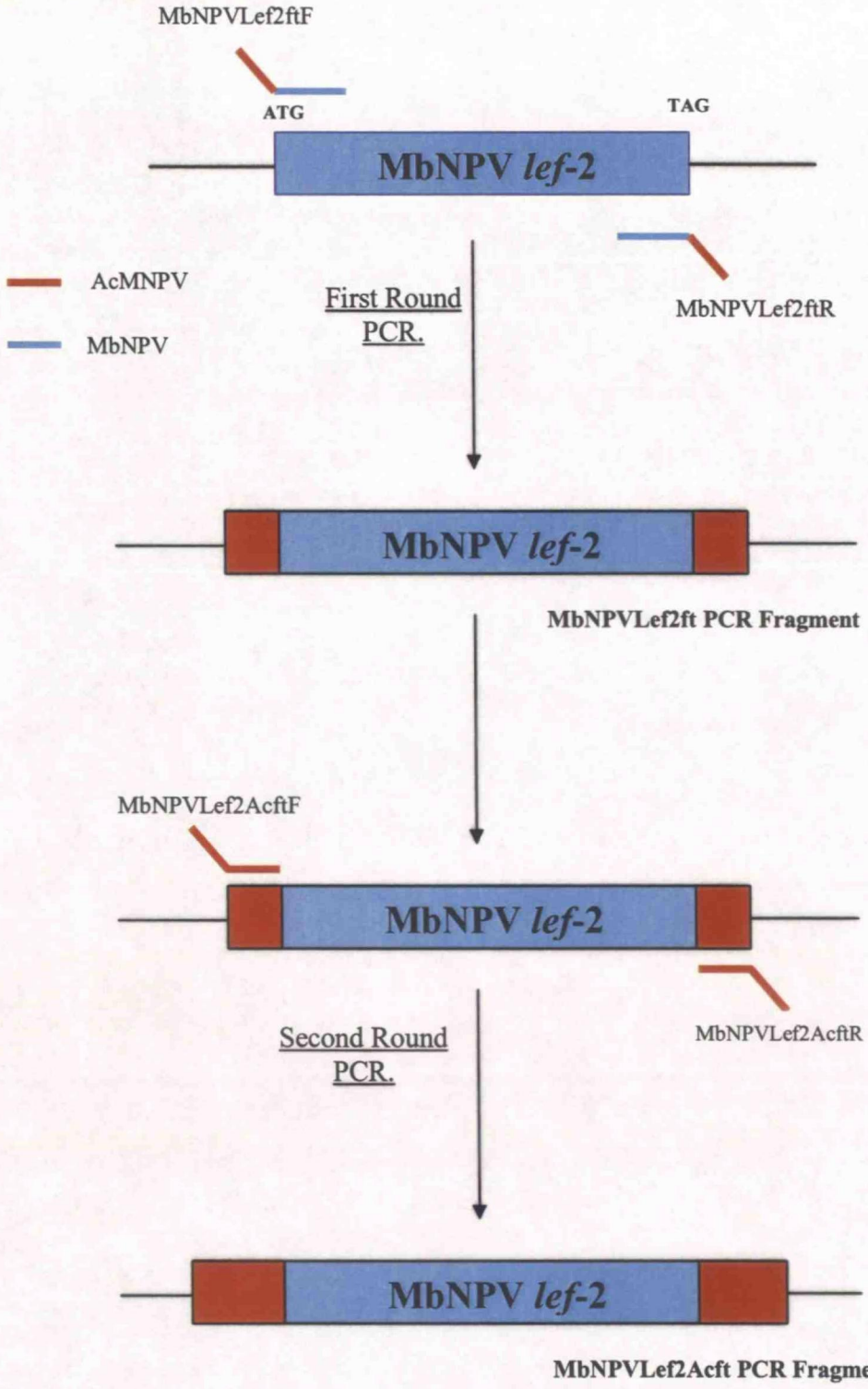

***Figure 5.9* – Construction of *lef*-2 hybrid PCR fragment with 50bp AcMNPV flanking regions.** MbNPV virus is being used as an example of the cloning strategy used. MbNPVLef2ftF and MbNPVLef2ftR were designed to amplify the MbNPV *Lef*-2 coding region as well as incorporating 32bp of AcMNPV flanking regions. The resulting fragment was denoted as MbNPVLef2Ft. Using this purified fragment as a template, the second round PCR was used with primers MbNPVLef2AcftF and MbNPVLef2Acft to incorporate the final 18bp of AcMNPV flanking regions.

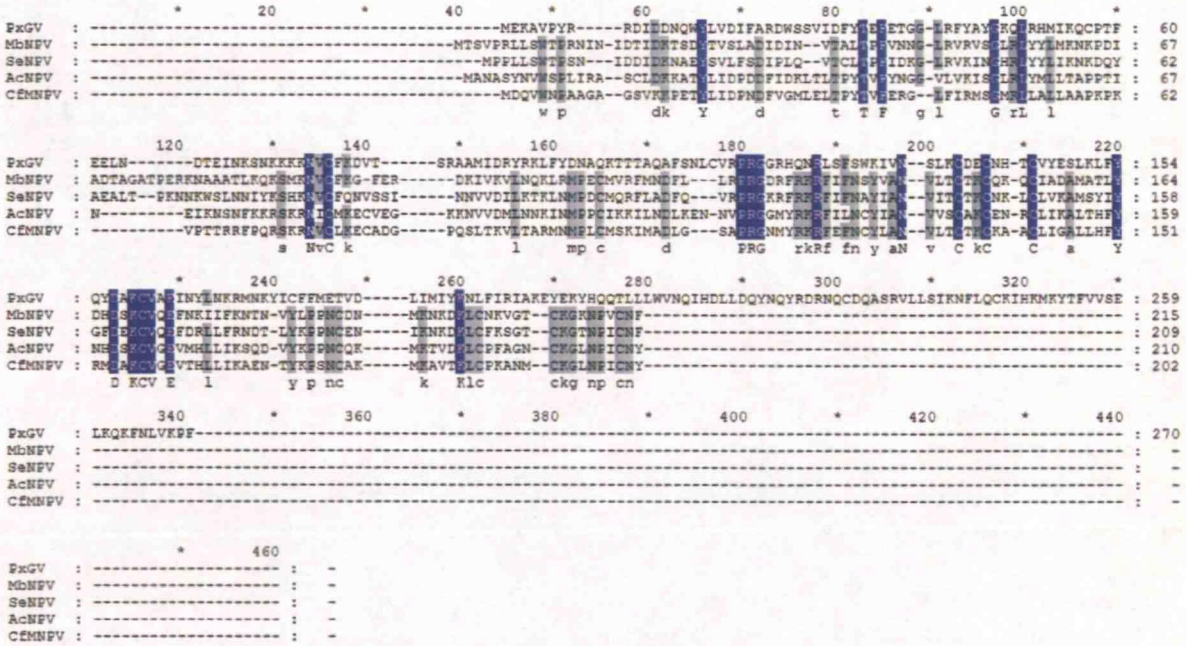

***Figure 5.10* – Alignment of viral LEF-2 protein sequences to be generated with AcMNPV 50bp flanking regions.** The LEF-2 protein sequence for AcMNPV, MbNPV, SeNPV, CfMNPV, and PxGV were obtained from Genbank (accession numbers are available from chapter two). The sequences were aligned using Clustal X (version 1.83) and two shading levels were set by GeneDoc: Dark blue for 100 identity and light blue for 85 identities.

The cotransfection was carried out with the virus *lef*-2 plasmids and Ac*Δlef*-2.neo + *Srf* I into *Sf*-21 cells. The samples were left to incubate at 28°C for 6dpi. Once again, the BV titre was determined by plaque assay (Fig 5.11). Plaques were only detected on AcMNPV and CfMNPV *lef*-2 dishes. Plaque assay analysis (Table 5.4) estimated a final BV titre of AcMNPV *lef*-2 and CfMNPV *lef*-2 at 1.9 x 10^7pfu/ml and 7.75 x 10^3pfu/ml respectively. When Ac*Δlef*-2.neo was solely cotransfected into *Sf*-21 cells no plaques were detected during plaque assay, which further confirmed previous results from this chapter (See Table 5.1).

***Table 5.3* – Sequencing summary of different baculovirus *lef*-2 with 50bp flanking regions of AcMNPV ligated into pGem-T vector.**

Plasmid Name	Nature of *Lef*-2	Forward FR	Reverse FR
AcMNPV *lef*-2	Complete	Complete	Complete
MbNPV *lef*-2	Complete	Complete	Sequence up to first primer (34bp flanking region)
SeNPV *lef*-2	Complete but a point mutation at SeNPV genomic position 16186 (K being replaced by N) Same mutation present in other sequenced clone.	Complete	Complete
PxGV *lef*-2	Complete	Sequence up to 40bp flanking region but has a point mutation seven bp from ATG of *lef*-2 (A has been replaced by E)	Sequence up to first primer (34bp flanking region)
CfMNPV *lef*-2	Complete but two point mutations at CfMNPV genomic positions 1811 and 1825 (P being replaced by T and G replaced by an A) respectively. Same mutation present in other sequenced clone.	Complete	Complete

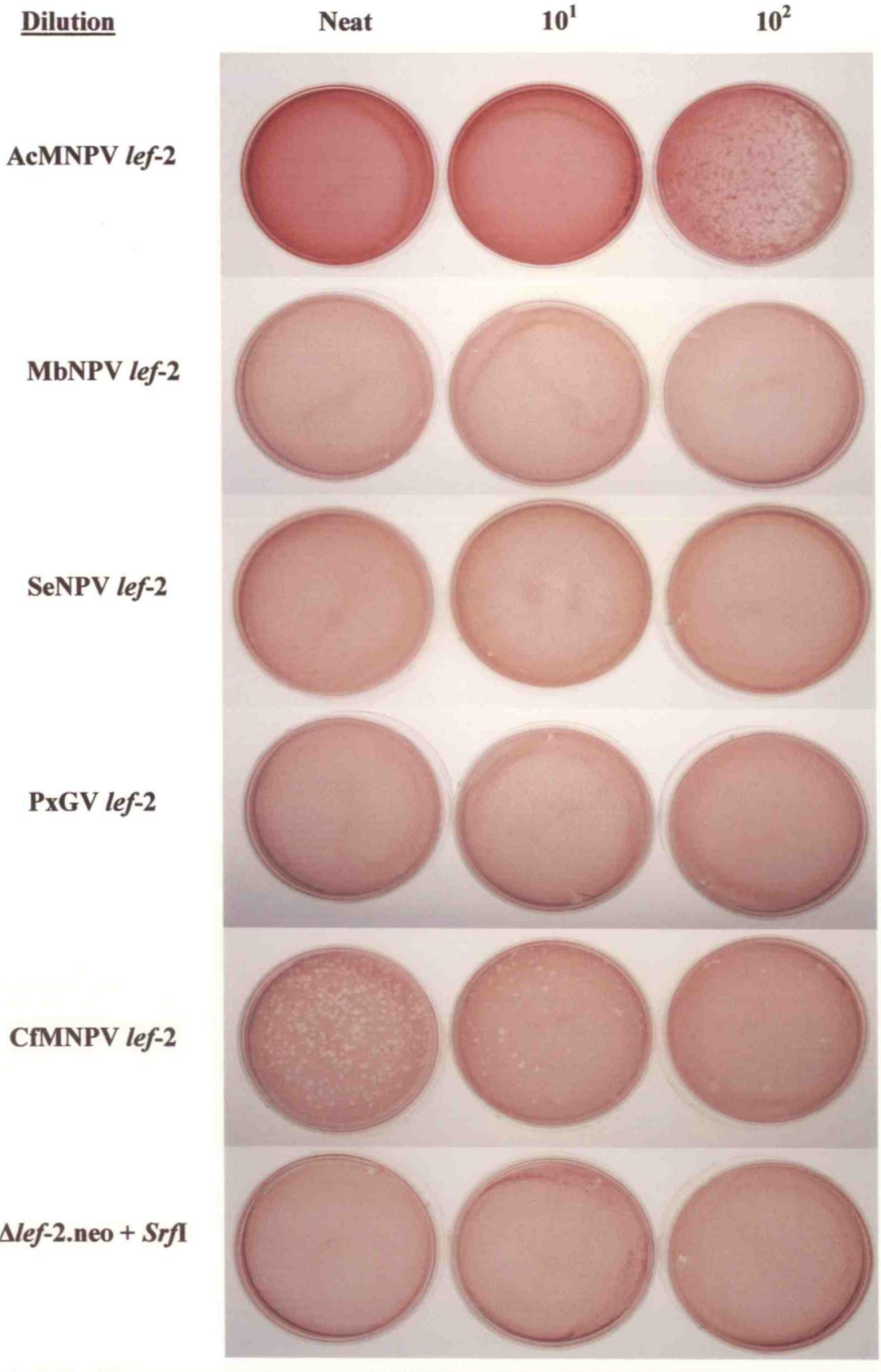

***Figure 5.11* - Plaque assay analysis of AcMNPV/ MbNPV/ SeNPV/ CfMNPV and PxGV *lef*-2 cotransfected with linearised AcΔ*lef*-2.neo.** Different virus *lef*-2 plasmids with linear AcΔ*lef*-2.neo DNA (digested with *Srf* I) were cotransfected into *Sf*-21 cells and left for 5dpi at 28°C. Afterwards, the medium was removed and titred by plaque assay. Plaques were visualized using neutral red at 5dpi.

Table 5.4 - **BV titre of different baculovirus *lef*-2 using linear AcΔ*lef*-2.neo**

Sample	Titre (pfu/ml)	Relative titre to AcMNPV *lef*-2 BV titre (%).
AcMNPV *lef*-2	1.90×10^7	100.00
MbNPV *lef*-2	0.00	0.00
SeNPV *lef*-2	0.00	0.00
CfMNPV *lef*-2	7.75×10^3	0.04
PxGV *lef*-2	0.00	0.00
AcΔ*lef*-2.neo	0.00	0.00

To further characterise the CfMNPV *lef*-2 recombinant viruses, five plaques were picked (Fig 5.12, panel A) and used to further infect *Sf*-21 cells. Total DNA was extracted from virus-infected cells and used as a template with CfMNPV *lef*-2-specific primers to detect the presence of the recombinant virus. The results were analysed using agarose gel electrophoresis. The presence of PCR products (approximate size of 370bp) was detected only in all of the CfMNPV *lef*-2 recombinant viruses 1 to 5 (Fig 5.12, panel B, lanes 2-6). However, no PCR product was present within the AcMNPV DNA or the negative control (water) (Fig 5.12, panel B, lanes 7 and 8).

A:

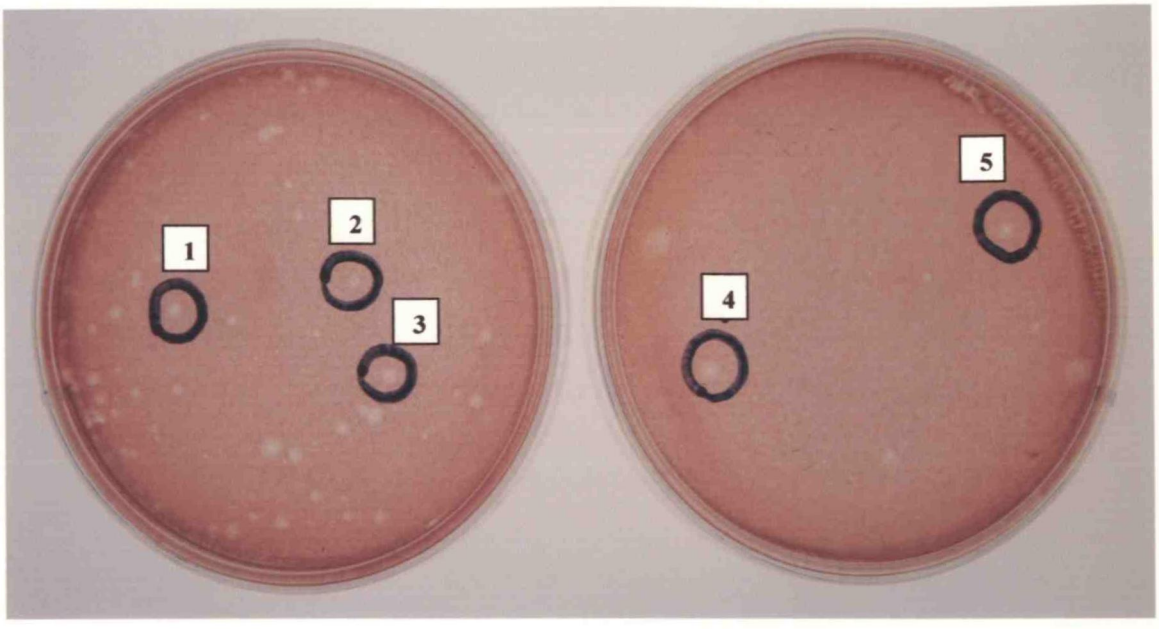

B:

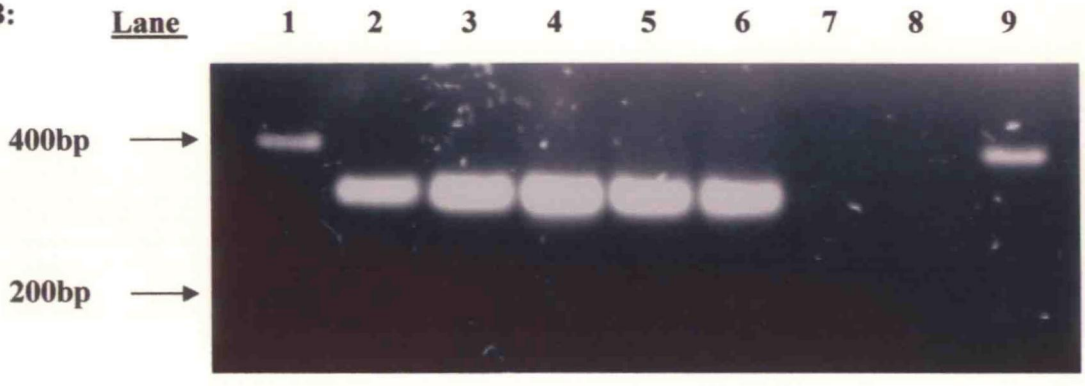

***Figure 5.12* –CfMNPV *lef*-2 recombinant viruses.** Panel A indicates the location of plaques picked using sterile Pasteur pipettes, which were placed into 0.5ml TC100 and stored at 4°C. Panel B represents the characterization of CfMNPV *lef*-2 recombinant viruses by PCR with specific CfMNPV *lef*-2 primers using a 1.2% agarose gel. Lanes 1 and 9 Bioline Hyperladder. Lanes 2 to 6 are CfMNPV *lef*-2 specific PCR products from plaque pick numbers (location of plaque picks see panel A) 1, 2, 3, 4, and 5; Lane 7 is AcMNPV DNA; Lane 8 is water (Negative Control).

5.3 Discussion

The initial aim of this chapter was to investigate critical residues within AcMNPV LEF-2 that were located close to the original VLD1 point mutation documented by Merrington *et al.* (1996). A multiple alignment of thirty-seven baculovirus LEF-2 sequences was produced. Overall, the multiple alignments highlighted that LEF-2 was highly conserved throughout the baculovirus family at both the N and C terminus. In agreement with previous research, the LEF-2 C-terminus comprised a cysteine-rich region with a high degree of conservation (Chen *et al.* 1999). Five cysteines were identified at positions (relative to AcMNPV LEF-2): 84 (cysteine 1), 143 (cysteine 2), 146 (cysteine 3), 150 (cysteine 4) and 165 (cysteine 5) with 95% identity applied across all 37 baculovirus examples of LEF-2. It was decided to take each cysteine residue individually and through site directed mutagenesis (Chapter four) to change it to a serine residue instead. A serine residue was selected because it was the closest amino acid that matched the cysteine residue both in molecular weight and charge. However, the cysteine residue does contain a sulphur atom within its R-group whereas the serine residue does not. The sulphur atom is important in the formation of di-sulphide bridges that are involved in the secondary structure of a protein. The only other known amino acid that contained a sulphur atom was methonine, and this was not used in this study.

Each of the cysteine residues was mutated using a two stage PCR approach that had been employed in chapter four to create the AcORF6^{3188} virus. To change the cysteine residue to a serine, a single point mutation was required to convert the triple codon from TCT to TGT respectively. To ensure that the point mutation had been successfully introduced into the PCR product and subsequently the completed plasmid, each of the cysteine-serine mutants was sequenced. It became apparent that cysteine-serine mutant number 5 would not be easy to produce. Sequence analysis revealed that the PCR templates for cysteine-serine number 5 had potentially annealed together at different locations to give an incomplete and obscure sequence. After several attempts to sequence different clones expressing the cysteine-serine

number 5 mutation with no success, it was decided to focus solely on the remaining four cysteine-serine mutants.

As described in chapter four, the AcΔ*lef*-2.neo virus was able to replicate and produce BV. To minimize any background noise created by the replication of the parental AcΔ*lef*-2.neo virus, the DNA was digested with *Srf* I prior to cotransfection. Unique to the AcΔ*lef*-2.neo virus was the addition of two *Srf* I restriction sites located either side of the neomycin fragment. By linearising the AcΔ*lef*-2.neo DNA with *Srf* I, the virus was rendered noninfectious unless a suitable *lef*-2 could circularize and subsequently rescue the virus.

Cotransfection with linearised AcΔ*lef*-2.neo DNA, revealed that cysteine-serine mutants' numbers 1 to 3 showed signs of BV production; evident by the presence of plaques. In contrast, both cysteine-serine mutant number 4 and individually AcΔ*lef*-2.neo+ *Srf* I did not produce any plaques. The cysteine-serine mutant number 4 was non-viable despite AcΔ*lef*-2.neo replicating and producing BV. This may have attributed to a dominant negative mutation in cysteine-serine mutant number 4 being present that resulted in an altered gene product being produced. As a result this may have affected the interaction of the mutant LEF-2 with other proteins abolishing DNA replication or late gene expression so that the virus could not be rescued. This further provides a potential understanding of the functioning of *lef*-2 in that it interacts with multiple proteins or transcription factors. The inability of AcΔ*lef*-2.neo + *Srf* I to replicate provided a means of virus separation. This gave the indication that any plaques present on rescued dishes were the result of the recombinant virus only. The highest BV titre value was produced by cysteine-serine number 2 with a relative titre of ~ 48% compared to wild type AcMNPV *lef*-2. In contrast, cysteine-serine number 3 BV titre shared only 0.08% relative titre with AcMNPV. Overall, the results show that collectively the cysteine residues contribute to the functioning of LEF-2, which is also illustrated by Sriram and Gopinathan. (1998). However, when the cysteine residues were examined individually, it was apparent that the consequences of such serine mutations exhibited varying effects

ranging from a 50% reduction in LEF-2 functioning to the total inability in rescuing the virus. Unfortunately, further characterization of the cysteine-serine mutant viruses was not possible in the time available. Future work such as sequencing analysis to ensure the presence of the mutations and investigating late or very late gene expression by q-PCR would be a very interesting course to pursue.

The multiple alignments of thirty-seven LEF-2 sequences showed a high degree of conservation across the baculovirus family. Chen *et al.* (1999) showed three regions of conservation across the baculovirus LEF-2. Region I was located in the N-terminal half with region II being notable for the cysteine-rich C-terminus. The final region, number III was only found in NPVs. Region I was placed in the N-terminal comprising of six conserved amino acids (relative to AcMNPV): P11, Y24, T41, F43, G47, and G54. The region between 20-60 amino acids has been suggested to be involved in the interaction of LEF-2 with LEF-1(Evans *et al.*, 1997). Chen *et al.* (1999) proposed that due to the divergence in this region, the interaction between LEF-1 and LEF-2 might be virus species–specific. This view was further supported experimentally by results obtained by Broer *et al.* (1998). Broer *et al.* (1998) examined the ability of SeMNPV to recognize and replicate AcMNPV *hr oris* and vice versa. Using a plasmid-based replication assay it was shown that SeMNPV *hr*6 could only replicate in the presence of SeMNPV and not AcMNPV. This was the same result for AcMNPV *hr5*, which suggested that DNA replication was *hr*-specific. Furthermore, it highlighted that a SeMNPV *lef*-2 could not replace AcMNPV *lef*-2 to support transient DNA replication (Broer *et al.*, 1998). As this study only focused on using *hrs oris* from one virus species, it was proposed to investigate the consequences of replacing AcMNPV *lef*-2 with other baculovirus *lef*-2s using the AcΔ*lef*-2.neo construct.

Due to the availability of LEF-2 sequences and the extent of the virus collection, five baculoviruses were chosen to represent a small cross section of group I (AcMNPV and CfMNPV) and II (SeNPV and MbNPV) NPVs and GVs (PxGV). To ensure the successfully insertion of the different virus *lef*-2 into AcΔ*lef*-2.neo

construct, 50bp AcMNPV flanking regions were incorporated into the final PCR product. Identical to the cysteine-serine work, the different baculovirus *lef*-2 were cotransfected with AcΔ*lef*-2.neo to give a mixture of small punctate and large well defined plaques. Therefore, the AcΔ*lef*-2.neo construct was digested with *Srf* I and the cotransfection repeated. Plaque assay analysis revealed the presence of plaques on AcMNPV *lef*-2 and CfMNPV *lef*-2 recombinant virus dishes. Characterisation of plaque picks taken from the CfMNPV dishes further confirmed the presence of the recombinant virus using virus species-specific *lef*-2 primers. The CfMNPV LEF-2 is calculated to share 53% of identical residues with AcMNPV LEF-2. Moreover, the CfMNPV titre was only determined to be 0.04% of the relative titre of AcMNPV *lef*-2. In contrast, SeNPV, MbNPV or PxGV *lef*-2 were unable to replace AcMNPV *lef*-2 and this may be reflected by the low percentage of identity of 38%, 37% and 13% respectively.

Unfortunately, the range of amino acid identity for LEF-2 across all baculovirus sequences is very limited because CfMNPV represents one of the higher values in the 28-54% range. After this range, a large jump is made to 94-95% amino acid identity to represent viruses such as BmNPV or RoNPV. However, there are no virus LEF-2 intermediates between the ranges of 55% to 90% that would provide useful to study in order to widen this investigation. This may suggest that there are other viruses yet to be discovered or that those *lef*-2s potentially present between 55%-90% are not viable.

There is a potential for gene replacement via ET recombination and using neomycin as a selectable marker. It would then be possible to transfect insect cells with high concentrations of bacmid DNA containing the gene replacement. This work could be expanded to include other genes such as *lef*-8 or *lef*-1 to examine if they can be replaced by other NPVs or GVs genes. It would be interesting to see if LEF-1 shares the same homology gap between 55%-90% as revealed in LEF-2. If not, what does this say about the functioning of *lef*-2 across the baculovirus family? This could imply that LEF-2 has evolved differently from LEF-1 in baculoviruses and that it

could have more than one function during infection than just a primase associated factor. Further questions that may arise are the determination of when a gene for one baculovirus cannot rescue AcMNPV and can it be considered the same gene? A gene can be classified according to its function within a system. However, when the same gene from one virus is replaced into another virus and is not able to perform the same function, is it really the same gene? Furthermore, even though the virus genes may share a degree of homology within both sequences; if they cannot share the same function does that make them different genes or is it just that other virus/ cell specific factors are required? This is really dependent upon the description or classification of a group of genes with a similar function or homology between sequences.

Chapter Six

Final Discussion

Chapter Six

6.1 Final Discussion.

Lef-2 is a highly conserved and important gene in baculovirus replication. It was proposed by Merrington *et al.* (1996) that *lef*-2 had a dual role in DNA replication and late gene expression. In this PhD study, I have obtained results that support the proposal of *lef*-2 having a dual role. However, some results have further questioned *lef*-2 as an essential replication *lef* within the baculovirus *lef* group. So in this final discussion, I am to reveal what future work should be conducted to extend our knowledge of LEF-2 function.

It is inferred that AcΔ*lef*-2.neo replication proceeds in the absence of *lef*-2. This was evident by q-PCR results which showed that despite virus replication occurring, it was severely compromised by the lack of *lef*-2. Early data suggested that *lef*-2 may play a more stimulatory role in DNA replication, but this has only been examined up to 72hpi. The AcΔ*lef*-2.neo virus is slow growing and to achieve a more detailed result, further characterisation is required. Low AcΔ*lef*-2.neo virus titres made it hard to do a one-step growth curve. One way that this could be achieved would be to expand the time-course to 168hpi and to examine both over a multi-step growth curve. However, growth curves are complicated by 5 day plaque assays and very small plaques. Using the techniques adopted in chapter three, the effect of the *lef*-2 null mutant virus on late and very late gene expression by q-PCR could be investigated, but *polyhedrin* would not be applicable because the AcΔ*lef*-2.neo is polyhedrin negative. Particular emphasis would be placed on late gene expression with structural genes such as *gp64* or *capsid* in attempt to explain the decreased levels in AcΔ*lef*-2.neo BV titre.

The work on AcΔ*lef*-2.neo and other *lef* mutants shows that the early studies by Miller *et al* to find *lef*s was not sensitive enough to find *lef*s that could be deleted in this way. *Lef*-2 was proposed as an essential *lef* because the omission of this gene from plasmid transient assays yielded no DNA replication. It is possible that replication was occurring but at such a low level that it was not detectable. The technology that has enabled us to delete the *lef*-2 could be applied to other replication *lefs* that have been noted as essential or stimulatory. Null

mutants have been increasingly used to determine the roles of *lef*s such as *lef*-6 and *lef*-12. The *lef*s were originally identified using transient assays and this method provided successful results, but in the case of *lef*-12, it was not discovered until a set of 18 plasmids expressing a single *lef* ORF with an eptiope-tagged fusion protein from the *Drosophila melanogaster* hsp70 promoter failed to support late gene expression in transient assays (Rapp *et al.*, 1998; Li *et al.*, 1999). *Lef*-11 was described as a transcription *lef* as the result of a transient assay. In contrast, it was shown that a *lef*-11 knockout bacmid was unable to replicate in *Sf*-9 cells. This was further supported by the reinsertion of the gene back into the DNA to rescue the defect. This may suggest that *lef*-11 needs to be further investigated as it possesses an essential role in DNA replication. I would like to expand this type of examination to the rest of the replication *lef*s to help determine if their classification is correct or needs potentially readjusting, which is the case of *lef*-2.

The cysteine-rich C-terminus is essential to the functioning of *lef*-2 as shown by Sriram and Gopinathan (1998) and my PhD work involving the site-directed mutagenesis of four cysteine residues. The work in chapter five highlighted that individual cysteines are affected differently by the mutagenesis to a serine residue. In some cases, the consequences of a serine mutation was definitive with no BV being produced, indicating that the alteration had disrupted the functioning of *lef*-2. Other cysteine-serine mutations were only affected by a 50% reduction with viable virus still being produced. DNA replication profiles of each virus would be examined to investigate the effect that the mutation exerted. Sriram and Gopinathan (1998) showed that the removal of 96 amino acids within the C-terminus of BmNPV LEF-2 resulted in the abolition of transcriptional activity of a minimal polyhedrin promoter. It would be very interesting to obtain the q-PCR profiles for each of the cysteine-serine recombinant viruses and to detect late and very late gene expression. Also we still need to characterise the cysteine-serine mutants further. This might help to determine if this region of LEF-2 is important in the role of late gene transcription. There are other highly conserved residues located throughout LEF-2 that could be modified to determine the consequences for LEF-2 function.

Measuring LEF-2 percentage identity compared to AcMNPV by phylogenetic analysis has provided tools in the examination of conservation across genes in virus families. The use of

LEF-2 across the baculovirus family highlighted the apparent absence of known viruses between 55-90% homology to AcMNPV LEF-2. This either indicated that there are still baculoviruses to be discovered or those *lef*-2s are not fully functional at that percentage. It would also be interesting and informative to construct chimeric *lef*-2 genes that contained 5' and 3' ends from different baculoviruses. This might help to differentiate between these regions required for DNA replication and late/ very late gene expression. It may be possible to expand this type of investigation to other genes such as LEF-1 across the baculovirus family. The interaction between LEF-1 and LEF-2 is well documented. It would be interesting to see if the high degree of conservation exhibited in LEF-2 is extended to LEF-1 across all sequenced genomes. Also it would be useful to determine the LEF-1 percentage identity across all baculoviruses compared to AcMNPV, to see if there is a break in homologies from 55-90% as highlighted in LEF-2. If so then this may indicate that there are other baculoviruses to be discovered. As it was possible to knock out the AcMNPV *lef*-2 using ET recombination, I would like to use the same technology to replace other baculoviruses *lef*s with different NPVs and GVs to see if the virus is still able to replicate and to what level.

The recombinant AcORF6^{3188} virus possesses a point mutation at the genomic position of 3188 within ORF6, or *lef*-2. This recombinant virus was constructed by co-transfecting a DNA fragment containing the mutation only with AcΔ*lef*-2^{100}.neo into insect cells. Unfortunately, the parental virus was able to persist despite several rounds of plaque picking as determined by PCR and *lef*-2 specific primers. Future work concerning the AcORF6^{3188} recombinant virus would involve the regeneration of this virus using AcΔ*lef*-2.neo digested with *Srf* I. This would enable the separation of the parental from the recombinant virus, a problem that proved impossible to solve by methods of plaque picking and plaque assays after circular DNA was used in a transfection. Afterwards, the DNA replication profile and late and very late gene expression levels can be measured by q-PCR. The contamination also suggests that such defective viruses are able to survive in a population as they act as parasites. Natural examples of parasite virus genomes are found in SeNPV populations, where virus genomes with large deletions are maintained in insects despite their viability to infect the host on their own (Munoz *et al.*, 1998).

Evidence by Evans *et al.* (1997) revealed that 20-60 amino acids of the LEF-2 N-terminus were essential to the interaction with LEF-1. None of the point mutations examined in this PhD study were located at these positions within *lef*-2. In fact, both mutations were situated near and within the cysteine-rich region of the C-terminus. Evidence by Merrington *et al.* (1996) and results in this PhD study show that despite the point mutation in AcORF6^{3260}-1, DNA replication was not affected. Furthermore, early studies involving the AcORF6^{3188} sample with AcΔ*lef*-2.neo showed that there was potentially no difference in DNA replication levels compared with AcMNPV, although this is to be further investigated. This suggested that the dual role of *lef*-2 in DNA replication and late gene expression could be sequence or region specific. To try and attempt to explain this observation, it would be interesting to mutate *lef*-2 by isolating either the N or C-terminus individually. This may be achieved by the construction of Bacmid DNA possessing the *lef*-2 mutations (Fig 6.1) and transfecting these into insect cells at high concentrations. These would have to made by making neomycin the selectable marker to insert the modified *lef*-2 into AcMNPV. If the recombinant virus is able to rescue, then both the DNA replication and late gene transcription can be examined using q-PCR, and the methods used throughout this PhD study. The isolation of large regions of *lef*-2 to produce hybrid fragments can be used to target much smaller regions that may show high conservation across the baculovirus family.

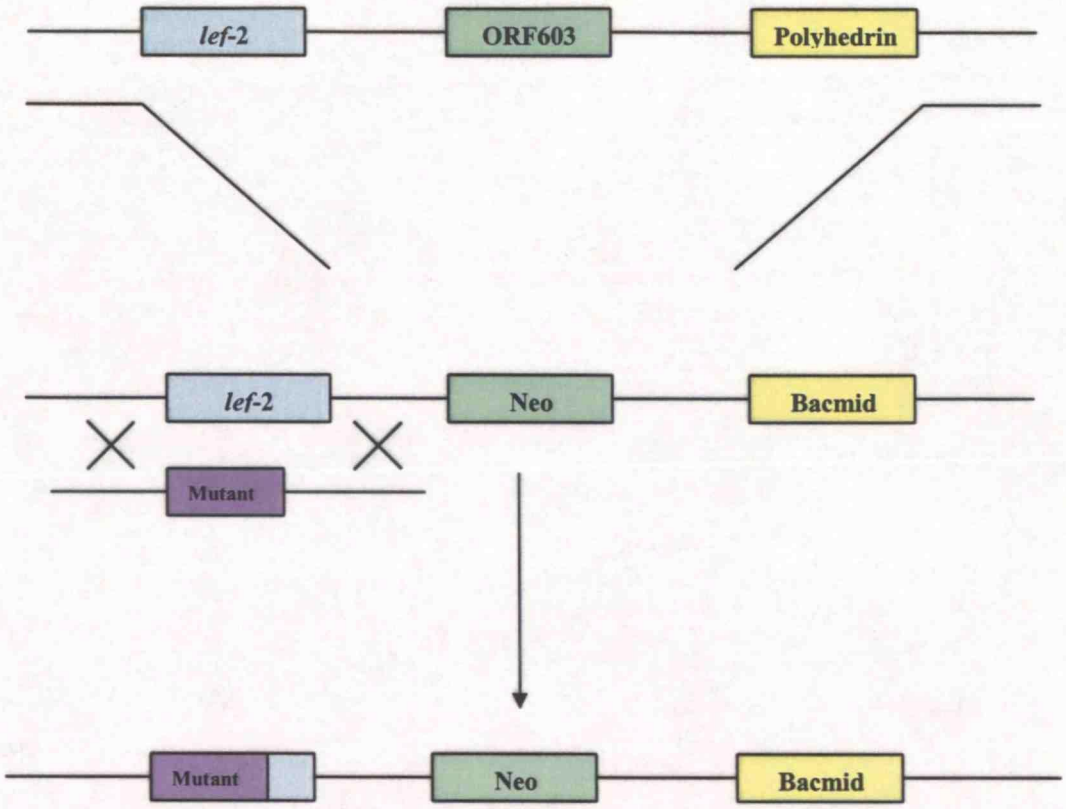

***Figure 6.1*- Construction of *lef*-2 N or C-terminus mutants by producing Bacmid DNA.** Bacmid DNA would be constructed through a bacterial system to replace ORF603 with the selectable neomycin fragment. The N or C-terminus *lef*-2 mutants would be generated by PCR and by ET recombination would replace the native *lef*-2.

References

References

ANON, pDraw32. URL: http://www.acaclone.com. Accessed 2005-2006.

ANON, Minitab Help. Minitab® Release 14 Statistical Software. URL: www.minitab.com. Accessed 2006

ANON, Rotorgene 6000 Online help. URL: http://www.corbettlifescience.com. Accessed 2004-2006

ANON. (2006) Rotor-gene 6000 Operator Manual. Corbett Life Sciences. URL: http://www.corbettlifescience.com. Accessed 2006

ACHARYA, A. & GOPINATHAN, K. P. (2002) Characterization of late gene expression factors *lef-9* and *lef-8* from *Bombyx mori* nucleopolyhedrovirus. *J Gen Virol,* 83, 2015-23.

ANGRAND, P. O., DAIGLE, N., VAN DER HOEVEN, F., SCHÖLER, H. R. & STEWART, A. F. (1999) Simplified generation of targeting constructs using ET recombination. *Nucleic Acids Research*, 27, e16 i- vi

AFONSO, C. L., TULMAN, E. R., LU, Z., BALINSKY, C. A., MOSER, B. A., BECNEL, J. J., ROCK, D. L. & KUTISH, G. F. (2001) Genome sequence of a baculovirus pathogenic for *Culex nigripalpus*. *J Virol,* 75, 11157-65.

AYRES, M. D., HOWARD, S. C., KUZIO, J., LOPEZ-FERBER, M. & POSSEE, R. D. (1994) The complete DNA sequence of *Autographa californica* nuclear polyhedrosis virus. *Virology,* 202, 586-605.

BAUMANN, M., FEEDERLE, R., KREMMER, E. & HAMMERSCHMIDT, W. (1999) Cellular transcription factors recruit viral replication proteins to activate the Epstein-Barr virus origin of lytic DNA replication, *oriLyt*. *EMBO Journal*, 18, 6095-6105.

BERRETTA, M. F., DESHPANDE, M., CROUCH, E. A. & PASSARELLI, A. L. (2006) Functional characterization of *Bombyx mori* Nucleopolyhedrovirus late gene transcription and genome replication factors in the non-permissive insect cell line SF-21. *Virology*, 348, 175-89.

BERRETTA, M. F. & PASSARELLI, A. L. (2006) Function of *Spodoptera exigua* nucleopolyhedrovirus late gene expression factors in the insect cell line SF-21. *Virology*, 355, 82-93.

BIJI, C. P., SUDHEENDRAKUMAR, V. V. & SAJEEV, T. V. (2006) Influence of virus inoculation method and host larval age on productivity of the nucleopolyhedrovirus of the teak defoliator, *Hyblaea puera* (Cramer). *J Virol Methods,* 133, 100-4.

BISWAS, N. & WELLER, S. K. (1999) A mutation in the C-terminal putative Zn2+ finger motif of UL52 severely affects the biochemical activities of the HSV-1 helicase-primase subcomplex. *J Biol Chem,* 274, 8068-76.

BLISSARD, G. W. & ROHRMANN, G. F. (1989) Location, sequence, transcriptional mapping, and temporal expression of the gp64 envelope glycoprotein gene of the *Orgyia pseudotsugata* multicapsid nuclear polyhedrosis virus. *Virology*, 170, 537-55

BLISSARD, G. W. & WENZ, J. R. (1992) Baculovirus gp64 envelope glycoprotein is sufficient to mediate pH-dependent membrane fusion. *J Virol,* 66, 6829-35.

BODMER-GLAVAS, M., EDLER, K. & BARBERIS, A. (2001) RNA polymerase II and III transcription factors can stimulate DNA replication by modifying origin chromatin structures. *Nucleic Acids Research*, 29, 4570-80.

BONFIELD, J. K., SMITH, K. & STADEN, R. (1995) A new DNA sequence assembly program. *Nucleic Acids Res,* 23, 4992-9.

BONFIELD, J. K. & STADEN, R. (1996) Experiment files and their application during large-scale sequencing projects. *DNA Seq,* 6, 109-17.

BROER, R., HELDENS, J. G., VAN STRIEN, E. A., ZUIDEMA, D. & VLAK, J. M. (1998) Specificity of multiple homologous genomic regions in *Spodoptera exigua* nucleopolyhedrovirus DNA replication. *J Gen Virol,* 79 (Pt 6), 1563-72.

BRUSCA, R. C., AND BRUSCA, G. J (1990) *Invertebrates,* Sunderland, Massachsetts, Sinauer Associates.

CANN, A. J. (1997) *Principles of Molecular Virology,* London, Academic Press.

CARSON, D. D., GUARINO, L. A. & SUMMERS, M. D. (1988) Functional mapping of an AcNPV immediately early gene which augments expression of the IE-1 trans-activated 39K gene. *Virology,* 162, 444-51.

CARSTENS, E. B., LU, A. L. & CHAN, H. L. (1993) Sequence, transcriptional mapping, and overexpression of *p47*, a baculovirus gene regulating late gene expression. *J Virol,* 67, 2513-20.

CHEN, C. J. & THIEM, S. M. (1997) Differential infectivity of two *Autographa californica* nucleopolyhedrovirus mutants on three permissive cell lines is the result of lef-7 deletion. *Virology,* 227, 88-95.

CHEN, X., IJKEL, W. F., DOMINY, C., DE ANDRADE ZANOTTO, P. M., HASHIMOTO, Y., FAKTOR, O., HAYAKAWA, T., WANG, C. H., PREKUMAR, A., MATHAVAN, S., KRELL, P. J., HU, Z. & VLAK, J. M. (1999)

Identification, sequence analysis and phylogeny of the *lef-2* gene of Helicoverpa armigera single-nucleocapsid baculovirus. *Virus Res,* 65, 21-32.

CHISOLM, G. E. & HENNER, D. J. (1988) Multiple early transcripts and splicing of the *Autographa californica* nuclear Polyhedrosis virus IE-1 gene. *J. Virol*, 62, 3193-3200.

CLEM, R. J., FECHHEIMER, M. & MILLER, L. K. (1991) Prevention of apoptosis by a baculovirus gene during infection of insect cells. *Science,* 254, 1388-90.

CLEM, R. J. & MILLER, L. K. (1993) Apoptosis reduces both the in vitro replication and the *in vivo* infectivity of a baculovirus. *J Virol,* 67, 3730-8.

COCHRAN, M. A. & FAULKNER, P. (1983) Location of Homologous DNA Sequences Interspersed at Five Regions in the Baculovirus AcMNPV Genome. *J Virol,* 45, 961-970.

DICKSON, J. A. & FRIESEN, P. D. (1991) Identification of upstream promoter elements mediating early transcription from the 35,000-molecular-weight protein gene of *Autographa californica* nuclear polyhedrosis virus. *J Virol,* 65, 4006-16.

DODSON, M. S., CRUTE, J. J., BRUCKNER, R. C. & LEHMAN, I. R. (1989) Overexpression and assembly of the herpes simplex virus type 1 helicase-primase in insect cells. *J Biol Chem,* 264, 20835-8.

DURANTEL, D., CROIZIER, G., RAVALLEC, M. & LOPEZ-FERBER, M. (1998) Temporal expression of the AcMNPV *lef-4* gene and subcellular localization of the protein. *Virology,* 241, 276-84.

ERLANDSON, M., KUZIO., J. & CARSTENS, E. B. (1984) Genomic variants of a temperature sensitive mutant of *Autographa californica* nuclear polyhedrosis virus containing specific reiterations of viral DNA. *Virus Res,* 1, 565-84.

EVANS, J. T., LEISY, D. J. & ROHRMANN, G. F. (1997) Characterization of the interaction between the baculovirus replication factors LEF-1 and LEF-2. *J Virol,* 71, 3114-9.

FAUQUET, C. M., MAYO, M. A., MANILOFF, J., DESSELBERGER, U. & BALL, L. A. (2005) *Virus Taxonomy- Eighth Report of the International Committee on Taxonomy of Viruses*. London, Elsevier.

FEDERICI, B. A. & HICE, R. H. (1997) Organization and molecular characterization of genes in the polyhedrin region of the *Anagrapha falcifera* multinucleocapsid NPV. *Arch Virol,* 142, 333-48.

FRIESEN, P. D. (1997) Regulation of Baculovirus Early Gene Expression. IN MILLER, L. K. (Ed.) *The Baculoviruses.* New York, Plenum Press, 141-66.

FRIESEN, P. D. & MILLER, L. K. (1987) Divergent transcription of early 35- and 94-kilodalton protein genes encoded by the HindIII K genome fragment of the baculovirus *Autographa californica* nuclear polyhedrosis virus. *J Virol,* 61, 2264-72.

FUCHS, L. Y., WOODS, M. S. & WEAVER, R. F. (1983) Viral transcription during *Autographa californica* Polyhedrosis virus infection: a novel RNA polymerase induced in infected *Spodoptera frugiperda* cells. *J. Virol*, 48, 641-6.

FUNK, C. J., BRAUNAGEL, S.C. & ROHRMANN, G. F (1997) Baculovirus Structure. IN MILLER, L. K. (Ed.) *The Baculoviruses.* New York, Plenum Press, 7-27.

GARCIA-MARUNIAK, A., MARUNIAK, J. E., ZANOTTO, P. M., DOUMBOUYA, A. E., LIU, J. C., MERRITT, T. M. & LANOIE, J. S. (2004) Sequence analysis of the genome of the *Neodiprion sertifer* nucleopolyhedrovirus. *J Virol,* 78, 7036-51.

GLOCKER, B., HOOPES, R. R., JR., HODGES, L. & ROHRMANN, G. F. (1993) *In vitro* transcription from baculovirus late gene promoters: accurate mRNA initiation by nuclear extracts prepared from infected *Spodoptera frugiperda* cells. *J Virol,* 67, 3771-6.

GOMI, S., MAJIMA, K. & MAEDA, S. (1999) Sequence analysis of the genome of *Bombyx mori* nucleopolyhedrovirus. *J Gen Virol,* 80 (Pt 5), 1323-37.

GORDON, J. D. & CARSTENS, E. B. (1984) Phenotypic characterization and physical mapping of a temperature-sensitive mutant of *Autographa californica* nuclear polyhedrosis virus defective in DNA synthesis. *Virology,* 138, 69-81.

GRANADOS, R. R., AND LAWLER, K. A (1981) *In Vivo* Pathway of *Autographa californica* Baculovirus Invasion and Infection. *Virology,* 108, 297-308.

GRANADOS, R. R., AND WILLIAMS, K. A (1986) In vivo Infection and Replication of Baculoviruses. IN GRANADOS, R. R., AND FEDERICI, B.A (Ed.) *The Biology of Baculoviruses.* Florida, CRC Press, 89-108.

GRIFFITHS, C. M., BARNETT, A. L., AYRES, M. D., WINDASS, J., KING, L. A. & POSSEE, R. D. (1999) *In vitro* host range of *Autographa californica* nucleopolyhedrovirus recombinants lacking functional *p35*, *iap1* or *iap2*. *J Gen Virol,* 80 (Pt 4), 1055-66.

GROSS, C. H. & SHUMAN, S. (1998) RNA 5'-triphosphatase, nucleotide triphosphatase and guanylyltransferase activities of baculovirus LEF-4 protein. *J. Virol*, 72, 10020-8.

GUARINO, L. A., DONG, W. & JIN, J. (2002a) *In vitro* activity of the baculovirus late expression factor LEF-5. *J Virol,* 76, 12663-75.

GUARINO, L. A., DONG, W., XU, B., BROUSSARD, D. R., DAVIS, R. W. & JARVIS, D. L. (1992) Baculovirus phosphoprotein pp31 is associated with virogenic stroma. *J Virol,* 66, 7113-20.

GUARINO, L. A., GONZALEZ, M. A. & SUMMERS, M. D. (1986) Complete Sequence and Enhancer Function of the Homologous DNA Regions of *Autographa californica* Nuclear Polyhedrosis Virus. *J Virol,* 60, 224-229.

GUARINO, L. A., JIN, J. & DONG, W. (1998a) Guanylyltransferase activity of the LEF-4 subunit of baculovirus RNA polymerase. *J Virol,* 72, 10003-10.

GUARINO, L. A., MISTRETTA, T. A. & DONG, W. (2002b) Baculovirus *lef-12* is not required for viral replication. *J Virol,* 76, 12032-43.

GUARINO, L. A. & SMITH, M. W. (1990) Nucleotide sequence and characterization of the 39K gene region of *Autographa californica* nuclear polyhedrosis virus. *Virology,* 179, 1-8.

GUARINO, L. A. & SUMMERS, M. D. (1986) Functional mapping of a trans-activating gene required for expression of a baculovirus delayed-early gene. *J Virol,* 57, 563-71.

GUARINO, L. A. & SUMMERS, M. D. (1987) Nucleotide Sequence and Temporal Expression of a Baculovirus Regulatory Gene. *J Virol,* 61, 2091-2099.

GUARINO, L. A., XU, B., JIN, J. & DONG, W. (1998b) A virus-encoded RNA polymerase purified from baculovirus-infected cells. *J Virol,* 72, 7985-91.

GUO, W., TANG, W. J., BU, X., BERMUDEZ, V., MARTIN, M. & FOLK, W. R. (1996) AP1 enhances polyomavirus DNA replication by promoting T-antigen-mediated unwinding of DNA. *J. Virol*, 70, 4914-8.

HABIB, S. & HASNAIN, S. E. (2000) Differential activity of two non-*hr* origins during replication of the baculovirus *Autographa californica* nuclear polyhedrosis virus genome. *J Virol,* 74, 5182-9.

HANG, X., DONG, W. and GUARINO, L. A. (1995) The *lef-3* gene of *Autographa californica* nuclear polyhedrosis virus encodes a single-stranded DNA-binding protein *J Virol,* **69,** 3924-8.

HANG, X. & GUARINO, L. A. (1999) Purification of *Autographa californica* nucleopolyhedrovirus DNA polymerase from infected insect cells. *J Gen Virol,* 80 (Pt 9), 2519-26.

HARWOOD, S. H., LI, L., HO, P. S., PRESTON, A. K. & ROHRMANN, G. F. (1998) AcMNPV late expression factor-5 interacts with itself and contains a zinc ribbon domain that is required for maximal late transcription activity and is homologous to elongation factor TFIIS. *Virology,* 250, 118-34.

HAWTIN, R. E., ZARKOWSKA, T., ARNOLD, K., THOMAS, C. J., GOODAY, G. W., KING, L. A., KUZIO, J. A. & POSSEE, R. D. (1997) Liquefaction of *Autographa californica* nucleopolyhedrovirus-infected insects is dependent on the integrity of virus-encoded chitinase and cathepsin genes. *Virology,* 238, 243-53.

HEFFERON, K. L. (2003a) Identification of a repressor of late gene expression within the AcMNPV genome. *Arch Virol*, 148, 1413-8.

HEFFERON, K. L. (2003b) Characterization of HCF-1, a determinant of *Autographa californica* multiple Nucleopolyhedrovirus host specificity. *Insect Molecular Biology*, 12, 651-8.

HEFFERON, K. L. (2004) Baculovirus late expression factors. *J Mol Microbiol Biotechnol,* 7, 89-101.

HEFFERON, K. L. & MILLER, L. K. (2002) Reconstructing the replication complex of AcMNPV. *Eur J Biochem,* 269, 6233-40.

HERNIOU, E. A., LUQUE, T., CHEN, X., VLAK, J. M., WINSTANLEY, D., CORY, J. S. & O'REILLY, D. R. (2001) Use of whole genome sequence data to infer baculovirus phylogeny. *J Virol,* 75, 8117-26.

HERSHBERGER, P. A., DICKSON, J. A. & FRIESEN, P. D. (1992) Site-specific mutagenesis of the 35-kilodalton protein gene encoded by *Autographa californica* nuclear polyhedrosis virus: cell line-specific effects on virus replication. *J Virol,* 66, 5525-33.

HERSHBERGER, P. A., LACOUNT, D. J. & FRIESEN, P. D. (1994) The apoptotic suppressor P35 is required early during baculovirus replication and is targeted to the cytosol of infected cells. *J Virol,* 68, 3467-77.

HOOPES, JR, R. R. & ROHRMANN, G. F (1991) *In vitro* transcription of baculovirus immediate early genes: accurate mRNA initiation by nuclear extracts from both insect and human cells, *Proc. Natl. Acad. Sci*, 88, 4513-7.

HUH, N. E. & WEAVER, R. F. (1990) Identifying the RNA polymerases that synthesize specific transcripts of the *Autographa californica* nuclear polyhedrosis virus. *J. Gen. Virol*, 71, 195-201.

HUIJSKENS, I., LI, L., WILLIS, L. G. & THEILMANN, D. A. (2004) Role of AcMNPV IE0 in baculovirus very late gene activation. *Virology,* 323, 120-30.

HUNTER-FUJITA, F.R., ENTWISTLE, P. F., EVANS, H. F. & CROOK, N. E. (1998). *Insect Viruses and Pest Management*, Somerset, New Jersey, USA, Wiley & Sons.

IJKEL, W. F. J., WESTENBERG, M., GOLDBACH, R. W., BLISSARD, G. W., VLAK, J. M. & ZUIDEMA, D. (2000) A novel baculovirus envelope fusion protein with a proprotein convertase cleavage site. *Virology*, 275, 30- 41.

JEHLE, J. A., BLISSARD, G. W., BONNING, B. C., CORY, J. S., HERNIOU, E. A., ROHRMANN, G. F., THEILMANN, D. A., THIEM, S. M. & VLAK, J. M. (2006) On the classification and nomenclature of baculoviruses: a proposal for revision. *Arch Virol,* 151, 1257-66.

JEHLE, J. A., VAN DER LINDEN, I. F., BACKHAUS, H. & VLAK, J. M. (1997) Identification and sequence analysis of the integration site of transposon TCp3.2 in the genome of *Cydia pomonella* granulovirus. *Virus Res,* 50, 151-7.

JIN, J., DONG, W. & GUARINO, L. A. (1998) The LEF-4 subunit of baculovirus RNA polymerase has RNA 5'-triphosphatase and ATPase activities. *J. Virol*, 72, 10011-19.

KELLY, B. J., KING, L. A., POSSEE, R. D. and CHAPPLE, S. D. (2006) Dual mutations in the *Autographa californica* nucleopolyhedrovirus FP-25 and p35 genes result in plasma-membrane blebbing in Trichoplusia ni cells. *J Gen Virol,* **87,** 531-6.

KING, L. A., AND POSSEE, R.D (1992) *The Baculovirus Expression System: A Laboratory Guide,* London, UK, Chapman and Hall.

KITTS, P. A. & POSSEE, R. D. (1993) A method for producing recombinant baculovirus expression vectors at high frequency. *Biotechniques*, 14, 810-7.

KNEBEL-MÖRSDORF, D., QUADT, I., MONTIER, L. & GUARINO, L. A. (2004) Expression of baculovirus late and very late genes depends on LEF-4, a component of the viral RNA polymerase whose guanyltransferase function is essential. *J. Virol*, 80, 4168-73.

KNOPF, C. W. (2000) Molecular mechanisms of replication of herpes simplex virus 1. *Acta Virol,* 44, 289-307.

KOGAN, P. H., CHEN, X. & BLISSARD, G. W. (1995) Overlapping TATA-dependent and TATA-independent early promoter activities in the baculovirus *gp64 envelope fusion protein* gene, *J. Virol*, 69, 1452-61.

KOOL, M., AHRENS, C. H., GOLDBACH, R. W., ROHRMANN, G. F. & VLAK, J. M. (1994) Identification of genes involved in DNA replication of the *Autographa californica* baculovirus. *Proc Natl Acad Sci U S A,* 91, 11212-6.

KOOL, M., VAN DEN BERG, P. M., TRAMPER, J., GOLDBACH, R. W. & VLAK, J. M. (1993) Location of two putative origins of DNA replication of *Autographa californica* nuclear polyhedrosis virus. *Virology,* 192, 94-101.

KOONIN, E. V., WOLF, Y. I., KONDRASHOV, A. S. & ARAVIND, L. (2000) Bacterial homologs of the small subunit of eukaryotic DNA primase. *J Mol Microbiol Biotechnol,* 2, 509-12.

KUZIO, J., PEARSON, M. N., HARWOOD, S. H., FUNK, C. J., EVANS, J. T., SLAVICEK, J. M. & ROHRMANN, G. F. (1999) Sequence and analysis of the genome of a baculovirus pathogenic for *Lymantria dispar*. *Virology,* 253, 17-34.

LAUFS, S., LU, A., ARRELL, K. & CARSTENS, E. B. (1997) *Autographa californica* nuclear polyhedrosis virus *p143* gene product is a DNA-binding protein. *Virology,* 228, 98-106.

LEE, H. Y. & KRELL, P. J. (1992) Generation and analysis of defective genomes of *Autographa californica* nuclear polyhedrosis virus. *J Virol,* 66, 4339-47.

LEISY, D. J. & ROHRMANN, G. F. (1993) Characterization of the replication of plasmids containing *hr* sequences in baculovirus-infected *Spodoptera frugiperda* cells. *Virology,* 196, 722-30.

LI, L., HARWOOD, S. H. & ROHRMANN, G. F. (1999) Identification of additional genes that influence baculovirus late gene expression. *Virology,* 255, 9-19.

LI, Q., DONLY, C., LI, L., WILLIS, L. G., THEILMANN, D. A. & ERLANDSON, M. (2002) Sequence and organization of the *Mamestra configurata* nucleopolyhedrovirus genome. *Virology,* 294, 106-21.

LI, Y., PASSARELLI, A. L. & MILLER, L. K. (1993) Identification, sequence, and transcriptional mapping of *lef-3*, a baculovirus gene involved in late and very late gene expression. *J Virol,* 67, 5260-8.

LIN, G. & BLISSARD, G. W. (2002a) Analysis of an *Autographa californica* multicapsid nucleopolyhedrovirus lef-6-null virus: LEF-6 is not essential for viral replication but appears to accelerate late gene transcription. *J Virol,* 76, 5503-14.

LIN, G. & BLISSARD, G. W. (2002b) Analysis of an *Autographa californica* nucleopolyhedrovirus lef-11 knockout: LEF-11 is essential for viral DNA replication. *J Virol,* 76, 2770-9.

LIN, G., SLACK, J. M. & BLISSARD, G. W. (2001) Expression and localization of LEF-11 in *Autographa californica* nucleopolyhedrovirus-infected Sf9 cells. *J Gen Virol,* 82, 2289-94.

LIU, G. & CARSTENS, E. B. (1999) Site-directed mutagenesis of the AcMNPV *p143* gene: effects on baculovirus DNA replication. *Virology,* 253, 125-36.

LU, A., KRELL, P. J., VLAK, J. M., AND ROHRMANN, G. F (1997) Baculovirus DNA Replication. IN MILLER, L. K. (Ed.) *The Baculoviruses.* New York, Plenum Press, 171-86.

LU, A. & CARSTENS, E. B. (1991) Nucleotide sequence of a gene essential for viral DNA replication in the baculovirus *Autographa californica* nuclear polyhedrosis virus. *Virology,* 181, 336-47.

LU, A. & MILLER, L. K. (1994) Identification of three late expression factor genes within the 33.8- to 43.4-map-unit region of *Autographa californica* nuclear polyhedrosis virus. *J Virol,* 68, 6710-8.

LU, A. & MILLER, L. K. (1995a) Differential requirements for baculovirus late expression factor genes in two cell lines. *J Virol,* 69, 6265-72.

LU, A. & MILLER, L. K. (1995b) The roles of eighteen baculovirus late expression factor genes in transcription and DNA replication. *J Virol,* 69, 975-82.

LU, A. & MILLER, L. K. (1996) Species-specific effects of the *hcf*-1 gene on baculovirus virulence. *J. Virol,* 70, 5123-30.

LU, A., AND MILLER, L. K (1997) Regulation of Baculovirus Late and Very Late Gene Expression. IN MILLER, L. K. (Ed.) *The Baculoviruses.* New York, Plenum Press, 193- 211.

LÜBBERT, H. & DOERFLER, W. (1984) Transcription of overlapping sets of RNAs from the genome of *Autographa californica* nuclear polyhedrosis virus: a novel method for mapping RNAs. *J Virol,* 52, 255-65.

LUNG, O., WESTENBERG, M., VLAK, J. M., ZUIDEMA, D. & BLISSARD, G. W. (2002) Pseudotyping *Autographa californica* multicapsid nucleopolyhedrovirus (AcMNPV): F proteins from group II NPVs are functionally analogous to AcMNPV GP64. *J Virol,* 76, 5729-36.

MERRINGTON, C. L., KITTS, P. A., KING, L. A. & POSSEE, R. D. (1996) An *Autographa californica* nucleopolyhedrovirus *lef-2* mutant: consequences for DNA replication and very late gene expression. *Virology,* 217, 338-48.

MIKHAILOV, V. S. & ROHRMANN, G. F. (2002) Baculovirus replication factor LEF-1 is a DNA primase. *J Virol,* 76, 2287-97.

MILLER, L. K., JEWELL, J. E. & BROWNE, D. (1981) Baculovirus induction of a DNA polymerase. *J Virol,* 40, 305-8.

MORRIS, T. D., TODD, J. W., FISHER, B. & MILLER, L. K. (1994) Identification of *lef-7*: a baculovirus gene affecting late gene expression. *Virology,* 200, 360-9.

MUNOZ, D., CASTILLEJO, J. I. & CABALLERO, P. (1998) Naturally occurring deletion mutants are parasitic genotypes in a wild-type nucleopolyhedrovirus population of *Spodoptera exigua*. *Appl Environ Microbiol,* 64, 4372-7.

NAGAMINE, T., KAWASAKI, Y. & MATSUMOTO, S. (2006) Induction of a subnuclear structure by the simultaneous expression of baculovirus proteins, IE1, LEF3, and P143 in the presence of *hr*. *Virology,* 352, 400-7.

NISSEN, M. S. & FRIESEN, P. D. (1989) Molecular analysis of the transcriptional regulatory region of an early baculovirus gene. *J Virol,* 63, 493-503.

OOMENS, A. G. P., MONSMA, S. A. & BLISSARD, G. W. (1995) The baculovirus GP64 envelope fusion protein: synthesis, oligomerization and processing. *Virology*, 209, 592-603.

O'REILLY, D. (1992) The Organisation and Regulation of Baculovirus Genes. IN VLAK, J. M., SCHLAEGER, J., AND BERNARD ROCHE, A. R (Ed.) *In Workshop on Baculovirus and Recombinant Protein Production Processes.* Basel, Switzerland.

PAGE, R. D. (1996) TreeView: an application to display phylogenetic trees on personal computers. *Comput Appl Biosci,* 12, 357-8.

PASSARELLI, A. L. & MILLER, L. K. (1993a) Identification and characterization of *lef-1*, a baculovirus gene involved in late and very late gene expression. *J Virol,* 67, 3481-8.

PASSARELLI, A. L. & MILLER, L. K. (1993b) Identification of genes encoding late expression factors located between 56.0 and 65.4 map units of the *Autographa californica* nuclear polyhedrosis virus genome. *Virology,* 197, 704-14.

PASSARELLI, A. L. & MILLER, L. K. (1993c) Three baculovirus genes involved in late and very late gene expression: *ie-1*, *ie-n*, and *lef-2*. *J Virol,* 67, 2149-58.

PASSARELLI, A. L. & MILLER, L. K. (1994) Identification and transcriptional regulation of the baculovirus lef-6 gene. *J Virol,* 68, 4458- 67.

PASSARELLI, A. L., TODD, J. W. & MILLER, L. K. (1994) A baculovirus gene involved in late gene expression predicts a large polypeptide with a conserved motif of RNA polymerases. *J Virol,* 68, 4673-8.

PEARSON, M., BJORNSON, R., PEARSON, G. & ROHRMANN, G. (1992) The *Autographa californica* baculovirus genome: evidence for multiple replication origins. *Science,* 257, 1382-4.

PEARSON, M. N., GROTEN, C. & ROHRMANN, G. F. (2000) Identification of the *Lymantria dispar* Nucleopolyhedrovirus envelope fusion protein provides evidence for a phylogenetic division of the *Baculoviridae*. *J. Virol*, 74, 6126-31.

POSSEE, R. D. & HOWARD, S. C. (1987) Analysis of the polyhedrin gene promoter of the *Autographa californica* nuclear Polyhedrosis virus. *Nucleic Acids Research*, 15, 10233-48.

POSSEE, R. D., AND ROHRMANN, G. F (1997) Baculovirus Genome Organisation and Evolution. IN MILLER, L. K. (Ed.) *The Baculoviruses.* New York, Plenum Press, 109- 34.

POSSEE, R. D., SUN, T. P., HOWARD, S. C., AYRES, M. D., HILL-PERKINS, M. & GEARING, K. L. (1991) Nucleotide sequence of the Autographa californica nuclear polyhedrosis 9.4 kbp EcoRI-I and -R (polyhedrin gene) region. *Virology,* 185, 229-41.

PRIKHOD'KO, E. A., LU, A., WILSON, J. A. & MILLER, L. K. (1999) *In vivo* and *in vitro* analysis of baculovirus *ie-2* mutants. *J Virol,* 73, 2460-8.

PRIKHOD'KO, E. A. & MILLER, L. K. (1998) Role of baculovirus IE2 and its RING finger in cell cycle arrest. *J Virol,* 72, 684-92.

QIN, J., LIU, A. & WEAVER, R. F. (1989) Studies on the control region of the p10 gene of the *Autographa californica* nuclear polyhedrosis virus. *J. Gen. Virol*, 70, 1273-9.

RAPP, J. C., WILSON, J. A. & MILLER, L. K. (1998) Nineteen baculovirus open reading frames, including LEF-12, support late gene expression. *J Virol,* 72, 10197-206.

RIBEIRO, B. M., HUTCHINSON, K. & MILLER, L. K. (1994) A mutant baculovirus with a temperature-sensitive IE-1 transregulatory protein. *J Virol,* 68, 1075-84.

RICE, W. C. & MILLER, L. K. (1986) Baculovirus transcription in the presence of inhibitors and in nonpermissive *Drosophila* cells. *Virus Res,* 6, 155-72.

RODEMS, S. M., PULLEN, S. S. & FRIESEN, P. D. (1997) DNA-dependent transregulation by IE1 of *Autographa californica* nuclear polyhedrosis virus: IE1 domains required for transactivation and DNA binding. *J Virol,* 71, 9270-7.

ROHRMANN, G. F. (1986) Polyhedrin structure. *J Gen Virol,* 67, 1499-513.

ROSINSKI, M., REID, S. & NIELSEN, L. K. (2002) Kinetics of baculovirus replication and release using real-time quantitative polymerase chain reaction. *Biotechnol Bioeng,* 77, 476-80.

SHERMAN, G., GOTTLIEB, J. & CHALLBERG, M. D. (1992) The UL8 subunit of the herpes simplex virus helicase-primase complex is required for efficient primer utilization. *J Virol,* 66, 4884-92.

SIMAKOV, O. MB Advanced DNA Analysis, Version 6.61.

SLACK, J. M. & BLISSARD, G. W. (1997) Identification of two independent transcriptional activation domains in the *Autographa californica* multicapsid nuclear polyhedrosis virus IE1 protein. *J Virol,* 71, 9579-87.

SRIRAM, S. & GOPINATHAN, K. P. (1998) The potential role of a late gene expression factor, *lef-2*, from *Bombyx mori* nuclear polyhedrosis virus in very late gene transcription and DNA replication. *Virology,* 251, 108-22.

STIRPE, F., AND FIUME, L. (1967) Studies on the Pathogenesis of Liver Necrosis by Alpha-Amanitin. *Journal of Biochemistry,* 105, 779-782.

TATUSOVA, T. A. & MADDEN, T. L. (1999) BLAST 2 Sequences, a new tool for comparing protein and nucleotide sequences. *FEMS Microbiol Lett,* 174, 247-50.

TENNEY, D. J., HURLBURT, W. W., MICHELETTI, P. A., BIFANO, M. & HAMATAKE, R. K. (1994) The UL8 component of the herpes simplex virus helicase-primase complex stimulates primer synthesis by a subassembly of the UL5 and UL52 components. *J Biol Chem,* 269, 5030-5.

THIEM, S. M. & MILLER, L. K. (1989) Identification, sequence, and transcriptional mapping of the major capsid protein gene of the baculovirus *Autographa californica* nuclear polyhedrosis virus. *J Virol,* 63, 2008-18.

THOMPSON, J. D., GIBSON, T. J., PLEWNIAK, F., JEANMOUGIN, F. & HIGGINS, D. G. (1997) The CLUSTAL_X windows interface: flexible strategies for multiple sequence alignment aided by quality analysis tools. *Nucleic Acids Res,* 25, 4876-82.

TITTERINGTON, J. S., NUN, T. K. & PASSARELLI, A. L. (2003) Functional dissection of the baculovirus *late expression factor-8* gene: sequence requirements for late gene promoter activation. *J Gen Virol,* 84, 1817-26.

TODD, J. W., PASSARELLI, A. L. & MILLER, L. K. (1995) Eighteen baculovirus genes, including *lef-11*, *p35*, *39K*, and *p47*, support late gene expression. *J Virol,* 69, 968-74.

TOMALSKI, M. D., WU, J. G. & MILLER, L. K. (1988) The location, sequence, transcription, and regulation of a baculovirus DNA polymerase gene. *Virology,* 167, 591-600.

VANARSDALL, A. L., OKANO, K. & ROHRMANN, G. F. (2004) Characterization of a baculovirus with a deletion of *vlf-1*. *Virology*, 326, 191-201.

VANARSDALL, A. L., OKANO, K. & ROHRMANN, G. F. (2005) Characterization of the replication of a baculovirus mutant lacking the DNA polymerase gene. *Virology*, 331, 175-80.

VANARSDALL, A. L., OKANO, K. & ROHRMANN, G. F. (2006) Characterization of the role of Very Late Expression Factor 1 in baculovirus capsid structure and DNA processing. *J Virol*, 80, 1724-33.

WESTENBERG, M., VEENMAN, F., ROODE, E. C., GOLDBACH, R. W., VLAK, J. M. & ZUIDEMA, D. (2004) Functional analysis of the putative fusion domain of the baculovirus envelope fusion protein F. *J Virol*, 78, 6946-54.

WEYER, U. & POSSEE, R. D. (1988) Functional analysis of the p10 5' leader sequence of the *Autographa californica* nuclear polyhedrosis virus. *Nucleic Acids Research*, 16, 3635- 53.

WEYER, U. & POSSEE, R. D. (1989) Analysis of the promoter of the *Autographa californica* nuclear polyhedrosis virus p10 gene. *J. Gen. Virol*, 70, 203-8.

WHITFORD, M., STEWART, S., KUZIO, J. & FAULKNER, P. (1989) Identification and sequence analysis of a gene encoding gp67, an abundant envelope glycoprotein of the baculovirus *Autographa californica* nuclear polyhedrosis virus. *J Virol*, 63, 1393-9.

WILLIAMS, G. V., AND FAULKNER, P (1997) Cytological and Viral Morphogenesis during Baculovirus Infection. IN MILLER, L. K. (Ed.) *The Baculoviruses*. New York, Plenum Press, 61- 96.

WILSON, J. A., FORNEY, S. D., RICCI, A. M., ALLEN, E. G., HEFFERON, K. L. & MILLER, L. K. (2005) Expression and mutational analysis of *Autographa californica* nucleopolyhedrovirus HCF-1: functional requirements for cysteine residues. *J. Virol*, 79, 13900-14.

WOOD, H.A. (1980) *Autographa californica* Nuclear Polyhedrosis Virus-induced proteins in tissue culture. *Virology*, 102, 21-27

WU, Y. & CARSTENS, E. B. (1996) Initiation of baculovirus DNA replication: early promoter regions can function as infection-dependent replicating sequences in a plasmid-based replication assay. *J. Virol*, 70, 6967-72.

WU, Y. & CARSTENS, E. B. (1998) A baculovirus single-stranded DNA binding protein, LEF-3, mediates the nuclear localization of the putative helicase P143. *Virology*, 247, 32-40.

YANG, S. & MILLER, L. K. (1999) Activation of baculovirus very late promoters by interaction with Very Late Factor 1. *J Virol*, 73, 3404-9.

ZANOTTO, P. M., SAMPAIO, M. J., JOHNSON, D. W., ROCHA, T. L. & MARUNIAK, J. E. (1992) The *Anticarsia gemmatalis* nuclear polyhedrosis virus polyhedrin gene region: sequence analysis, gene product and structural comparisons. *J Gen Virol,* 73 (Pt 5), 1049-56.

ZANOTTO, P. M., KESSING, B. D. & MARUNIAK, J. E. (1998) Phylogentic interrelationships among baculoviruses: evolutionary rates and host associations. *J. Invert. Pathol*, 62, 147-64.